D.M. RICHARDS

THE MINIMUM WEIGHT DESIGN OF COMPRESSION STRUCTURES INCLUDING PLASTICITY EFFECTS.

College of Aeronautics

Submission for the degree of Ph.D., November 1977

CRANFIELD INSTITUTE OF TECHNOLOGY

COLLEGE OF AERONAUTICS

Submission for the award of the degree of PhD.

by

D.M. RICHARDS

THE MINIMUM WEIGHT DESIGN OF COMPRESSION STRUCTURES INCLUDING PLASTICITY EFFECTS.

Supervisor:

Professor D. Howe.

November 1977

DEDICATION

With humility and love, I dedicate this work to my children

Ursula, Helen and Caroline.

ACKNOWLEDGEMENT

I would like to express my deepest gratitude to Joyce Carberry for the very special care she has given to the preparation of this text.

SUMMARY

The minimum weight design of a wide range of structures required to resist compressive loading is considered. Items which have been analysed in detail include struts of various sorts, thin plates, honeycomb core sandwich panels, wide column stiffened panels, stiffened panels with optimised support locations, and cylindrical shells stiffened by axial stiffners and rings. A further study is concerned with the effects of imperfections on a tower with corrugation stiffened walls, loaded in compression.

Except for the corrugated tower, each analysis includes the effects of plasticity in a direct and realistic way by characterising stress-strain behaviour in the manner suggested by Ramberg and Osgood.

Results for each type of structure are presented, together with the appropriate computer programmes.

CONTENTS

FIGURES

FOREWORD

The training of structural engineers is traditionally almost exclusively devoted to the analysis, experimental and theoretical, of structures with members of given size, subjected to loads of given distribution and intensity. In this way, an appreciation of structural behaviour is acquired, including an understanding of structural failure. Thus the young engineer may become well equipped to evaluate the performance of a given structure. However, if he should be asked to recommend ways in which a defective structure might be modified so that it becomes reliable and safe, he will suddenly be on more uncertain ground. His difficulties will increase if he is asked to suggest the best way of doing this. The change in outlook required in making the step from analysis, by way of design to optimisation is a radical one.

Perhaps the structural design problem which exemplifies this notion best is that of the large scale multi-element, highly redundant structure. The American engineer Cilly[1], at a time when systematic methods of analysis for redundant structures were first becoming available, strongly advocated the use of statically determinate configurations, mainly on the grounds of certainty of analysis and freedom from thermal stresses.

The problems of analysis of complex structures without the aid of computers were quite formidable in themselves, without the added complication of variable structural sizes. Thus designers were, and often still are, forced to adopt the design-analysis-redesign sequence without really being sure that such a cycle would produce either a safer, or a more efficient structure. Quite a lot is now known[2,3] about this process, but much of the mystery remains.

The arrival of powerful computers coincided with an increasing incentive to make complex structures lighter. This arose from the needs of the aerospace designer, who could afford to spend a large amount on structural refinement, because the payoff was, and indeed is so great. The approach adopted[4,5] was to utilise the techniques of mathematical programming, exploring the multidimensional design space defined by member sizes in the search for the lightest safe design. A typical problem might involve many hundreds of design variables, dozens of design cases, and many different failure criteria, coupled with restrictions on maximum and minimum member sizes. These methods have proved largely unsuccessful, mainly because of the difficulties of generalisation, computing expense and the absence of any guarantee of the achievement of a global optimum.

Important improvements in computing efficiency have been made using optimality criteria[6,7] methods for the design of structures of this type. These procedures are more directly related to the behaviour of the structure, and the characteristics of the optimum solution, and show greatly improved convergence characteristics, but are still nevertheless likely to remain beyond the reach of designers of a wide range of structures.

Perhaps the most directly practical developments in optimisation offering immediately tangible benefits are those concerned with the design of individual components and elements.

Studies of this type, which form the basis of the present work, are designed to produce sub-routines which may be amalgamated with large scale analysis schemes to ensure a uniformly high standard of element design.

It is becoming clear that an energy starved world cannot afford the luxury of excess structure weight, especially if that weight displaces useful payload as part of a vehicle structure. Optimisation techniques of the type described here, firmly based on practical engineering concepts, can play a useful role in promoting the more efficient deployment of increasingly scarce material resources.

Chapter 1

INTRODUCTION

General

Empirical stress-strain relations have been extensively applied to many problems of structural analysis Even though materials whose manufacture is tightly controlled will in practice vary significantly in this respect from point to point within a single piece (see for instance Butterworth [8]), there nevertheless exists a vital need to standardise the characterisation of behaviour in order to ensure a consistency of assumed performance between designers. This assumed standard may be revised as required, in the light of achieved performance, by the appropriate central authority.

The analyst is concerned primarily to forecast the behaviour of a given structure in terms of stiffness, strength and stability, etc. All of these properties are seriously eroded by the onset of plasticity which must therefore be accurately and realistically modelled in order that the necessary calculations will be reliable, thus verifying the structure to be safe under the specified loading.

From the point of view of initial design and optimisation, for which purpose the expected loads are assumed to be known, it is required to fix structural dimensions with maximum economy and guaranteed safety, and therefore for this purpose the precise characterisation of material properties is of no less importance. Since structural forms and dimensions will be varied in a systematic and continuous way in the quest for maximum efficiency, the expression of stress-strain properties in a continuous functional form as opposed, for instance, to a graphical presentation, becomes particularly advantageous.

The work presented here is concerned with the establishment of methods for the minimum weight design of structures for which stability considerations are important. Attention is confined to compression structures, and includes struts, isotropic flat plates, honeycomb sandwich plates, wide column surfaces, and cylindrical shells with axial wide-column type stiffening systems.

Throughout, the objective has been to devise optimisation methods which are as direct as possible, and which are based on a well established, reliable characterisation of buckling failure taking appropriate and realistic account of the effects of plasticity. Thus almost all of the relationships governing structural failure are drawn from other works. What is new is the way in which these relationships are inverted and adapted to the design and optimisation process, so that safe and efficient structures may be thereby devised to equilibrate loadings of given magnitude.

A number of authors have published significant papers on the subject of design for stability including Lagrange[9] Farrar[10], Shanley [11], Hoff [12], Gerard [13] and Keller [14] among many others. However, perhaps the most distinguished contributions in both depth and scope have been made by Cox[15,16,17] who has consistently demonstrated the very special, complex character of the design problem per se.

The essential features of any analysis of the buckling behaviour of a given structure are the load intensity at which buckling occurs, and the mode or deformed shape associated therewith. The most significant part of the answer is the load itself, but the mode is also important in the sense that if the mode is wrong, the associated load will be too high, i.e. unconservative. There is also a pictorial interest in mode shapes on behalf of the analyst, who needs to build up experience to enable him to make the informed guesses for application to other similar problems, which are useful in some methods of analysis. In the optimisation process, the detailed characteristic dimensions of the structure are varied, and this may significantly affect the character of the solution.

Thus in the case of the rectangular sandwich panel loaded in compression considered in chapter 4, both plasticity in the faceplates and transverse shear flexibility in the core will tend to reduce buckled wavelength, in extreme cases to a fraction of plate width.

Stress-strain functions

A number of authors have proposed empirical functions which may be used to describe the stress-strain behaviour of strain hardening materials, including Nadai[18], Ylinen[19] and Hsu and Bertels[20]. However by far the most successful formulation measured in terms of general usage has been that due to Ramberg and Osgood [21] who suggested the following relationship between uniaxial strain and stress f

$$\varepsilon = \frac{f}{E} + \alpha\left(\frac{f}{E}\right)^{n} \qquad \ldots (1)$$

Among the most important advantages of this expression are included simplicity of mathematical form enabling worthwhile analytical development, and the segregation of strain into elastic and plastic (i.e. irrecoverable) components.

Three parameters are required, E which is the ideal or initial plastic modulus, the exponent n and the coefficient α. For most common engineering metals, the exponent n takes a value in the range 10-30. Two extreme cases may be identified, when n = 1, equation (1) corresponds to linear elastic behaviour (with some modification to the meaning of E), and as $n \to \infty$ a representation of elastic-perfectly plastic behaviour is obtained.

The physical meaning of the coefficient α, which is usually a very large number perhaps of the prder 10^{50}, is less obvious.

However the transformation of equation (1) worked out in Appendix A in terms of the 0.2% proof stress f_2, is more amenable to interpretation, and offers many advantages from the point of view of computation.

A representative selection of stress-strain curves based on equation (1) is shown plotted in figure A1.

A frequently quoted version of the Ramberg Osgood equation is

$$\varepsilon = \frac{f}{E} + \frac{3}{7}\frac{f_r}{E}\left(\frac{f}{f_1}\right)^n \qquad \ldots (2)$$

The stress f_r is introduced which is the stress at which the secant modulus is reduced to 70% of the fully elastic value E.

The introduction of a totally artificial quantity of this sort may in the past have helped the slide rule operator somewhat, but otherwise has no merit is a modern context.

The transformation already mentioned, utilising the proof stress f_2 which is the upper limit to stress in compression imposed by many design authorities, proves to be entirely satisfactory especially in the derivation of the various moduli, etc. required in buckling analysis.

A further significant advantage of the present formulation accrues from the maintenance of homogeneity in the various functions in terms of the dimensionless stress f/E. This renders the algebraic treatment of the analysis comparatively straightforward and elegant, while effectively reducing the number of independent material parameters to two, which are here chosen to be f_2/E and n.

When a particular material is needed to illustrate the results obtained, values of $f_2/E = 0.005$ and $n = 15.0$ are used. These figures correspond with reasonable accuracy to the sort of aluminium alloy of medium strength widely used in aircraft construction (e.g. L73) and on this basis should therefore give a fairly direct impression of the physical significance of the examples shown.

Imperfections

Following the work of Van der Neut[22] and Thompson[23] , a great deal of attention has been recently directed towards the influence of small imperfections on the behaviour and hence performance of compression structures. It has been shown that quite small dimensional irregularities could in principle significantly erode the strength of compression structures of a wide variety of forms especially when dimensions are chosen so that different modes of instability are made to coincide. There is as yet little experimental evidence of the practical importance of these effects, and no case seems to be on record of a structure of major importance whose failure can be traced directly to this phenomenon. One major difficulty facing the designer who seeks to allow for imperfections, lies in the lack of statistical information relating

to the occurrence and magnitude of imperfections in real, practical structures and the way in which this data correlates with the variations in structural dimensions that the design and optimisation process contemplates.

Certain methods of analysis incorporated in the present text in effect already incorporate some allowance for imperfections. Thus in the case of column buckling the effects of plasticity on buckling load are expressed by using the tangent modulus E_t in place of the elastic modulus E in Euler's equation. This accords well with experimental observation and is widely accepted as a safe and reliable procedure by design authorities. In fact, it may be shown [38] that for real (imperfect) struts, the tangent modulus load is not correct, and may be either too high or too low, depending on the degree of imperfection. It seems to happen, however, that the magnitude of imperfection that actually occurs in real structures must be just about that value which allows the tangent modulus theory to give good answers.

A similar phenomenon seems to have occurred in the analysis of buckling of thin rectangular plates including the effects of plasticity. Illyushin [24] based his analysis on the flow theory of plasticity, but predicted buckling loads which were significatly higher than those observed in the laboratory. On the other hand, Stowell [25] using the less respectable deformation theory of plasticity derived solutions which correlate very well with the experiment. The implication is that small imperfections in practice reduce buckling loads sufficiently to bring them in line with the Stowell theory. This idea is substantiated by Hutchinson and Budiansky [26], who have analysed the buckling of cruciform sections by both plasticity theories, also including explicitly the effects of imperfections to show that the differences between the theories match the effects of feasible imperfection magnitudes.

In the present work, the optimisation of struts is based on the tangent modulus theory, and that of plates on Stowell's analysis in the knowledge that some account is thereby being taken of imperfection effects in real structures, and that the resulting designs will emerge as safe after checking by these widely accepted engineering procedures.

In chapter 8, a direct contribution is made to the effects of imperfection on the optimisation of structures when the design of an axially loaded tower with corrugated walls is considered. The structure is assumed to be perfectly manufactured in every way except that the walls contain imperfections of the Euler mode form. It is found possible to incorporate these effects directly into the design process, and to obtain optimum dimensions for the entire structure. The example is used to contrast the sensitivity of tower strength to imperfections for a given tower weight, with the sensitivity of tower weight to the same effects for given tower strength.

Computation

The analysis reported here is geared to the possibility of producing directly useful numerical results by digital computation. A significant number of Fortran IV programmes have been written and

developed, and these are reported in detail in appropriate appendices, including information which will allow the preparation and interpretation of input and output data.

The procedures involved are mostly fairly standard methods of numerical analysis including interpolation, the solution of high order polynomials, and the determination of the minimum values of given functions.

The policy throughout has been to maintain a non-dimensional form for the analyses, and in the event this has led to natural and efficient procedures with the natural benefit of great generality.

All programmes have been written so that they may conveniently be used by remote access terminal.

Chapter 2

THE STRUT

General

The design of struts provides an appropriate starting point to a study of compression structures. Struts are generally simple in form and have structural properties which are comparatively well understood and readily characterised.

It is required to design a structure which will equilibrate without failure a pair of opposing coaxial compressive forces P of given magnitude applied a distance L apart. The structure will have the character of a beam, in that it will lie essentially along the centre line joining the applied loads, and will require significant axial, bending, torsional and transverse shear stiffnesses.

The structure will be fabricated from a homogenous isotropic material whose unaxial stress-strain properties may be adequately characterised by the Ramberg-Osgood[21] law. Boundary conditions are taken to be simple supports at each point of load application, with freedom of rotation about all axes contained within the plane perpendicular to the strut axis at those places.

Perhaps the most thorough text available on this subject is that due to Cox[17] who considered elastic designs utilising a variety of cross sectional forms. Some of the results obtained by him have been incorporated in this text, although the explicit incorporation of plasticity effects naturally leads to significant changes in the style of presentation. The structures considered are assumed to be perfect in the sense that individual dimensions are assumed to have precisely the values ascribed to them, nominally straight lines are truly straight, and flat surfaces are indeed flat. This is not to imply that some degree of imperfection is not already accounted for in the relationships used to characterise buckling behaviour. These relationships are drawn from accepted engineering practice and as such refer to the real, as opposed to the ideal world.

However imperfections of the sort considered by Van der Neut,[22] Thompson and Lewis,[27] Cox and Grayley,[28] and Crawford and Hedgepeth[29] are not explicitly included.

The range of cross sectional forms considered here is wide but not exhaustive. However most of the configurations which might be considered in practical circumstances are included, at least by implication.

Spanwise variations

The problem of how to distribute structural material along the length of the strut so that either for a given total volume of material the buckling load is maximised, or alternatively (and equivalently), that a minimum volume of material is utilised to achieve a given buckling load, invites a formulation utilising the notation of the calculus of variations. A number of authors have achieved significant results in this area. The form and character of any solution will depend strongly on the relationship assumed to connect the two essential structural properties concerned, namely cross section area, and second moment of area.

The case that might be considered first is that for which all sections remain geometrically similar, so that second moment of area I is related to area A by an expression of the form

$$I = \beta A^2 \qquad \ldots (3)$$

where the coefficient β contains the dimensionless ratios required to describe the cross section shape, and will be discussed in detail under a later heading.

The volume of elastic material V required so that Euler buckling shall not occur under a load P for a strut of this kind is given by

$$\frac{V}{L^3} = \frac{\gamma_1}{\beta^{\frac{1}{2}}} \cdot \frac{1}{\pi}\left[\frac{P}{EL^2}\right]^{\frac{1}{2}} \qquad \ldots (4)$$

The numerical quantity γ_1 is the factor by which the volume required is changed relative to that of a prismatic strut of the same buckling strength. Keller[14] showed the minimum value of γ_1 to be $\sqrt{(3/4)}$ which is achieved when material is distributed along the strut according to the following relations

$$\left.\begin{aligned} \frac{A}{L^2} &= \frac{4}{3}\frac{V}{L^3}\sin^2\theta \\ \frac{x}{L} &= \frac{1}{\pi}(\theta - \frac{1}{2}\sin 2\theta) \end{aligned}\right\} \qquad \ldots (5)$$

where x = distance along strut axis from one end

θ = a parameter varying in the range $0 \leq \theta \leq \pi$

Thus the maximum amount of material that can be saved by varying a section of this kind is about 13.4%.

Prager and Taylor [30] considered the case of a linear relationship between I and A which would correspond, for instance, to a sandwich strut of constant depth h having thin faceplates each of area (A/2) supported by a weightless core which is rigid under transverse shear forces but infinitely flexible under axial stresses.

The volume of active material required for such a strut is given by

$$\frac{V}{L^3} = \gamma_2 \cdot \frac{4}{\pi^2} \cdot \left(\frac{L}{h}\right)^2 \left[\frac{P}{EL^2}\right] \qquad \ldots (6)$$

where γ_2 is volume relative to that of a constant section strut of the same strength.

Prager and Taylor[30] showed the minimum value of γ_2 to be $(\pi^2/12)$ for which faceplate material must be distributed according to

$$\frac{A}{L^2} = 6\,\frac{V}{L^3} \cdot \frac{x}{L}\left(1 - \frac{x}{L}\right) \qquad \ldots (7)$$

The maximum amount of material that can be saved in this case is therefore about 17.7%

A problem of this class was investigated by Venkayya, Khot and Berke[31]. The distribution of material along the strut was represented by 10 equal length uniform elements, and the optimum distribution of material between these elements was obtained by a numerical search procedure. The results obtained approximate closely the ideal distribution given by (7) with a total volume about 2.5% higher than the ideal.

The ideal distributions specified above, which are shown plotted in Figure 1 , have the common feature of zero area and hence infinite stress at each pinned end. Prager and Taylor[30] have accounted for this by introducing a minimum size constraint for which they have given a general solution.

Solid section

Equations 5 and 7 are based on the elastic design of struts whose cross sections are solid, singly connected, and with convex profiles. These provisos effectively eliminate the possibility of all forms of instability other than Euler buckling.

Keller[14] reports that the ideal cross section of this sort will have the property of equal second moment of area about all axes. Thus an appropriately representative range of designs is provided by regular polygons of m sides, where

$$3 \leq m \leq \infty$$

which includes the triangle and circle as extreme cases.

Plasticity will be accounted for by replacing the elastic modulus E by the tangent modulus E_t, which is accepted engineering practice accounting as it does for some small degree of imperfection. E_t may be readily expressed as a function of applied stress as is shown in Appendix 1.

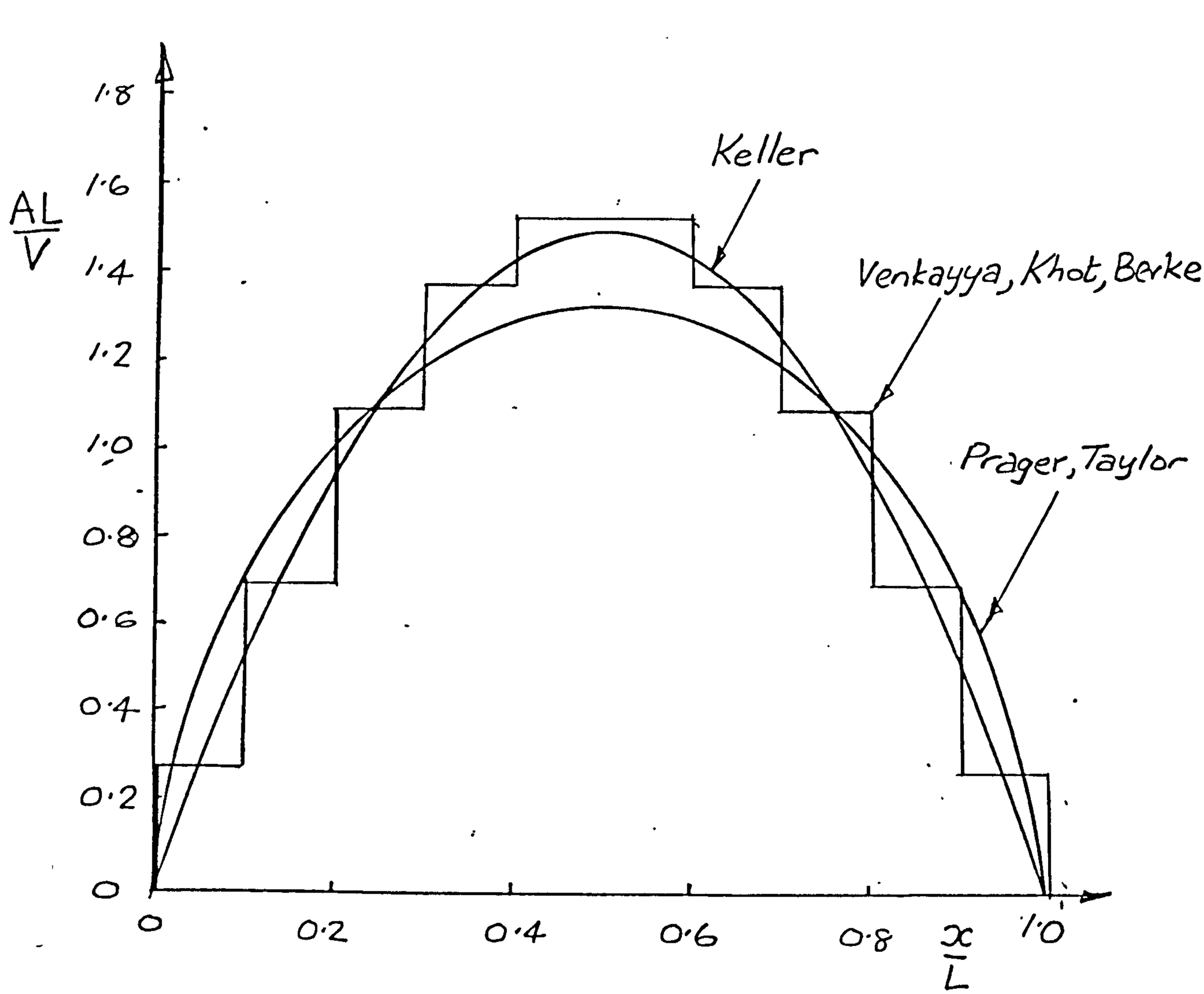

Figure 1. DISTRIBUTIONS OF MATERIAL FOR OPTIMUM PIN-ENDED STRUTS

Euler's equation therefore becomes

$$P = \frac{\pi^2 E_t I}{L^2}$$

which for design purposes, may be expressed in terms of stress using equation (A3) from Appendix A which process gives

$$\frac{E}{E_t} = 1 + n\phi$$

where $$\phi = \alpha\left(\frac{f}{E}\right)^{n-1}$$

so that $$\frac{\beta\pi^2 P}{EL^2} = \left(\frac{f}{E}\right)^2\left[1 + n\phi\right] \qquad \ldots (8)$$

The right hand side of (9) is a function of stress alone, so that for any given material a data sheet may be plotted which may be read directly to give design stress values for any given combination of load, length and cross section shape parameter β. This is illustrated in figure (2) for a typical aluminium alloy type material.

For the regular polygon with m sides, section properties are given by the following equations.

$$\left.\begin{aligned} A &= m R^2 \tan\left(\frac{\pi}{m}\right) \\ I &= \frac{m}{12} \cdot R^4 \tan\left(\frac{\pi}{m}\right)\left[2 + \sec^2\left(\frac{\pi}{m}\right)\right] \end{aligned}\right\} \qquad \ldots (9)$$

so that, from (3), the shape parameter is given by

$$\beta = \frac{I}{A^2} = \frac{1}{12m}\left[\frac{2 + \sec^2\left(\frac{\pi}{m}\right)}{\tan\left(\frac{\pi}{m}\right)}\right] \qquad \ldots (10)$$

Note that for the circle ($m = \infty$), $\beta = \frac{1}{4\pi}$

Stress is always a direct measure of efficiency, so that for elastic designs ($\phi = 0$), equation (8) gives $f\alpha\beta^{\frac{1}{2}}$ and the various possible shapes may be ranked quantitatively as shown below

Merit factors for solid elastic polygonal struts

m	3	4	5	6	∞
$\beta^{\frac{1}{2}}$	0.3102	0.2887	0.2845	0.2832	0.2821

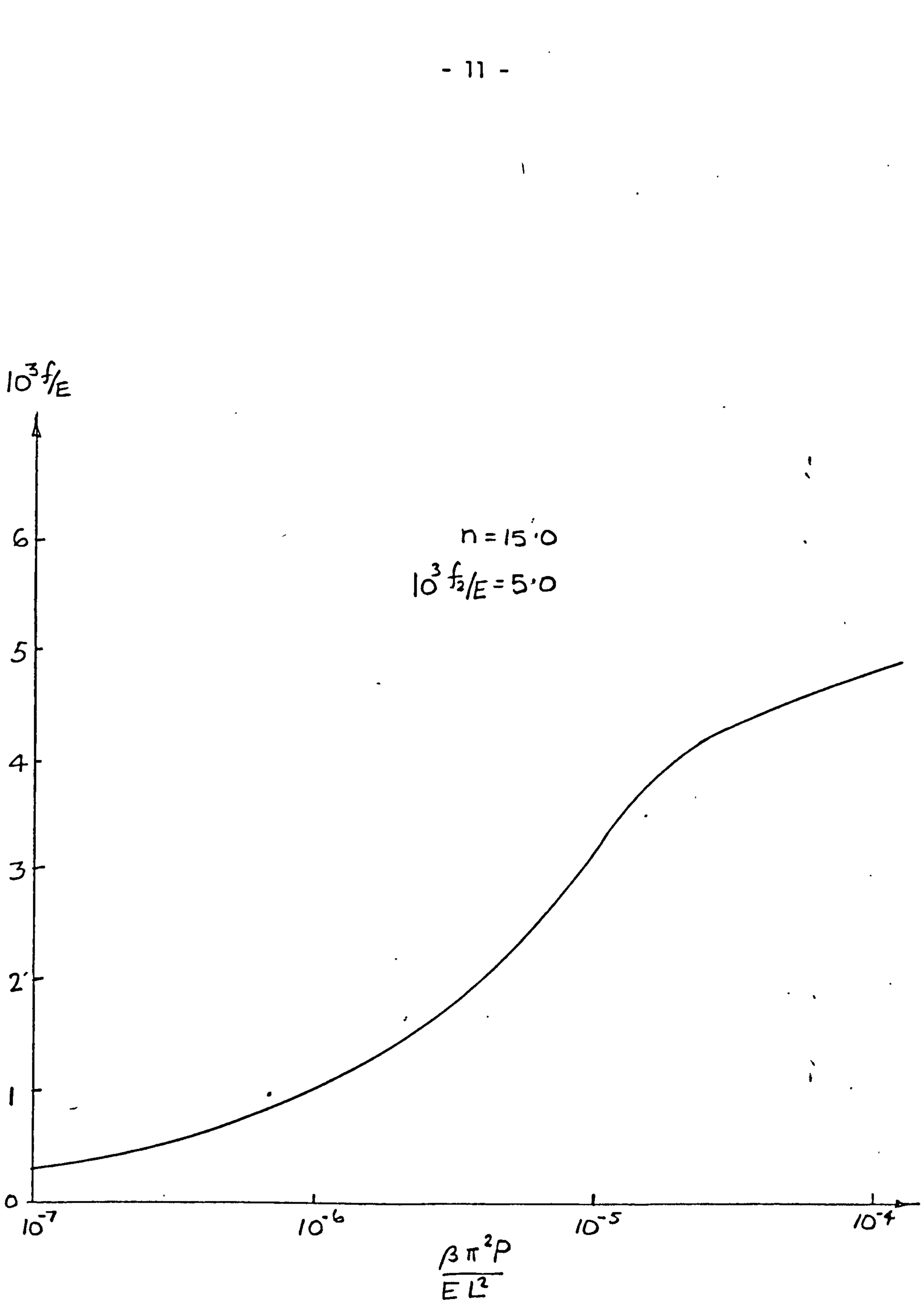

Figure 2. OPTIMUM STRESS FOR SOLID POLYGONAL STRUTS.

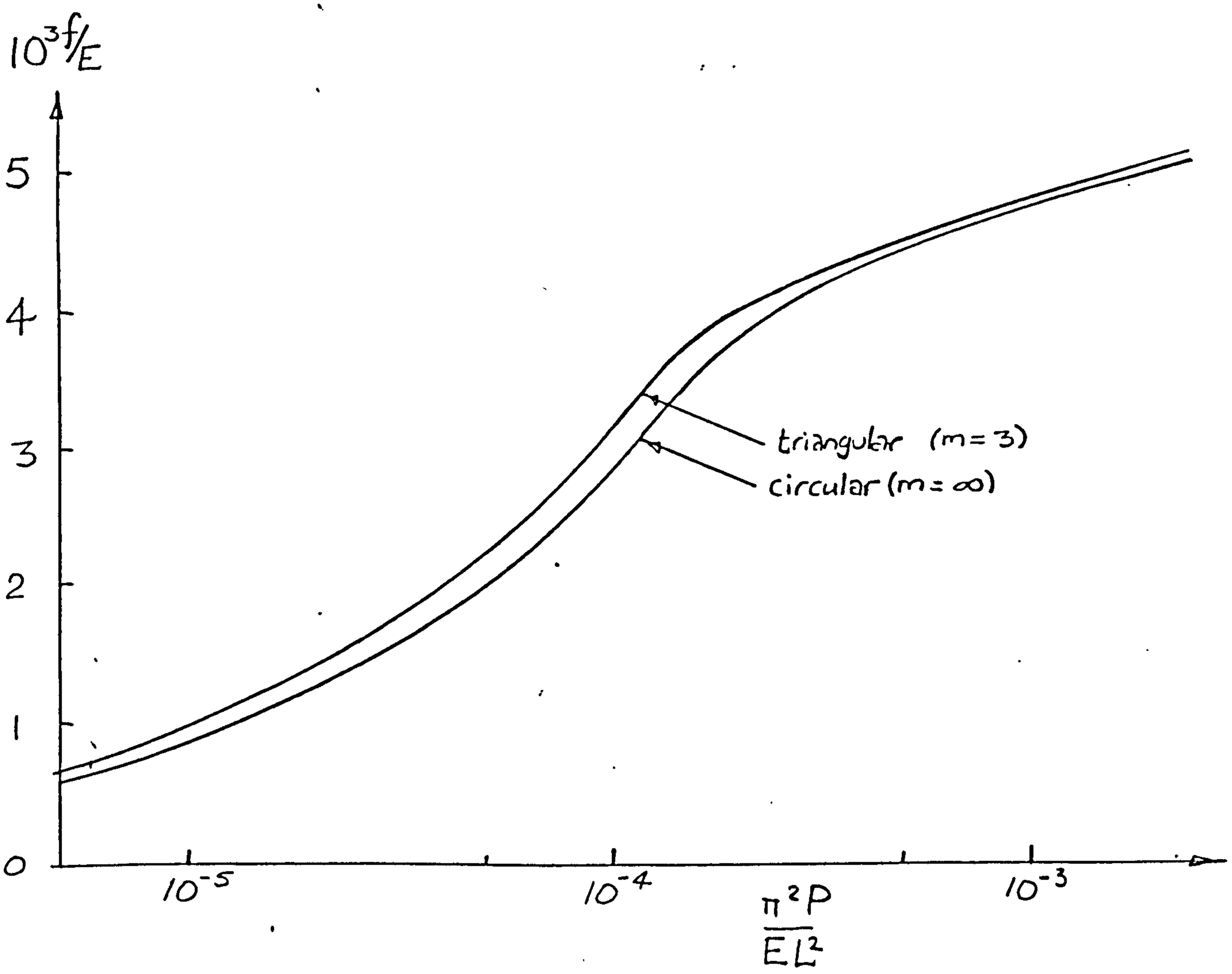

Figure 3. EFFECT OF POLYGON ORDER ON OPTIMUM STRESS FOR SOLID POLYGON STRUTS

The triangular section struts require some 10% less material than the circle, but the other intermediate sections are at most 2.5% lighter.

The intervention of plasticity at higher load intensities has the effect of smoothing the differences between sections, as may be seen from figure 3.

Thin walled multi-flat tubes

Three orders of dimension may be identified in the geometry of the thin walled multi-flat tube, each having an individual significance in the description of buckling behaviour. These groups are exemplified by the characteristic leading dimensions strut length L, flat width b, and wall thickness t. The groups are separated from each other by at least one order of magnitude, on which basis the following relationships governing buckling behaviour may be written.

Euler buckling:

$$\frac{f}{E} \leq K_1 \cdot \frac{E_t}{E} \left(\frac{b}{L}\right)^2 \qquad \ldots (11)$$

Local buckling:

$$\frac{f}{E} \leq K_2 \cdot \frac{E_t}{E} \cdot \left(\frac{t}{L}\right)^2 \left(\frac{L}{b}\right)^2 \qquad \ldots (12)$$

Equilibrium:

$$\frac{f}{E} = K_3 \cdot \left(\frac{P}{EL^2}\right) \cdot \left(\frac{L}{t}\right) \cdot \left(\frac{L}{b}\right) \qquad \ldots (13)$$

The use of tangent modulus in equation(12) may be justified on the basis of accepted current engineering practice. For local buckling Stowell[25] has analysed a wide range of boundary conditions for plates in compression including the effects of plasticity. Although the theory of plasticity used is imperfect being based on the deformation as opposed to the more correct flow theory, his answers nevertheless accord well with experimental observation. This apparent paradox maybe accounted for by the presence of small imperfections which would reduce buckling strength towards the lower values predicted by deformation theory. Indeed detailed analysis by Hutchinson[26] has shown this to be precisely so in the case of cruciform struts buckling by torsional instability at stress levels for which plasticity is significant. Thus Stowell's results may be accepted for engineering purposes on this basis.

A survey of his results shows that the tangent modulus is in effect a lower bound to all the cases he has considered, and since as the design proceeds the boundary conditions for each flat will be varying themselves, a safe and sensible course is to assume the tangent modulus throughout. A not insignificant benefit of this assumption is

the comparative simplicity of the resulting analysis.

The coefficients K_1, K_2 and K_3 are functions of the dimensionless ratios describing the detailed layout of the cross section. Thus

$$K_1 = \pi^2 \frac{I}{Ab^2} \qquad \ldots (14)$$

which may be written down explicitly for any given class of sections, and will be independent of the dimensions b and t since for thin walled sections

$$I \alpha tb^3$$

and $$A \alpha tb$$

The local buckling coefficient K_2 may be expressed explicitly only in a few rare cases since its value depends on a detailed, usually numerical evaluation of local buckling with the appropriate boundary conditions of the sort to be found in the ESDU data sheets[32]. However appropriate results are widely available [33, 34] from a number of sources for various structural forms.

The equilibrium coefficient is simply given by

$$K_3 = \frac{tb}{A} \qquad \ldots (15)$$

and may always be written explicitly.

On the understanding that the dimensionless ratios relating the quantities in each group to the leading dimensions in that group may be separately varied at a later stage, the coefficients $K_{1,2,3}$ may be regarded as fixed and an optimum solution to (11), (12) and (13) sought.

We therefore require the values of the leading variables (b/L) and (t/L) so that the relations (11), (12) and (13) are satisfied in such a way that the stress (f/E) is maximised.

Again the Ramberg-Osgood relationship for tangent modulus may be used to establish the optimum solution.

Consideration is given first to the satisfaction of the Euler buckling criterion.

From (11) and (13), for a structure on the point of Euler buckling

$$\frac{b}{L} = \frac{1}{K_1^{\frac{1}{2}}} \left[\frac{f}{E} \cdot (1 + n\phi)\right]^{\frac{1}{2}} \qquad \ldots (16)$$

$$\frac{t}{L} = K_1^{\frac{1}{2}} K_3 \left(\frac{P}{EL^2}\right) \left[\left(\frac{f}{E}\right)^3 (1 + n\phi)\right]^{-\frac{1}{2}} \qquad \ldots (17)$$

These relations allow the Euler failure boundary to be plotted in (b/L)~(t/L) space (see figure 4), but it is of more immediate significance that equation(16)shows (b/L) to be a monotonically increasing function of stress, which indicates that from the point of view of this criterion alone, (b/L) should be as large as possible (see figure 5).

From equations (12) and (13), and for local buckling

$$\frac{b}{L} = K_2^{\frac{1}{4}} K_3^{\frac{1}{2}} \left(\frac{P}{EL^2}\right)^{\frac{1}{2}} \left[\frac{1}{\left(\frac{f}{E}\right)^3 (1 + n\phi)}\right]^{\frac{1}{4}} \quad \ldots (18)$$

$$\frac{t}{L} = \left(\frac{K_3^2}{K_2}\right)^{\frac{1}{4}} \cdot \left(\frac{P}{EL^2}\right)^{\frac{1}{2}} \left[\frac{1 + n\phi}{K_2 (f/E)}\right]^{\frac{1}{4}} \quad \ldots (19)$$

Equation (18) shows that (b/L) is a monotonically decreasing function of stress for this criterion, indicating that optimum local buckling performance requires (b/L) to be unconditionally as small as possible (see figure 6 for example). Thus equations (16) and (18) taken together demonstrate conclusively that the minimum weight design will have coincident modes of buckling even when plasticity effects are explicitly included.

The ideal optimum design may now be identified by the establishment of (11) and (12) as equations, giving finally

$$\left[K_1^2 K_2 K_3^2\right]^{\frac{1}{2}} \frac{P}{EL^2} = \left(\frac{f}{E}\right)^{\frac{5}{2}} (1 + n\phi)^{\frac{3}{2}} \quad \ldots (20)$$

$$K_1^{\frac{1}{2}} \cdot \frac{b}{L} = \left(\frac{f}{E}\right)^{\frac{1}{2}} (1 + n\phi)^{\frac{1}{2}} \quad \ldots (21)$$

$$(K_1 K_2)^{\frac{1}{2}} \cdot \frac{t}{L} = \left(\frac{f}{E}\right) (1 + n\phi) \quad \ldots (22)$$

These design functions are shown plotted in figure(7) for a typical material.

From (20) the best shape of design is that for which the quantity $K_1^2 K_2 K_3^2$ is a maximum. For elastic designs ($\phi = 0$) optimum design stress is given by

$$\frac{f}{E} = \left[K_1^2 K_2 K_3^2\right]^{\frac{1}{5}} \left[\frac{P}{EL^2}\right]^{\frac{2}{5}}$$

$$= F \left[\frac{P}{EL^2}\right]^{\frac{2}{5}}$$

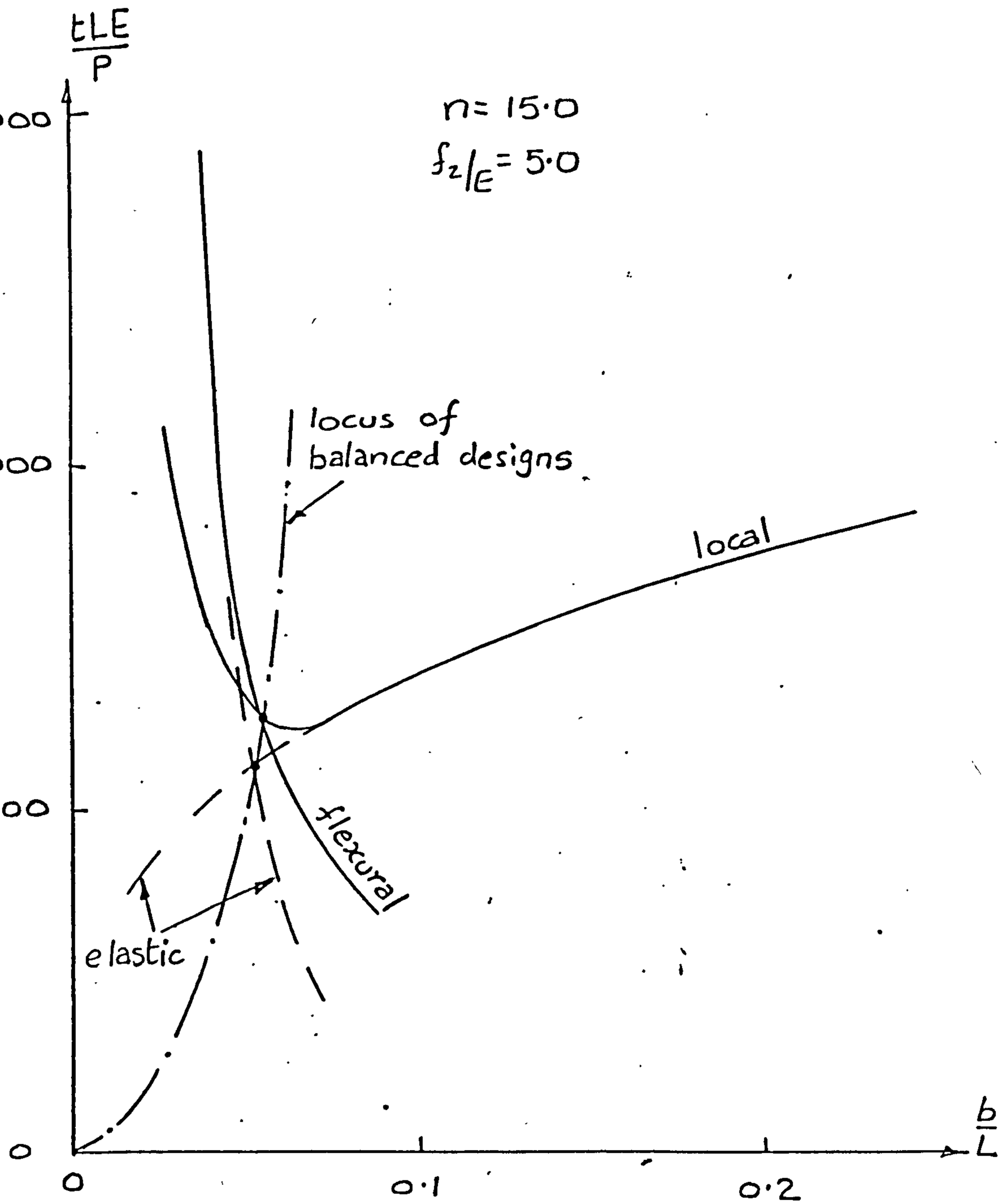

Figure 4. DESIGN SPACE WITH PLASTICITY FOR THIN-WALLED MULTI-FLAT TUBULAR STRUTS.

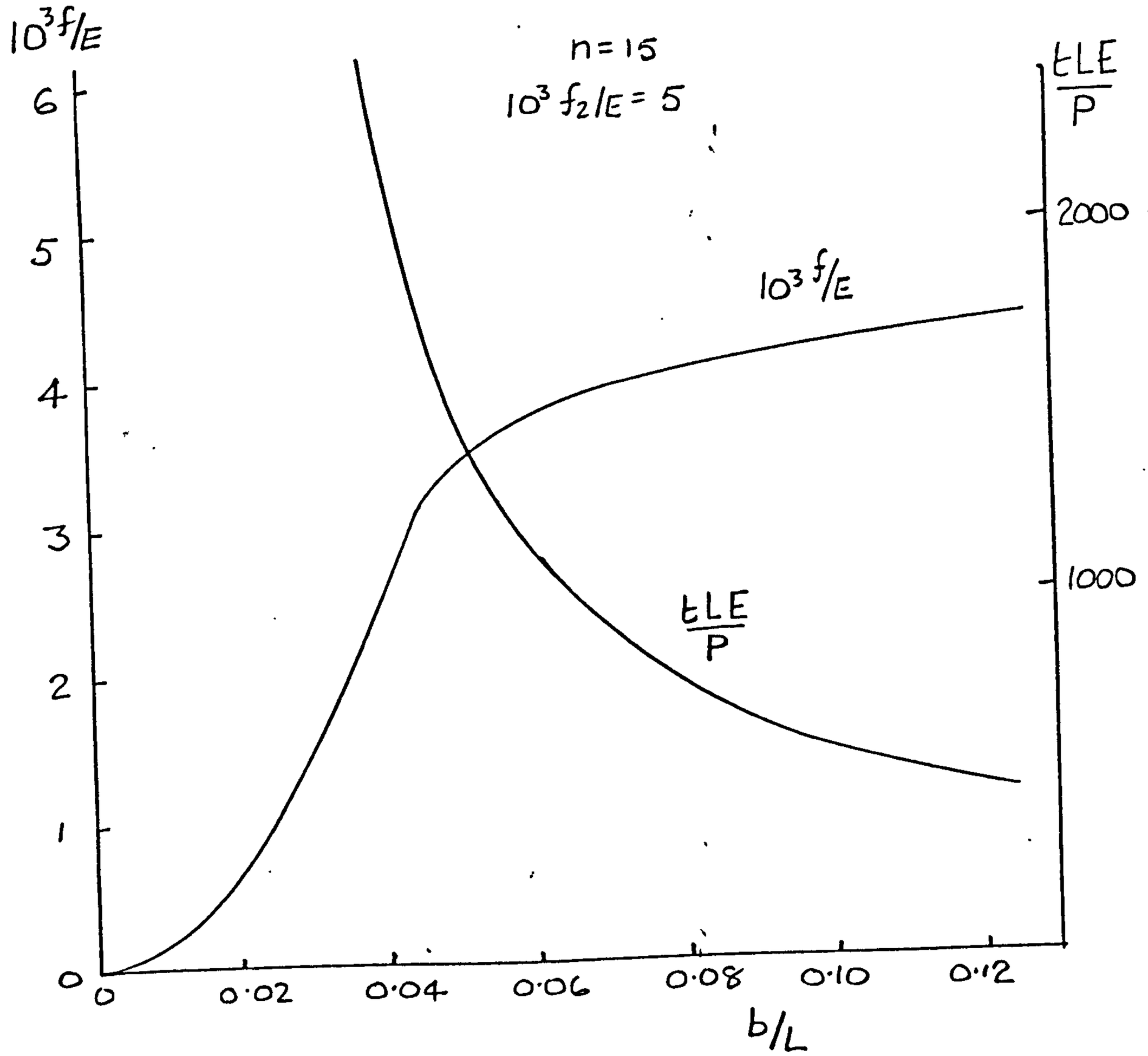

Figure 5. EULER BUCKLING CRITERION FOR THIN-WALLED POLYGONAL STRUTS.

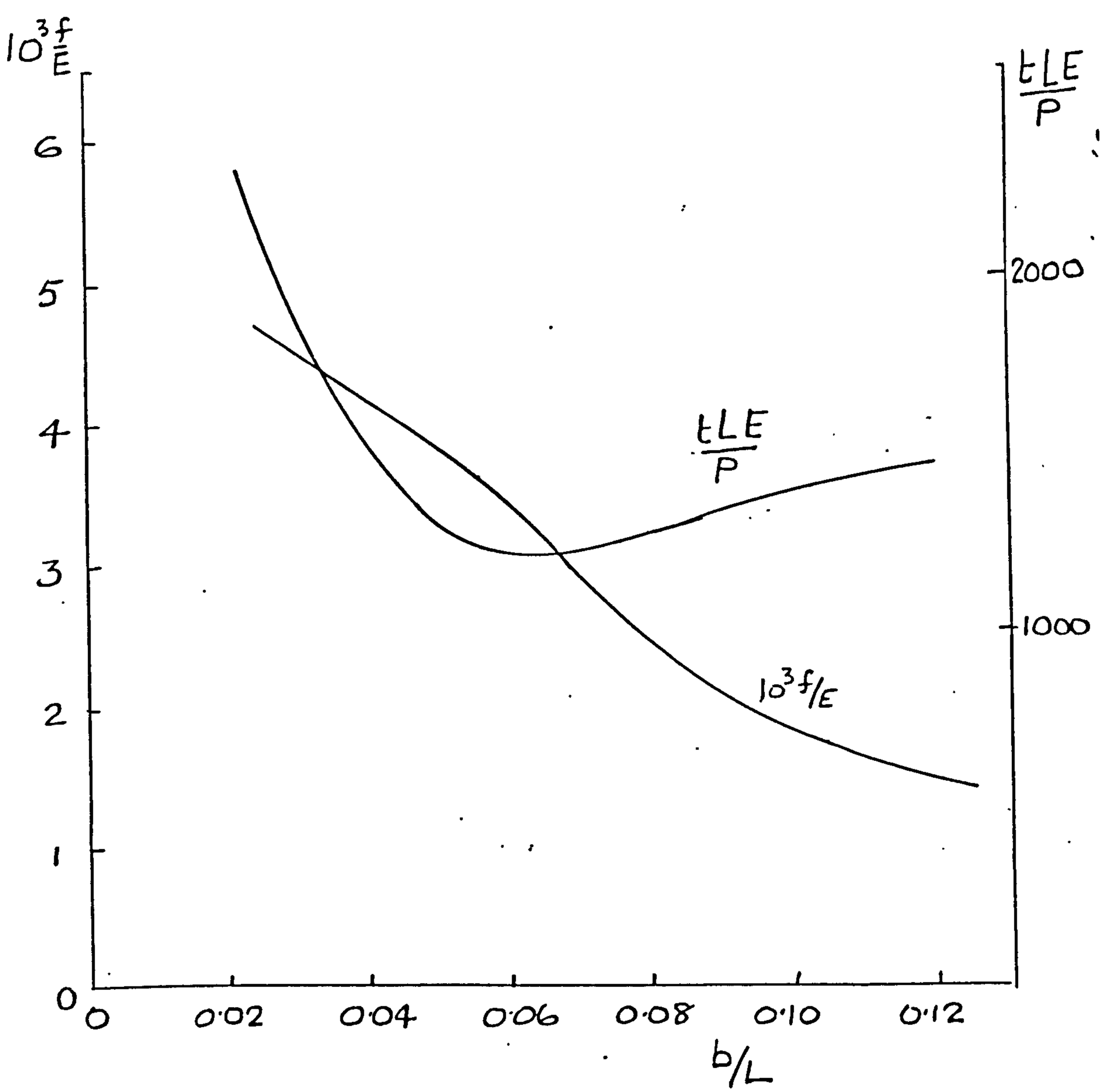

Figure 6. LOCAL BUCKLING CRITERION FOR THIN-WALLED POLYGONAL STRUTS

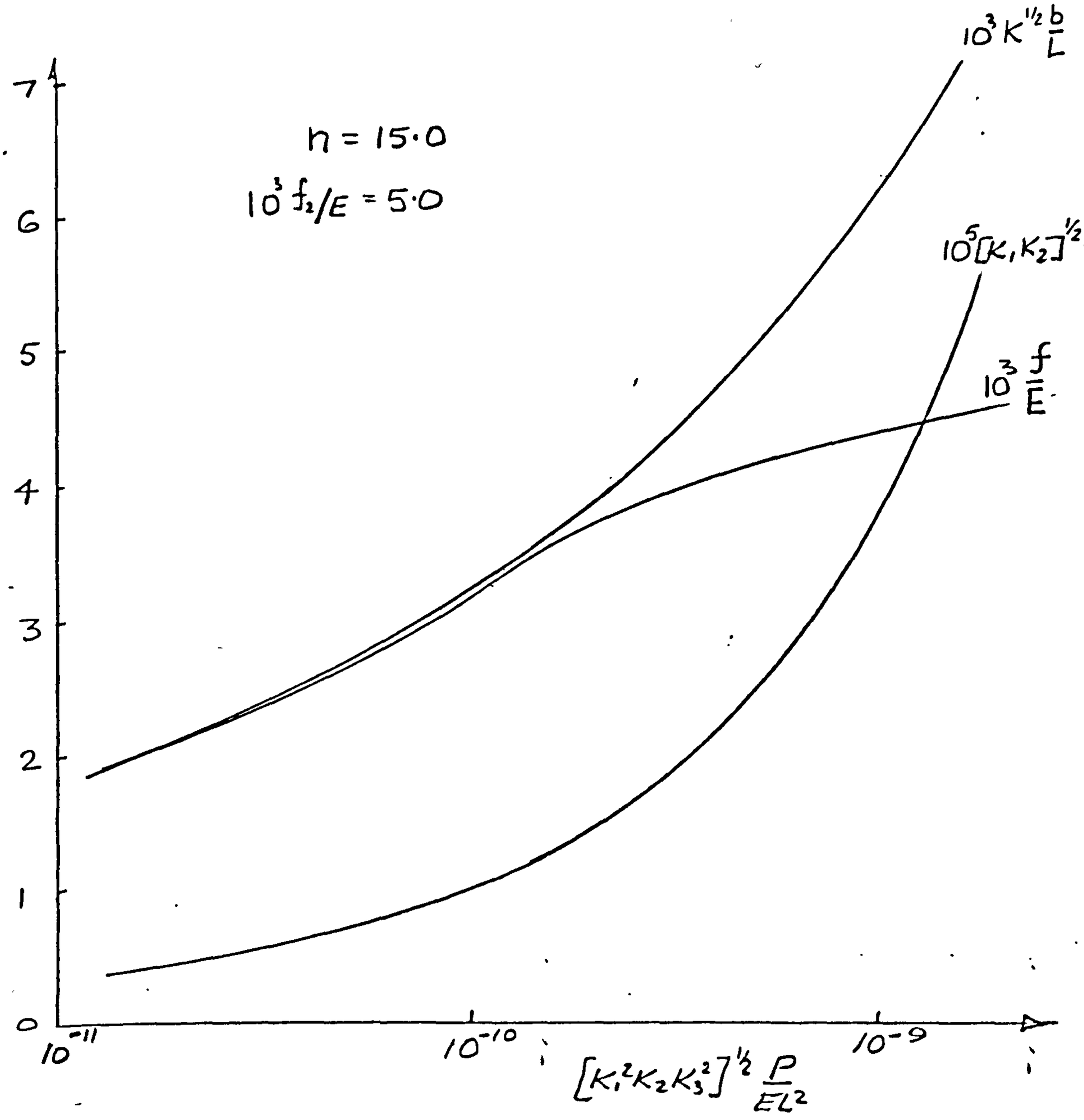

Figure 7. DESIGN DATA FOR THIN-WALLED POLYGONAL TUBES

For the regular polygon

$$I = \frac{nb^3t}{24} \frac{\left[3 + \tan^2\frac{\pi}{n}\right]}{\tan^2\frac{\pi}{n}}$$

$$A = nbt$$

so that from (14) and (15)

$$K_1 = \frac{\pi^2}{24} \frac{\left[3 + \tan^2\frac{\pi}{n}\right]}{\tan^2\frac{\pi}{n}}$$

$$K_3 = \frac{1}{n}$$

The values of K_2 given by Cox [17] may now be utilised to determine the coefficient : F for each regular polygon shape.

n	3	4	5	6	7	8	9	10
K_1	.823	1.645	2.748	4.112	5.731	7.602	9.724	12.097
K_2	4.31	3.62	3.87	3.62	3.76	3.62	3.69	3.62
F	.798	.907	1.032	1.112	1.203	1.267	1.339	1.396

Efficiency is seen to increase with the number of polygon sides. However, according to Cox [17], the local buckling analysis becomes unreliable when n > 12, since movement of the vertices in the buckling mode must be considered, leading to shell-like behaviour.

It may be that the optimum stress indicated by equation (20) is higher than some pre-specified allowable maximum value f_t.

In this case. although the efficiency of the strut is now invariant in weight terms, the designer has some freedom of choice in the dimensions. This freedom is probably best exercised by introducing factors of safety r_1, r_2 for each mode of buckling. These factors will in general be different, however for the present analysis it will be assumed that $r_1=r_2=r$, giving a balanced design. Thus the design equations become

$$r\left(\frac{f_t}{E}\right) = K_1 \cdot \frac{E_t^*}{E}\left(\frac{b}{L}\right)^2 \quad \ldots (23)$$

$$r\left(\frac{f_t}{E}\right) = K_2 \cdot \frac{E_t^*}{E}\left(\frac{t}{L}\right)^2\left(\frac{L}{b}\right)^2 \quad \ldots (24)$$

$$\frac{f_t}{E} = K_3 \cdot \left(\frac{P}{EL^2}\right)\left(\frac{L}{t}\right)\left(\frac{L}{b}\right) \quad \ldots (25)$$

where the tangent modulus E_t^* must be calculated at the factored stress

$$f^* = rf_t$$

The transition value of endload intensity P_t is found from equation (20) to be

$$\frac{P_t}{EL^2} = \frac{\left(\frac{f_t}{E}\right)^{\frac{5}{2}} (1 + n\phi_t)^{\frac{3}{2}}}{(K_1^2 K_2 K_3^2)^{\frac{1}{2}}} \qquad \ldots (26)$$

So equations (23), (24), and (25) hold when $P \geq P_t$, and these can then be solved to give structural dimensions in the following form.

$$\left.\begin{aligned} \frac{t}{L} &= \left[\frac{K_3^4 K_1}{K_2}\right]^{\frac{1}{6}} \left[\frac{P}{f_t L^2}\right]^{\frac{2}{3}} \\ \frac{b}{L} &= \left[\frac{K_3^2 K_2}{K_1}\right]^{\frac{1}{6}} \left[\frac{P}{f_t L^2}\right]^{\frac{1}{3}} \end{aligned}\right\} \qquad \ldots (27)$$

Note that for all balanced designs, including the ideal optimum, the following relationship holds (from (23) and (24))

$$\frac{b}{L} = \left(\frac{K_2}{K_1}\right)^{\frac{1}{4}} \left(\frac{t}{L}\right)^{\frac{1}{2}} \qquad \ldots (28)$$

The reserve factor r is given in implicit form in terms of the design endload by the following equation

$$\frac{P}{P_t} = \left[\frac{(1 + n\phi^*)\left(\frac{f^*}{E}\right)}{(1 + n\phi_t)\left(\frac{f_t}{E}\right)}\right]^{\frac{3}{2}} \qquad \ldots (29)$$

where the stress function $\phi^* = \alpha\left(\frac{f^*}{E}\right)^{n-1} = \alpha\left(\frac{rf_t}{E}\right)^{n-1}$

This relationship is shown plotted in figure 9 for a typical material.

The locus of balanced designs is also shown in the typical design space plotted in figure 8 with the aid of equations (16), (17), (18) and (19), which may be used to visualise directly the effects on the design of imposing dimensional constraints on the quantities t and b, enabling an appropriate analytical strategy to be devised.

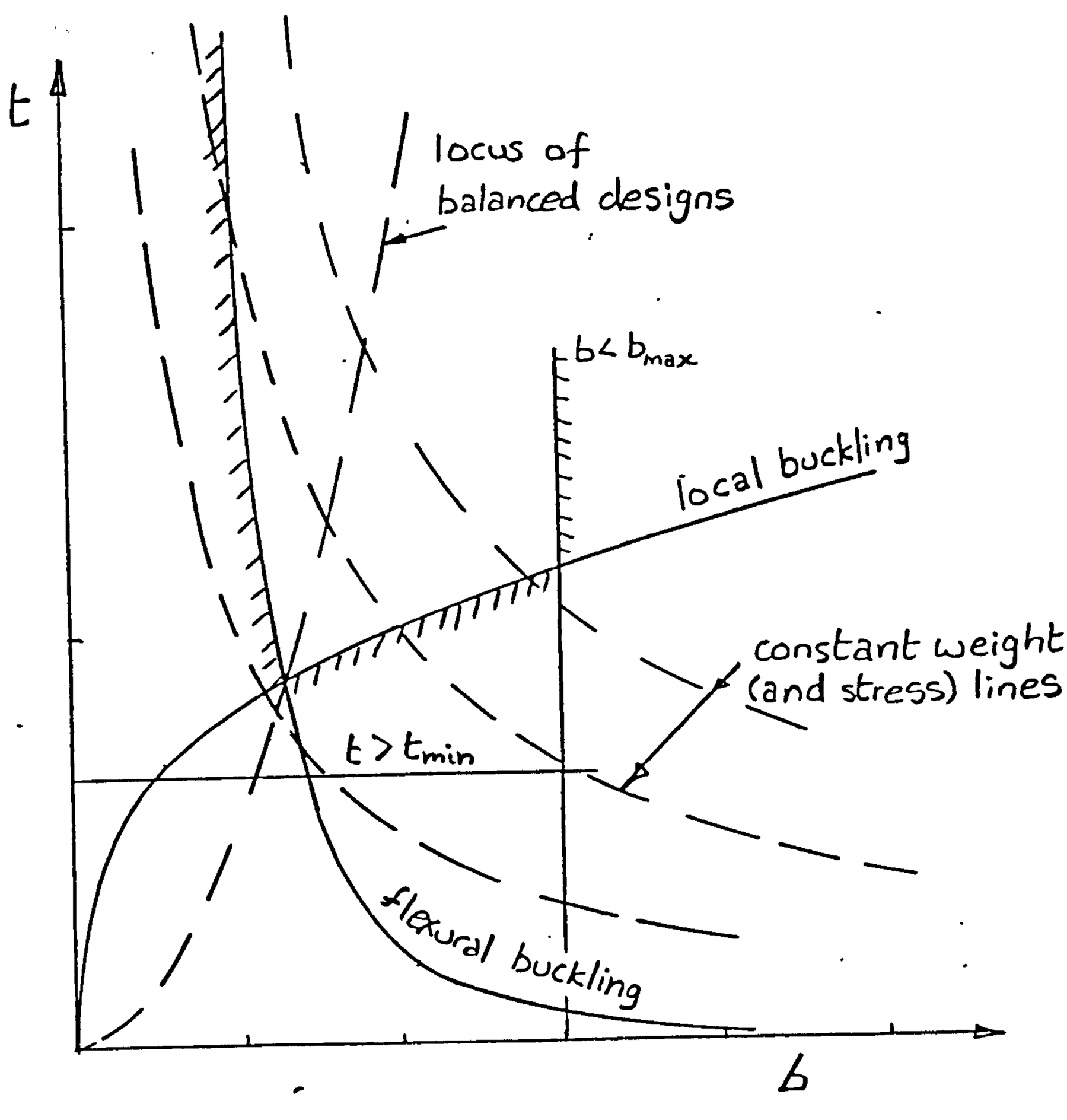

Figure 8. ELASTIC DESIGN SPACE FOR THIN-WALLED POLYGONAL TUBES WITH CONSTRAINTS.

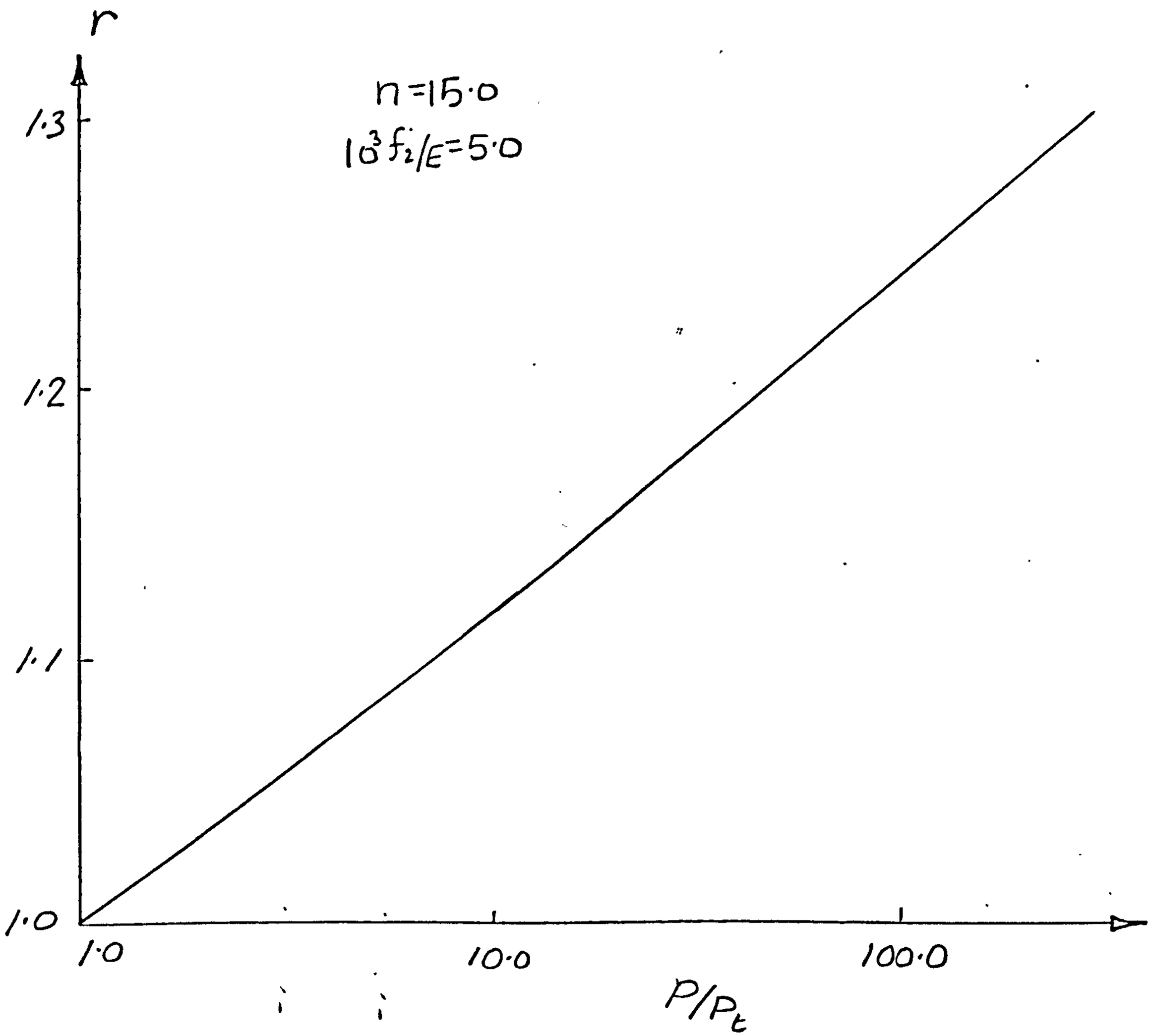

Figure 9. RESERVE FACTORS FOR MAXIMUM STRESS CONSTRAINED THIN-WALLED POLYGONAL TUBES.

Round tubes

In strictly geometric terms, the round tube is a regular polygon with an infinite number of sides.

However, from the point of view of structural behaviour there are significant differences between the local buckling of the round tube and that of the lower order polygons as mentioned in the previous section. A quite different relationship is required to characterise short wave or local buckling and Timoshenko and Gere [35] give

$$\frac{f}{E} = K_s \left(\frac{E_t}{E}\right)^{\frac{1}{2}} \cdot \left(\frac{t}{L}\right) \cdot \left(\frac{L}{D}\right) \qquad \ldots (30)$$

where D = tube mean diameter

t = wall thickness

The ideal value of the buckling coefficient K_s is about 1.12, but the inevitable existence of small imperfections even in carefully manufactured tubes may reduce this to as low as 0.25.

The Euler buckling stress is

$$\frac{f}{E} = \frac{\pi^2}{8} \cdot \frac{E_t}{E} \cdot \left(\frac{D}{L}\right)^2 \qquad \ldots (31)$$

and equilibrium requires that

$$\frac{f}{E} = \frac{1}{\pi} \cdot \left(\frac{L}{D}\right) \cdot \left(\frac{L}{t}\right) \cdot \left(\frac{P}{EL^2}\right) \qquad \ldots (32)$$

The requirement that the achievement of maximum stress requires coincident buckling modes may be confirmed by noting first, from (30), and (32), that the tube diameter required to resist Euler buckling is

$$\frac{D}{L} = \left[\frac{8}{\pi^2} \cdot \frac{f}{E}(1 + n\phi)\right]^{\frac{1}{2}} \qquad \ldots (33)$$

which is a monotonically increasing function of stress, whereas for local buckling, (31) and (32) give

$$\frac{D}{L} = \left[K_s \frac{P}{EL^2}\right]^{\frac{1}{2}} \frac{1}{\left(\frac{f}{E}\right)(1 + n\phi)^{\frac{1}{4}}} \qquad \ldots (34)$$

which decreases monotonically with stress. Since the achievable stress is the lower envelope of these two functions, they must coincide to obtain the maximum possible stress.

Equations (30), (31) and (32) may on that basis be solved for the relevant design variables, giving the following results

$$\frac{\pi}{8} K_s \left(\frac{P}{EL^2}\right) = \left(\frac{f}{E}\right)^3 (1 + n\phi)^{\frac{3}{2}} \quad \ldots (35)$$

$$\frac{\pi}{\sqrt{8}} \cdot \left(\frac{D}{L}\right) = \left(\frac{f}{E}\right)^{\frac{1}{2}} (1 + n\phi)^{\frac{1}{2}} \quad \ldots (36)$$

$$\frac{\pi}{\sqrt{8}} K_s \left(\frac{t}{L}\right) = \left(\frac{f}{E}\right)^{\frac{3}{2}} (1 + n\phi) \quad \ldots (37)$$

These functions are shown plotted for a typical material in figure 10 It is of interest to note from (35), (36) and (37) that the optimum wall thickness to diameter ratio which is given by

$$\frac{t}{D} = \left[\frac{\pi}{8} \cdot \frac{1}{K_3^2} \cdot \frac{P}{EL^2}\right]^{\frac{1}{3}} \quad \ldots (38)$$

is quite independent of any plasticity effects and depends only on structural index and elastic modulus.

If a maximum allowable stress f_t is specified, from (35) at design loads higher than

$$P_t = \frac{8}{\pi K_s} \cdot f_t L^2 \cdot \left[\frac{f_t}{E}\right]^2 (Hn\phi_t)^{\frac{3}{2}} \quad \ldots (39)$$

it will be necessary to introduce a safety factor r in each mode so that the design equations become

$$r \frac{f_t}{E} = K_s \left(\frac{E_t^*}{E}\right)^{\frac{1}{2}} \left(\frac{t}{L}\right) \left(\frac{L}{D}\right) \quad \ldots (40)$$

$$r \frac{f_t}{E} = \frac{\pi^2}{8} \left(\frac{E_t^*}{E}\right) \cdot \left(\frac{D}{L}\right)^2 \quad \ldots (41)$$

$$\frac{f_t}{E} = \frac{1}{\pi} \left(\frac{L}{D}\right) \cdot \left(\frac{L}{t}\right) \cdot \frac{P}{EL^2} \quad \ldots (42)$$

where E_t^* corresponds to the stress (rf_t).

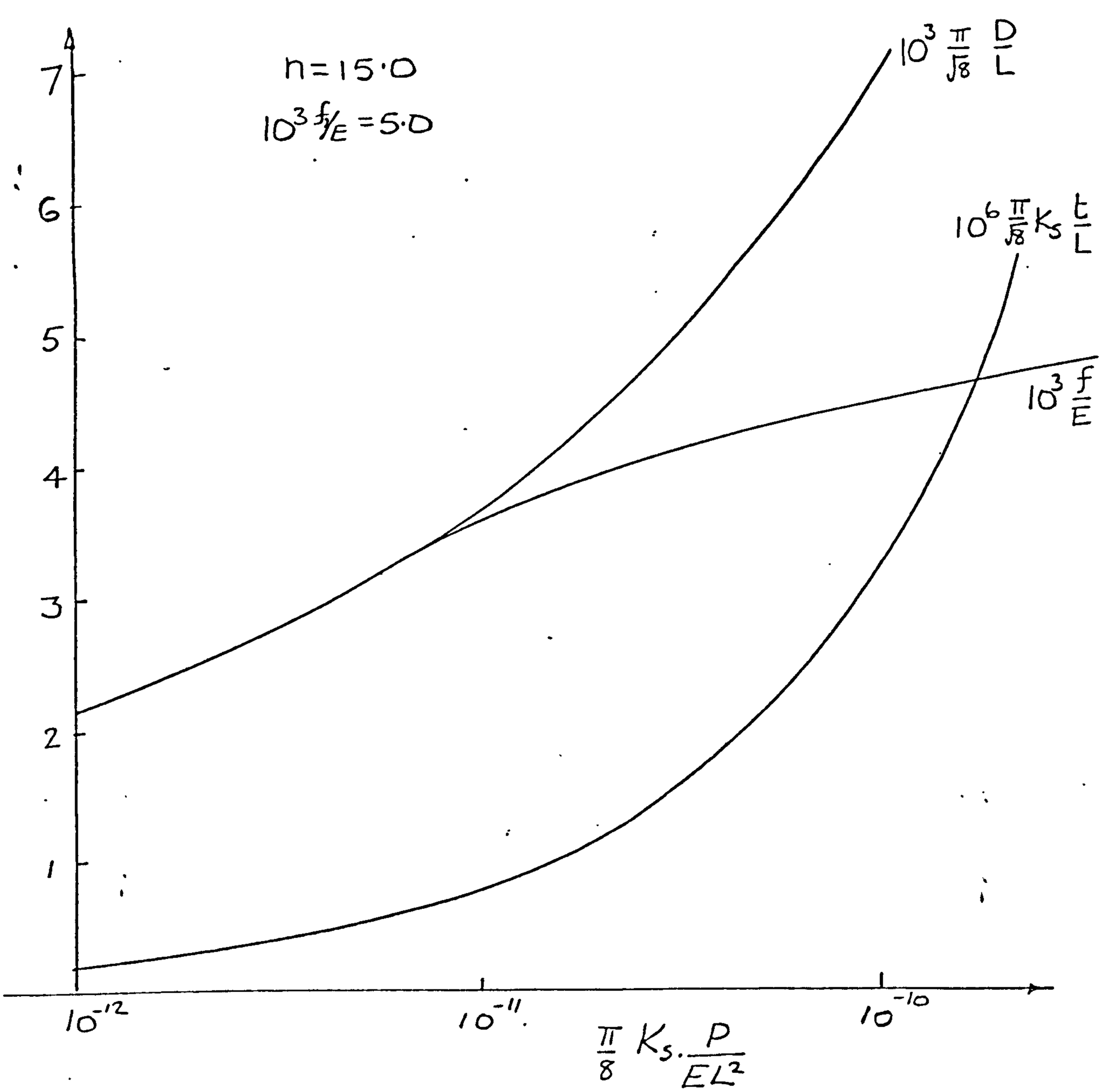

Figure 10. OPTIMUM DESIGN DATA FOR ROUND TUBES

These equations may be solved to give

$$\frac{D}{L} = \left(\frac{8K_s}{\pi^3}\right)^{\frac{1}{4}} \cdot \left(\frac{P}{f_t L^2}\right)^{\frac{1}{4}} \cdot (1 + n\phi^*)^{\frac{1}{8}} \quad \ldots (43)$$

$$\frac{t}{L} = \left(\frac{1}{8\pi K_s}\right)^{\frac{1}{4}} \cdot \left(\frac{P}{f_t L}\right)^{\frac{3}{4}} \cdot \frac{1}{(1 + n\phi^*)^{\frac{1}{8}}} \quad \ldots (44)$$

where $\phi^* = \alpha\left(\frac{rf_t}{E}\right)^{n-1}$

and the safety factor r must be found from the following implicit relationship.

$$\frac{\pi}{8} K_s \left(\frac{P}{f_t L^2}\right) = \left(\frac{f^*}{E}\right)^2 (1 + n\phi^*)^{\frac{3}{2}} \quad \ldots (45)$$

where $f^* = rf_t$.

The equations are shown plotted in figure 11 and are used in the construction of the D/L~t/L design space shown in figure 12 .

Honeycomb sandwich

A potentially efficient form of strut may be devised from a strip of honeycomb core sandwich panel of the sort discussed earlier by Wittrick [36] . In the analysis which follows, attention is concentrated on struts of this sort which have ideal isotropic honeycomb cores manufactured from the same material as the faceplates. Core properties are typified by transverse shear stiffness G_c, direct stiffness normal to faceplates E_c and mean density ρ_c.

If the strut is narrow, then structural behaviour and consequent design properties are independent of width, so that the appropriate loading quantity is axial load per unit width ω.

For this type of structure the Euler buckling equation which is based on flexural action only is in general inadequate, and some allowance for the destabilising effect of finite transverse shear flexibility is essential.

The analysis of Timoshenko and Gere[35] is reliable for this purpose and leads to the following equation for buckling load

$$\frac{\omega}{EL} = \frac{1}{\frac{2}{\pi^2} \cdot \frac{E}{E_t} \cdot \frac{L}{t} \cdot \left(\frac{L}{h}\right)^2 + \frac{E}{G_c}\left(\frac{L}{h}\right)} \quad \ldots (46)$$

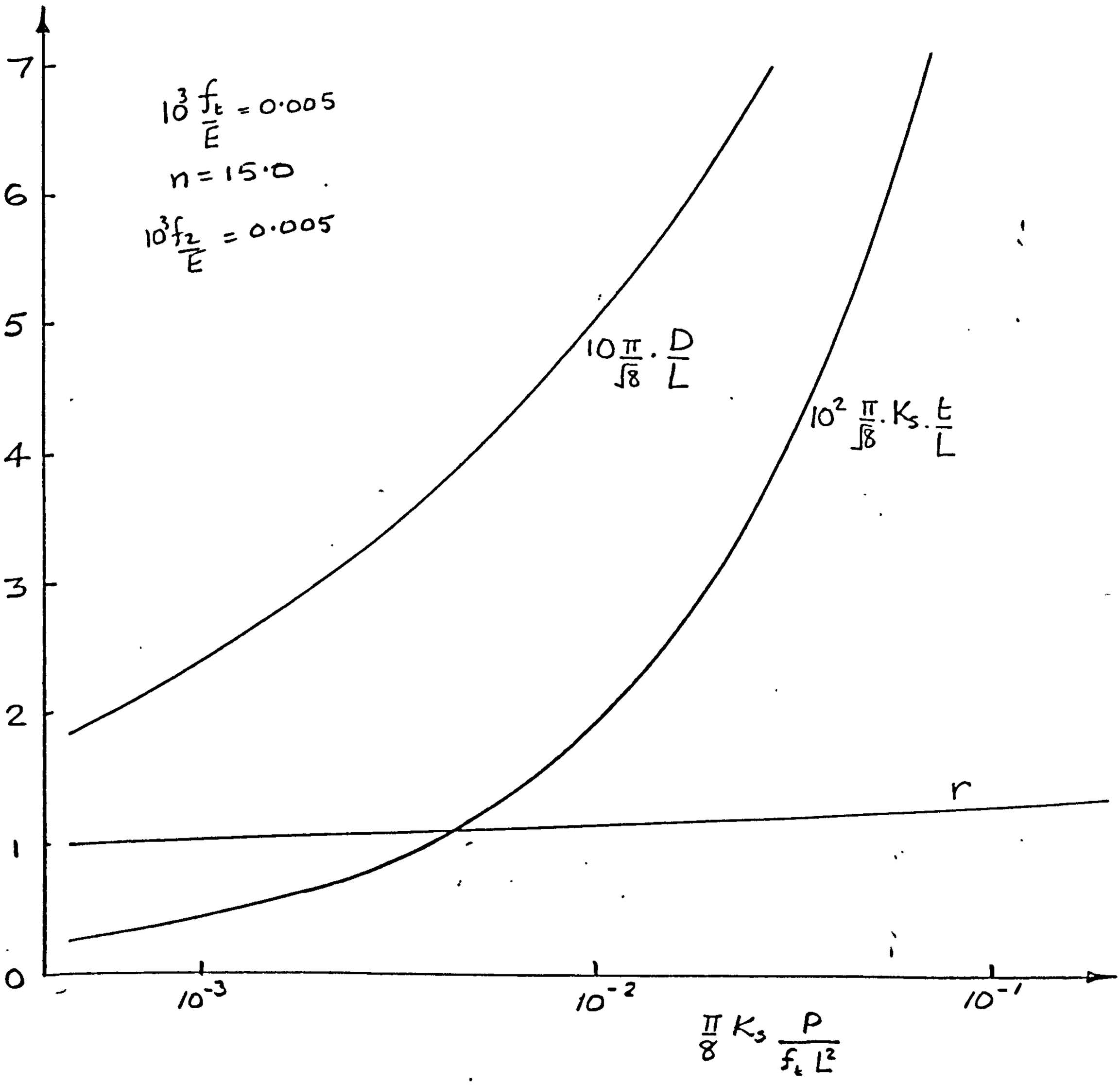

Figure 11. OPTIMUM ROUND TUBE DESIGN WITH ACTIVE STRESS CONSTRAINT

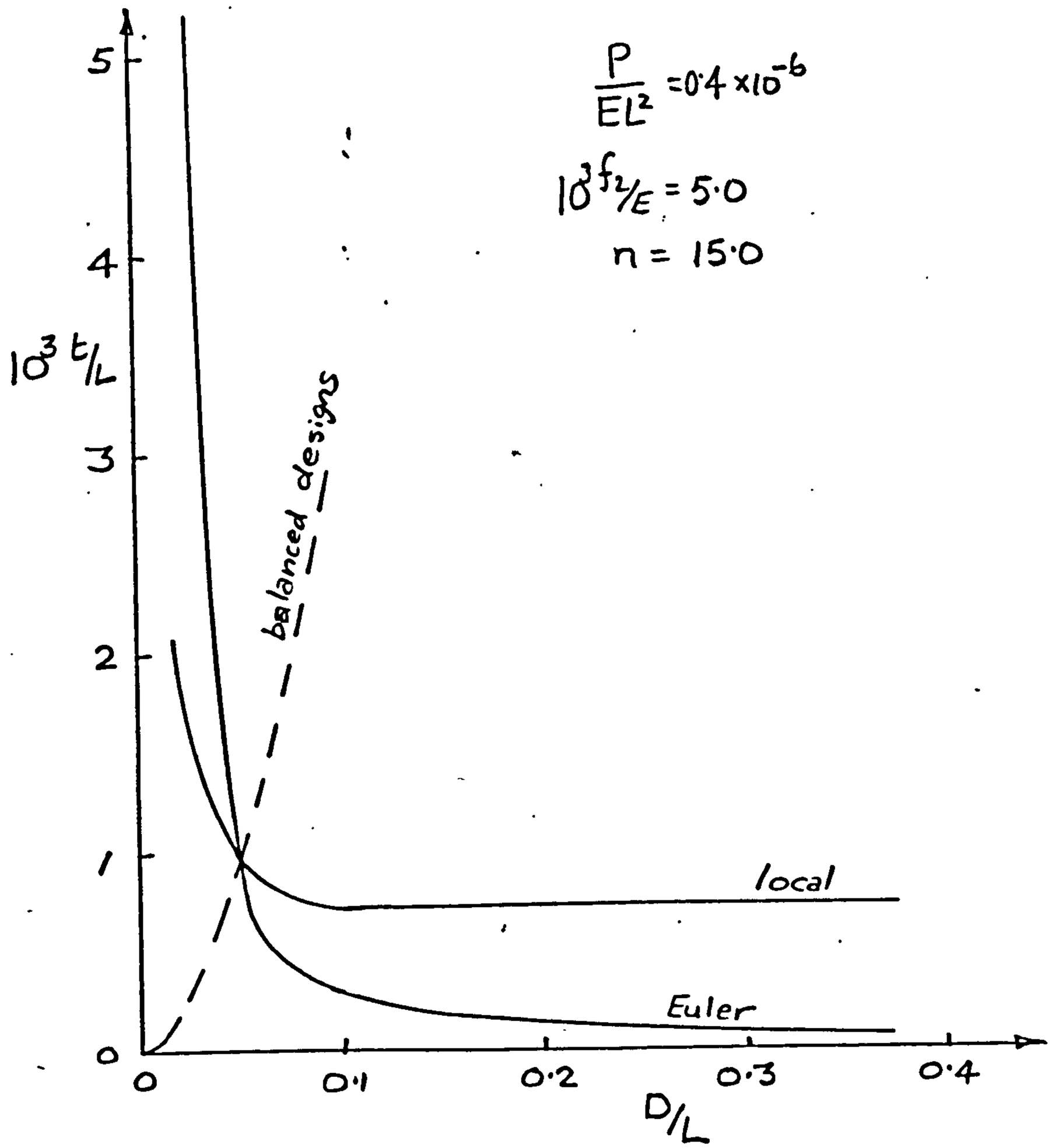

Figure 12. DESIGN SPACE FOR ROUND TUBULAR STRUTS

where t = faceplate thickness
h = distance between faceplate centroids
L = strut simply supported length.

Faceplate thickness may be expressed in terms of surface stress

$$\frac{t}{L} = \frac{1}{2}\frac{\omega}{EL} \Big/ \frac{f}{E} \qquad \ldots (47)$$

so that (46) may be solved for sandwich depth to give

$$\frac{h}{L} = \frac{1}{2}\frac{\omega}{EL}\cdot\frac{E}{G_c} + \left\{\frac{1}{4}\left(\frac{\omega}{EL}\right)^2\left(\frac{E}{G_c}\right)^2 + \frac{4}{\pi^2}\frac{E}{E_t}\cdot\frac{f}{E}\right\}^{\frac{1}{2}} \qquad \ldots (48)$$

Core shear modulus is determined by the need to prevent wrinkling instability of the faceplates. The stress at which this is likely to occur is given by Plantema[37] in the following form

$$f = K_w(EE_cE_g)^{\frac{1}{3}} \qquad \ldots (49)$$

where E_g is the geometric modulus at stress f given by

$$\frac{E_g}{E} = \frac{4E_t}{\left[E^{\frac{1}{2}} + E_t^{\frac{1}{2}}\right]^2} \qquad \ldots (50)$$

and K_w is the wrinkling coefficient, a conservative estimate for which is given by Plantema[37] to be 0.5.

For an ideal honeycomb core from reference 46 it may be shown that

$$\frac{E_c}{E} = \frac{64}{15}(1+\nu)\cdot\frac{G_c}{E}$$

so that the core shear modulus required to prevent wrinkling may now be expressed as a function of stress, giving

$$\frac{G_c}{E} = \left\{\frac{15}{1+\nu}\right\}^{\frac{1}{2}}\left\{\frac{1}{4K_w}\right\}^{\frac{3}{2}}\left\{\frac{f}{E}\right\}^{\frac{3}{2}}\cdot\left\{\frac{E}{E_g}\right\}^{\frac{1}{2}} \qquad \ldots (51)$$

The equivalent or weight thickness of the strut is given by

$$\frac{t^e}{L} = \frac{2t}{L} + \frac{\rho_c}{\rho}\cdot\frac{h}{L}$$

where ρ_c = core density

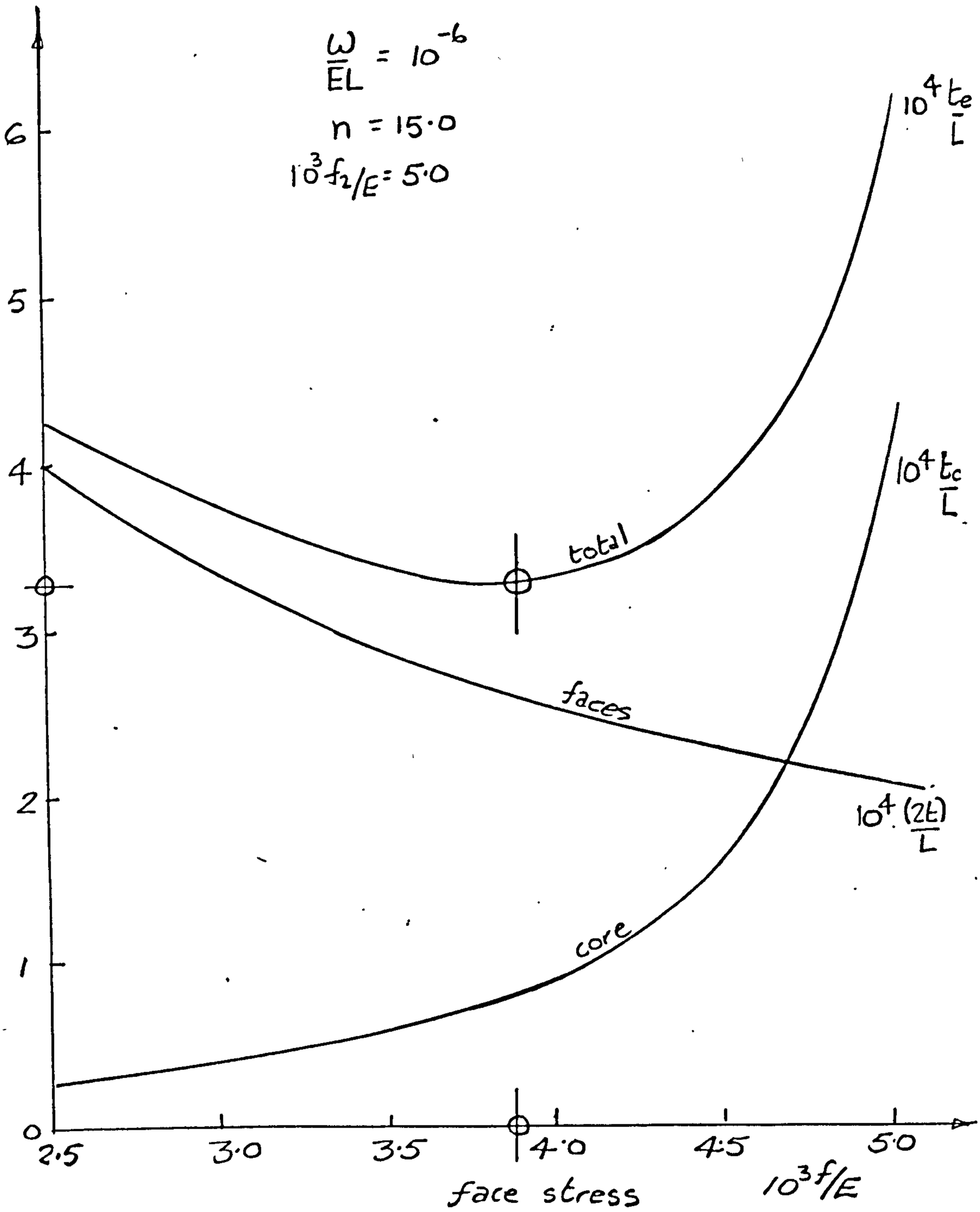

Figure 13. SANDWICH STRUT ELEMENT THICKNESSES RELATED TO FACE STRESS

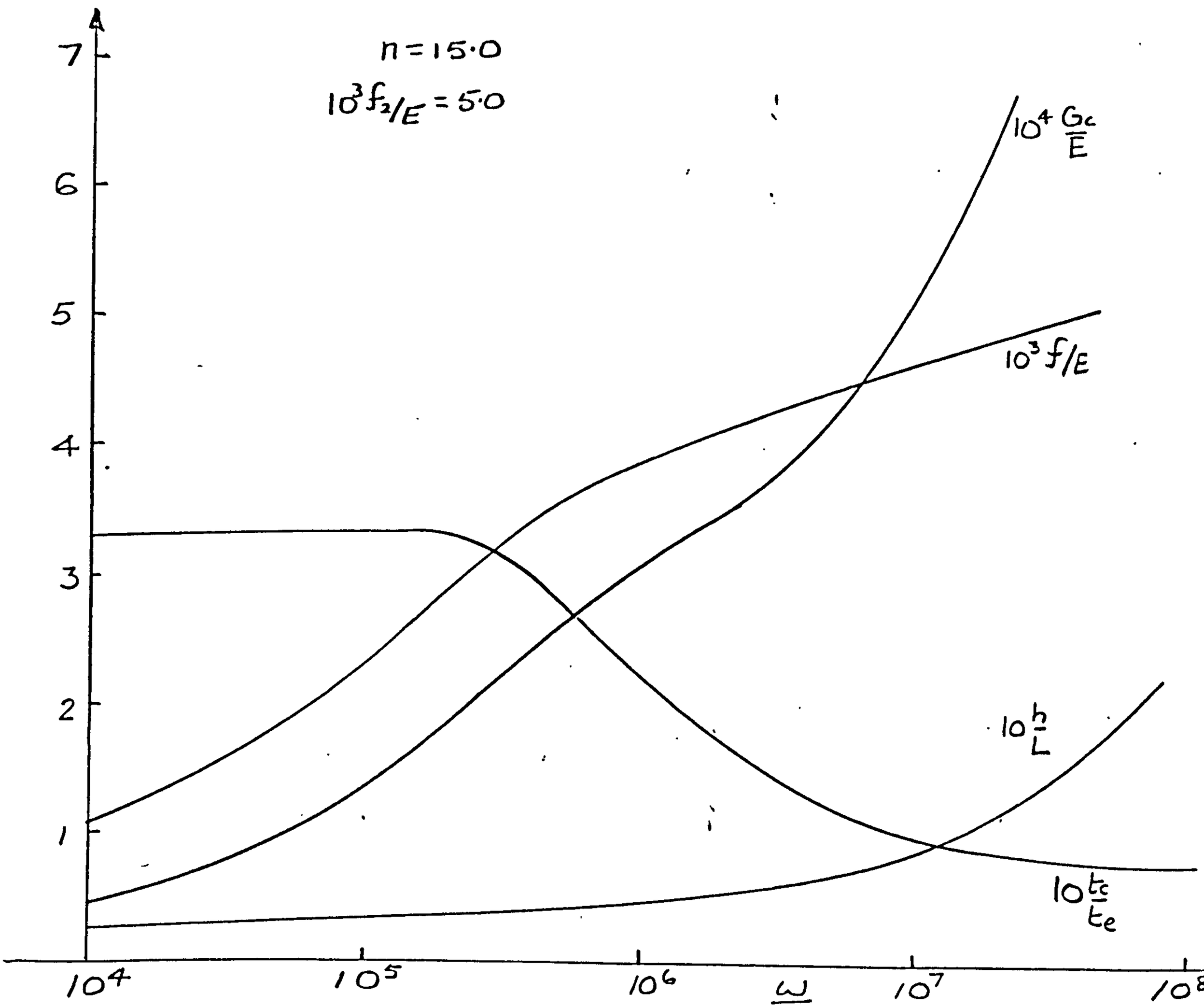

Figure 14. OPTIMUM SANDWICH STRUT PARAMETERS

and since, for honeycomb made from faceplate material

$$\frac{\rho_c}{\rho} = \frac{64}{15}(1+\nu)\frac{G_c}{E}$$

then $$\frac{t_e}{L} = \frac{\omega}{EL}\frac{E}{f} + \frac{64}{15}(1+\nu)\frac{h}{L}\cdot\frac{G_c}{E} \qquad \ldots (52)$$

where $\frac{h}{L}$ is given by equation (48).

Thus using (50) and (51) the equivalent thickness of the strut may be expressed entirely in terms of surface stress which may be varied as shown in figure (13). determine the optimum design, including all the quantities necessary to define it completely.

On this basis a simple numerical interpolation procedure has been devised to determine optimum sandwich strut properties for any given material and load intensity parameter ω/EL. Details of the relevant computer programme (SAST) are given in Appendix B.

Comparisons

From the point of view of performance as individual struts, direct comparisons may only be made between solid, thin walled polygonal, and circular tube struts for which the load intensity parameter is $\frac{P}{EL^2}$.

The sandwich strut design is of an essentially two dimensional character, all characteristic quantities including the applied load being ascertainable only per unit width. Thus the appropriate load intensity parameter for sandwich struts is $\frac{\omega}{EL}$.

One way in which a unified comparison may be made is to consider individual struts as being arranged into a contiguous linear array. This requires the introduction of a transverse dimension in each case to give a value to the spacing of the otherwise isolated struts. This matter will be explored at a later stage.

- First, the individual struts will be considered.

From equations (8), (20) and (35) for solid struts, thin walled polygons and circular tubes respectively

$$\frac{P}{EL^2} = \frac{1}{\beta\pi^2}\left(\frac{f}{E}\right)^2(1+n\phi) \qquad \ldots (53)$$

$$\frac{P}{EL^2} = \frac{1}{(K_1^2 K_2 K_3^2)^{\frac{1}{2}}}\left(\frac{f}{E}\right)^{\frac{5}{2}}(1+n\phi)^{\frac{3}{2}} \qquad \ldots (54)$$

$$\frac{P}{EL^2} = \frac{8}{\pi K_s}\left(\frac{f}{E}\right)^3(1+n\phi)^{\frac{3}{2}} \qquad \ldots (55)$$

All of these relationships have the following form

$$\frac{P}{EL^2} = C\left(\frac{f}{E}\right)^R(1+n\phi)^S \qquad \ldots (56)$$

For perfectly elastic behaviour, $\phi \to 0$, so that

$$\frac{f}{E} = \left(\frac{1}{C}\cdot\frac{P}{EL^2}\right)^{\frac{1}{R}} \qquad \ldots (57)$$

If we consider two competing types of design characterised by the parameters $C_{1,2}$ and $R_{1,2}$, they will have identical efficiencies (i.e. design stresses), when the load intensity parameter is

$$\left(\frac{P}{EL^2}\right)^* = \left[\frac{C_1^{R_1}}{C_2^{R_2}}\right]^{\frac{1}{R_1-R_2}} \qquad \ldots (58)$$

for which the common design stress will be

$$\left(\frac{f}{E}\right)^* = \left(\frac{1}{C_i}\right)^{\frac{1}{R_i}}\left(\frac{C_1}{C_2}\right)^{\frac{R_2}{R_1-R_2}} \qquad \ldots (59)$$

Equation (59) shows that an exchange of pre-eminence will always occur at some load intensity unless $R_2 = R_1$. We may explore the possibilities between the groups under consideration by considering the available ranges of the various parameters

For solid sections, $R = 2$, $S = 1$ and

$$1.053 < C < 1.2732$$

For thin walled polygons, $R = 2.5$, $S = 1.5$

$$0.4343 < C < 1.7579$$

and for round tubes, $R = 3.0$, $S = 1.5$ and $C = 10.19$.

Thus from equation (59) the range of possible elastic intercept stresses may be determined, giving the following results.

For solid and thin walled polygons,

$$0.3588 \leq (f/E)^* < 8.595$$

for solid struts and round tubes

$$0.1034 < (f/E)^* < 0.1250$$

and for thin walled polygons and round tubes

$$0.0018 < (f/E)^* < 0.0298$$

For all common structural metals, yield stresses are at the very most equal to 0.02E. It follows that when behaviour is perfectly elastic, an interchange of supremacy is only feasible between the best thin-walled polygon (the decagon) and the round tube.

Behaviour at high load intensities, when plasticity is important, may be investigated in a parallel way by noting that at high stresses,

$$n\phi >> 1.0$$

so that (56) becomes, for perfectly plastic behaviour,

$$\frac{P}{EL^2} = C\left(\frac{f}{E}\right)^R . (n\phi)^S$$

$$= C(0.002n)^S \left(\frac{f_2}{E}\right)^{R-S} \left(\frac{f/E}{f_2/E}\right)^{[R+S(n-1)]}$$

and therefore optimum stress is given by

$$\frac{f}{E} = \left(\frac{f_2}{E}\right)^{\left[\frac{n}{n-1+R/S}\right]} \left[\frac{1}{C(0.002n)^S} . \frac{P}{EL^2}\right]^{\left[\frac{1}{R+S(n-1)}\right]} \quad \ldots (60)$$

It may be noted immediately, that for the three categories of design under consideration, since R/S = 2, 5/3 and 2 respectively and n is a number of the order of 15, design stress is almost proportional to the proof stress f_2.

For any given material characterised by the quantities n and f_2/E, a similar intercept feasibility exercise may be performed for ideal elastic behaviour above. The following results are obtained for n = 15, f_2/E = 0.005.

For solid and thin walled polygon designs

$$0.005900 < (f/E)^* < 0.007291$$

for solid polygons, and round tubes

$$0.006528 < (f/E)^* < 0.006685$$

and for thin walled polygons and round tubes

$$0.001818 < (f/E)^* < 0.02980.$$

Thus an interchange of supremacy is possible between all combinations of designs for perfectly plastic behaviour. However, many design codes limit design stresses to the f_2, at which level the characteristic quantities are very much in transition between elastic and entirely plastic behaviour, and the full equation must be solved. This is conveniently accomplished by interpolation, and an efficient programme to do this (SCOM) is described in Appendix B. The fully elastic and ideally plastic solutions provide an upper bound to the correct design stress at any particular load intensity and are therefore not conservative. Differences from the true solution are significant in the transition region, as may be seen in Figure 15 which shows results for a representative range of design concepts.

Comparisons will now be made with the honeycomb sandwich strut. For this purpose, the other three types of strut must be grouped into linear arrays, and the governing parameters redefined in terms of end load per unit width. The load carried by an individual strut must be spread over a transverse dimension, which will in effect be that part of the array occupied by one strut. Since all the struts considered are regular polygons, the question of strut spacing may be settled by considering that each strut is located at the centre of its own circumscribing circle.

The equivalent endload per unit width thus derived will only be comparable from one type of design to another on average over an integral number of units. However, the degree of abstraction involved is no greater than that by which the stresses arising from a so-called point load are assumed to be distributed over the finite dimensions of the cross section of an individual strut.

The solid polygonal strut with m sides and of radius R has a cross section area given by equation (9)

$$A = mR^2 \tan \frac{\pi}{m}$$

The mean array loading due to load P on each element is

$$\omega = \frac{P}{2R}$$

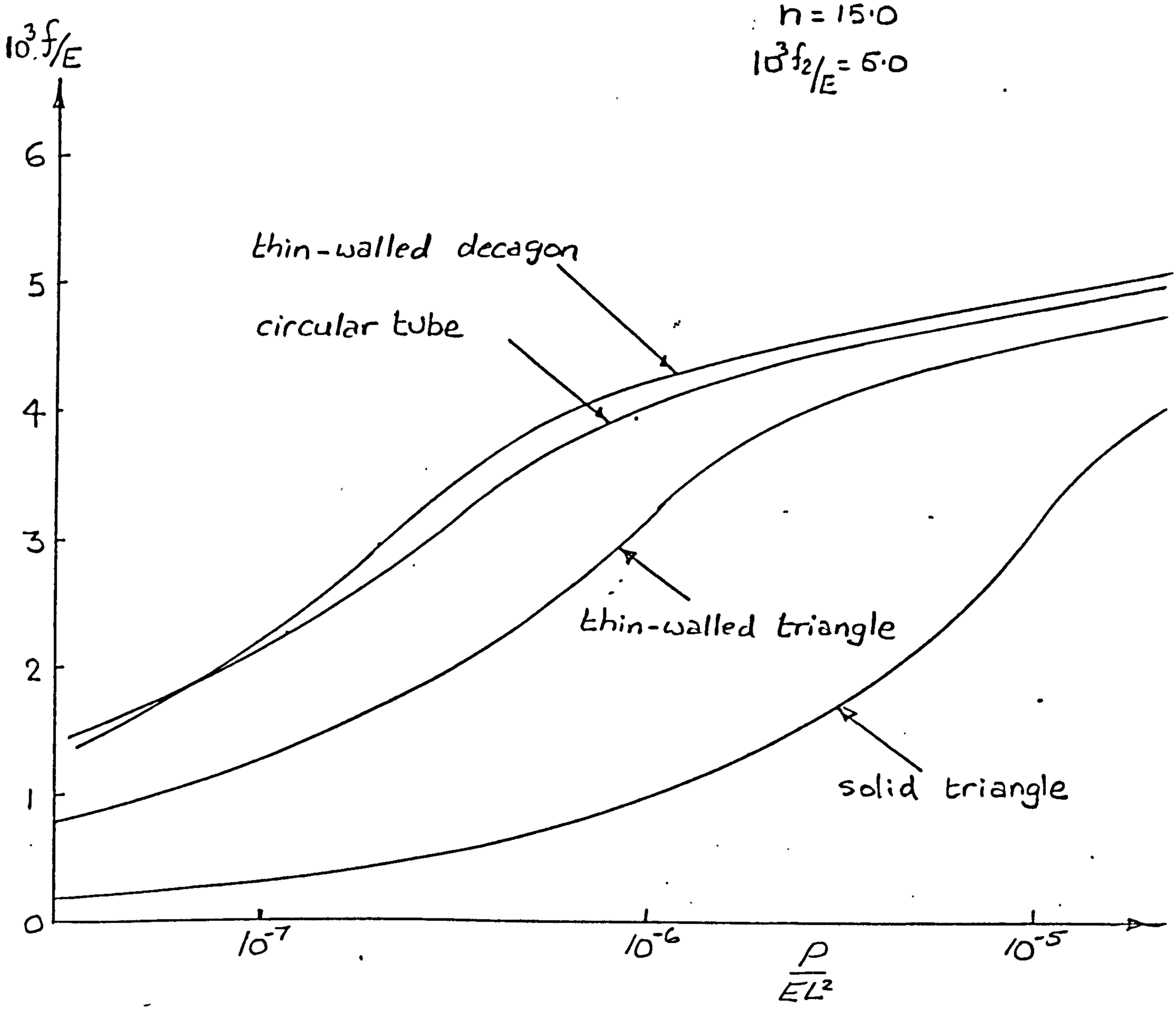

Figure 15. DESIGN STRESSES FOR VARIOUS STRUT CONFIGURATIONS

and design stress is

$$f = \frac{P}{A}$$

It follows that the design point load P may now be expressed in terms of an equivalent array loading w and the design stress f to give

$$P = \frac{4w^2}{mf\tan(\pi/m)} \qquad \ldots (61)$$

This may be substituted into the original design equation (8), which after reorganisation leads to

$$\frac{\omega}{EL} = F\left(\frac{f}{E}\right)^R (1 + n\Phi)^S \qquad \ldots (62)$$

where

$$C = \left[\frac{3}{\pi^2}\frac{m^2\tan^2(\pi/m)}{3+\tan^2(\pi/m)}\right]^{\frac{1}{2}} \qquad \ldots (63)$$

$$R = 1.5 \; ; \quad S = 0.5$$

For elastic designs, $\phi = 0$ and equation (62) may be inverted to give design stress, a direct measure of relative merit

$$\frac{f}{E} = F\left[\frac{\omega}{EL}\right]^{\frac{2}{3}} \qquad \ldots (64)$$

where $F = \left[\frac{1}{C}\right]^{\frac{2}{3}}$

m	3	4	5	6	10	circle
C	1.1695	1.1027	1.0663	1.0461	1.0165	1.0
F	0.9009	0.9369	0.9581	0.9704	0.9891	1.0

It is worth noting that on this basis, the order of merit in terms of polygon order m is reversed compared with the isolated strut, the circular section is now best by a maximum margin of about 10%.

From equations (20) and (21) for the isolated thin walled polygon

$$\frac{P}{EL^2} = \frac{1}{\left[K_1^2 K_2 K_3^2\right]^{\frac{1}{2}}} \left(\frac{f}{E}\right)^{\frac{5}{2}} (1 + n\phi)^{\frac{3}{2}}$$

$$\frac{b}{L} = \frac{1}{K_1^{\frac{1}{2}}} \left(\frac{f}{E}\right)^{\frac{1}{2}} (1 + n\phi)^{\frac{1}{2}}$$

The circumscribing radius is

$$R = \frac{b}{2\sin(\pi/m)}$$

so that $P = 2R\omega = \frac{b}{\sin(\pi/m)}$

The design stress equation may now be compounded, giving

$$\frac{\omega}{EL} = C\left(\frac{f}{E}\right)^R (1 + n\phi)^S$$

where

$$C = \left[\frac{24}{K_2}\right]^{\frac{1}{2}} \cdot \frac{m\sin(\pi/m)\tan(\pi/m)}{\pi\left[3 + \tan^2(\pi/m)\right]^{\frac{1}{2}}} \qquad \ldots (65)$$

the K_2 values are given in the table on page 20, and

$$R = 2.0 \quad ; \quad S = 1.0$$

so that for elastic design

$$\frac{f}{E} = F\left(\frac{\omega}{EL}\right)^{\frac{1}{2}}$$

where $F = \left(\frac{1}{C}\right)^{\frac{1}{2}}$

m	3	4	5	6	7	8	9	10
C	1.380	1.159	0.901	0.778	0.654	0.584	0.514	0.467
F	0.851	0.929	1.054	1.134	1.237	1.309	1.395	1.463

The values of the efficiency factor F, which in this case corresponds precisely to that due to Farrar[10] for wide column compression panels, indicate significant advantages for the higher order polygons. In fact the higher efficiencies shown above exceed by a significant margin those which have been noted for more conventional panels (e.g. for Z stiffeners F = 0.95, and for trapezoidal corrugations F = 1.26).

From equations (35) and (36), for round tubes

$$\frac{P}{EL^2} = \frac{8}{\pi K_s}\left(\frac{f}{E}\right)^3 (1 + n\phi)^{\frac{3}{2}}$$

$$\frac{D}{L} = \frac{\sqrt{8}}{\pi}\left(\frac{f}{E}\right)^{\frac{1}{2}} (1 + n\phi)^{\frac{1}{2}}$$

and with $P = \omega D$

$$\frac{\omega}{EL} = \frac{P/EL^2}{D/L} = \frac{\sqrt{8}}{K_s}\left(\frac{f}{E}\right)^{\frac{5}{2}} (1 + n\phi) \qquad \ldots (66)$$

so that, in this case, with $K_s = 0.25$

$$C = 4\sqrt{8} = \underline{11.314} \; ; \quad R = 2.5 \; ; \quad S = 1.0$$

and for elastic design

$$\frac{f}{E} = F\left(\frac{\omega}{EL}\right)^{\frac{2}{5}}$$

where $F = \left[\frac{K_s}{\sqrt{8}}\right]^5 = \underline{0.379}.$

The governing equations for each of the three types of design are of the form of equation (56), and may therefore be solved using the routine SCOM (see Appendix B).

The sandwich strut results are produced by the routine SAST (see Appendix B) and can now be directly compared.

Figure 16 shows comparative efficiencies of arrays made up of a number of representative strut designs, together with the sandwich strut results for a typical aluminium alloy type material.

At low load intensities, the sandwich strut is always superior. However, at higher loads, the sandwich design is overtaken by the round tube and the decagon, subject to the reservations about local buckling behaviour referred to on p.20.

The solid triangular and circular designs are greatly inferior over most of the loading range, but will actually emerge as the best designs of all at extremely high load intensities. The corresponding stresses are extremely high, and would be well beyond those allowed as an overriding maximum by most design codes.

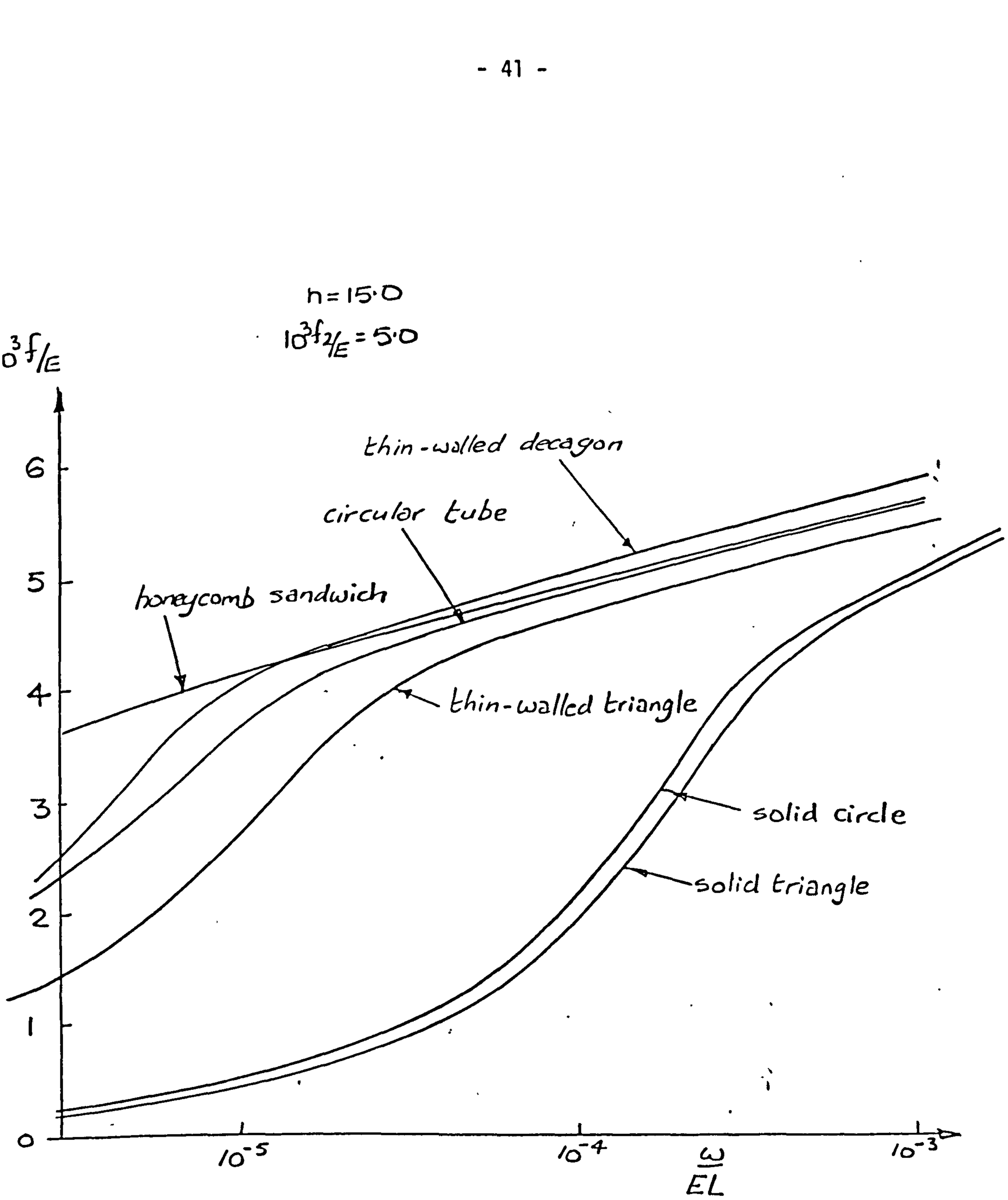

Figure 16. COMPARATIVE DESIGN STRESSES FOR ARRAYS OF VARIOUS STRUT DESIGNS

Chapter 3

THE RECTANGULAR PLATE

Elastic Analysis

A uniform, thin, flat, isotropic, perfectly elastic, simply supported rectangular plate compressed in its own plane by a uniform loading applied to two opposite edges will buckle when that loading reaches a value given by

$$\omega = KE\frac{t^3}{b^2} \qquad \ldots (67)$$

where E = Young's modulus
t = plate thickness
b = plate width (transverse to loading direction)
K = buckling coefficient

given by Timoshenko[35] to be

$$K = \frac{\pi^2}{12(1-\nu^2)}\left[m\left(\frac{b}{a}\right) + \frac{1}{m}\left(\frac{a}{b}\right)\right]^2 \qquad \ldots (68)$$

where ν = Poisson's ratio
a = plate length
m = the number of half waves of the buckle mode in the direction of loading.

All integral values of m correspond to exact solutions of the equations of equilibrium in the buckled state. However as the loading increases from zero, buckling will naturally occur at that value of m corresponding to the lowest load.

As plate aspect ratio a/b increases from zero, the appropriate values of K will therefore be those which correspond to the lower envelope of equation (68) incorporating in turn all integral values of m.

It may be readily demonstrated that this condition leads to the following relationships for m which allow K to be precisely determined as a function of a/b.

$$m = m_i \quad \text{if} \quad a/b \leq (a/b)^*$$

$$m = m_i + 1 \quad \text{if} \quad a/b > (a/b)^*$$

where m_i = integral part of a/b

$$(a/b)^* = (m_i(m_i+1))^{\frac{1}{2}}$$

The design of such a plate requires that for a given load ω the least value of plate thickness t be found which prevents buckling.

So that from (67)

$$\frac{t}{b} = \left[\frac{1}{K} \cdot \frac{\omega}{Eb}\right]^{\frac{1}{3}} \qquad \ldots (69)$$

This equation together with the buckling coefficient given by (68) is shown plotted in figure 17.

The essential feature from a design point of view is that wavelength and hence buckling coefficient are functions of plate aspect ratio alone, and as such may be pre-determined independently of material properties as in the case of the analysis of a given plate.

Analysis with Plasticity Effects

A reliable analysis of plasticity effects in flat plates has been given by Stowell[25].

His analysis of rectangular plates with a variety of boundary conditions is based on the work of Ilyushin[24], who uses a deformation plasticity theory. This theory is known to be inconsistent in some respects, compared with the more widely accepted flow theory. An important feature of the Stowell analysis is the assumption that no strain reversal occurs before maximum load is reached, which is consistent with Shanley's strut theory. The Shanley[11] assumption of irreversibility can be proved to be in error for real (imperfect) struts. However it gives results which are in good agreement with experiment.

Handelman and Prager[39] used a more refined incremental plasticity theory to develop a plate analysis. However, Stowell reports that this work leads to optimistic values of plate strength compared with NACA tests, and justifies his results, which are lower, on this basis for engineering purposes.

Much more recently, Hutchinson and Budiansky[26] have demonstrated that for cruciform struts, the differences arising from the various plasticity theories correspond to those which might reasonably arise from small imperfections in the structure. This explanation neatly accounts for the apparent success of the Stowell plate and Shanley strut theories, and justifies in some measure their use in determining engineering solutions. The utilisation of more precise theories must await the development of a more complete treatment of imperfection effects, as well as the statistical quantification of imperfections in engineering structures. A wide spectrum of plasticity effects in buckling has recently been thoroughly reviewed by Hutchinson[40].

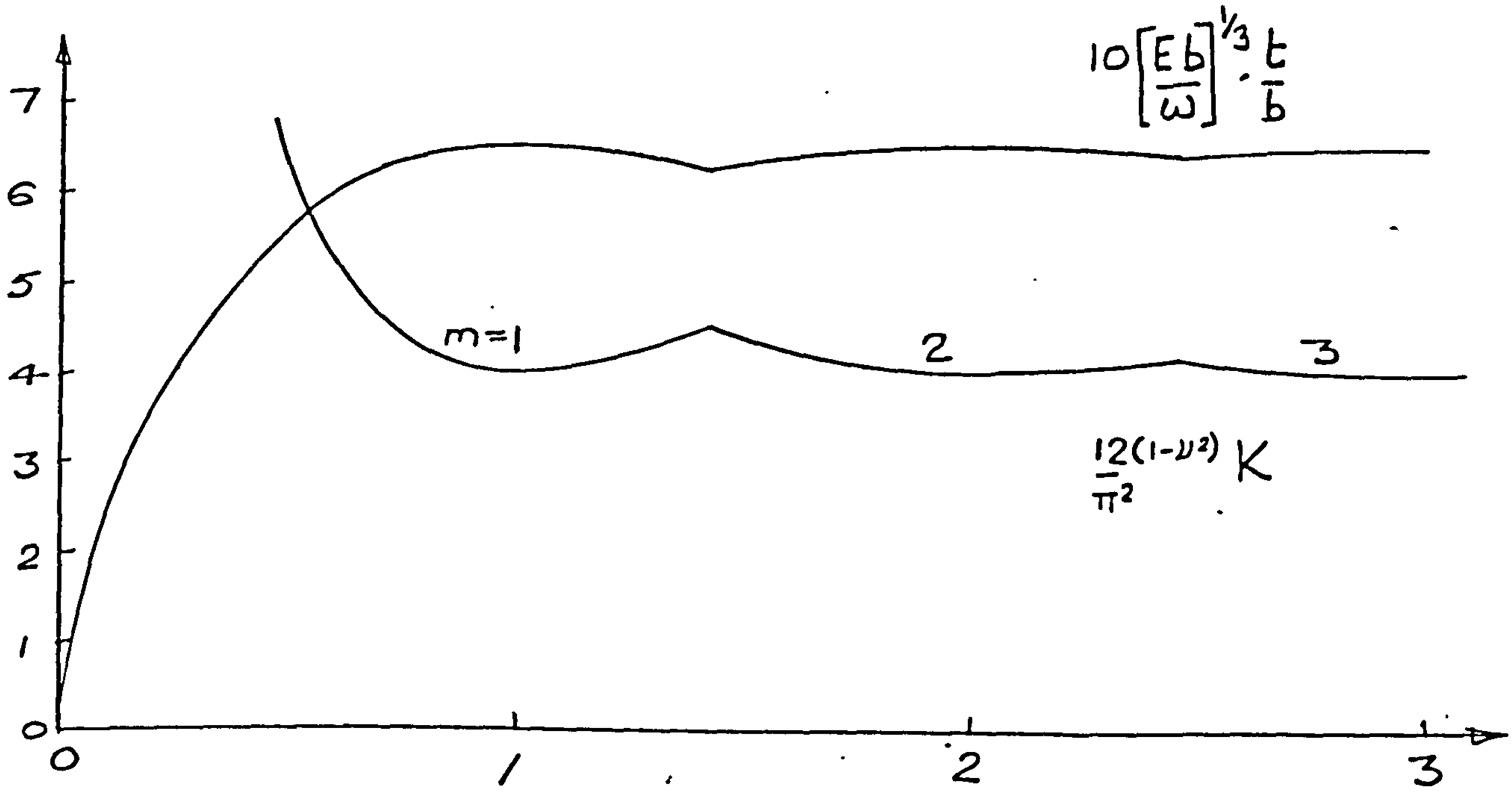

Figure 17. BUCKLING COEFFICIENTS AND DESIGN THICKNESSES FOR ELASTIC RECTANGULAR PLATES.

From the work of Stowell the following relationship for buckling load allowing for plasticity effects may be obtained.

$$\frac{\omega}{Eb} = \left[\frac{1}{4}\left(1+3\frac{E_t}{E_s}\right)\left(\frac{mb}{a}\right)^2 + \left(\frac{a}{mb}\right)^2 + 2\right]\cdot\frac{\pi^2}{12(1-\nu^2)}\cdot\frac{E_s}{E}\cdot\left(\frac{t}{b}\right)^3 \qquad \ldots (70)$$

This expression avoids the assumption of Stowell[25] that $\nu = 0.5$, but is otherwise unchanged.

Handelman and Prager [39] using a more sophisticated plasticity theory obtain the following analagous expression

$$\frac{\omega}{Eb} = \left[D'_{11}\left(\frac{mb}{a}\right)^2 + D'_{22}\left(\frac{a}{mb}\right)^2 + 2D'_{12}\right]\frac{\pi^2}{12(1-\nu^2)}\left(\frac{t}{b}\right)^3 \qquad \ldots (71)$$

The coefficients D'_{11} , D'_{22} and D'_{12} contain the effects of plasticity, and may be obtained by the following rather lengthy sequence of substitutions from basic material properties.

$$\left.\begin{aligned} D'_{11} &= 1 - c\delta(2-\nu)^2 \\ D'_{12} &= 1 - c\delta(2-\nu)(2\nu-1) \\ D'_{22} &= 1 - c\delta(2\nu-1)^2 \end{aligned}\right\} \qquad \ldots (72)$$

where $\delta = \frac{1}{4}\left[2 - 3\zeta + \zeta^3\right]$

$$\left.\begin{aligned} c &= \frac{\lambda-1}{(5-4\nu)\lambda-(1-2\nu)^2} \\ \zeta &= \alpha + (\alpha^2-1)^{\frac{1}{2}} \\ \alpha &= 1 - \frac{2}{c(5-4\nu)} \end{aligned}\right\} \qquad \ldots (73)$$

$$\lambda = E/E_t = 1 + n\phi \qquad \ldots (74)$$

As plasticity develops $0 < \phi < \infty$, so that the range of behaviour between perfect elasticity, and advanced plasticity may be bracketed for the above quantities in the following way.

$$1.0 < \lambda < \infty$$

$$0 < c < \frac{1}{(5-4\nu)}$$

$$-\infty < \alpha < -1.0$$

$$
\begin{aligned}
0 &> \zeta > -1.0 \\
0.5 &< \delta < 1.0 \\
1.0 &> D'_{11} > 1 - \frac{(2-\nu)^2}{(5-4\nu)} \\
1.0 &< D'_{12} < 1 - \frac{(2-\nu)(2\nu-1)}{(5-4\nu)} \quad \text{(since } \nu \leq 0.5\text{)} \\
1.0 &> D'_{22} > 1 - \frac{(2\nu-1)^2}{(5-4\nu)}
\end{aligned}
$$

The coefficients D'_{11} , D'_{22} and D'_{12} have the general character of plate bending stiffnesses. As such their erosion due to plasticity will have a destabilising effect, as well as leading to changes in the buckling mode.

Somewhat surprisingly, although D'_{11} and D'_{22} decrease with increasing plasticity, D'_{12} in fact increases in the Handelman-Prager analysis.

If the Stowell-Ilyushin coefficients are identified in an analagous way, using the same notation without the prime,

$$
\left.
\begin{aligned}
D_{11} &= \frac{1}{4}\left(\frac{E_s}{E} + 3\,\frac{E_t}{E}\right) \\
D_{12} = D_{22} &= \frac{E_s}{E}
\end{aligned}
\right\} \qquad \ldots (76)
$$

all of which decrease monotonically with increasing stress. Numerical analysis based on the more correct theory of plasticity utilised by Handelman and Prager leads to consistently higher buckling strengths than the Stowell analysis which, however, gives a much better correlation with experimental observation.

The missing element of course is the effect of manufacturing imperfections on plate strength, which is not included in either of the above analyses. As with the tangent modulus theory of strut buckling, it is possible to conclude as suggested by Hutchinson [40] that the conservatism engendered by the approximate plasticity theory endows a reduction in buckling strength which compensates for the de-stabilising effects of imperfections of the magnitude commonly found in real structures.

In the absence of a satisfactory analysis for the maximum load of plates with imperfections, a sensible engineering approach is to use the Stowell analysis in the expectation that if a plate were too imperfect, the solution could be non-conservative. However the evidence is that such degrees of imperfection are unlikely to occur often in practice, assuming adequate standards of care in manufacture, inspection and quality control.

Design

Stowell's equation (70) will be used as a basis for the design of simply supported plates of finite proportions. By noting the relationship between plate thickness, endload intensity and design stress in the following form,

$$\frac{t}{b} = \frac{\omega}{Eb} / \frac{f}{E} \qquad \ldots (77)$$

equation (70) may be transformed into a relationship between design endload intensity and stress only, giving

$$\frac{\omega}{Eb} = \frac{(f/E)^{\frac{3}{2}} \left\{12(1+\phi)\left[1-\left\{\frac{\nu_e+\phi\nu_p}{1+\phi}\right\}^2\right]\right\}^{\frac{1}{2}}}{\pi\left\{\frac{1}{4}\left[1+\frac{3(1+\phi)}{(1+n\phi)}\right]\left(\frac{mb}{a}\right)^2+\left(\frac{a}{mb}\right)^2+2\right\}^{\frac{1}{2}}} \qquad \ldots (78)$$

Integral numbers of half waves m must always be chosen so that the denominator of (78) is a minimum.

For long plates, m may be regarded as a continuous number, on which basis Stowell[25] has found wavelength λ to be given by

$$\frac{\lambda}{b} = \left[\frac{1}{4}+\frac{3}{4}\frac{E_t}{E_s}\right]^{\frac{1}{4}} \qquad \ldots (79)$$

The results obtained in Appendix A give

$$\frac{E_t}{E_s} = \frac{1+\phi}{1+n\phi} \leq 1$$

since $n > 2, \phi \geq 0$ and so $\frac{\lambda}{b} \leq 1$

Thus the effect of plasticity on wavelength as far as long plates is concerned is to reduce it below the elastic value, which is confirmed in effect by calculation for plates of finite length also. In the limit, the ultimate effect of plasticity on wavelength may be investigated by noting that

$$\left[\begin{matrix}\text{limit}\\ f \to \infty\end{matrix}\right](\phi) = \infty$$

so that

$$\frac{E_t}{E_s} \to \frac{1}{n}$$

and the wavelength function enclosed within (79) which must always be minimised becomes

$$\psi(m) = \frac{1}{4}\left(1 + \frac{3}{n}\right)\left(\frac{mb}{a}\right)^2 + \left(\frac{a}{mb}\right)^2 + 2 \qquad \ldots (80)$$

This function may best be discussed in terms of the values of plate proportion $\left(\frac{a}{b}\right)^*$ at which transition occurs between successive numbers of half waves, from m to (m+1) say, for which

$$\psi(m) = \psi(m+1)$$

This condition gives, from (80)

$$\frac{1}{4}\left(1+\frac{3}{n}\right)\frac{m^2}{(a/b^*)^2} + \frac{(a/b^*)^2}{m^2} = \frac{1}{4}\left(1+\frac{3}{n}\right)\frac{(m+1)^2}{(a/b^*)^2} + \frac{(a/b^*)^2}{(1+m)^2}$$

which may be solved for $\left(\frac{a}{b}\right)^*$ to give

$$\left(\frac{a}{b}\right)^* = \left[\frac{m}{2}(1+m)\left(1+\frac{3}{n}\right)^{\frac{1}{2}}\right]^{\frac{1}{2}} \qquad \ldots (81)$$

The perfectly elastic solution is given precisely by n = 1. For higher values, transition occurs at smaller plate proportions until for large n, the change takes place at plate proportions which are reduced by a factor of $1/\sqrt{2}$ compared with elastic values.

Equation (80) which is plotted in figure (18) is confirmed by the results obtained using the programme PDES, which indicates a consistent reduction in wavelength due to plasticity effects.

These observations have an important effect on computation strategy.

In the search for the correct number of half waves for any particular plate, the elastic solution gives a definite value which is now seen as a minimum. The computer is then instructed to consider increasing values until the least plate strength is discovered. This is now known to be the required solution.

On this basis the programme PDES which is described in Appendix C has been written.

For given material properties, plate proportions and endload intensity the design stress which satisfies equation (78) is sought.

The interpolation procedure adopted depends on the magnitude of the design stress.

For high stresses, when plasticity effects predominate, it is convenient and economical to use plastic strain as a basis for interpolation. At low stresses, the stress itself may be used. The demarcation between the two methods is taken to be the stress f_{05} at which plastic strain equals 0.0005. The endload intensity ω_{05} corresponding to this stress is found directly from (78) and the branching between interpolation procedures is accomplished by applying the simple test

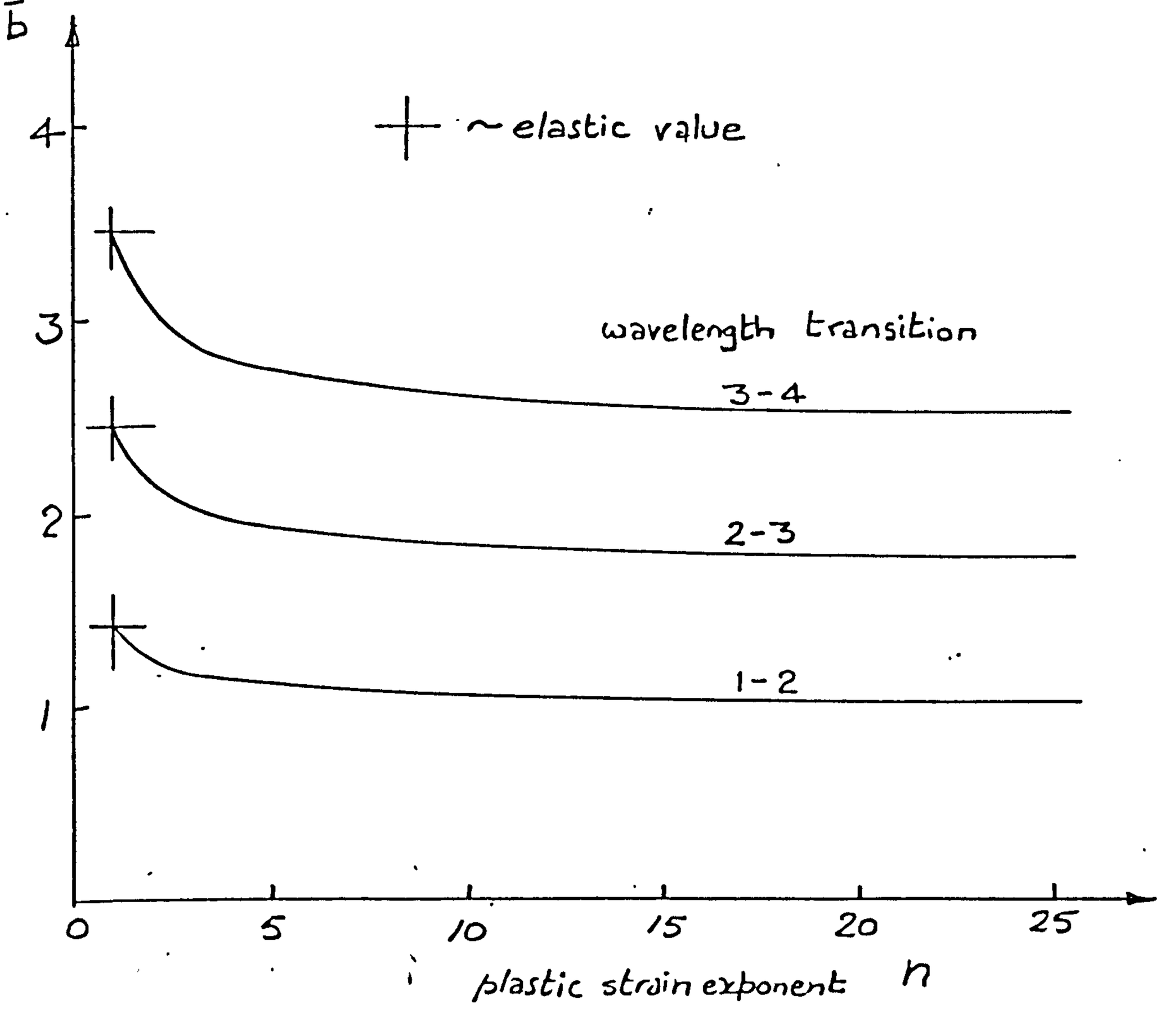

Figure 18. THE EFFECT OF EXTREME PLASTICITY ON WAVELENGTH TRANSITION ASPECT RATIOS

$$\omega \gtrless \omega_{05}$$

Output gives plate aspect ratios, design stress, number of half waves, thickness and normalised thickness.

Normalised thickness is based on the ideal elastic solution given by equation (69) to be

$$\frac{[t/b]}{[\omega/Eb]^{\frac{1}{3}}} = \left[\frac{1}{K}\right]^{\frac{1}{3}} \qquad \ldots (82)$$

with $\nu = 0.3$

(= 0.6513 for long elastic plates)

The general effect of plasticity is to increase this value, although the corresponding changes in Poisson's ratio will have a compensating influence.

The Handelman-Prager analysis has been programmed also (see PDEP described in Appendix C) and used as a basis for comparison between the two theories in design terms.

Numerical results

Results obtained from the programmes are shown plotted in Figures 19 to 22 . The parameters explored include plate aspect ratio, material proof stress, plasticity exponent and primary Poisson's ratio values.

Figure 19 which shows plate thickness as a function of plate proportions for a given load intensity and plate material, illustrates the difference in design terms between the Illyushin-Stowell and the Handelman-Prager theories. The material chosen is that used by Handelman and Prager ($n = 8.613$, $f_2/E = 0.00463$) and the results indicate the conservative character of Stowell's solution. The results are quite sensitive to the value of Poisson's ratio chosen, the higher perfectly plastic value being seen to have a stabilising influence.

Increasing proof stress for a given load intensity will obviously tend to reduce plasticity effects up to the point when perfectly elastic behaviour becomes possible. This feature is illustrated in figure 20.

If the proof stress is fixed and the plastic strain exponent n is varied, the effect is for higher values of n to give improved stability below the proof stress, but performance is degraded at higher stress levels since the loss of slope (tangent modulus) is more severe in this regime. This effect is reflected in the results shown in figure 21, which indicates reducing plate thicknesses for lower values of n for very short plates as design stress increases.

The plot of equation (80) shown in figure 18 confirms the features discussed above, and when plate design results are plotted in terms of design stress as in figure 22, the doubly asymptotic character of the mode transition lines between perfectly elastic and plastic values is clearly revealed.

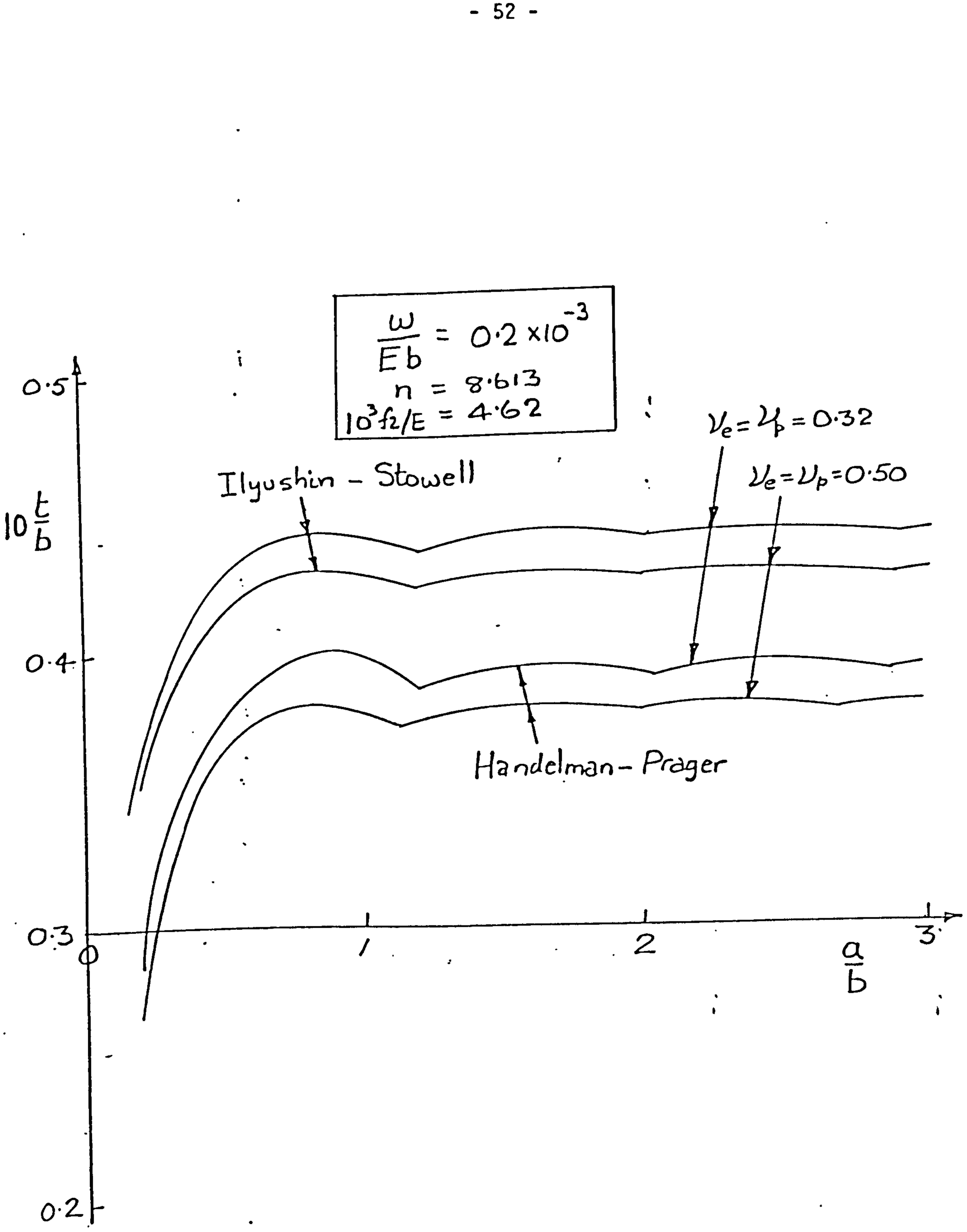

Figure 19. PLATE DESIGN THICKNESSES FOR TWO PLASTIC PLATE BUCKLING THEORIES

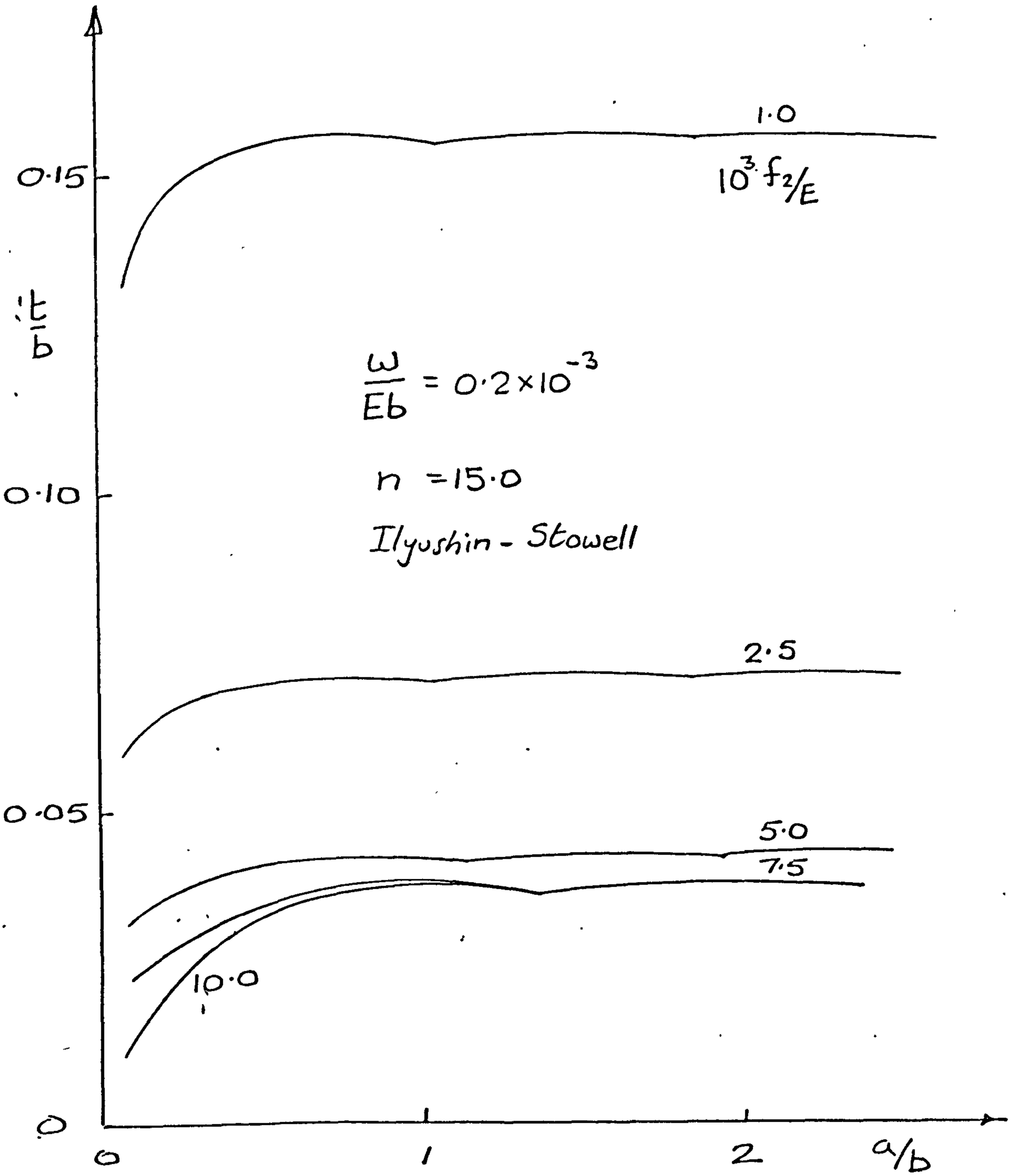

Figure 20. PLATE DESIGN THICKNESSES RELATED TO PROOF STRESS.

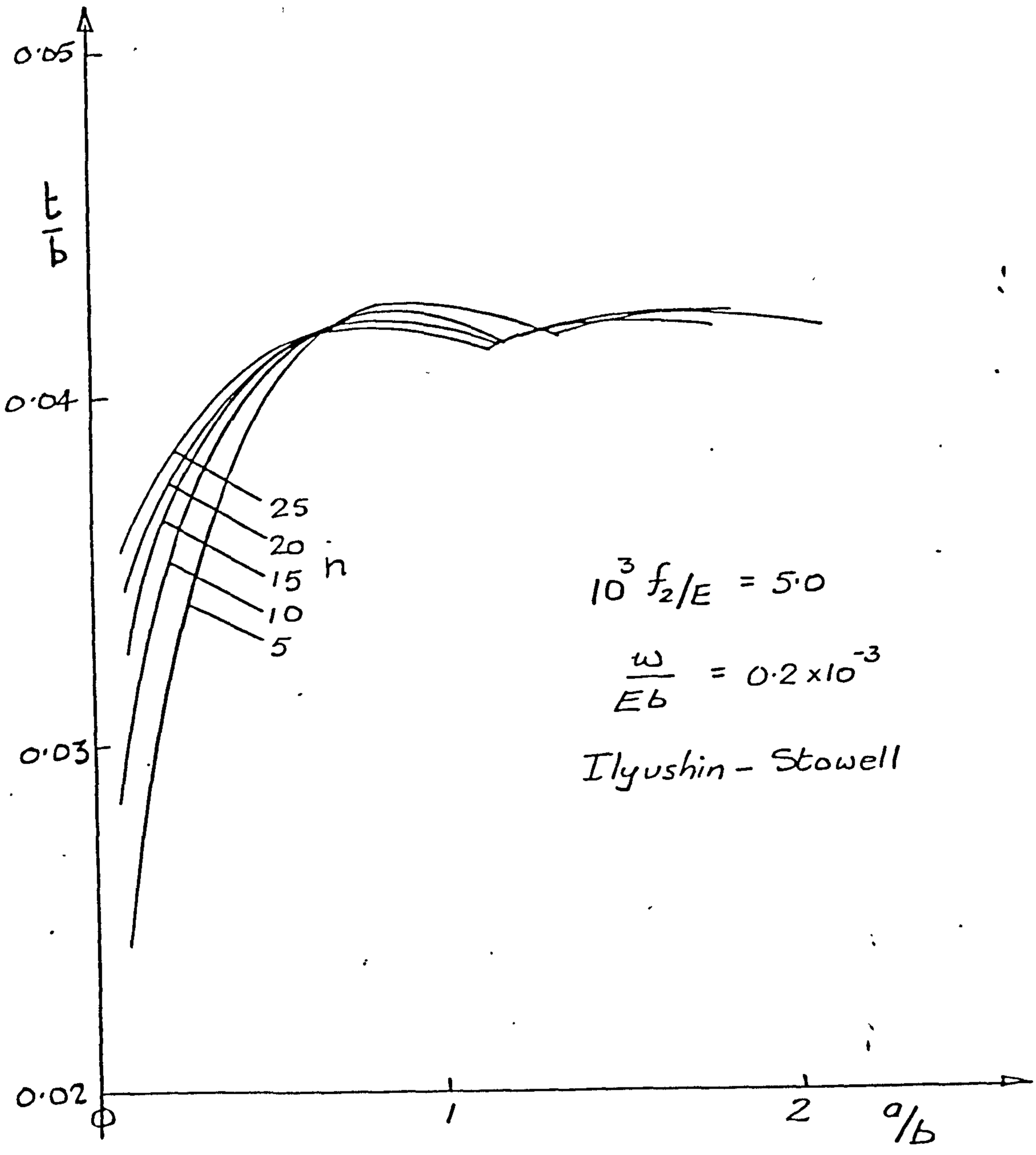

Figure 21. PLATE DESIGN THICKNESSES RELATED TO PLASTIC STRAIN EXPONENT

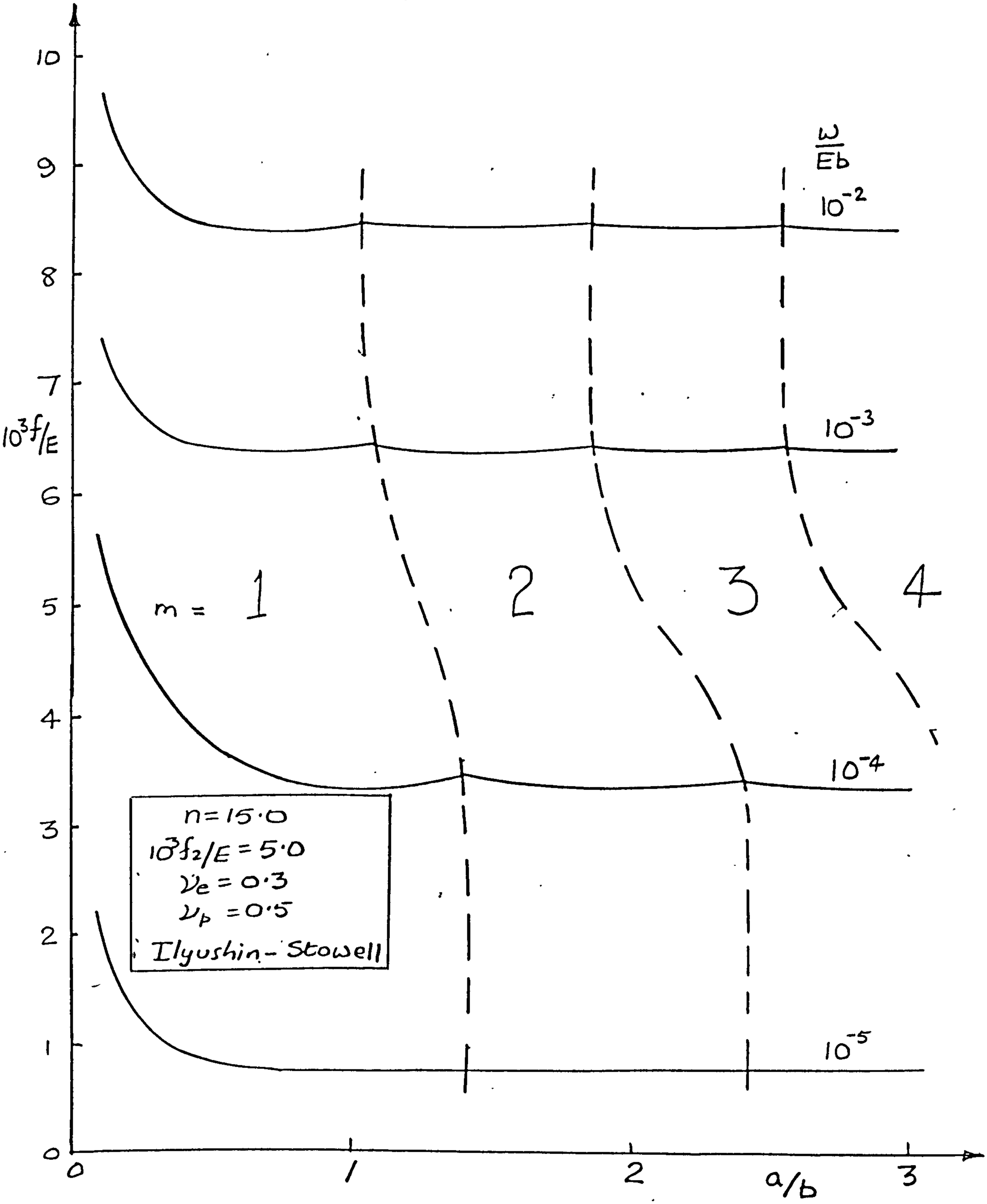

Figure 22. PLATE DESIGN STRESSES RELATED TO LOAD INTENSITY AND ASPECT RATIO

Chapter 4

THE HONEYCOMB SANDWICH PLATE

General

The weight of uniform isotropic elastic plate of the sort described in chapter 3, which is required to be just stable under edgewise compressive loading, will be proportional to material density ρ, and inversely proportional to the cube root of the elastic modulus E (as indicated by equation (69)).

For most engineering metals used in the fabrication of structures, elastic modulus is almost proportional to density, within quite close limits. Thus plate weight will be approximately proportional to density raised to the two thirds power, and lower density materials of this sort will always have an intrinsic advantage.

Thus aircraft structures which in the first instance are frequently stability critical are typically manufactured from aluminium rather than steel, and on this basis an advantage could be shown for beryllium and magnesium were it not for certain practical fabrication problems. Higher density materials such as titanium and steel are only used if some additional influence, such as the need to resist high temperatures, should intervene.

Clearly therefore there are practical limits to the process of improvement in efficiency by simply choosing lower density materials. An alternative approach is to lower the effective density of the structure by dispersing the structural material in space. This notion is the essence of the stiffened plate structure which, though complicated and expensive to manufacture, offers greatly increased efficiency compared with the solid plate, and indeed is a commonplace in structural design practice.

The most common form of stiffening involves the addition of folded or extruded beamlike members to a flat sheet. In its simplest form, this results in the wide-column stiffened plate which is considered in the next chapter.

An attractive alternative method is to divide the basic sheet into two, and to separate the panels so formed by a low density medium which provides a shear connection between the faces, analogous to the web of an I-beam. A further advantage lies in the continuous, albeit elastic, foundation which provides a stable mounting for the faceplates. The sandwich panel so formed has found many applications in aerospace and other structures for which efficiency is at a premium.

Many materials have been used for the core including organic foam, balsa wood and honeycomb fabricated from a wide variety of materials such as aluminium, paper, fibreglass, etc.

The structure considered here utilises a hexagonal core honeycomb, which is assumed to have been fabricated from the same material as the faceplates. This form of construction has been widely used (e.g. aluminium/aluminium) and will be sufficient to illustrate the design problem with which this work is concerned. Generalisation to other combinations of materials is straightforward. Many authors have published work relating to the analysis and design of this form of construction, particularly in the 1950's when it seemed as if the sandwich panel combination of high efficiency and good surface finish would be particularly valuable to the supersonic aeroplane.

The fundamental problem of the buckling of the faceplates on the elastic foundation provided by the core was considered originally by Gough, Elam and de Bryne [41], and this work was continued by Hoff and Mautner [42] and Yusuff.[43]

Design problems were considered by Wittrick[31] and Williams[44] who neglected two dimensional plate effects however, and Bijlaard[45]. A comprehensive design treatment was given by Kaechele [46], who noted the superiority of sandwich at low load intensities on the rather uncertain foundation of a structural index comparison with wide column designs using differing dimensional bases. Perhaps the best modern text on sandwich construction is that of Plantema[37], which covers comprehensively most aspects of sandwich behaviour, including plasticity effects, although little note is taken explicitly of design problems. There is also a somewhat more limited text due to Allen[47], which nevertheless contains much useful data.

Analysis

Compared with the uniform isotropic plate, two additional characteristics must be considered in the design of sandwich panels. These are faceplate wrinkling, a form of local instability characterised by very short wavelengths, and transverse shear flexibility.

Faceplate wrinkling stress is given by the well established relationship

$$f = K_W[E_f E_c G_c]^{\frac{1}{3}} \qquad \ldots (83)$$

where E_f = faceplate modulus.

To allow for plasticity, Plantema[37] suggests the use of the geometric modulus given by

$$\frac{E_f}{E} = \frac{4E_t}{\left[E^{\frac{1}{2}} + E_t^{\frac{1}{2}}\right]^2} \qquad \ldots (84)$$

E_c = core direct modulus measured normal to faceplate.

G_c = core shear modulus under transverse shear forces.

It will be assumed that G_c is constant in all planes normal to the faceplate surface, although methods of manufacture used for honeycomb usually lead to increased stiffness in particular directions.

The buckling coefficient K_W has been assigned various values by different authors. A conservative lower bound is $K_W = 0.5$ which takes account of the destabilising effects of manufacturing imperfections in both the faces and core.

For an ideal honeycomb core, shear and direct modulus may be related by geometric considerations leading to

$$E_c = \frac{64}{15}(1+\nu_e)G_c \qquad \ldots (85)$$

Equations (84) and (85) may now be used in conjunction with the expressions for tangent modulus as a function of stress given by (A4) and (A7) to develop a relationship between the faceplate stress and the core shear modulus required to prevent wrinkling in the following form

$$\frac{G_c}{E} = \frac{1}{16}\left[\frac{15}{(1+\nu_e)K_W^3}\right]^{\frac{1}{2}} \left(\frac{f}{E}\right)^{\frac{3}{2}} \left[1 + (1+n\phi)^{\frac{1}{2}}\right] \qquad \ldots (86)$$

This equation is shown plotted in figure 23 for a typical aluminium alloy ($n = 15$, $f_2/E = 0.005$, $\nu = 0.3$).

The very lightest aluminium honeycomb core quoted by Allen [47] is made from 0.0007 in foil with 0.25 in cells and has a mean value of $G_c/E = 0.00153$.

It may be seen from figure 23 that a core of this stiffness would be sufficient to stabilise faces made of the example material over the entire range of stress up to 0.2% proof stress, which is often taken as the maximum allowable.

It follows that core stiffness requirements for resistance to wrinkling can be expected to be easily satisfied from a design point of view, and the incorporation of a practical minimum core stiffness constraint will be essential in any design routine.

Plantema [37] has derived a solution for the compressive loading at which overall buckling will occur in a simply supported sandwich plate which may be written in the following form

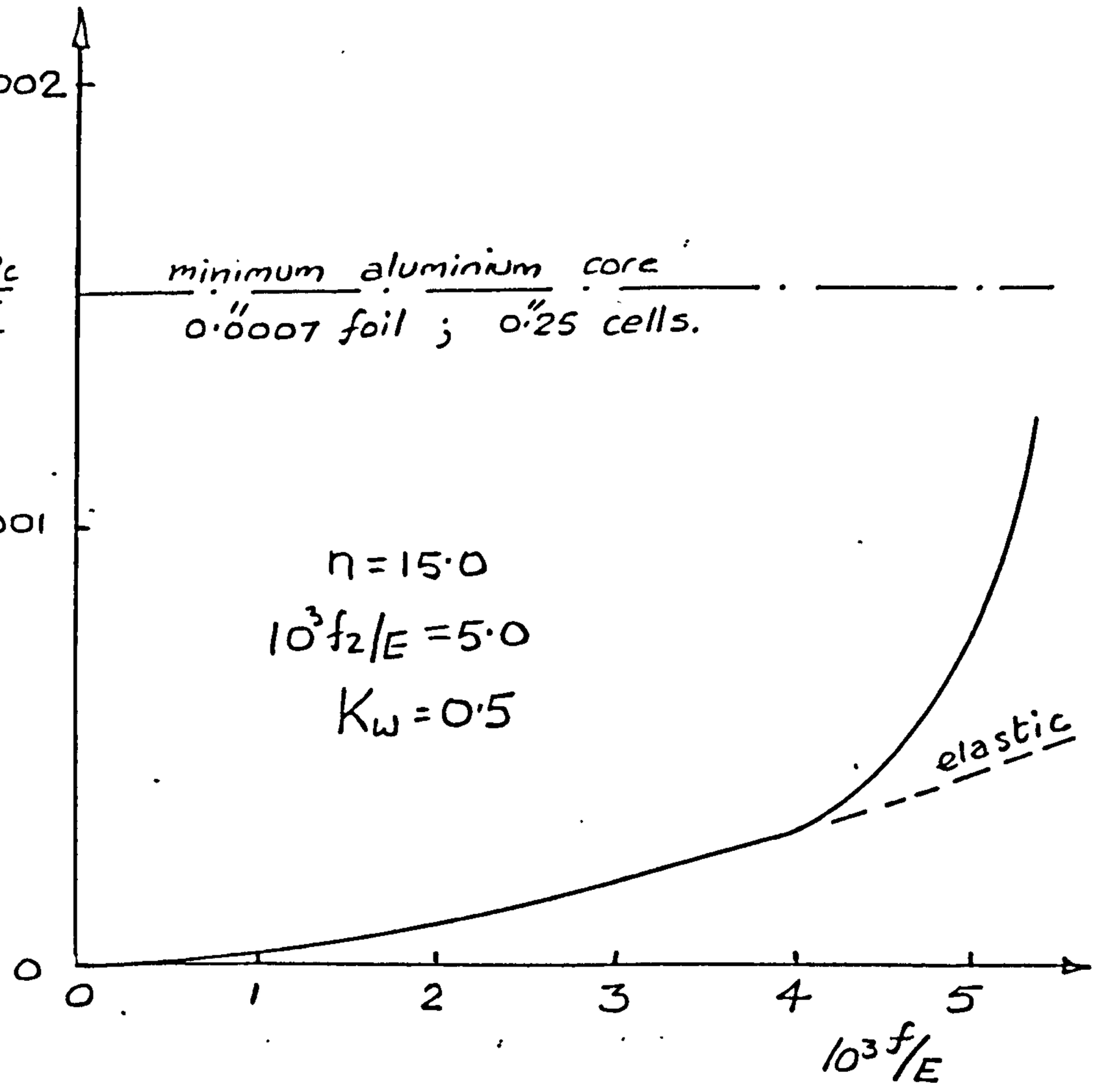

Figure 23. CORE STIFFNESS REQUIRED TO PREVENT FACEPLATE WRINKLING

$$\frac{\omega}{Eb} = \frac{\frac{h}{b}\cdot\frac{E_r}{E}\cdot\frac{G_c}{E}(1+\lambda)^2}{1+\lambda\left[1+\frac{2(1-\nu_e^2)}{\pi^2}\frac{G_c/E}{t/b\,h/b}\right]} \qquad \ldots (87)$$

where t = faceplate thickness
h = panel depth
b = panel width transverse to loading direction
ω = compressive endload intensity per unit width

Plantema suggests the use of the reduced modulus to represent the effects of plasticity on faceplate stiffness, so that

$$E_r = \frac{2EE_t}{E+E_t} = \frac{2E}{2+n\phi} \qquad \ldots (88)$$

λ = wavelength parameter = $(\frac{a}{mb})^2$

b = panel length

m = number of half waves in direction of loading which for a given panel must be chosen to minimise ω.

Equation (87) is based on the usual sandwich assumptions that transverse shear forces are carried by the core, and bending stiffness is provided entirely by the faceplates which are thin relative to sandwich depth.

The elastic solution to (87) is shown plotted in figure 24 which has been transcribed from Plantema The parameter 1/S is proportional to shear flexibility, expressed as a ratio to bending flexibility. As shear flexibility increases, it may be noted that buckling strength is eroded, and also that buckle wavelength is reduced. With zero shear flexibility, the solution reduces to that of the thin isotropic plate.

Design

The design variables whose values are to be fixed include core density, panel depth and faceplate thickness from which faceplate stress follows directly since design endload is given

i.e.

$$2\cdot\frac{f}{E}\cdot\frac{t}{b} = \frac{\omega}{Eb}$$

The wrinkling condition defines core density in terms of faceplate stress, so that (87), which is quadratic in sandwich depth, may be solved to give sandwich depth as a function of stress only, in the following form.

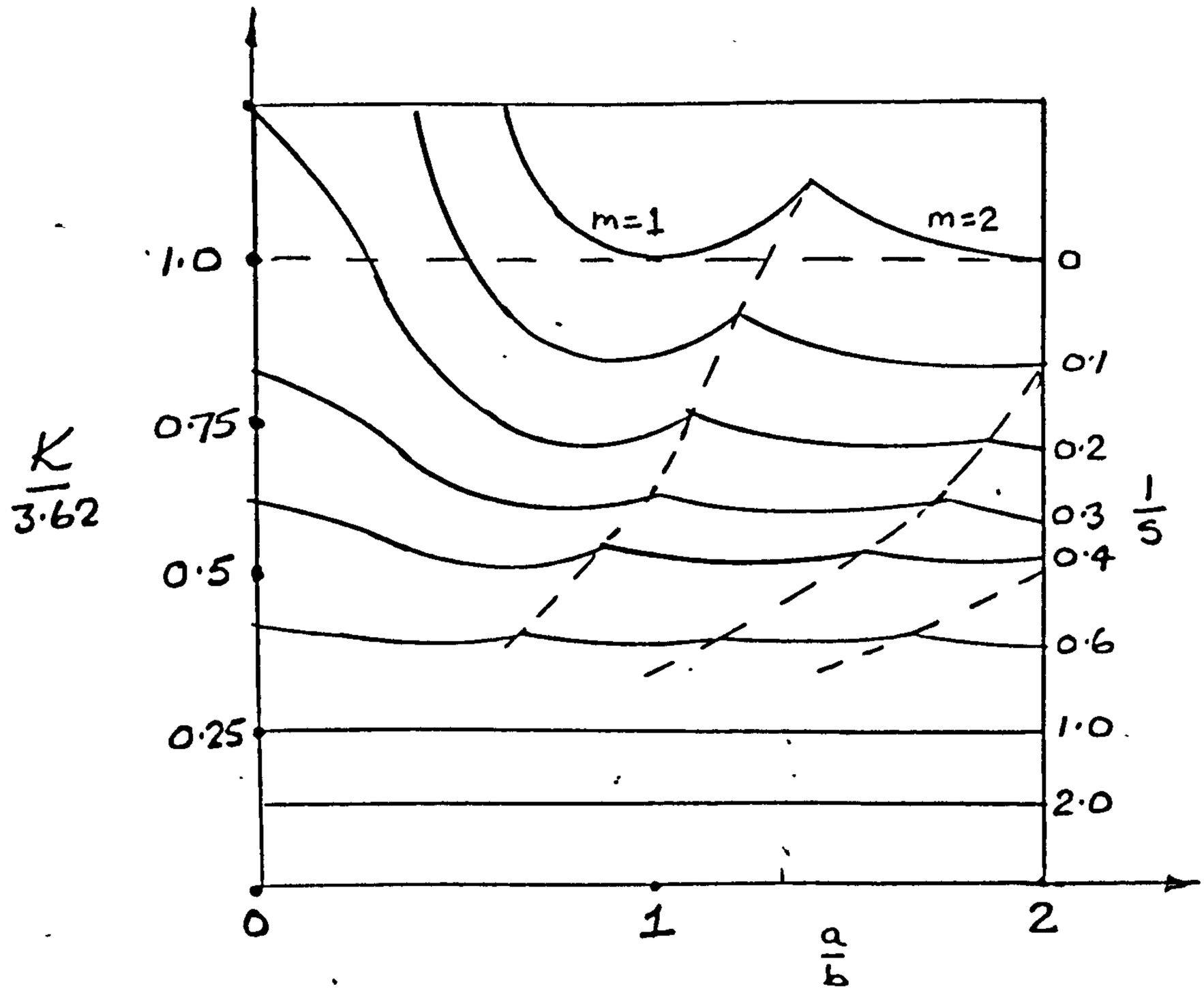

Figure 24. THE EFFECT OF TRANSVERSE SHEAR FLEXIBILITY ON PLATE BUCKLING STRESS (AFTER PLANTEMA 37)

$$\frac{h}{b} = \frac{\frac{\omega}{Eb}}{2(1+\lambda)\frac{G_c}{E}\cdot\frac{E_r}{E}}\left[1+\left\{1+\frac{16(1-\nu_e^2)}{\pi^2}\cdot\frac{f}{E}\cdot\frac{E_r}{E}\left[\frac{G_c/E}{/Eb}\right]^2\lambda\right\}^{\frac{1}{2}}\right] \quad \ldots (89)$$

Wave length must be chosen to give maximum panel depth h for any given value of surface stress.

The quantity relating directly to efficiency is the panel equivalent thickness t* which allows for core weight, so that

$$t^* = 2t + \frac{\rho_c}{\rho} \cdot h$$

where ρ_c = core density

ρ = faceplate density

For a honeycomb core using the same material as the faceplates

$$\frac{\rho_c}{\rho} = \frac{64}{15}(1+\nu_e)\cdot\frac{G_c}{E} \quad \ldots (90)$$

so that finally

$$\frac{t^*}{b} = \frac{\omega}{Eb}\Big/\frac{f}{E} + \frac{64}{15}(1+\nu_e)\frac{G_c}{E}\cdot\frac{h}{b} \quad \ldots (91)$$

which is a function of faceplate stress alone.

An investigation of this function by varying faceplate stress reveals well ordered behaviour with high values of equivalent thickness at low stress when face thicknesses predominate, and again at high stresses when core weight becomes excessive. At some intermediate stress a well defined optimum design may be found as shown in figure 25 which may be accurately determined by numerical interpolation. This task is performed by the programme COSA which is described in Appendix D.

Constraints

An investigation of ideal optimum designs for a range of materials, load intensities and panel proportions reveals that a number of the design variables may assume unrealistic values in certain regimes. The core stiffness problem was noted above at the analysis stage, but other features which emerge include very thin faceplates, excessive faceplate stress, and sometimes excessive sandwich depth.

Fortunately it has proved possible in COSA to allow the successive application of these constraints, namely

$$G_c \geq (G_c)_{min}$$
$$t \geq (t)_{min}$$
$$f \leq (f)_{max}$$
$$h \leq (h)_{max}$$

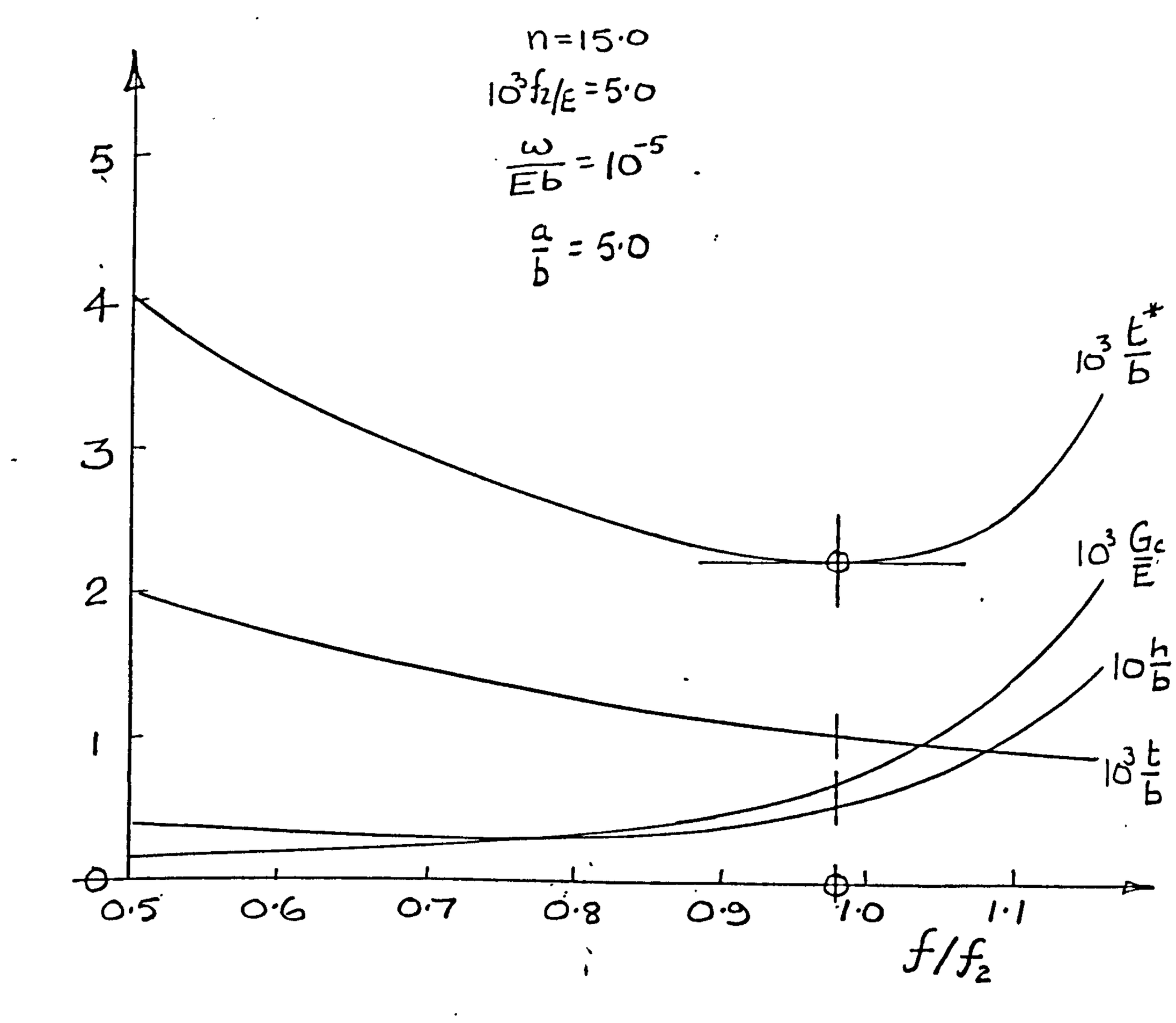

Figure 25. VARIATION OF SANDWICH DESIGN VARIABLES TO DETERMINE MINIMUM WEIGHT

in such a way that when any combination of these are violated, a revised strategy is found which leads to a constrained optimum design.

This process is outlined below, but for more details reference should be made to Appendix D .

The first objective is to determine the ideal (unconstrained) optimum design.

Since end load is given, constraints on face stress and thickness have essentially the same character; and these are checked next. If a violation occurs, the constrained value of stress or face thickness is applied so that effectively design stress is reduced from the optimum value. Core modulus required to prevent wrinkling may now be reduced, but must also be continuously checked against its minimum value. Sandwich thickness required to resist panel buckling may now be determined, and subsequently subjected to its own maximum value check.

When stress/thickness are unconstrained, core modulus may be too low, in which case with a constrained value inserted, face stress may rise to some value bracketed between the ideal optimum and the maximum permitted. New constrained dimensions are then immediately established, and the revised design is again available for the sandwich thickness check.

If maximum sandwich thickness is exceeded, the revised constrained design will work at some lower face stress with a corresponding lower core stiffness if possible. Stress and face thickness constraints cannot now be freshly violated and the constrained design may be completed.

Throughout the computation the sandwich thickness relationship must be frequently solved which requires that the panel buckling wavelength be chosen as an integral part of panel length. A fortunate feature of sandwich panel behaviour in this respect is that both transverse shear flexibility and plasticity reduce buckle wavelength so that the thin elastic plate value may always be used as a lower bound starting point in the search for the correct value.

Design space topology

In order to effectively discuss the philosophy underlying the optimisation routine outlined above; it is essential to consider in detail the characteristic topology of the appropriate design space. The two primary design variables are surface stress and core stiffness (proportional to core density), assuming that faceplate material properties are given.

Following extensive numerical investigation, two types of behaviour may be distinguished which depend broadly on design load intensity. Typical design spaces for each type are illustrated in figures 26 and 27 The design spaces show contours of constant equivalent panel thickness (which we seek to minimise), together with panel depth contours and the wrinkling criterion discussed earlier. At low load intensities, panel buckling is primarily flexural in character and panel depth required to prevent this is found to be almost independent of core stiffness.

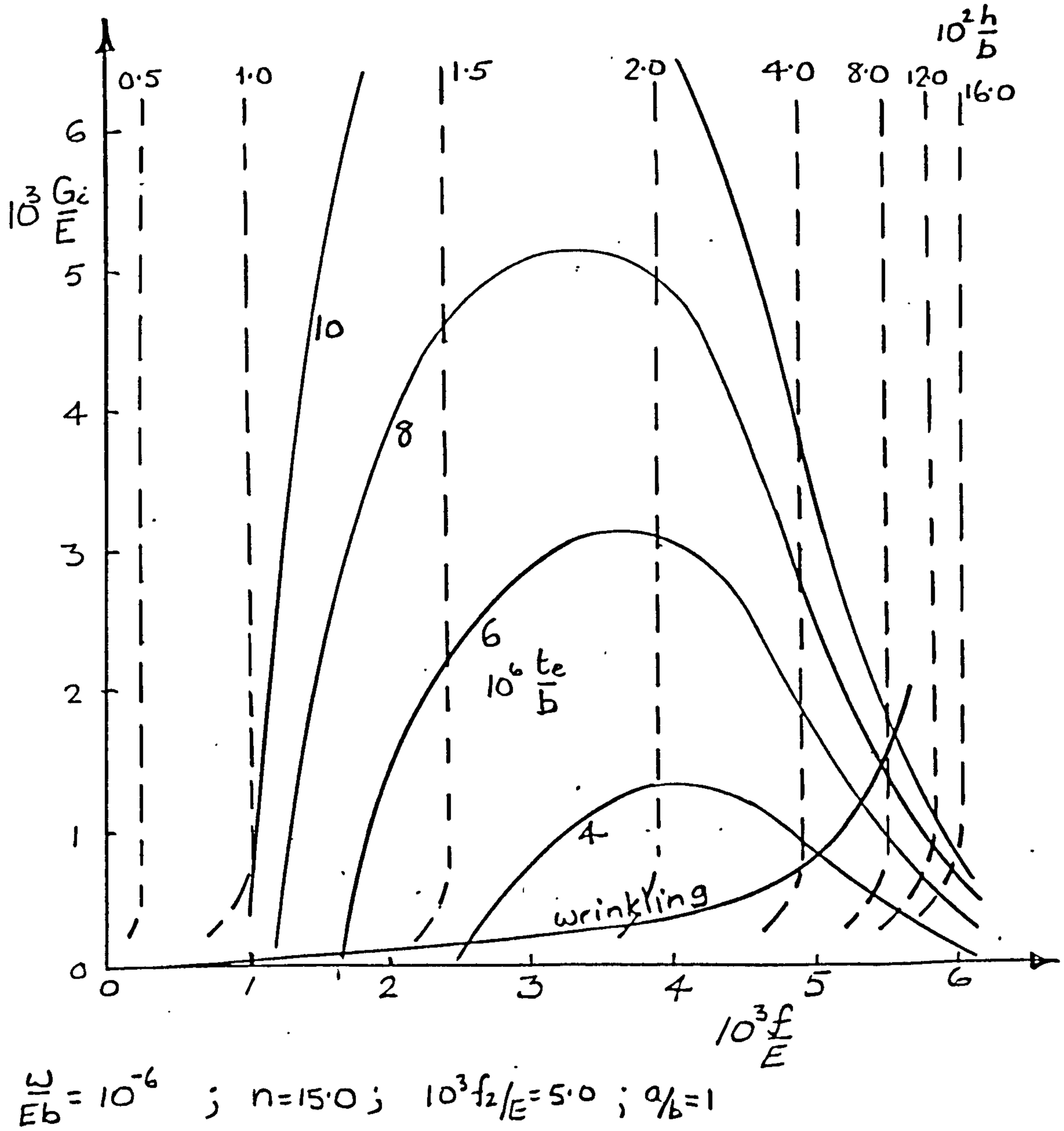

$\frac{\omega}{Eb} = 10^{-6}$; $n = 15.0$; $10^3 f_2/E = 5.0$; $a/b = 1$

Figure 26. HONEYCOMB SANDWICH PLANEL DESIGN SPACE: LOW LOAD INTENSITY

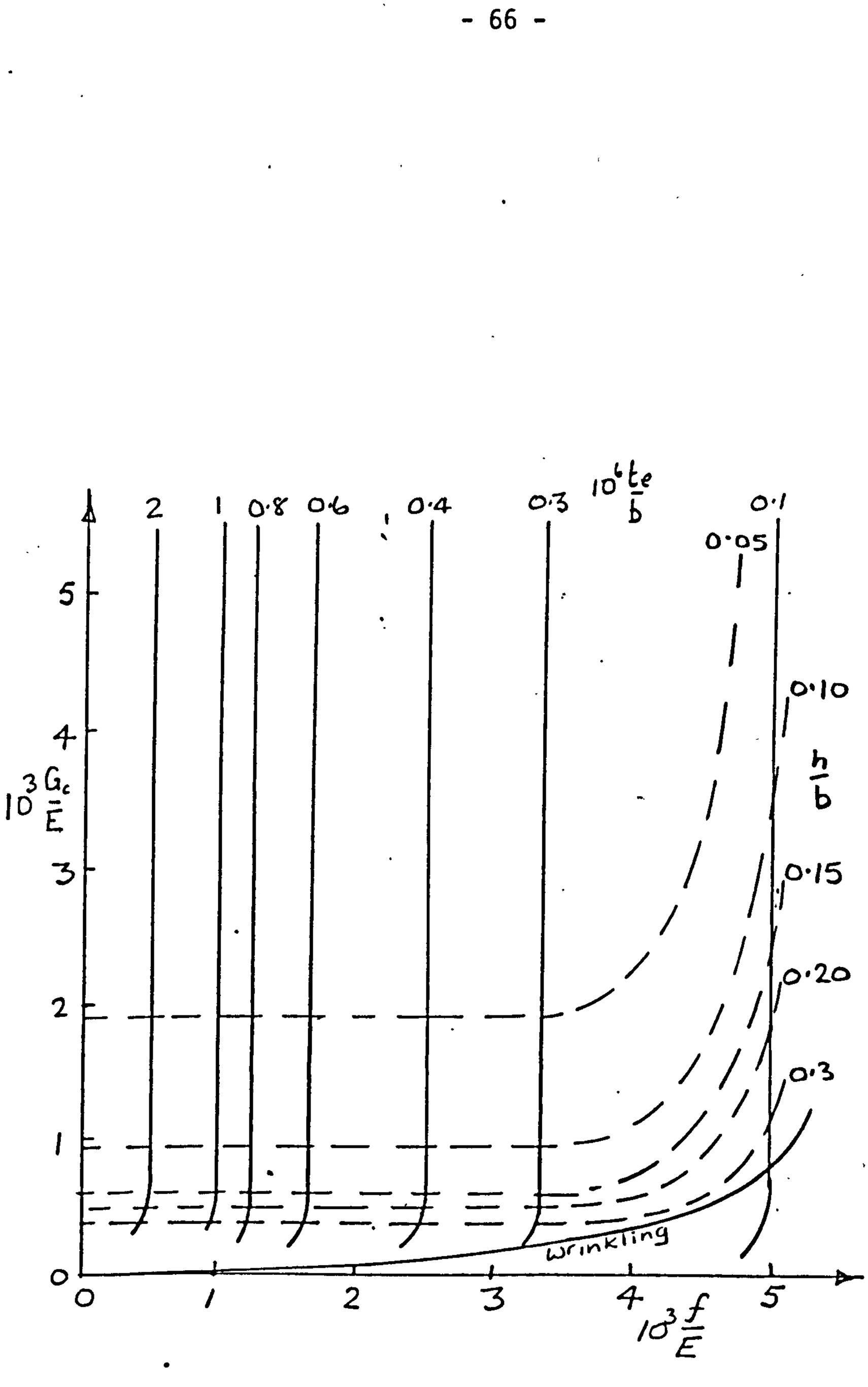

$\frac{\omega}{E b} = 10^{-3}$; $n = 15.0$; $10^3 f_2/E = 5.0$; $a/b = 1$

Figure 27. HONEYCOMB SANDWICH PANEL DESIGN SPACE: HIGH LOAD INTENSITY

Equivalent thickness however increases monotonically with core stiffness, which must therefore always be assigned its minimum possible value at any given stress level. Clearly the panel should always be designed to just meet the wrinkling criterion, unless minimum core stiffness or maximum faceplate stress constraints intervene. In these circumstances the equivalent thickness contour pattern indicates that an optimum faceplate stress may always be found.

When load intensities are high (or, equivalently, the panel is very short), transverse shear flexibility begins to dominate panel buckling behaviour. It is found that a reciprocal relationship becomes established between core stiffness and panel depth so that the product of these two qualities (to which equivalent thickness is proportional), becomes constant. Thus panel equivalent thickness is effectively independent of core stiffness, and depends only on faceplate stress. Designs in this regime will therefore tend to be either maximum stress or wrinkling stress limited, and the underlying conception of always minimising core stiffness remains valid. Panel depths may get quite large for designs at high load intensities, and will therefore frequently be constrained in this respect. However, observation of the appropriate design space topology has enabled a proper solution sequence allowing for all real contingencies to be worked out, and this has been incorporated in the programme COSA.

Optimisation

An examination of the design space layout indicates that a combination of wrinkling and panel buckling is invariably critical for the ideal optimum designs, and a routine to determine this is comparatively straightforward to devise. As was shown above, both criteria may be expressed as a function of faceplate stress alone, which may then be varied until the lightest design is located. A review of the results obtained from this optimisation process gives definite indications of the ways in which engineering practicalities may preclude the use of the ideal optimum.

The very high intrinsic stability of this form of construction leads often to either extremely thin faceplates or very high faceplate stresses (or both). Since design endload intensity is given, these two constraints may be interchangeably expressed either in stress or thickness terms, and a logical programme sequence to cater for a prespecified restriction of these variables is easily devised.

Minimum thickness must be specified as a proportion of panel width, and a typical value might be given by

$$t \geq t_{min} = 0.001b \qquad \ldots (92)$$

Maximum stress depends on the appropriate design code, but might often be the 0.2 per cent proof stress.

The core stiffness required to avoid wrinkling, and to give the panel sufficient transverse shear stiffness in the panel buckling mode is often quite small in relation to the types of core available as was noted above, so that core stiffness will always be bounded from below.

A typical value for this restriction might be

$$G_c \geq G_{c\,min} = 0.001E \qquad \ldots (93)$$

Designs for very short, or heavily loaded panels are likely to be dominated by transverse shear stiffness, and the ideal optimisation process leads to large panel depths.

The buckling load in the pure shear mode is given by

$$\omega = h\,G_c$$

As the core contribution to panel weight is proportional to hG_c also, core weight therefore tends to be invariant in these circumstances, and consequently the panel tends to become deeper to minimise the weight of faceplate material required to provide the necessary minimum flexural strength.

When panel depth is restricted to a value smaller than the optimum, this usually implies that core density must rise, leaving the wrinkling criterion 'submerged' and irrelevant.

Core stiffness will then be fixed by panel buckling requirements with panel depth given.

It may be noted that in these circumstances, the panel buckling equation (87) is linear in core modulus, and may be solved to give

$$\frac{G_c}{E} = \frac{\frac{\omega}{Eb}(1+\lambda)}{\left[\frac{h}{b}\cdot\frac{E_r}{E}(1+\lambda)^2 - \frac{4(1-\nu^2)}{\pi^2}\cdot\lambda\,\frac{f}{E}\cdot/\cdot\frac{h}{b}\right]} \qquad \ldots (94)$$

For any given stress level, the wavelength parameter λ must be chosen to maximise the core stiffness G_c since the panel will always fail in its weakest mode.

The denominator of (94) can become zero when

$$\frac{f}{E} = \frac{\pi^2}{4(1-\nu^2)}\cdot\frac{(1+\lambda)^2}{\lambda}\cdot\frac{E_r}{E}\cdot\left(\frac{h}{b}\right)^2 \qquad \ldots (95)$$

This is precisely the condition for panel buckling by purely flexural action, i.e. with infinite transverse shear flexibility. Care must be taken to cater for this singularity in the coding of the depth constraint routine.

A typical panel depth restriction might be

$$h \leq h_{max} = 0.1b \qquad \ldots (96)$$

The constraint values quoted above in (92), (93) and (96) are typical values which have been used here for illustration. The programme COSA will accept any values the designer may wish to impose.

Ideal elastic design

A solution may be derived for the optimum design of perfectly elastic long sandwich panels of the type under discussion.

From equation (89), the panel depth required to prevent general instability may be written in the form

$$\frac{h}{b} = \frac{B}{1+\lambda}\left[1 + [1 + C\lambda]^{\frac{1}{2}}\right] \qquad \ldots (97)$$

where

$$B = (\omega/Eb)/(2G_c/E)$$

$$C = \frac{16(1-\nu^2)}{\pi^2} \cdot \frac{f}{E}\left(\frac{G_c/E}{\omega/Eb}\right)^2$$

and for elastic behaviour $E_r = E$.

The wavelength parameter λ may be regarded as a continuous variable for long panels, and must be chosen to maximise h/b, i.e.

$$\frac{\partial(h/b)}{\partial \lambda} = 0$$

which leads to the quadratic form

$$(1 + C\lambda) + 2(1 + C\lambda)^{\frac{1}{2}} - (C - 1) = 0$$

for which the significant root is

$$\lambda = 1 - 2/C^{\frac{1}{2}} \qquad \ldots (98)$$

therefore

$$\frac{h}{b} = \frac{B}{2-2/C^{\frac{1}{2}}}\left[1 + [1 + C - 2C^{\frac{1}{2}}]^{\frac{1}{2}}\right] \qquad \ldots (99)$$

The core shear modulus required to prevent wrinkling under elastic conditions (ϕ = 0) at surface stress f is given by (86) to be

$$G_c/E = A\left[f/E\right]^{\frac{3}{2}} \qquad \ldots (100)$$

where

$$A = \frac{1}{8}\left[\frac{15}{(1+\nu)K_w^{\,3}}\right]^{\frac{1}{2}}$$

Finally (99) and (100) may be used together with (91) to develop an expression for equivalent panel thickness in the following form (when C>>1),

$$\frac{t^*}{b} = \frac{J}{(f/E)} + L(f/E)^2 \qquad \ldots (101)$$

where $J = \omega/Eb$

and $L = \left[\frac{64(1+\nu)(1-\nu^2)}{15\pi^2 K_w^3}\right]^{\frac{1}{2}}$

$(= 2.0227 \text{ for } K_w = 0.5, \nu = 0.3)$

The stress which minimises equivalent thickness may be found by differentiating (101), which process allows the following properties of the optimum elastic sandwich to be derived

$$\left.\begin{aligned} \frac{f}{E} &= 0.6276\left(\frac{\omega}{Eb}\right)^{\frac{1}{3}} \\ \frac{h}{b} &= 0.2406\left(\frac{\omega}{Eb}\right)^{\frac{1}{6}} \\ \frac{t^*}{b} &= 2.3901\left(\frac{\omega}{Eb}\right)^{\frac{2}{3}} \\ \frac{f^*}{b} &= 0.4184\left(\frac{\omega}{Eb}\right)^{\frac{1}{3}} \end{aligned}\right\} \qquad \ldots (102)$$

where $f^* = \omega/t^*$ = equivalent design stress.

It may be further noted that for this design, the core contributes precisely one third of total sandwich weight.

The above results represent an absolute upper bound to sandwich efficiency and as such provide a useful basis for comparison with results obtained from COSA. This enables the erosion of the ideal optimum due to plasticity, and dimensional constraints to be viewed in perspective.

Numerical results

The programme COSA has been used to generate a range of results which serve to illustrate the quantitative effect on sandwich design of various fundamental parameters. The important given quantities include load intensity, panel aspect ratio, material proof stress, and dimensional constraint values.

The choice of parameter magnitudes has been made in the perspective of values which would be appropriate to panels made from a typical medium strength aluminium alloy for which

$$f_2/E = 0.005$$
$$n = 15.0$$

Load intensities and proof stresses are considered within the ranges

$$10^{-7} \geq \omega/Eb \geq 10^{-4}$$

$$0.0025 \geq f_2/E \geq 0.010$$

Constraints were applied with the following values

$$f/E \leq f_2/E$$

$$G_c/E \geq 0.001$$

$$h/b \leq 0.1$$

$$0 \leq t/b \leq 0.001$$

Results for panels of low aspect ratio ($0 \leq a/b < 3.0$) are shown plotted in figures (29) to (31) for a range of proof stresses and two load intensities ($\omega/Eb = 10^{-6}, 10^{-4}$). Unconstrained optimum values are given for equivalent thickness, panel depth and core modulus which show the characteristic overlapping sequence of integral wavelength values. The results indicate only small variations in properties for panel aspect ratios greater than about 1.5, with increasing core modulus and panel equivalent thickness as proof stress is reduced.

The effects of varying proof stress and load intensity are best illustrated by restricting attention to long panels ($a/b = 5.0$ in this case). Figure (32) shows equivalent panel stress related to these parameters, and graphically illustrates the importance of high proof stress for this form of construction. The upper bound to equivalent stress is provided by the ideal elastic solution given by equations (102), which are confirmed by running COSA with a very high proof stress ($f/E = 0.05$) so that plasticity effects are negligible.

Constraint effects are illustrated by again using long panels of constant proportions. Figures (33), (34) and (35) corresponding to $f/E = 0.005$ and 0.05 show how the imposition of practical limitations on both faceplate thickness and core modulus make serious inroads into the ideal theoretical efficiency of sandwich panels of this type over the practical range of load intensities.

Conclusion

An analysis has been developed for the optimum design of rectangular honeycomb core sandwich panels which are required to be stable when loaded by uniaxial compressive forces. Panels are simply supported and of finite proportions. The calculations allow for the effects of plasticity in the faceplates, and both wrinkling and panel buckling modes are considered. Account is also taken of engineering constraints on faceplate stress and thickness, core modulus and panel depth.

The results obtained show the importance of these constraints, particularly face thickness and core modulus, and also how the inherent stability of this form of construction makes possible the exploitation of any improvement in proof stress.

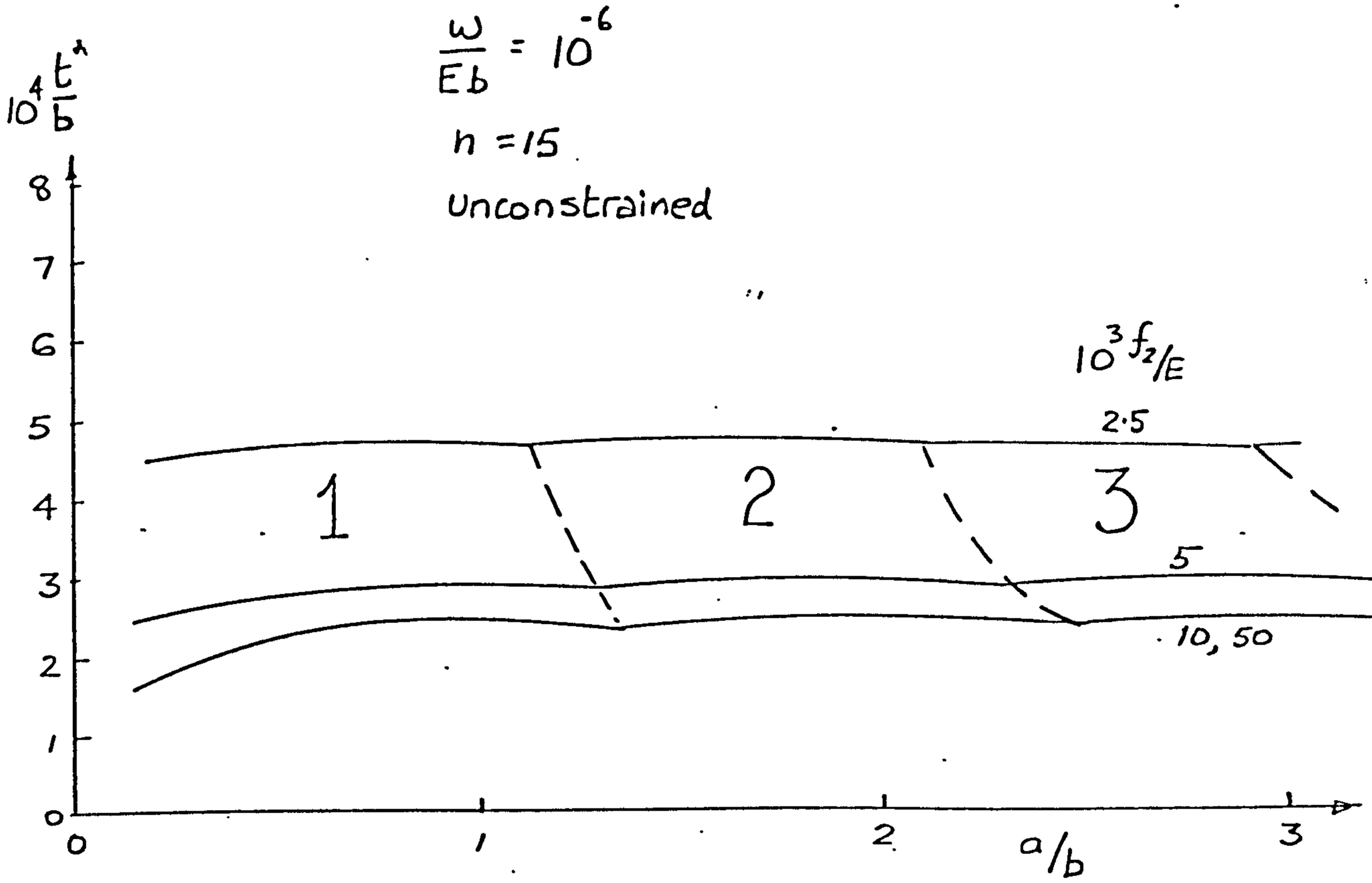

Figure 28. UNCONSTRAINED OPTIMUM EQUIVALENT THICKNESSES FOR HONEYCOMB PANELS

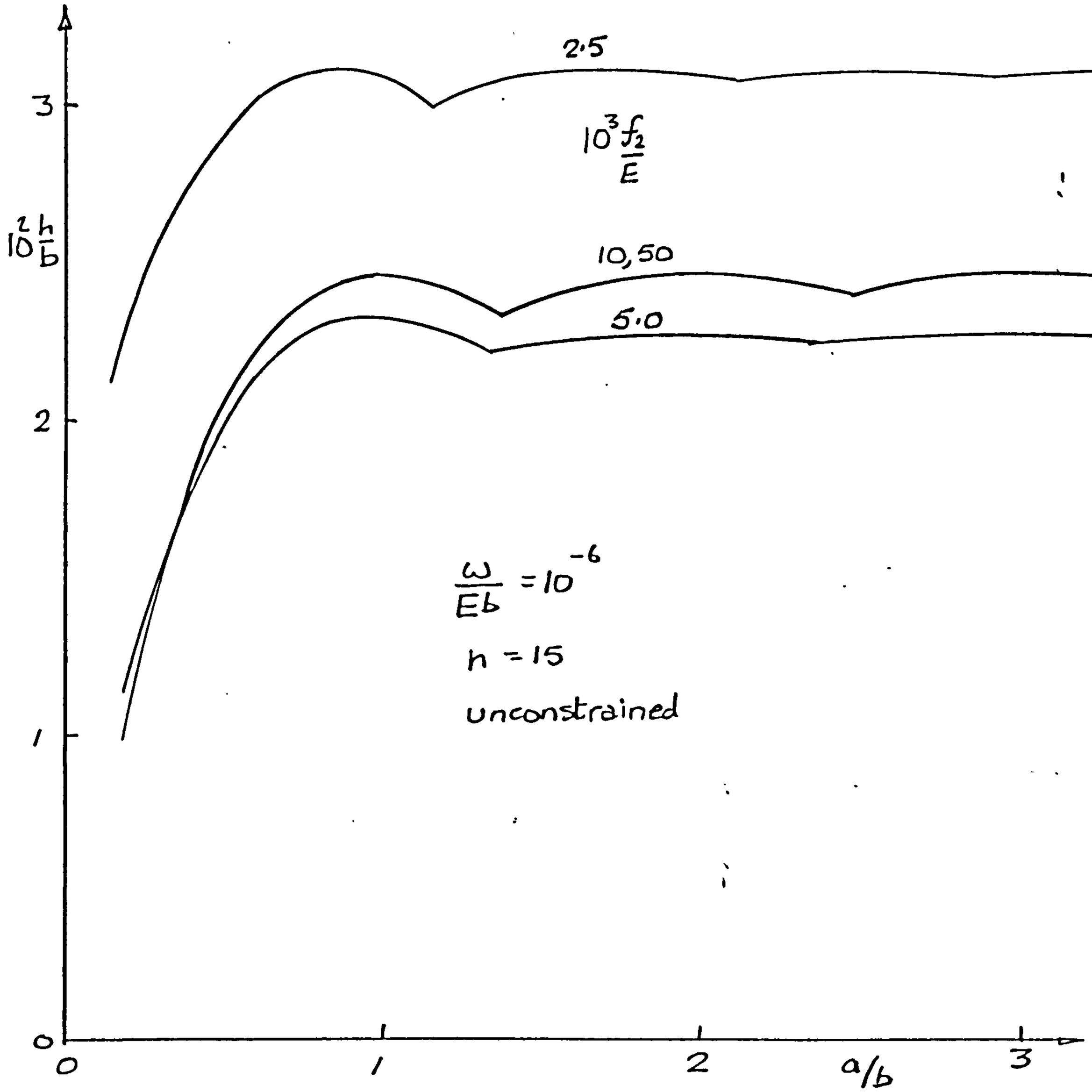

Figure 29. UNCONSTRAINED OPTIMUM SANDWICH DEPTHS FOR HONEYCOMB PANELS.

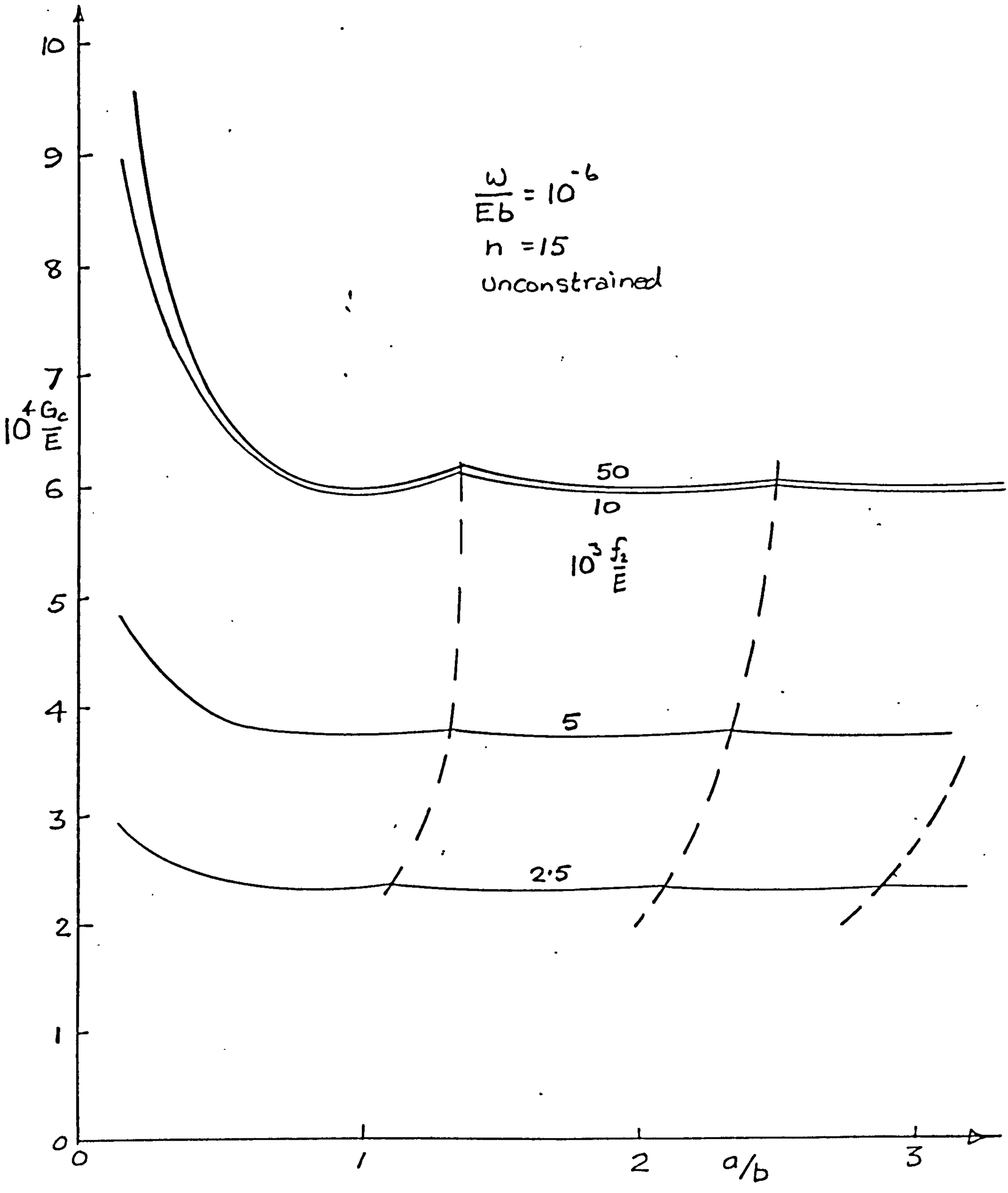

Figure 30. UNCONSTRAINED OPTIMUM CORE MODULI FOR HONEYCOMB PANELS

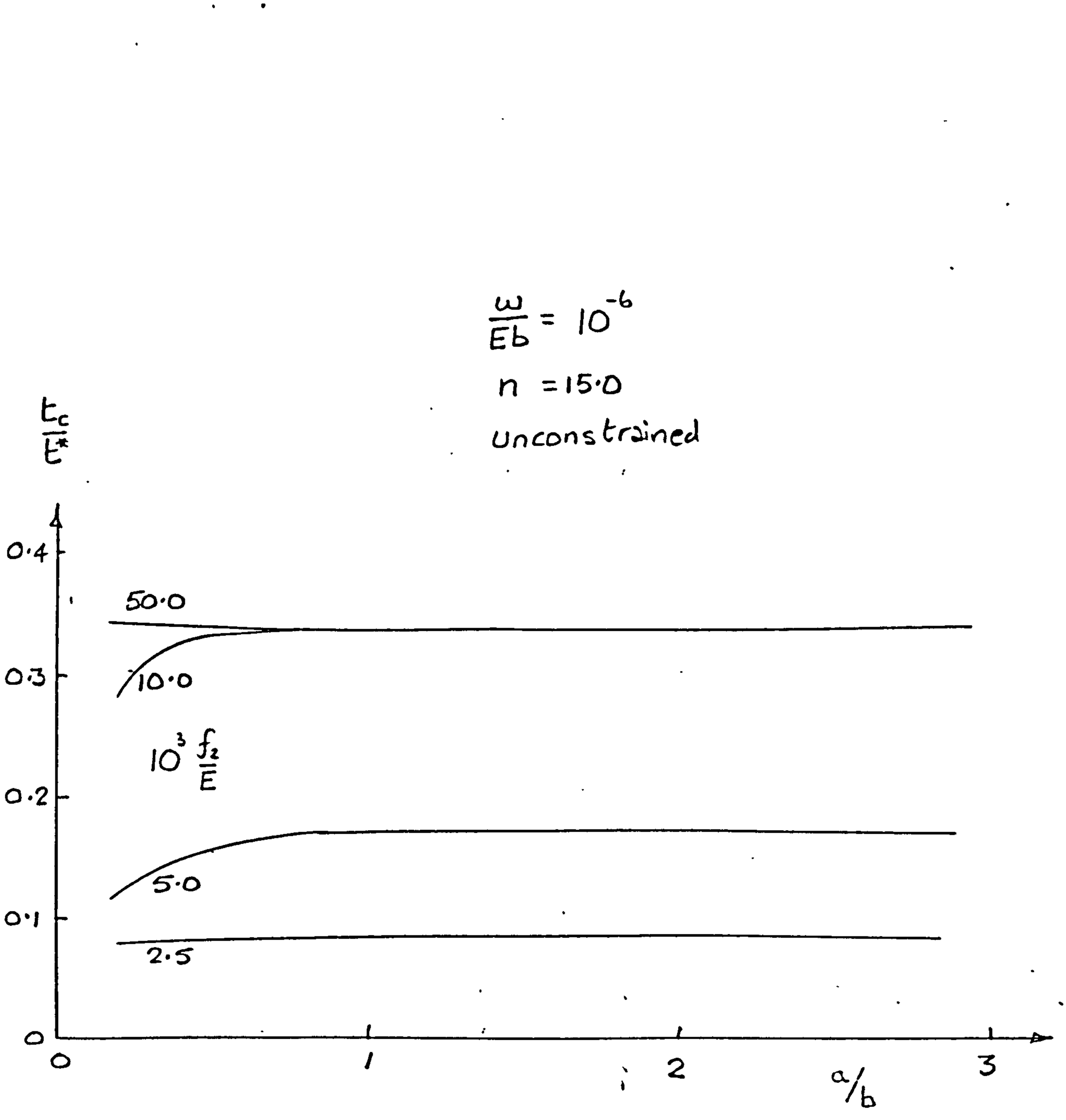

Figure 31. UNCONSTRAINED OPTIMUM CORE PROPORTION OF TOTAL THICKNESS FOR HONEYCOMB PANELS

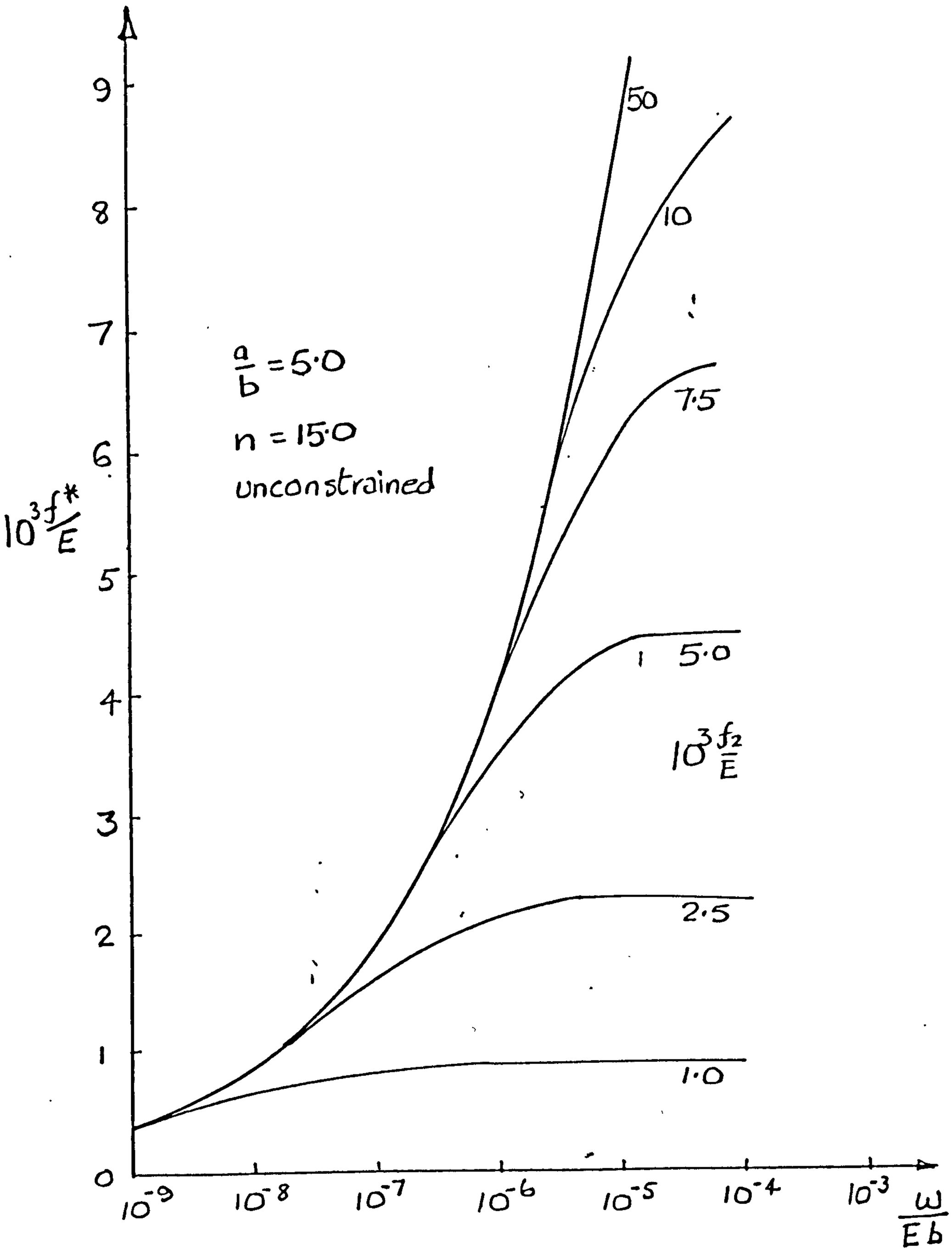

Figure 32. UNCONSTRAINED OPTIMUM EQUIVALENT STRESS FOR HONEYCOMB PANELS

PAGE

MISSING

IN

ORIGINAL

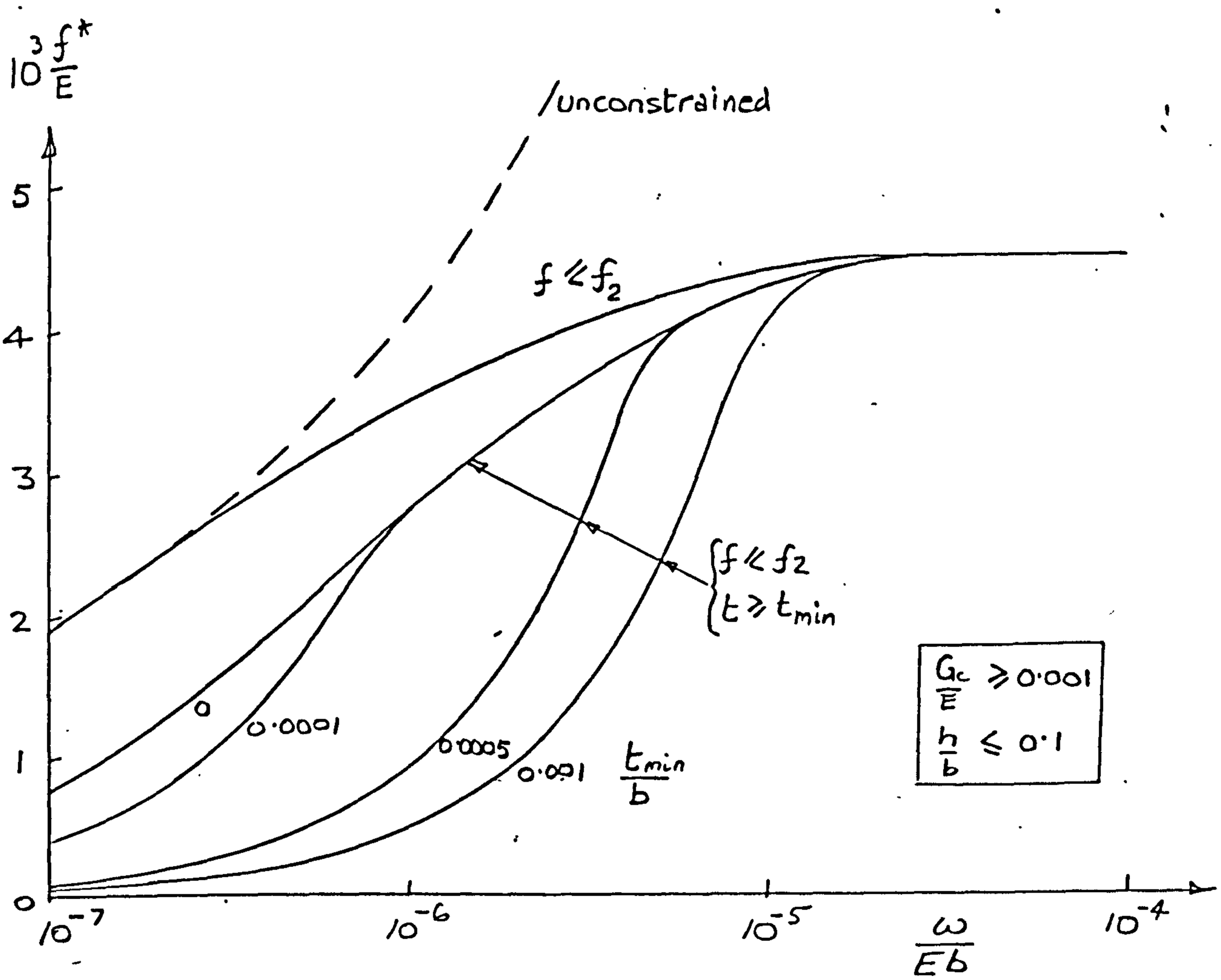

Figure 34. CONSTRAINT EFFECTS ON HONEYCOMB PANEL DESIGN
($f_2/E = 0.005$, $n = 15.0$)

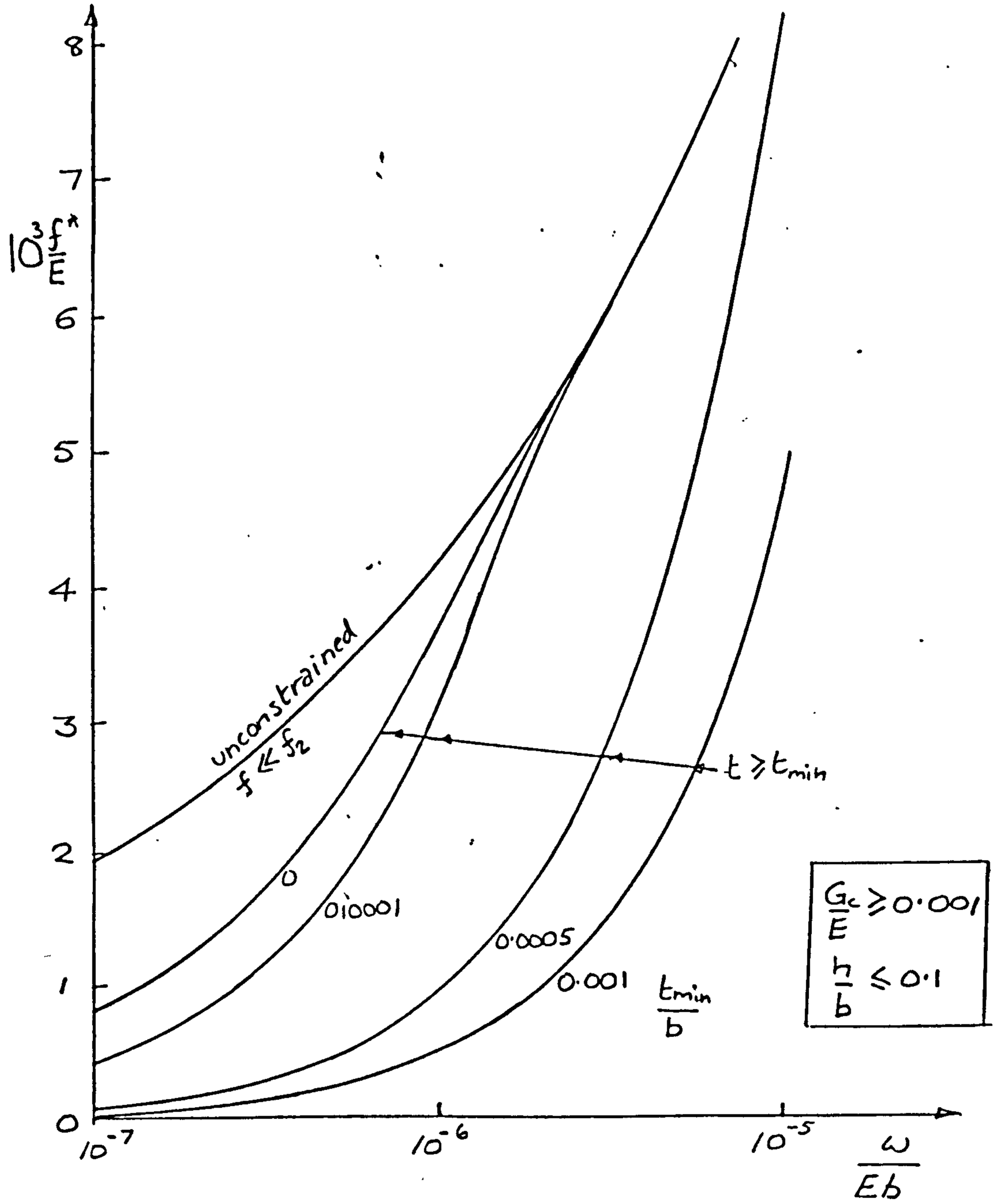

Figure 35. CONSTRAINT EFFECTS ON HONEYCOMB PANEL DESIGN
(f_2/E = 0.05, n = 15.0)

Chapter 5

THE WIDE COLUMN STIFFENED PLATE

Introduction

The most widely utilised form of compression surface in structural engineering is the wide column type stiffened plate.

This typically consists of a single thin flat sheet which is stabilised by a unaxial array of prismatic stiffeners, arranged to run in the direction of the applied compressive loading. Such a plate might form the compression surface of a thin walled box beam loaded by bending moments. For a structure of this type, with given major cross-section dimensions, the bending moment may be transformed to give an equivalent compressive load per unit width in the surface as the primary design loading. The effect of varying cross-section dimensions with the design bending moment becoming the primary loading quantity, is considered at a later stage for the particular case of the circular shell.

Plates of this type are cheap and simple to manufacture, and their behaviour under load may be reliably analysed by well established methods.

Materials used are mostly isotropic metals such as steel and aluminium, although more exotic construction with fibre reinforced composites is increasingly being considered in situations when the payoff for advanced efficiency is sufficiently high.

A significant advantage of this form of construction from a design point of view is that a smooth continuous surface is provided to perform secondary operational functions, as in the case of the aeroplane wing and fuselage which require aerodynamic smoothness, or the bridge deck for which surface traffic must be accommodated. A penalty must be paid for this property, e.g. the intrinsically more efficient form is the symmetric trapezoidal corrugation which is not smooth. A further consideration is that a continuous shear flow path is provided enabling the box to transmit torque and transverse shear forces effectively.

Widespread application in aerospace structures has led to intense study of the efficiency of this form of construction, notably by Cox[16], Farrar[10], Catchpole[48], Gerard[13], Richards[49] and many others.

Recently attention has been concentrated on the effects of manufacturing imperfections, on efficient designs, particularly in the work of Van der Neut,[22] Thompson,[23] Tvergaard,[50] Cox and Grayley[28] and Crawford and Hedgepeth[29]. A later section of this work deals with one - aspect of this behaviour as it affects the design of a corrugated tower - in compression. However, in the present context the problem of the imperfection sensitivity of designs which have near simultaneous modes of failure is in a sense avoided by specifying simultaneous failure criteria, which may incorporate appropriate factors whose proper magnitude future research will, hopefully, identify.

This type of plate is typically utilised in conjunction with a regular array of transverse frames or bulkheads, which enforce nodes in the Euler buckling mode. The function, design and optimum spacing of these members will be considered in detail in the next chapter. Thus for the present analysis, the axial spacing of transverse supports will be regarded as pre-specified.

Dimensional variables

Three groups of dimensional variables may be identified, differing from each other by at least one order of magnitude.

The first (largest) group is led by frame pitch L, and includes such dimensions as box width C, and circular shell diameter D. This group defines the major dimensions of the structure, and are regarded as pre-specified for this section of the work.

The second order group includes dimensions comparable with the stiffener spacing b. Thus stiffener height h and flange width d are included.

The third order group is characterised by the skin thickness t, and includes stiffener web thickness t_s and flange thickness t_f, for example. The separate identification of the above groups is important since their relative magnitudes are decisive in determining the form of the relevant buckling equations. Also, only members of the same group are used in non-dimensionalising operations, so that non-dimensional quantities defining surface detail are maintained to be of the order of 1.0, which helps to keep arithmetic operations well ordered.

Design criteria

Three modes of buckling may be considered as significant for wide column surfaces.

These include Euler buckling for which the axial stress may be written

$$f_1 = K_1 E_t \left(\frac{b}{L}\right)^2 \qquad \ldots (103)$$

The coefficient K_1, which is a function of the dimensionless ratios describing the proportions of the surface cross-section, i.e. $\frac{t_s}{t}, \frac{t_f}{t}, \frac{h}{b}$, etc., is a geometric property of the cross section and may be written down in explicit algebraic form. It is usually assumed for this purpose that simple support conditions are provided at the boundaries of the panel which are spaced L apart, and that applied compressive loading is uniform over that panel span.

The use of the tangent modulus to account for the effects of plasticity is governed by the same considerations as those affecting the design of isolated struts as discussed in Chapter 2.

Local buckling with wavelengths of the order of stiffener pitch b is characterised by

$$f_2 = K_2 E_t \left(\frac{t}{b}\right)^2 \qquad \ldots (104)$$

Again the buckling coefficient K_2 depends on the same set of dimensionless ratios as K_1, however in general the relationship is not explicit, since the analysis of this form of buckling almost invariably depends on numerical solution of the appropriate equations. Thus these coefficients are usually available only in numerical or graphical form,[32,33,34] or as fairly complex computer subroutines.

An alternative approach is to approximate local buckling behaviour by imposing assumed boundary conditions on the individual elements involved in the cross-sections. This procedure, which renders the analysis explicit while entailing some compromise on accuracy which is not necessarily conservative, will be explored for one form of construction later in this section.

If the transverse members which delineate panel boundaries in the loaded direction have inadequate bending stiffness, then the effects of long wave buckling may propagate over a number of spans. This general form of instability will be discussed in detail in the next chapter, when the design of an array of panels is considered. Meanwhile it will be assumed here that such transverse members are always just sufficiently stiff to provide simple support conditions.

The final restriction on panel design is the maximum allowable surface stress in compression. This will vary depending on the prevailing design regulations. However the value imposed on aircraft structures designed in the United Kingdom which is the 0.2% proof stress is a reasonably typical value, and will be used here.

The buckling stresses defined above may be conveniently related to the design endload per unit width ω by the following equilibrium equation

$$f = K_3 . \frac{\omega}{t} \qquad \ldots (105)$$

where the coefficient K_3, being the ratio between skin thickness t and equivalent surface thickness t_e, is a function of the geometric properties of the particular form of construction under consideration, and as such may always be expressed as an explicit algebraic function of the dimensionless ratios which comprise the design variables.

Design

It may be readily shown that the highest stress will be achieved when $f = f_1 = f_2$, so that equations (103), (104) and (105) may be combined to give design stress, and the leading dimensions t and b in the following form which was originally derived by Farrar.[10]

$$f = F\left[\frac{\omega E_t}{L}\right]^{\frac{1}{2}} \quad \ldots (106)$$

$$b = B\left[\frac{\omega L^3}{E_t}\right]^{\frac{1}{4}} \quad \ldots (107)$$

$$t = T\left[\frac{\omega L}{E_t}\right]^{\frac{1}{2}} \quad \ldots (108)$$

where

$$F = \left[K_1 K_2 K_3{}^2\right]^{\frac{1}{4}} \quad \ldots (109)$$

$$B = \left[\frac{K_2 K_3{}^2}{K_1{}^3}\right]^{\frac{1}{8}} \quad \ldots (110)$$

$$T = \left[\frac{K_3{}^2}{K_1 K_2}\right]^{\frac{1}{4}} \quad \ldots (111)$$

It may be noted that the coefficients F, B and T are functions only of the dimensionless design variables t_s/t, h/b, etc. Thus these quantities may be independently varied to maximise the stress coefficient F to which surface stress and hence efficiency is proportional. A number of authors[10, 48, 51] have performed these calculations for various forms of construction, resulting in optimum values for the design variables, which in turn fix the coefficients B and T enabling the complete design to be specified. Typical results are shown in the following table.

	F_o	B_o	T_o	ref.
	0.95	0.92	0.42	10
	0.81	1.30	0.50	48
	1.27	1.05	0.59	49

Approximate optimisation

It is a common practice in stress analysis to approximate the local buckling behaviour of built up structures by checking individual elements, assuming simplified boundary conditions. Only two possibilities are envisaged, either edges are free or they are simply supported.

From the point of view of estimating overall buckling stresses, these assumptions may be optimistic for some configurations, and it is therefore worthwhile investigating the consequences in design terms.

The form of construction chosen for analysis is the unflanged integrally stiffened panel originally studied by Catchpole.[48] This example has the advantage of dimensional simplicity, together with a well established set of results already available for comparison.

The following dimensions may be defined as a basis for the design variables.

t = skin thickness
t_s = stiffener thickness
b = stiffener spacing
h = stiffener height

so that the design variables become

$$r_t = t_s/t$$
$$r_b = h/b$$

and the following geometric quantities may be derived

$$K_1 = 2.05477 r_b^4 \frac{(4 + 2.4983 r_b^2)}{(1 + 2.4983 r_b^2)^2} \quad \ldots (112)$$

$$K_3 = \frac{1}{1 + 2.4983 r_b^2} \quad \ldots (113)$$

The approximate analysis of local buckling may be considered in various ways, based on the independent treatment of elements.

If the skin is assumed simply supported at the stiffener junctions

$$f_{2t} = 3{,}62 E_t \left(\frac{t}{b}\right)^2 \quad \ldots (114)$$

For the flanges, with one edge free a widely utilised compromise between simple and fixed support at the skin gives

$$f_{2s} = 0.58 E_t \left(\frac{t_s}{h}\right)^2 \quad \ldots (115)$$

For trueindependence

$$f_2 = \min(f_{2t}, f_{2s})$$

The boundary between the regions dominated by each element is given by

$$f_{2t} = f_{2s}$$

so that

$$3.62 E_t \left(\frac{t}{b}\right)^2 = 0.58 E_t \left(\frac{t_s}{h}\right)^2$$

giving

$$r_t = 2.4983 r_b$$

thus when $r_t < 2.4983 r_b$, $K_2 = 0.58\left(\frac{r_t}{r_b}\right)^2$ ... (116)

and $r_t > 2.4983 r_b$, $K_2 = 3.62$ ... (117)

Equations for the stress coefficient F may now be written down for each domain, giving the following results

flanges critical:

$$F = 0.83107\left[\frac{r_t^3 r_b(4+r_t r_b)}{(1+r_t r_b)^4}\right]^{\frac{1}{4}} \quad \ldots (118)$$

skin critical:

$$F = 1.31358\left[\frac{r_t r_b^3 (4+r_t r_b)}{(1+r_t r_b)^4}\right]^{\frac{1}{4}} \quad \ldots (119)$$

Stress coefficients based on these relationships are shown plotted as contours against an appropriate range of r_t and r_b in figure (36), together with the corresponding results transcribed from Catchpole[48] who used the correct analysis for local buckling without approximation. The optimum solution, which lies on the intersection when both local buckling criteria are coincident is as follows.

$r_t = 1.799$
$r_b = 0.720$
$F = 0.7859$

which may be compared with Catchpole's[48] more accurate solution which used the local buckling analysis due to Cox.[52]

$r_t = 2.250$
$r_b = 0.650$
$F = 0.810$

In the region of the optimum solution, the approximate analysis of local buckling is conservative since elastic rotational restraints against skin buckling are largely ignored. This not only leads to the somewhat lower efficiency indicated, but also imposes significant changes in the optimum values of the design variables.

It may therefore be concluded that despite the computational convenience of the approximate procedure outlined above, the correct characterisation of local buckling behaviour should be utilised wherever possible. Alternatively, an approximate analysis of the type recently proposed by Yussuf[53] may prove convenient.

Apart from the examples due to Catchpole[48] and Farrar,[10] particular analyses have been performed by Richards,[49] and Emero and Spunt,[51] for a number of different forms of construction.

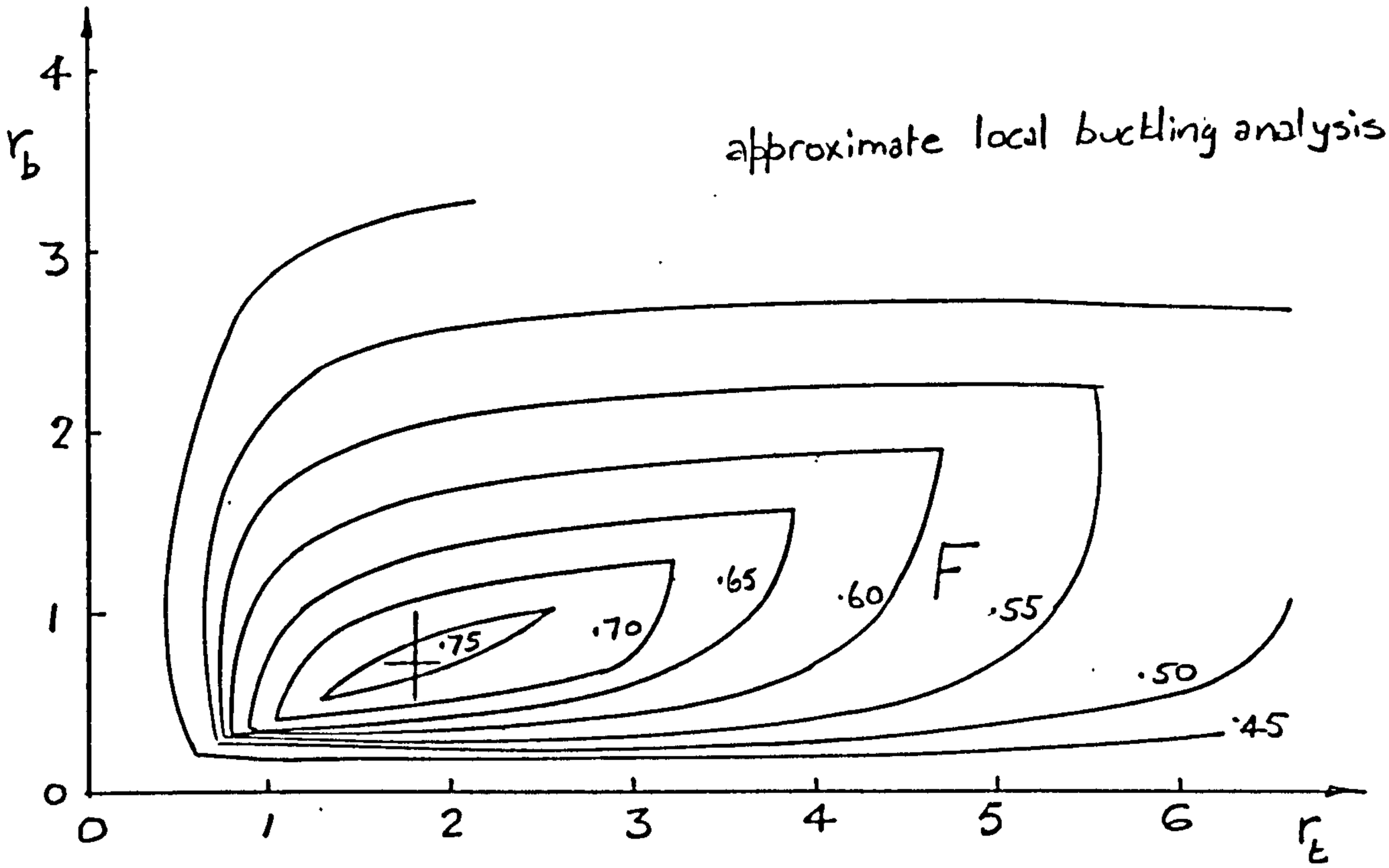

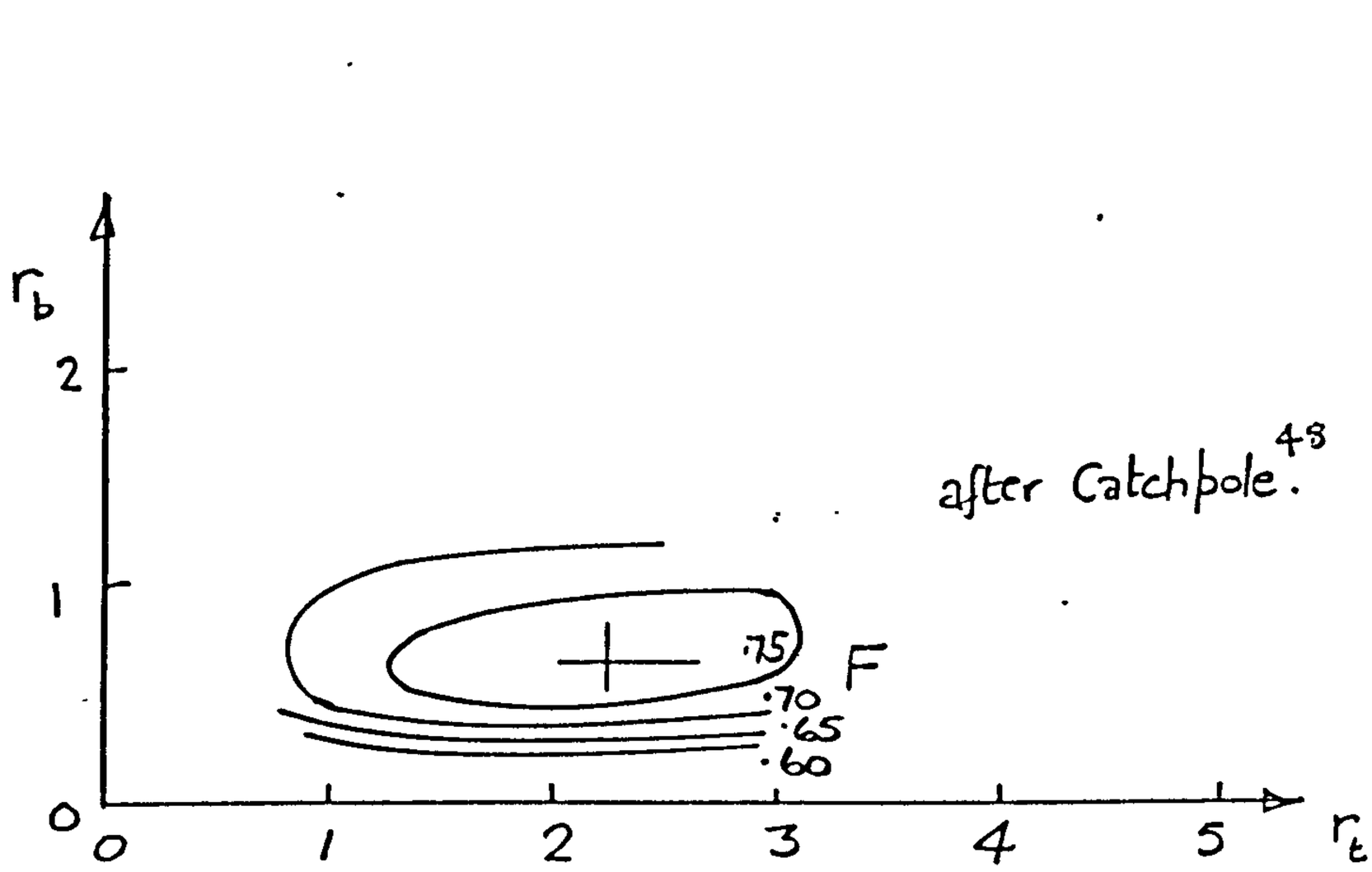

Figure 36. STRESS COEFFICIENT DISTRIBUTIONS FOR UNFLANGED INTEGRAL PANELS

Plasticity effects

The influence of pasticity on the results contained in equations (106) to 108) is expressed by the tangent modulus, which is a function of surface design stress. Thus in the plastic region the relationships are not explicit.

This difficulty may be conveniently resolved in a manner which will subsequently prove to be of much wider utility, by expressing the tangent modulus as a function of stress. Equations (106) to (108) may then themselves be recast as functions of surface stress alone in the following way, using the results established in Appendix A for material properties.

$$\frac{F^2\omega}{EL} = \left(\frac{f}{E}\right)^2\left[1 + n\phi\right] \qquad \ldots (120)$$

$$\frac{Ft}{TL} = \left(\frac{f}{E}\right)\left[1 + n\phi\right] \qquad \ldots (121)$$

$$\frac{F^{\frac{1}{2}}b}{BL} = \left(\frac{f}{E}\right)^{\frac{1}{2}}\left[1 + n\phi\right]^{\frac{1}{2}} \qquad \ldots (122)$$

where from equation (A4), $\phi = \alpha\left(\frac{f}{E}\right)^{n-1}$.

These equations may be used to prepare data sheets for any given material which are quite general for this form of construction, since all detailed section properties are segregated with the depedent variables.

It is of interest to note that an invariant relationship (independent of plasticity effects) exists between skin thickness and stiffener spacing, for by squaring equation (122) the resulting right hand side will equal that of equation (121), which gives for all optimum designs

$$t = \frac{Tb^2}{B^2L} \qquad \ldots (123)$$

Equations (120)(121) and (122) have been utilised to plot design data for a typical range of materials in figures (37), (38) and (39) as a function of the load intensity parameter, using the programme ZEDS which is based on a coding originally devised by Fews [54].

Both skin thickness and stiffener spacing are seen to be monotonically increasing functions of load intensity, and monotonically decreasing functions of proof stress. Perhaps the more significant relationship is between design stress and load intensity.

Figure (37) confirms that design stress increases monotonically with load intensity for any given material, and that for a given value of the plastic strain exponent n, improvement will be continuous as proof stress increases.

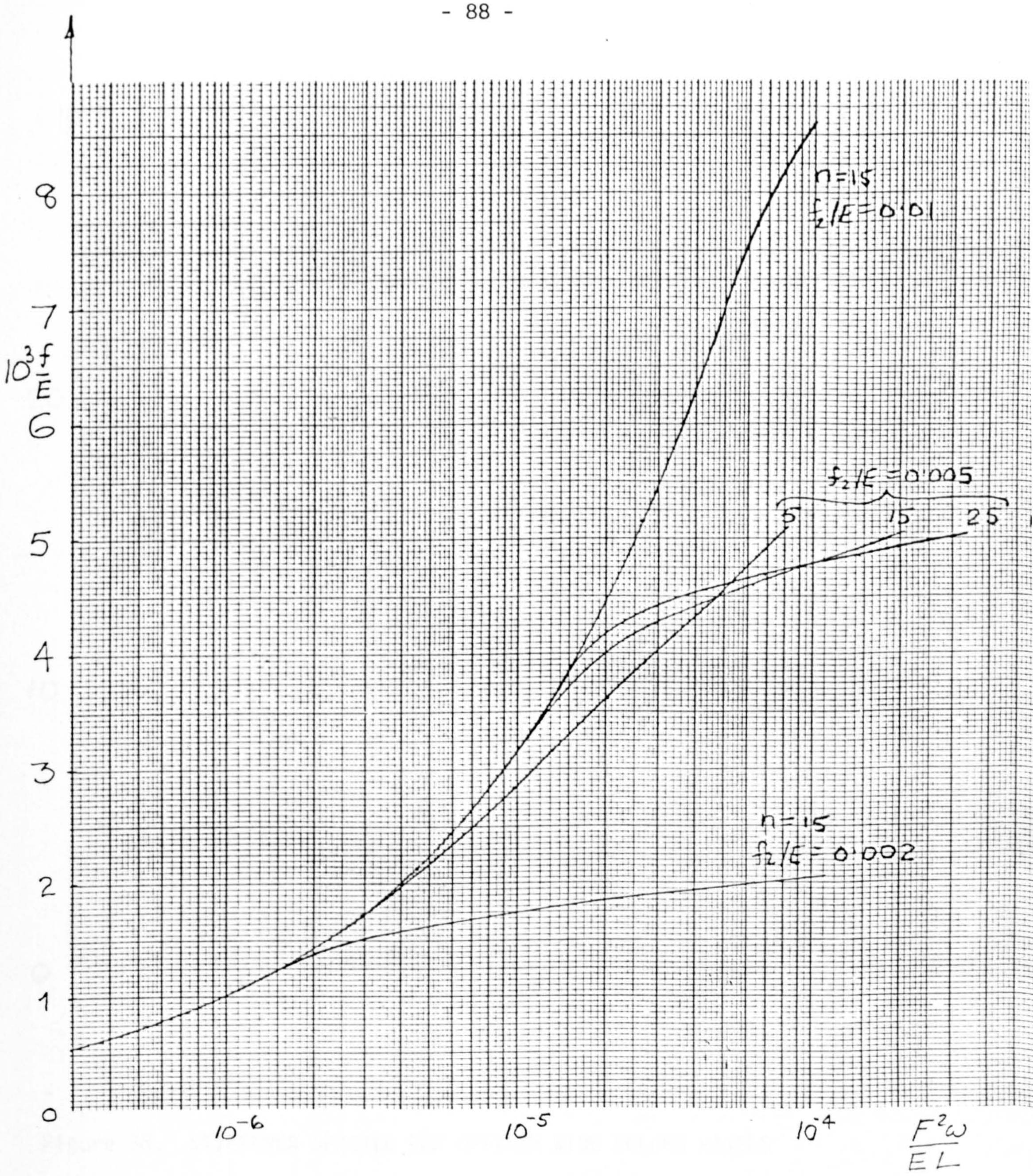

Figure 37. DESIGN STRESSES FOR OPTIMUM WIDE COLUMN PANELS

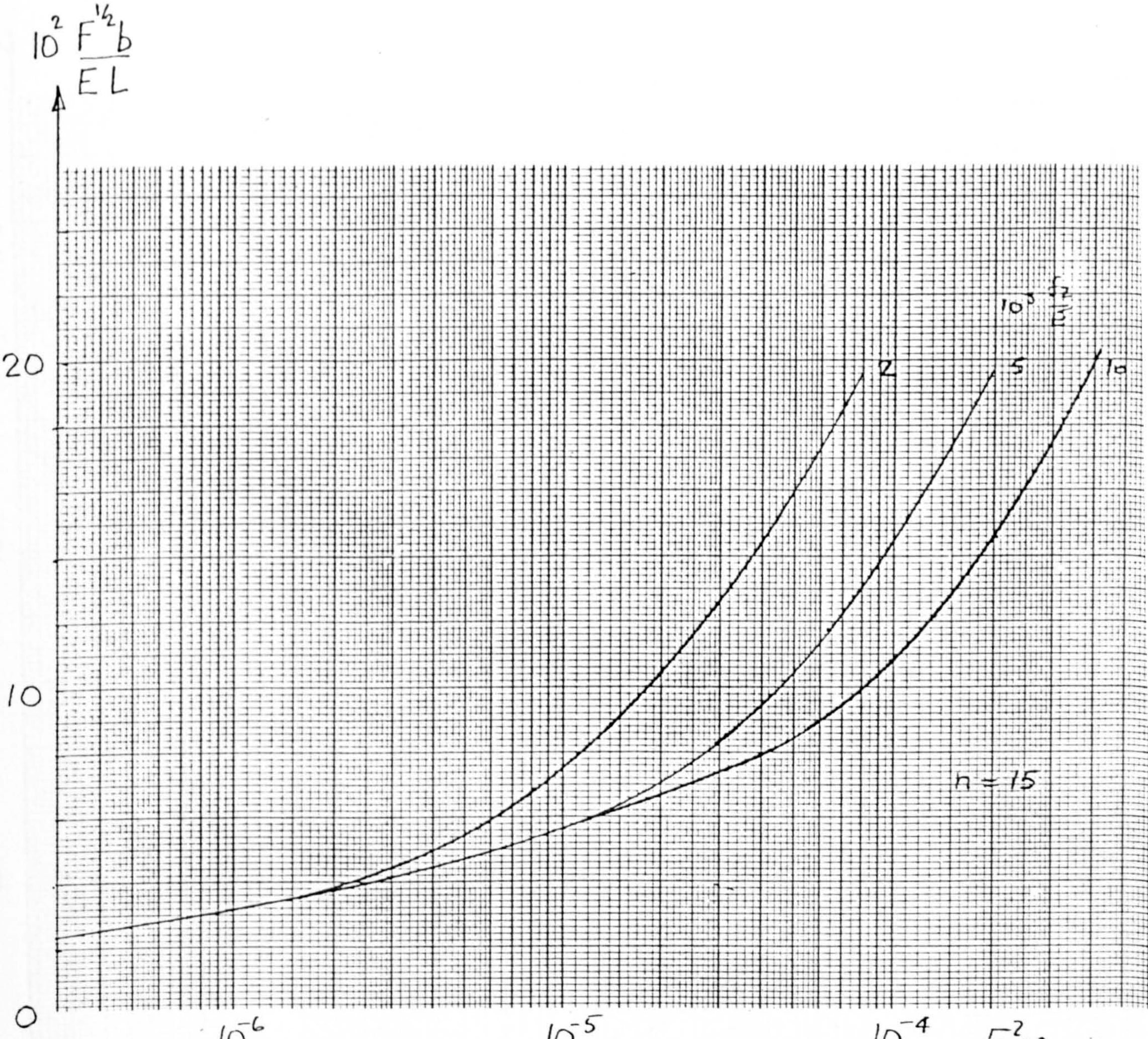

Figure 38. STIFFENER SPACING FOR OPTIMUM WIDE COLUMN PANELS

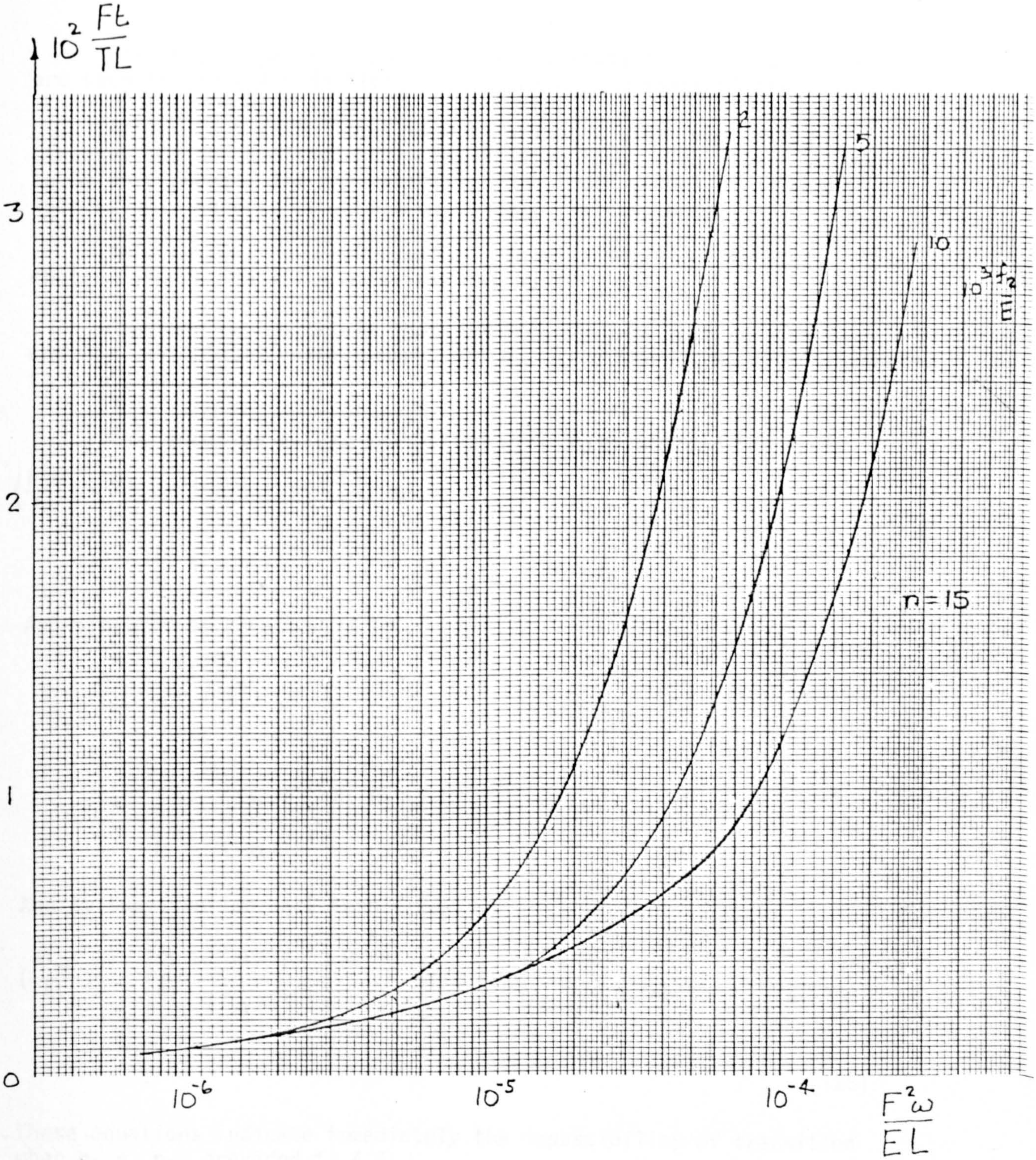

Figure 39. SKIN THICKNESS FOR OPTIMUM WIDE COLUMN PANELS

However, if proof stress is fixed, variations of the quantity n are seen to exert a significant influence on the shape of the curve.

At low load intensities, low values of n give lower design stresses and hence efficiency. But at high load values there is seen to be an exchange, and the materials with lower values of n become increasingly superior to the more sharply yielding ones.

This feature is worth examining in more detail since clearly the choice between competing materials may be affected.

Consider two materials characterised by 0.2% proof stress f_{21} and f_{22}, and plastic strain exponents n_1, n_2. Young's modulus is assumed to be common.

From equation (120), transition will occur at load intensity $\left(\frac{F^2\omega}{EL}\right)^*$ with design stress $\left(\frac{f^*}{E}\right)$ when

$$\left(\frac{f^*}{E}\right)^2\left[1 + \alpha_1 n_1\left(\frac{f^*}{E}\right)^{n_1-1}\right] = \left(\frac{f^*}{E}\right)^2\left[1 + \alpha_2 n_2\left(\frac{f^*}{E}\right)^{n_2-1}\right]$$

And since, from equation (A2)

$$\alpha = \frac{0.002}{(f_2/E)^n}$$

$$\frac{f^*}{E} = \left[\frac{n_2}{n_1}\cdot\frac{(f_{21}/E)^{n_1}}{(f_{22}/E)^{n_2}}\right]^{\frac{1}{n_1-n_2}} \quad \ldots (124)$$

And by substitution back into (120)

$$\left(\frac{f^2\omega^*}{EL}\right) = \left[\frac{n_2}{n_1}\cdot\frac{(f_{21}/E)^{n_1}}{(f_{22}/E)^{n_2}}\right]^{\frac{2}{n_1-n_2}}\left[1+0.002\left\{\frac{(f_{21}/E)^{n_1(n_2-1)}}{(f_{22}/E)^{n_2(n_1-1)}}\cdot\frac{n_2^{(n_1-1)}}{n_1^{(n_2-1)}}\right\}^{\frac{1}{n_1-n_2}}\right] \quad \ldots (125)$$

These equations indicate immediately the impossibility of transition when $n_1 = n_2$, provided $f_{22} \neq f_{21}$.

However, when $f_{21} = f_{22} = f_2$, equations (124) and (125) reduce to become

$$\frac{f^*}{E} = \left[\frac{n_2}{n_1}\right]^{\frac{1}{n_1-n_2}}\cdot\frac{f_2}{E} \quad \ldots (126)$$

and

$$\frac{F^2\omega^*}{EL} = \left[\frac{n_2}{n_1}\right]^{\frac{2}{n_1-n_2}} \left(\frac{f_2}{E}\right)^2 \left[1 + 0.002\left\{\frac{n_2^{(n_1-1)}}{n_1^{(n_2-1)}}\right\}^{\frac{1}{n_1-n_2}} \cdot \frac{1}{f_2/E}\right] \quad \ldots (127)$$

Note that the case when $n_1 = n_2$ may be deduced by taking limits. Thus it may be shown that

$$\lim_{n_2 \to n_1} \left(\frac{f^*}{E}\right) = \frac{f_2}{E} e^{-\frac{1}{n}} \quad \ldots (128)$$

and

$$\lim_{n_2 \to n_1} \left(\frac{F^2\omega^*}{EL}\right) = \left(\frac{f_2}{E}\right)^2 e^{\frac{-2}{n}} + 0.002\left(\frac{f_2}{E}\right) e^{\left(\log_e n - 1 - \frac{1}{n}\right)} \quad \ldots (129)$$

These values are useful in calculating with equations (126) and (127) to produce data of the type illustrated in figures (40) and (41).

From these figures it may be noted that the intersection functions are symmetric with respect to the two plastic strain exponents (this follows because of the interchangeability of the suffices).

For the materials chosen, intersections are seen to occur at load intensity values which increase monotonically with n. Within the practical range of n values chosen, all intersections are found to occur at stresses less than the common 0.2% proof value.

Comparison with experimental data

Williams and Mikulas[55] have collected together a very large number of test results relating to aluminium compression panels of the type discussed here which have been tested at various times by or for NASA.

The results have been correlated by plotting panel weight per unit area W divided by span L, against failure load per unit width w also divided by L, using logarithmic scales.

Two basic types of behaviour may be readily described using a scheme of this sort.

For panels which fail by buckling without the intervention of plasticity effects, equation (120) gives (with $\phi = 0$)

$$\frac{f}{E} = F\left[\frac{\omega}{EL}\right]^{\frac{1}{2}}$$

Panel weight per unit area is material density ρ multiplied by equivalent surface thickness t_e.

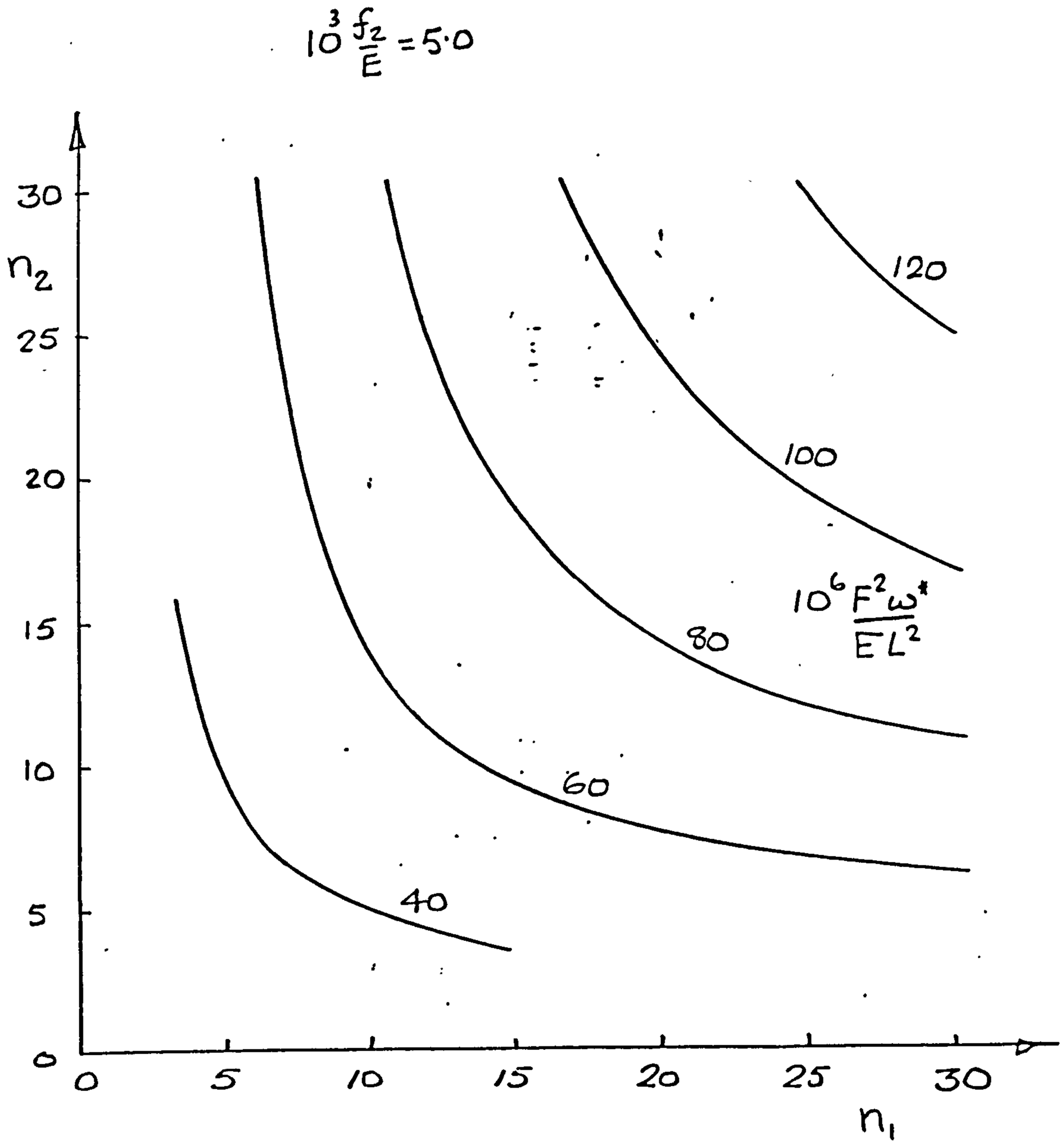

Figure 40. ENDLOAD INTENSITY FOR EXCHANGE OF SUPREMACY BETWEEN TWO MATERIALS WITH EQUAL PROOF STRESS.

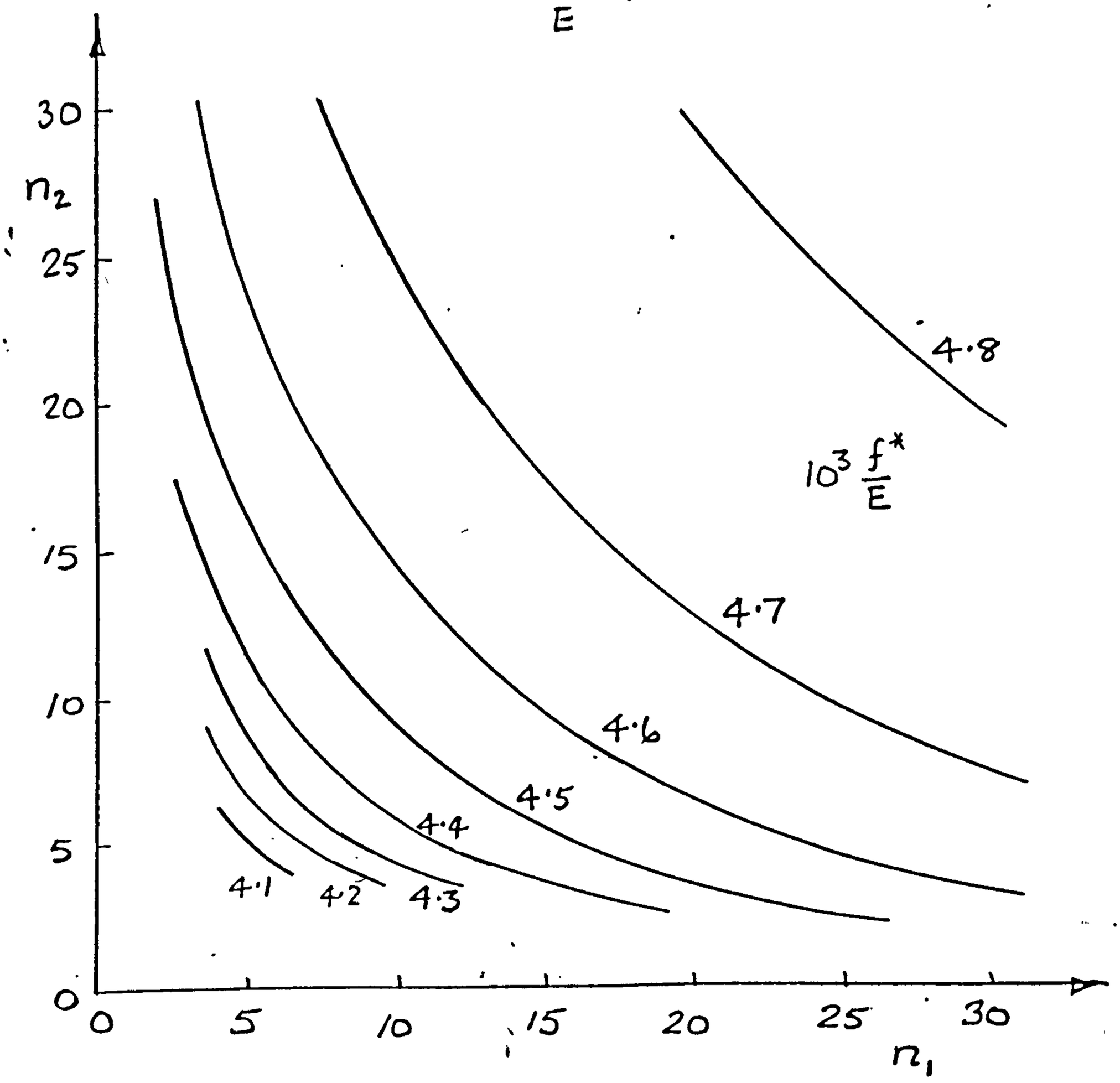

Figure 41. DESIGN STRESS FOR EXCHANGE OF SUPEREMACY BETWEEN TWO MATERIALS WITH EQUAL PROOF STRESS

Thus

$$\frac{W}{L} = \frac{\rho t_e}{L} = \frac{\rho W}{fL} = \frac{\rho}{FE^{\frac{1}{2}}} \cdot \left[\frac{W}{L}\right]^{\frac{1}{2}} \qquad \ldots (130)$$

When plotted using log scales this relationship will be linear, with slope equal to 0.5.

The second primary property is the limitation exercised by the imposition of a maximum allowable stress, which for the present purpose is taken to be f_2 the 0.2% proof stress. For panels restricted in this way

$$\frac{W}{L} = \frac{\rho}{f_2}\left[\frac{W}{L}\right] \qquad \ldots (131)$$

which is also, naturally, linear.but with unit slope.

The analysis which has been evolved here, envisaging as it does the gradual onset of plasticity, provides a realistic transition between the two primary forms of behaviour given by (130) and (131). This point is emphasised by the results shown in figure (42), which has been adapted from references (55) and (56) to show the NASA data in relation to the present analysis.

A particular point of interest is that for the medium strength material ($f_2/E = 0.005$) which might be regarded as typical, the overwhelming majority of test points displayed occur in the region of transition between elastic stability and strength dominated designs, where the methods derived here have their greatest effect.

Dimensional constraints

The analysis up to now has been concerned with the determination of ideal dimensions which specify a design which will safely equilibrate the given loading.

In practical circumstances, a number of considerations may hold which may make it impossible to utilise the optimum dimensions. These may, for instance, be due to the limitations of manufacturing techniques, availability of material sizes, or perhaps the existence of secondary functions (other than the transmission of the design compressive loading) which may be required in operation. Constraints of this sort may be expressed as inequalities such as

$$\begin{aligned} t_{min} \leq t \leq t_{max} \\ b_{min} \leq b \leq b_{max} \end{aligned} \qquad \ldots (132)$$

Violation of these constraints is revealed immediately the ideal optimum design has been worked out.

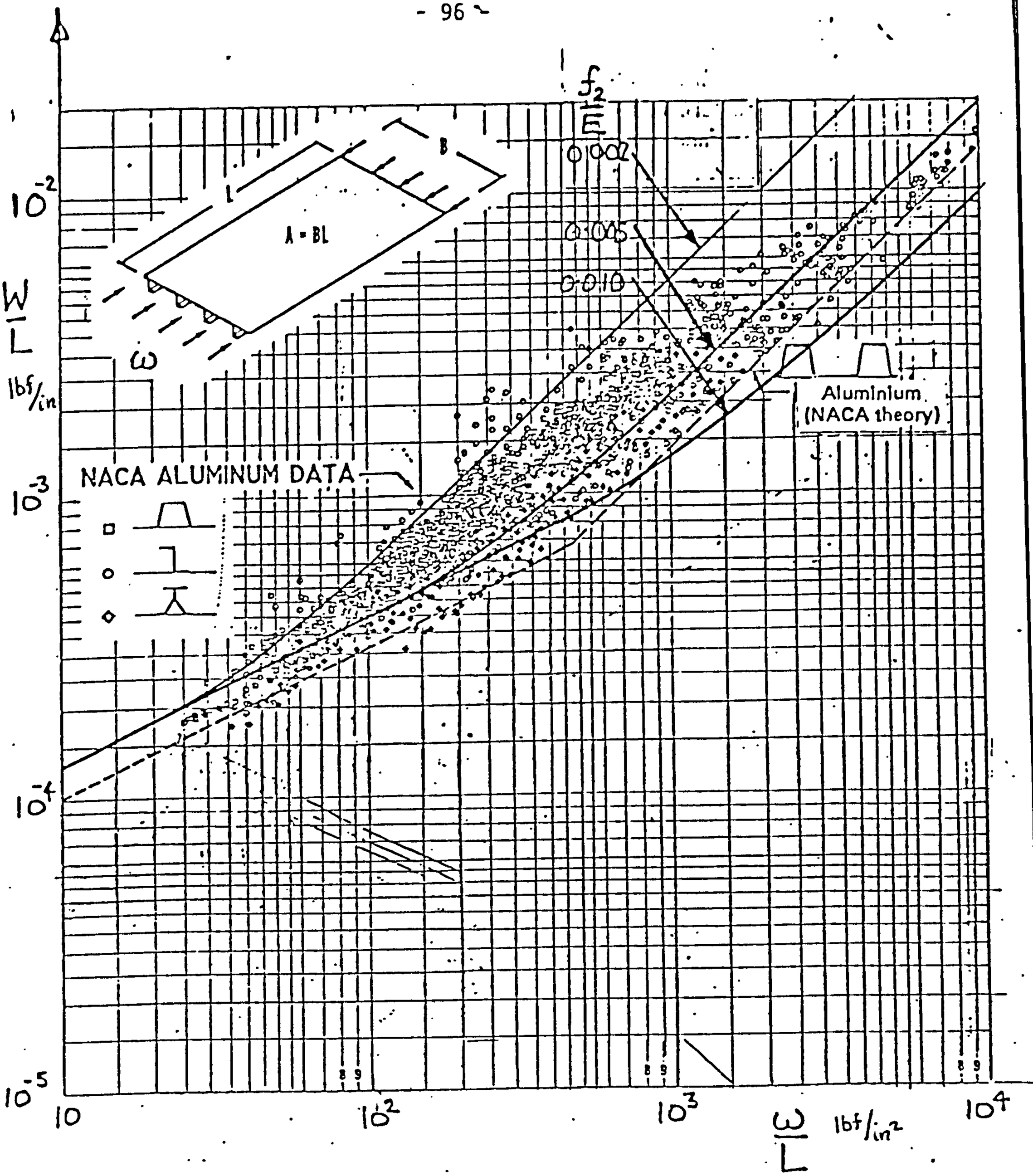

Figure 42. PANEL WEIGHT STATISTICAL DATA FROM REFS.(55) AND (56) RELATED TO PRESENT ANALYSIS

For elastic designs, the relationships already devised may be sufficient to allow the surface detail to be re-organised to take account of one or more active constraints.

These possibilities will now be explored, using the unflanged integrally stiffened panel as an example.

Single constraint violated

From equations (107), (108), the skin thickness and stiffener spacing coefficients may be written for elastic designs

$$B = b\left[\frac{E}{wL^3}\right]^{\frac{1}{4}} \qquad \ldots (133)$$

$$T = t\left[\frac{E}{wL}\right]^{\frac{1}{2}} \qquad \ldots (134)$$

Corresponding quantities relating to other dimensions may be written in an analogous way, e.g. stiffener height

$$H = h\left[\frac{E}{wL^3}\right]^{\frac{1}{4}} = \frac{h}{b} \cdot B \qquad \ldots (135)$$

and stiffener thickness

$$T_s = t_s\left[\frac{E}{wL}\right]^{\frac{1}{2}} = \frac{t_s}{t} \cdot T \qquad \ldots (136)$$

Each of these coefficients will have a specific value corresponding to the optimum value of F as previously described.

However, if the optimum solution violates (132) in one respect, then that dimension must be constrained, and a constrained value of the appropriate coefficient determined from the appropriate one of equations (133) to (136).

The available variations of B, T, etc. may be mapped in the design space defined in this case by the design variables t_s/t and h/b. These mappingsare illustrated in figures (43) to (46) for the particular form of construction under consideration.

The constraintcoefficient value will now define a specific contour in the design space which will connect all designs satisfying the active constraint.

This contour will describe a path across the stress coefficient (F) map, from which values may be transcribed to determine once more the combination of the design variables which maximise F, and hence the surface stress. This will define the constrained optimum design. Thus if the complete plots are available, the entire range of feasible constraints may be charted, together with corresponding dimensional data.

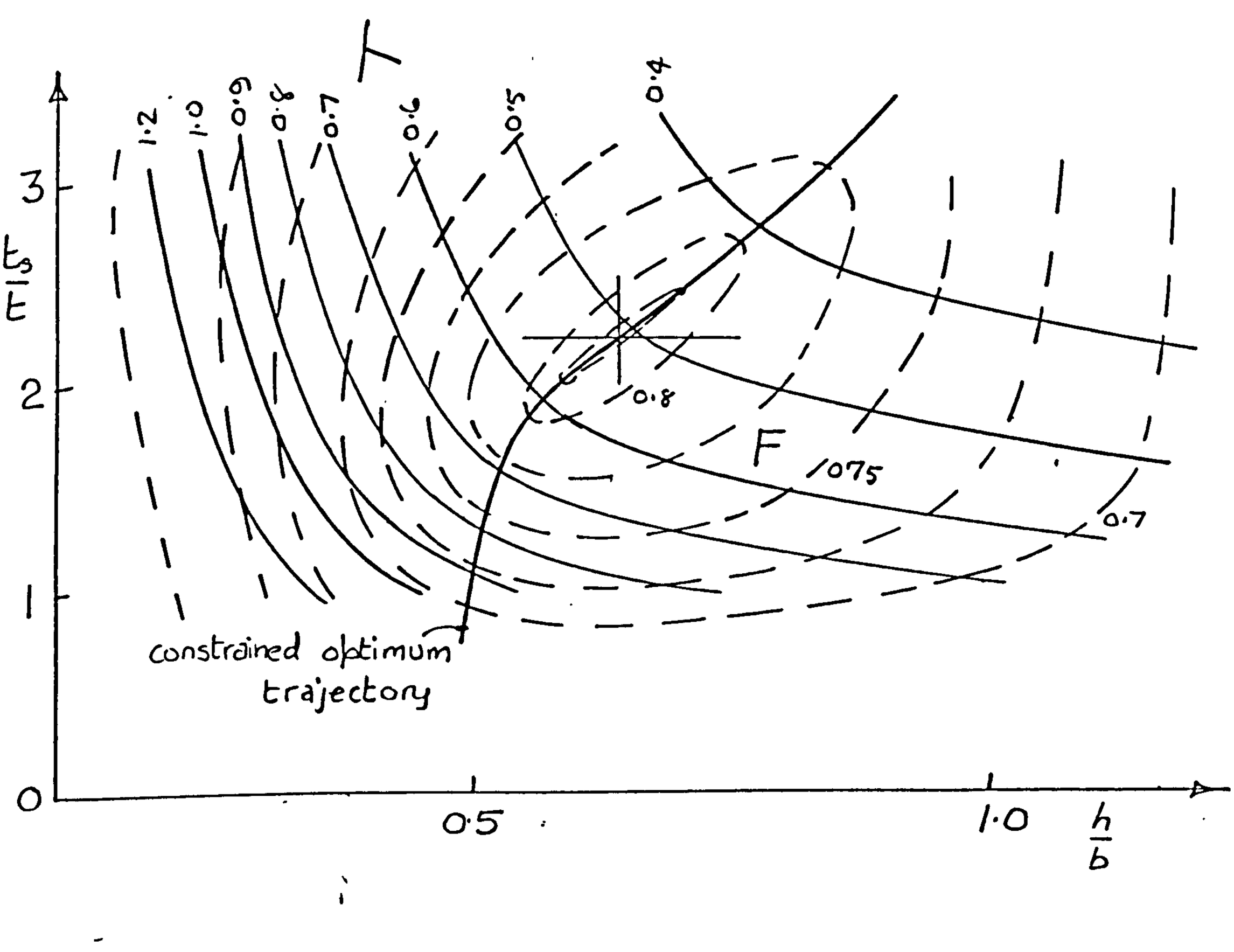

Figure 43. INTEGRAL PANEL DESIGN SPACE WITH SKIN THICKNESS CONSTRAINTS

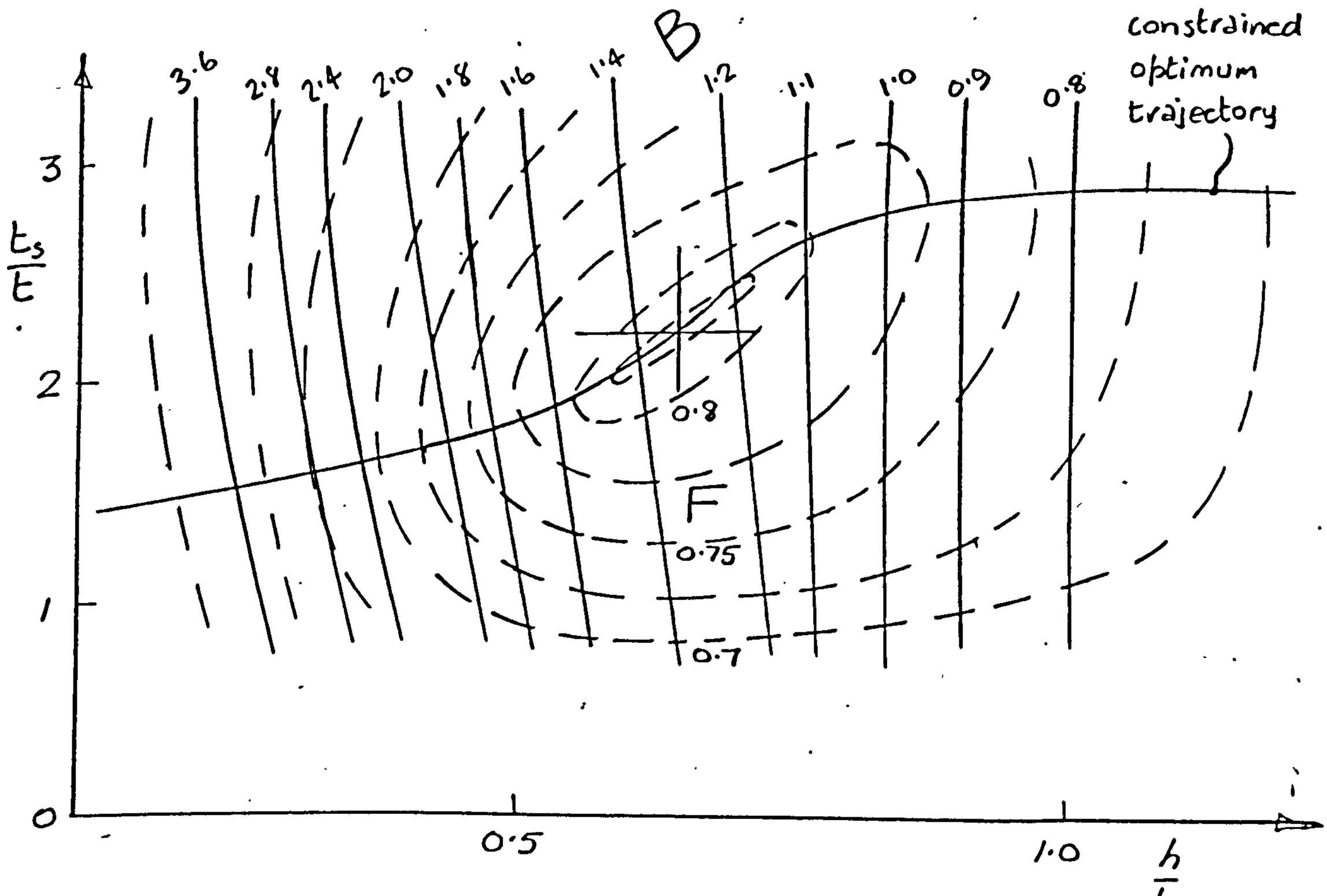

Figure 44. INTEGRAL PANEL DESIGN SPACE WITH STIFFENER SPACING CONSTRAINTS

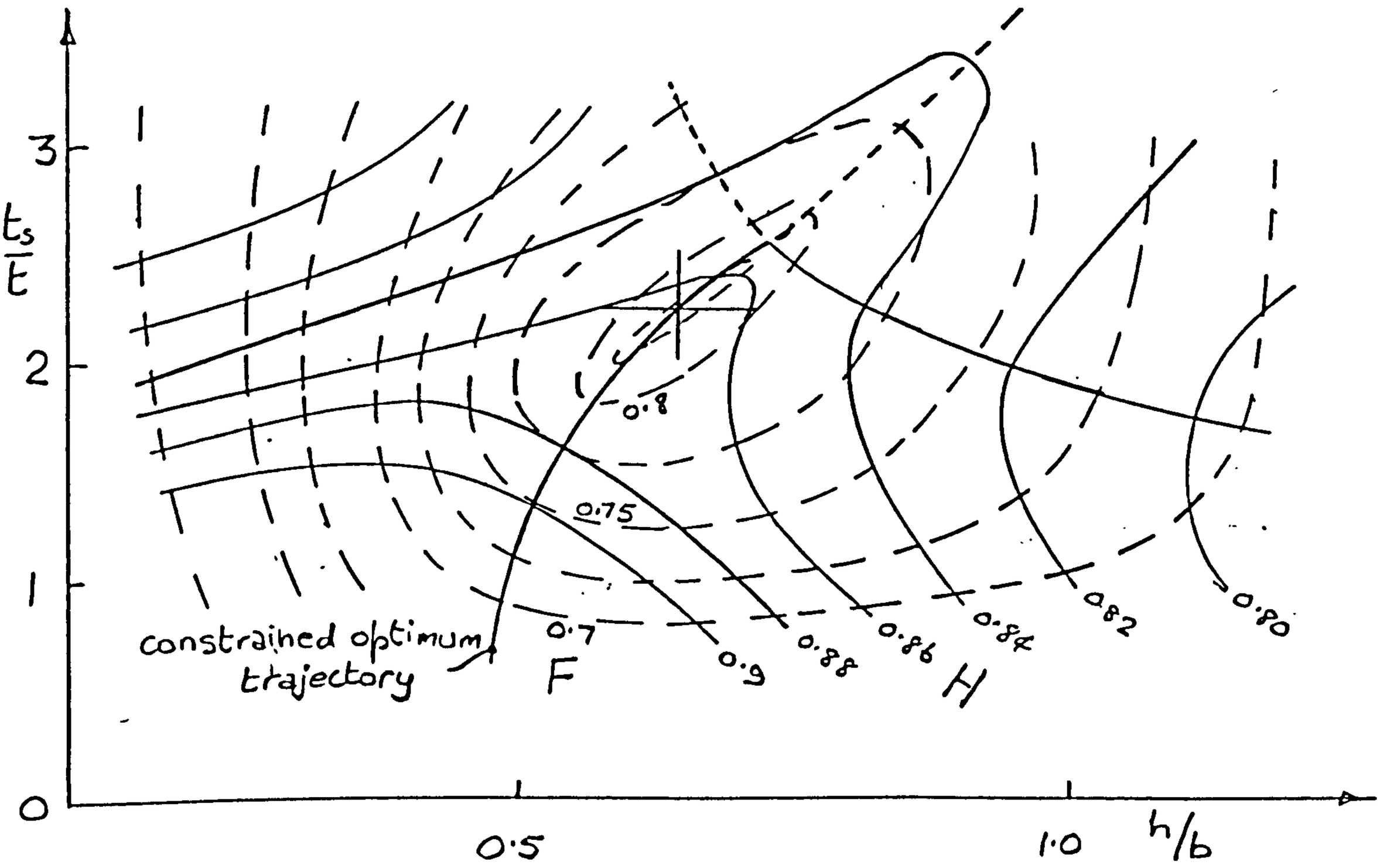

Figure 45. INTEGRAL PANEL DESIGN SPACE WITH STIFFENER HEIGHT CONSTRAINTS

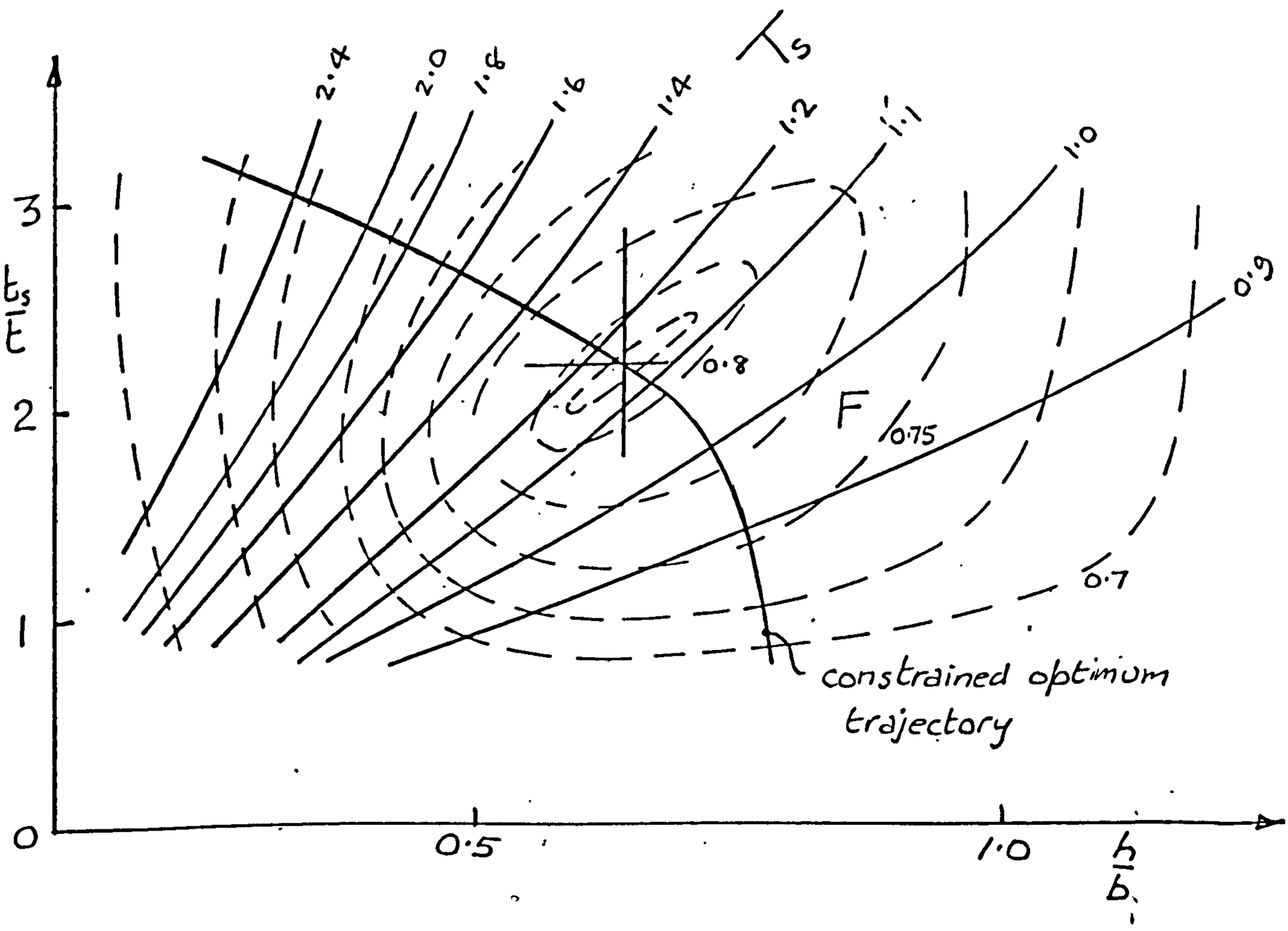

Figure 46. INTEGRAL PANEL DESIGN SPACE WITH STIFFENER THICKNESS CONSTRAINTS

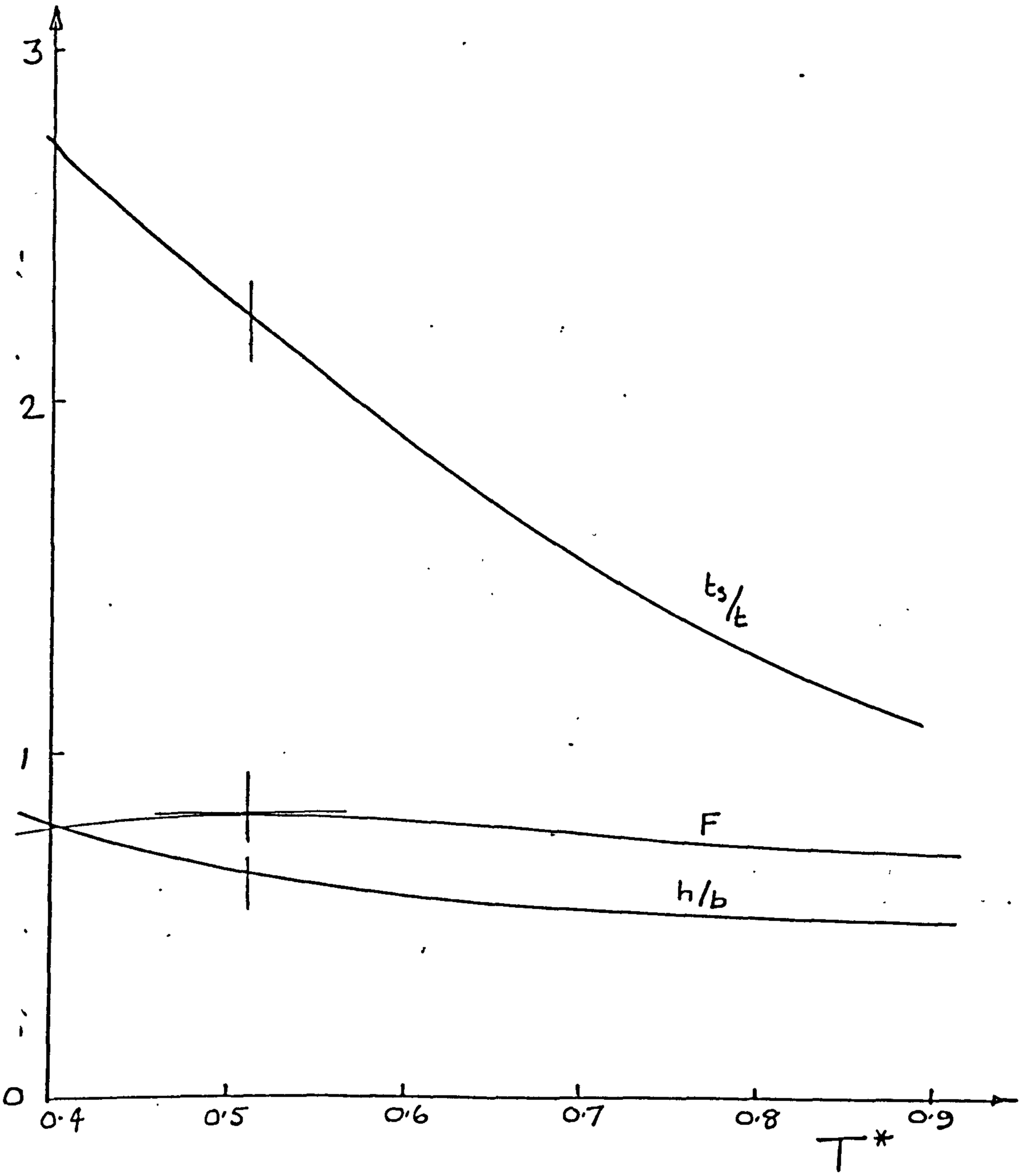

Figure 47. OPTIMUM INTEGRAL PANEL WITH SKIN THICKNESS CONSTRAINT

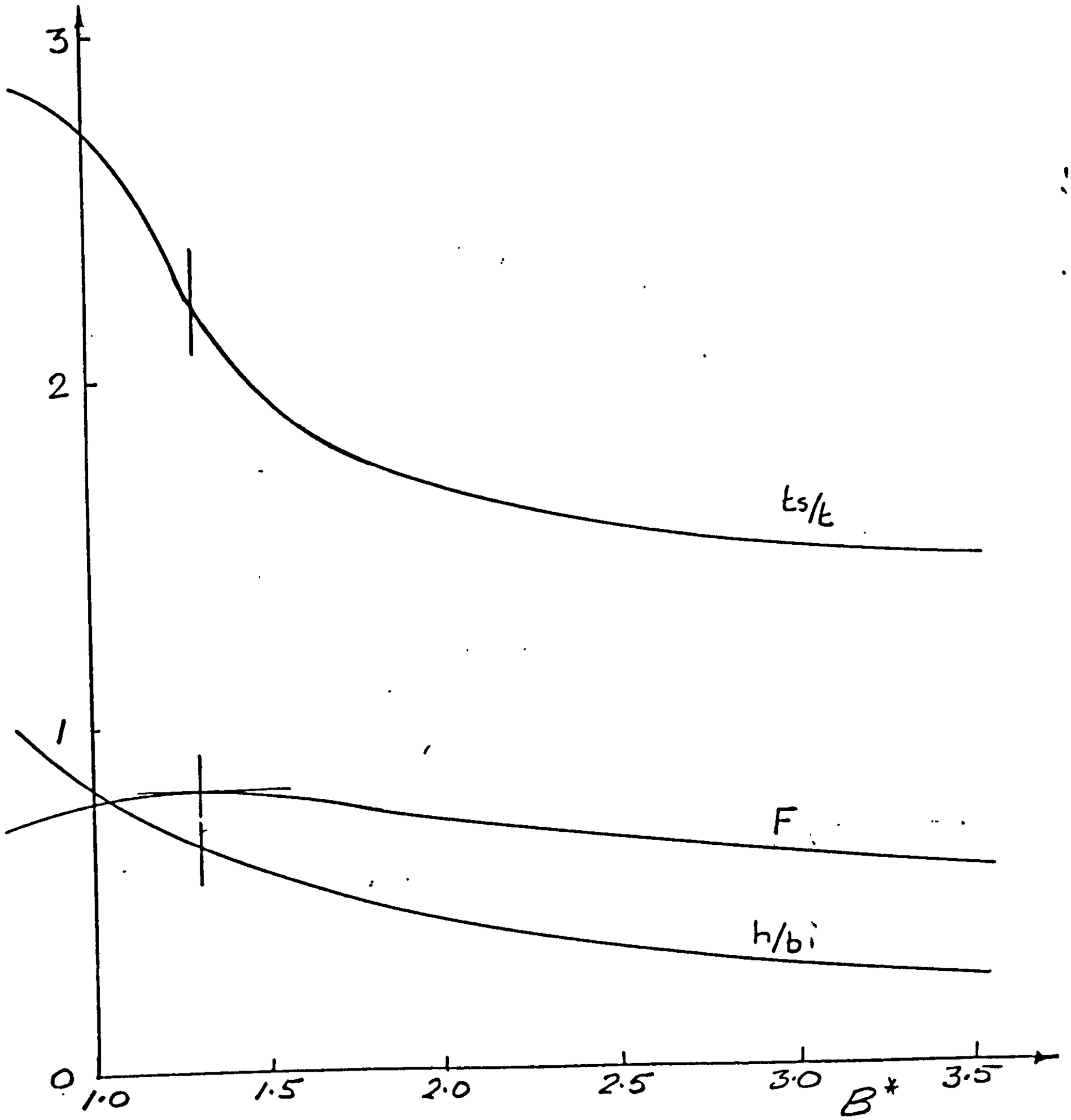

Figure 48. OPTIMUM INTEGRAL PANEL WITH STIFFENER SPACING CONSTRAINT

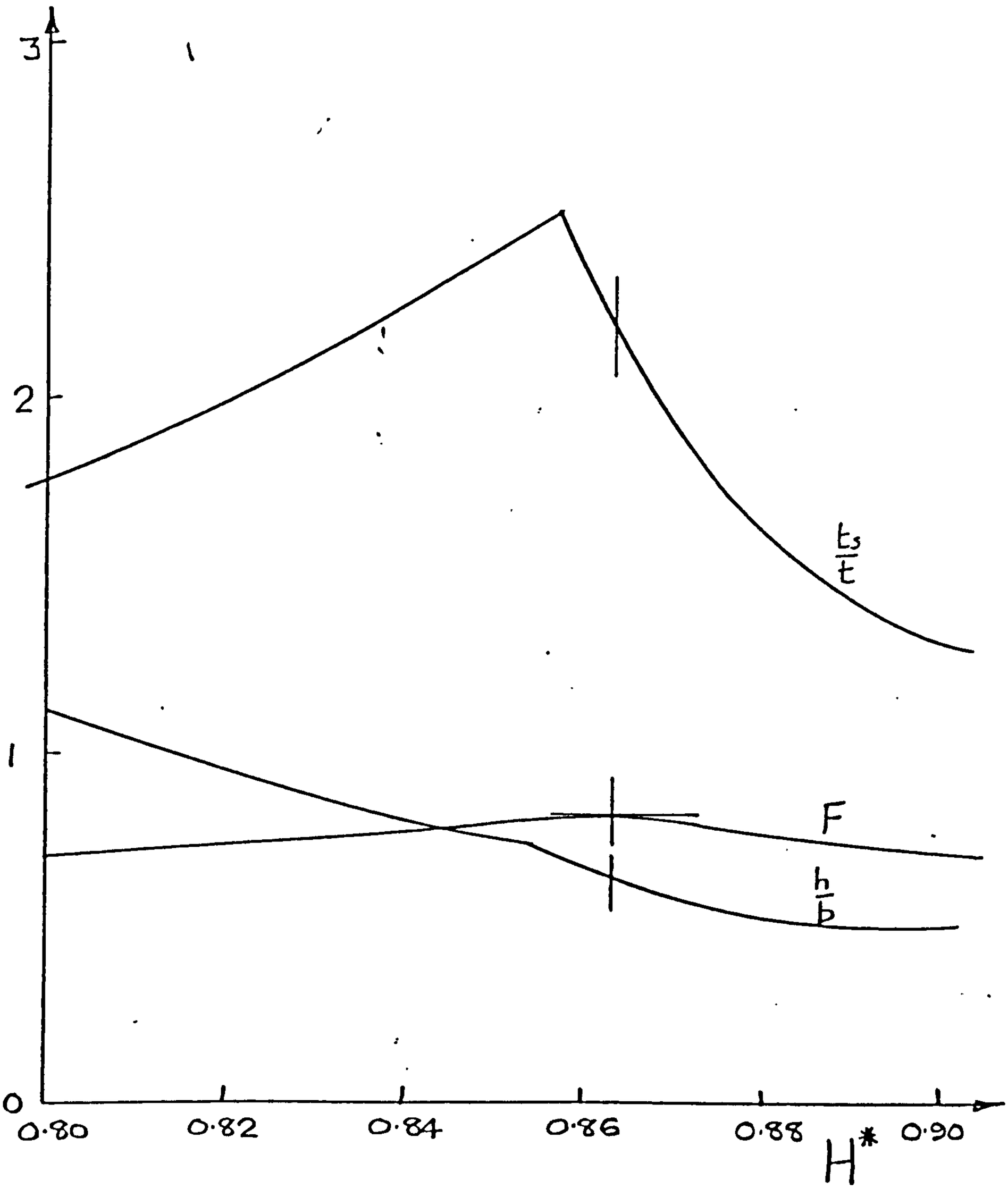

Figure 49. OPTIMUM INTEGRAL PANEL WITH STIFFENER HEIGHT CONSTRAINT

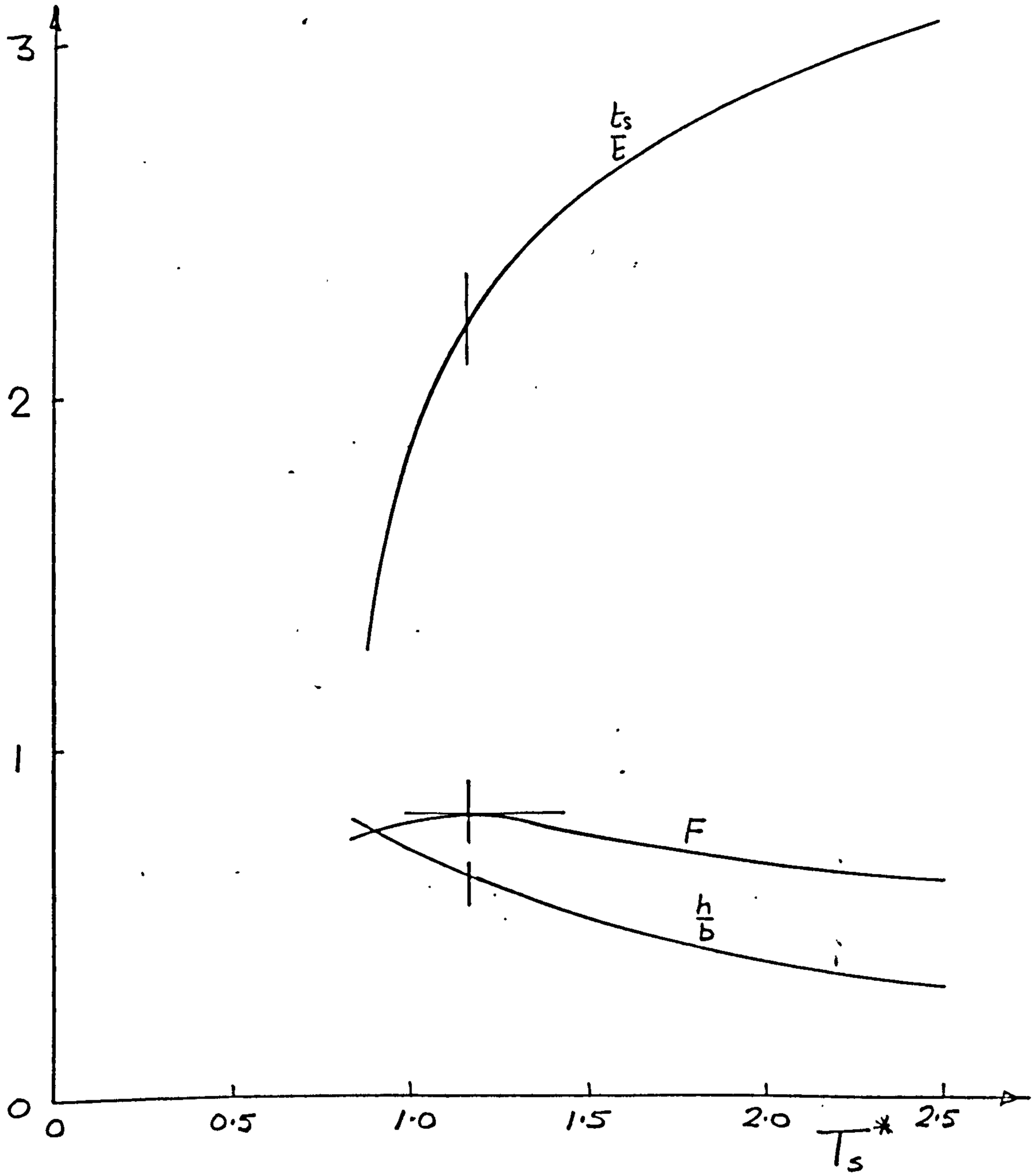

Figure 50. OPTIMUM INTEGRAL PANEL WITH STIFFENER THICKNESS CONSTRAINT

The superimposed coefficient plots are shown in figures (43) to (46), together with the constrained optimum trajectories. These have been transcribed to give, in figures (47) to (50) the optimum parameters as a function of each constrained coefficient value.

It may be noted that all constraints except stiffener height give smooth, continuous results.

The stiffener height parameter H has a more complex characteristic which leads to a bifurcation of the optimum trajectory. There is, however, no difficulty in choosing the best path by reference to the stress coefficient plot upon which it is superimposed in figure (45).

Dual violation

When two dimensional constraints are violated, the problem is reduced to the determination of a single solution within the available range.

This process is illustrated in figures (51) to (56) which show the six combinations of dimensional coefficients (T/B, T/H, T/T_s, B/H, B/T_s, H/T_s) overlaid in the design space.

All except the T/H and B/H combinations are seen to offer unique solutions to the coincident constraint problem within the available data range.

In the exceptional cases, multiple solutions are available and reference must be made to the appropriate region of the stress coefficient chart to determine which solution is best.

More than two variables

The promotion of two of the inequalities to be equalities together with the buckling and equilibrium equations creates a complete set of five equations which may in effect be solved for the five unknown design quantities in this case, namely f, t, b, t_s/t and h/b.

If more constraints are applicable, clearly the buckling criteria cannot be satisfied, although safety must be ensured.

For the present example, the procedure with more than two (e.g. three) constraints active is quite straightforward.

With only four dimensions required to define the structures completely, if three are fixed it remains only to find the smallest value of the remaining free variable which gives a safe structure if such a value exists. If four are fixed, a simple yes/no answer as to safety is all that is required, otherwise a design is impossible. In this context it should again be emphasised that the constraints are inequalities which could become released when further constraints are added. Thus all such options should be kept open until all the logical possibilities have been explored.

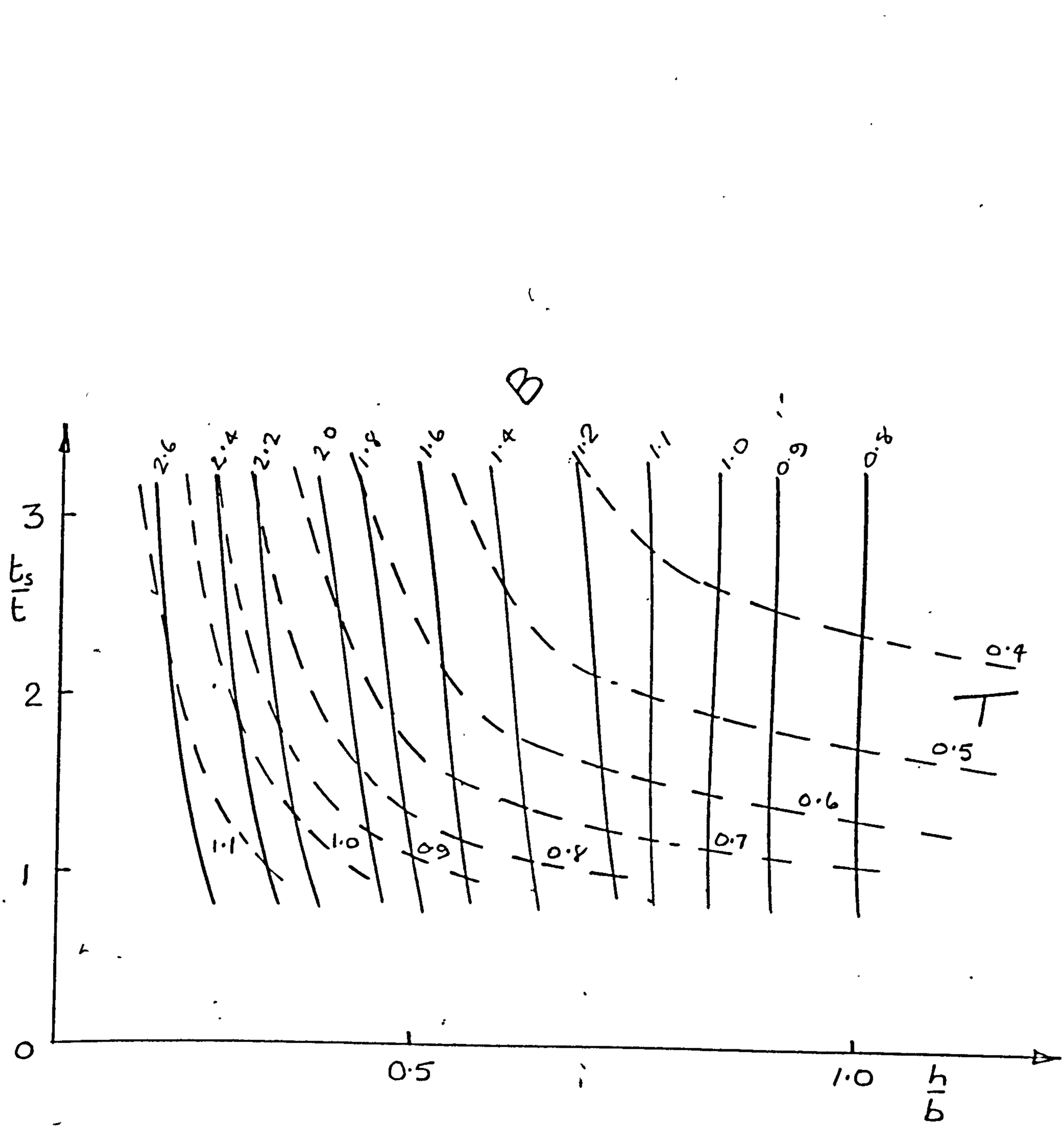

Figure 51. OPTIMUM INTEGRAL PANELS WITH DUAL CONSTRAINTS (SKIN THICKNESS, STIFFENER SPACING)

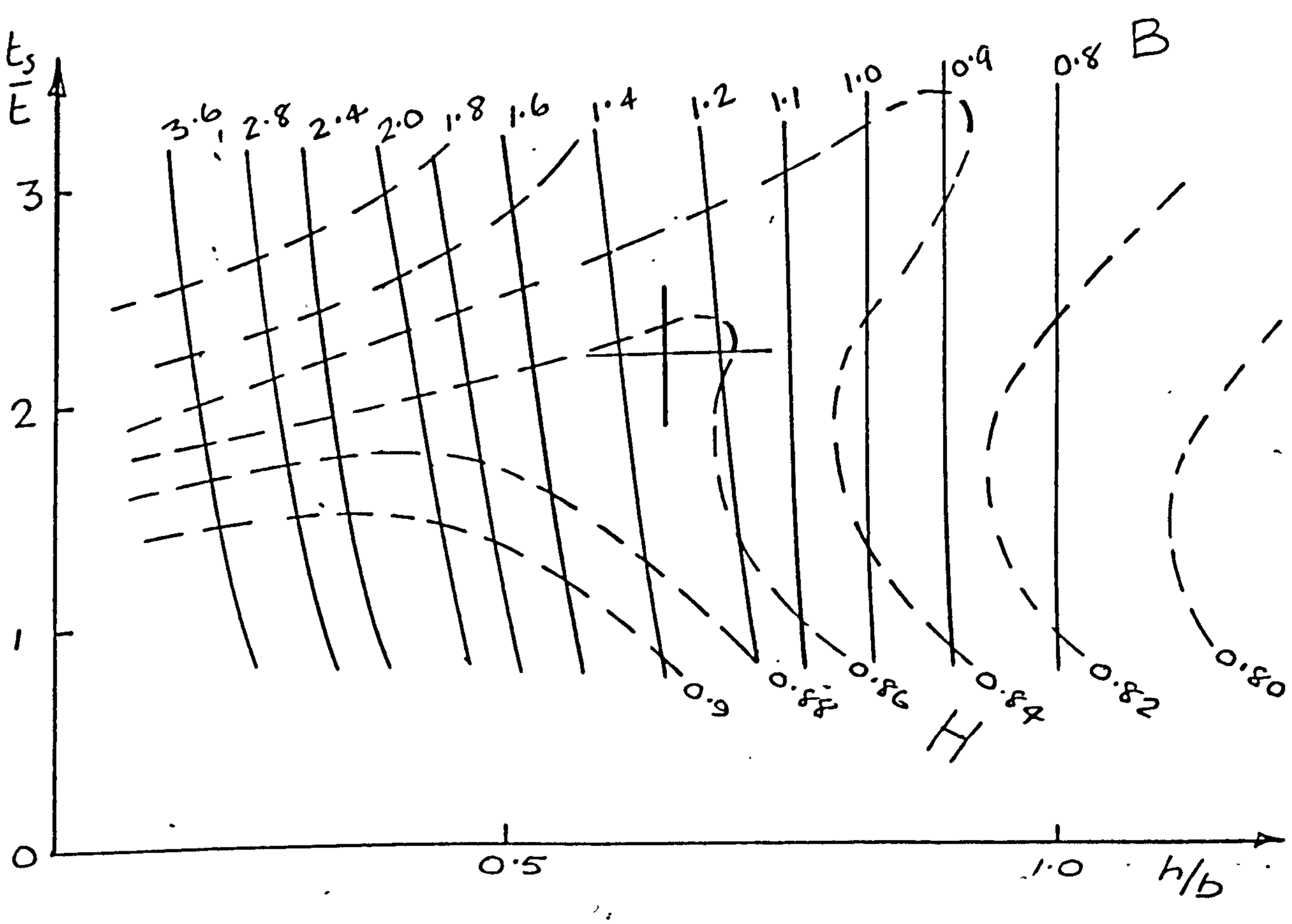

Figure 52. OPTIMUM INTEGRAL PANELS WITH DUAL CONSTRAINTS (STIFFENER SPACING AND HEIGHT)

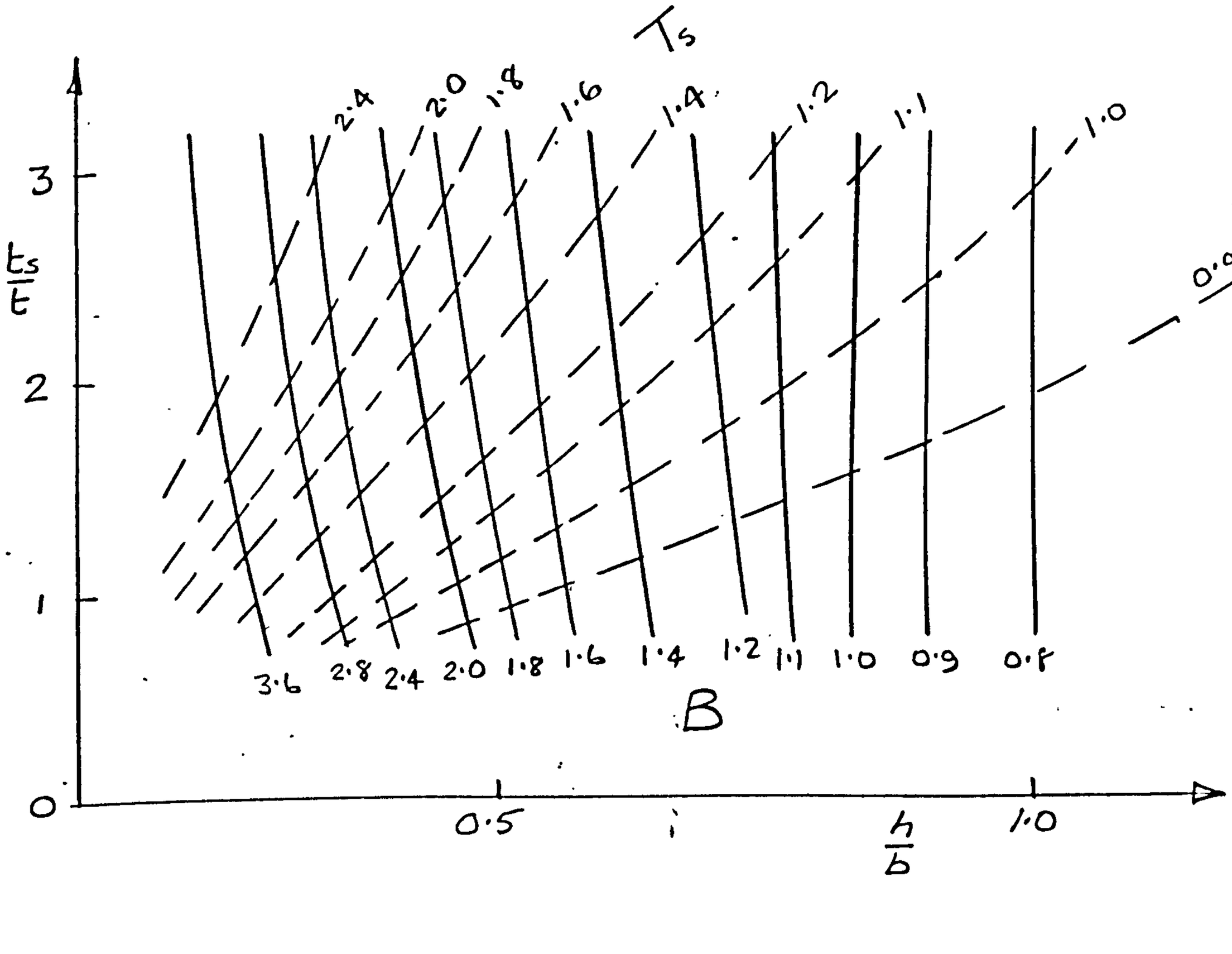

Figure 5.3. OPTIMUM INTEGRAL PANELS WITH DUAL CONSTRAINTS (STIFFENER SPACING AND THICKNESS)

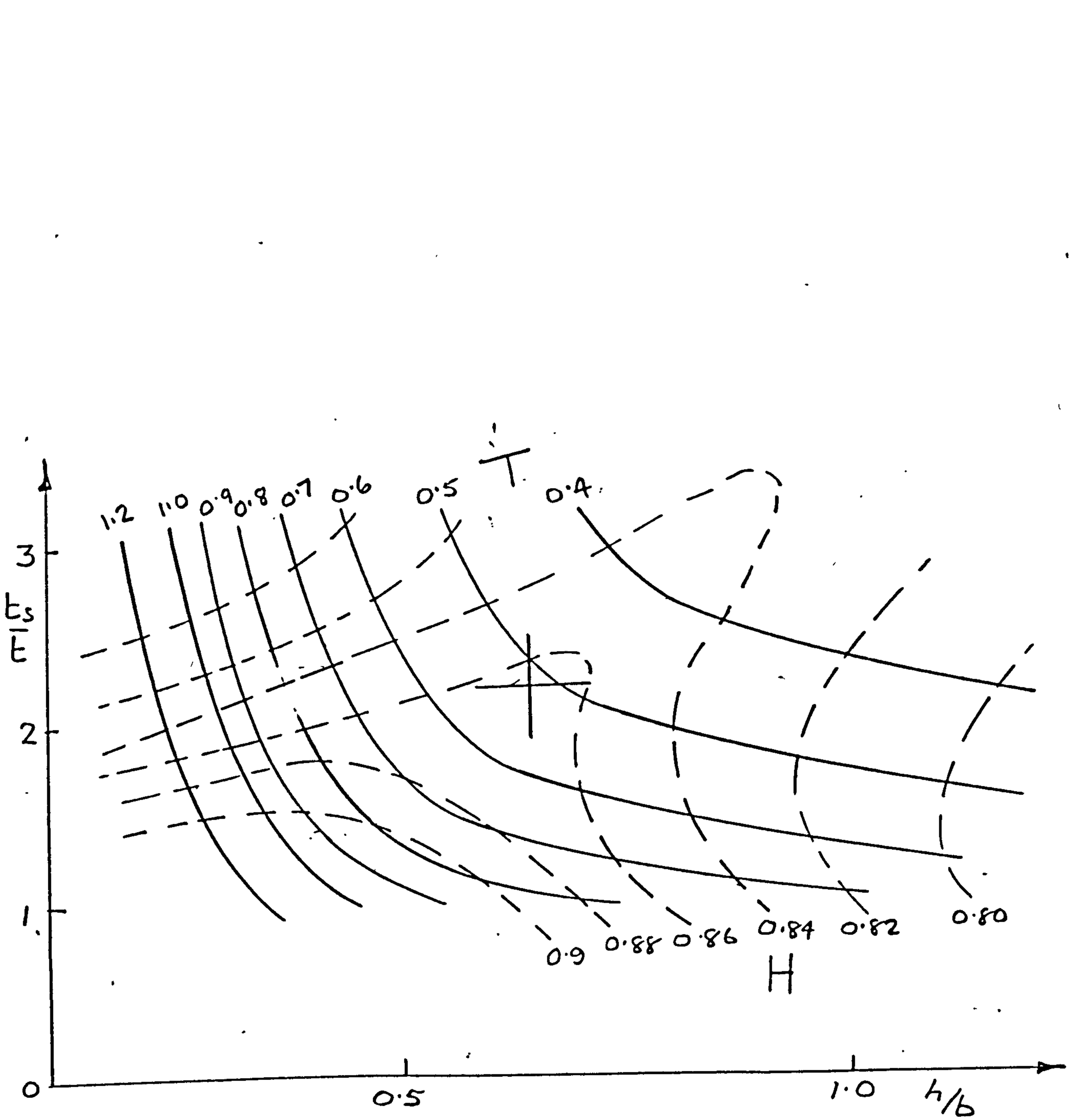

Figure 54. OPTIMUM INTEGRAL PANELS WITH DUAL CONSTRAINTS (SKIN THICKNESS, STIFFENER HEIGHT)

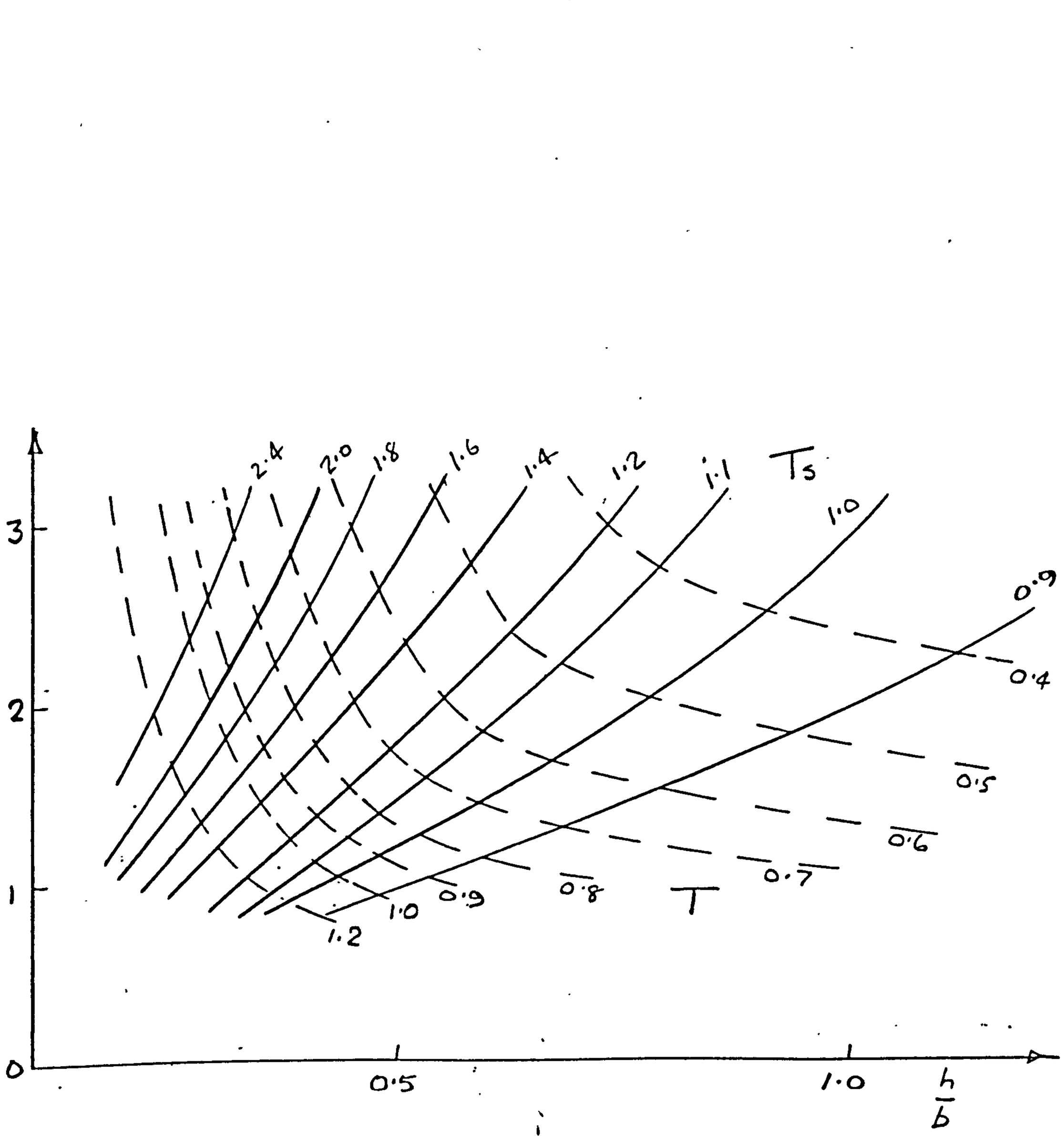

Figure 55. OPTIMUM INTEGRAL PANELS WITH DUAL CONSTRAINT (SKIN AND STIFFENER THICKNESSES)

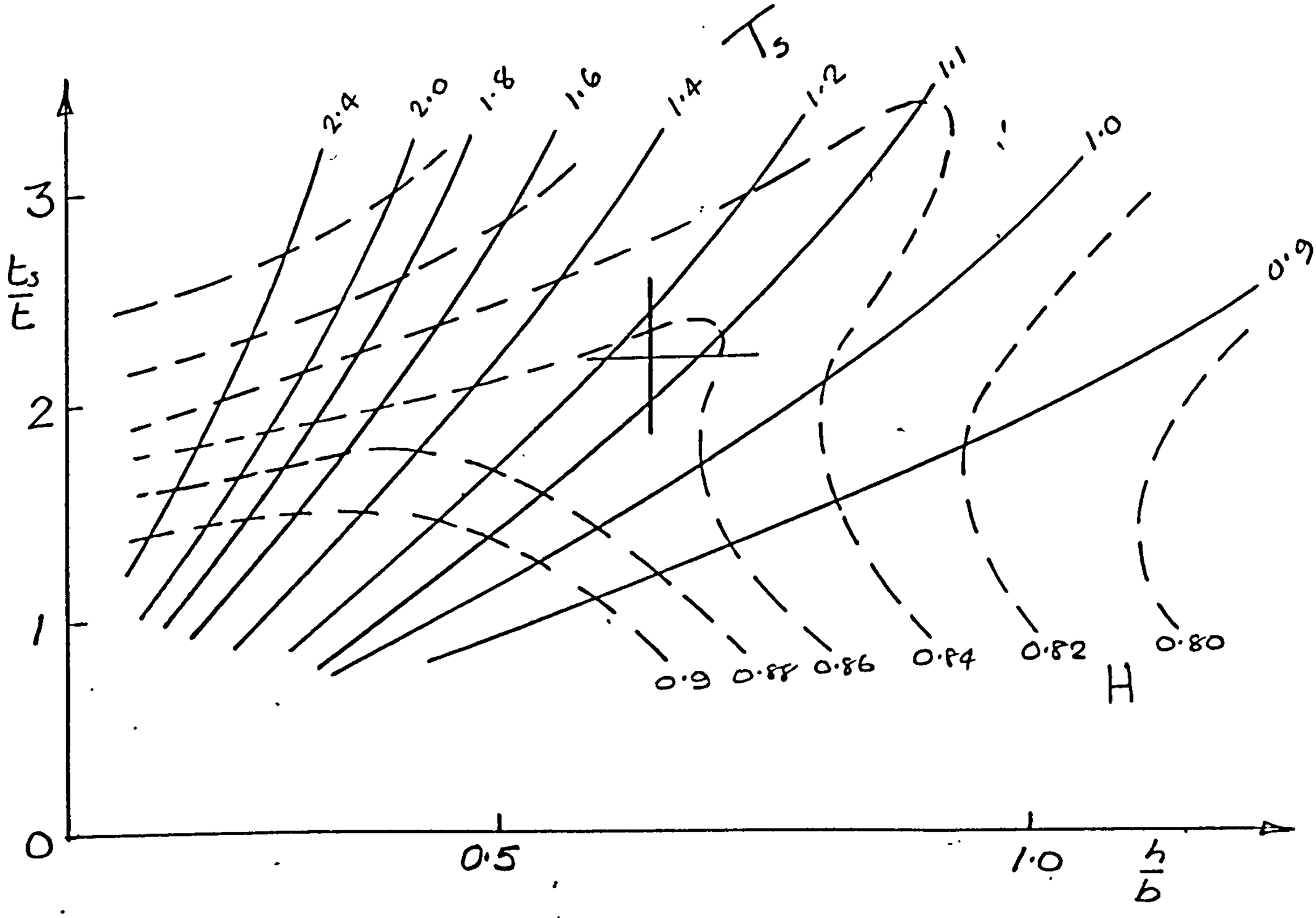

Figure 56. OPTIMUM INTEGRAL PANELS WITH DUAL CONSTRAINTS (STIFFENER HEIGHT AND THICKNESS)

Maximum stress constraint

At a certain level of load intensity w*, the design surface stress indicated by equation (120) will exceed the maximum allowed, say f*. From (120), this load intensity is given directly by

$$\frac{F^2\omega^*}{EL} = \left(\frac{f^*}{E}\right)^2\left[1 + n\phi^*\right] \qquad \ldots (137)$$

At higher load intensities, the optimum design will therefore have a reserve of stability which is best used by the designer to provide a margin of strength in each mode. If the margin is equalised between the modes, it may be expressed as a reserve factor, r, so that equations (103) and (104) become

$$rf^* = K_1 E_T\left(\frac{b}{L}\right)^2 \qquad \ldots (138)$$

and

$$rf^* = K_2 E_T\left(\frac{t}{b}\right)^2 \qquad \ldots (139)$$

$$r \geq 1.0$$

In effect this amounts to exchanging the reserve factor for the surface stress f as a design variable.

Equations (120), (121) and (122) may now be re-written to give

$$\frac{F^2 w}{EL} = \frac{1}{r}\left(\frac{rf^*}{E}\right)^2\left[1 + n\phi^*\right] \qquad \ldots (140)$$

$$\frac{Ft}{TL} = \left(\frac{rf^*}{E}\right)\left[1 + n\phi^*\right] \qquad \ldots (141)$$

$$\frac{F^{\frac{1}{2}} b}{BL} = \left(\frac{rf^*}{E}\right)^{\frac{1}{2}}\left[1 + n\phi^*\right]^{\frac{1}{2}} \qquad \ldots (142)$$

where $\phi^* = \alpha\left(\frac{rf^*}{E}\right)^{n-1}$ from (A4)

For elastic design these equations reduce to

$$r = F^2 . \frac{E}{f^*} . \left[\frac{w}{Lf^*}\right] \qquad \ldots (143)$$

$$\frac{t}{L} = TF . \left[\frac{w}{Lf^*}\right] \qquad \ldots (144)$$

$$\frac{b}{L} = F^{\frac{1}{2}} B . \left[\frac{w}{Lf^*}\right]^{\frac{1}{2}} \qquad \ldots (145)$$

The above relationships may be directly evaluated when preparing design data sheets by selecting increasing values of $r > 1.0$, thereby calculating the right hand sides of equations (140), (141) and (142) for any given material. The programme ZOPTIMUM, the coding for which is given in reference (56) performs this task.

Chapter 6

WIDE COLUMN PANELS WITH OPTIMISED SUPPORT LOCATIONS

General

In chapter 5, the design of wide column stiffened panels was considered for which the panel span L measured in the direction of loading was assumed to be pre-specified.

If the dimension L is now regarded as a design variable, the general character and design of the supports which are thus located immediately becomes an important issue.

Equation (120), which measures the efficiency of panels of fixed span, indicates that design stress will increase monotonically as span is reduced. And since such a reduction can only be achieved by devoting increasing quantities of structural material to the support function, clearly at some point reductions in span must become counter-productive. Thus the existence of an optimum span appropriate to any given set of design conditions is indicated.

In order to determine that optimum, suitable relationships between support function and weight must be established.

Support function

The purpose of the supports which are considered here is to provide 'simple' support i.e. to prevent significant transverse displacement at their locations should buckling take place in the Euler mode. The slope of the panel at these points is assumed to be uninhibited. It should be noted that Cox[17] has shown that a sinking support may give a somwhat lighter struct

The supports will be assumed to be fabricated as uniform transverse beams which are flexible in bending, but have insignificant transverse shear flexibility.

Since the wide-column behaves to all intents and purposes like an array of individual thin-walled struts, the effect of the supports will be to act as springs placed at regular intervals L along the length of the structure.

Timoshenko and Gere [35] have considered in detail a problem which corresponds precisely to the one outlined above. They show that in order for an infinitely long strut to carry the Euler load P_E corresponding to simple supports regularly spaced at intervals L, the spring stiffness provided at each support should be at least that which is given by

$$k = \frac{4P_E}{L} \qquad \ldots (146)$$

By analogy, this expression may be varied to apply to the case of the wide column loaded by the uniformly distributed compressive loading, w, so that

$$k = \frac{p}{y} = \frac{4w}{L} \qquad \ldots (147)$$

where p is the local value of a transversely distributed loading, and y is the corresponding displacement.

In order to determine an appropriate stiffness, a sinusoidally distributed transverse loading will be considered.

The boundaries of the support beam will be taken to occur at the extreme transverse edges of the panel which is of width c. These boundaries will be considered to provide either simple support or complete clamping.

The equation governing the deflection of the support is obtained from elementary beam theory to be

$$p_o \sin(\frac{\pi x}{c}) = EI \frac{d^4y}{dx^4} \qquad \ldots (148)$$

where the coordinate x is measured along the beam from one end, y is the deflection at x, and p_o is the notional transverse loading at midspan when x = c/2.

Depending on the boundary conditions assumed, equation (148) may be directly integrated to give the deflected shape of the beam. Thus for simple supports

$$y = \frac{p_o c^4}{\pi^4 EI} \sin(\frac{\pi x}{c}) \qquad \ldots (149)$$

The displacement is therefore proportional to the transverse loading at each point along the beam making the choice of location for the application to equation (147) arbitrary. The mid span values may therefore be used so that a combination of (147) and (149) gives for the required bending stiffness of the beam

$$EI = \frac{4}{\pi^4} \cdot \frac{c^4 w}{L} \qquad \ldots (150)$$

and for fixed ends

$$EI = \frac{(4-\pi)}{\pi^4} \cdot \frac{c^4 w}{L} \qquad \ldots (151)$$

Gerard [13] confirms the value of $\frac{4}{\pi}_4$ as the coefficient for the simple support case, but quotes 1/125 for the fixed end value, which is some 9.2% less than the value obtained above.

When wide column type stiffening is used in conjunction with ring frames to fabricate cylindrical shells, a corresponding analysis of the required ring stiffness may be performed.

Shanley [11] correlated a large number of test results for such structures, linking frame stiffness with the type of observed failure by the parameter

$$c_f = \frac{EIL}{MD^2} \qquad \ldots (152)$$

where M = bending moment at failure
D = shell diameter

For a thin walled shell, maximum compressive loading due to bending moment M is given by

$$w = \frac{4M}{\pi D^2}$$

which may be used to re-cast (152) in the form of (150) and (151) giving

$$EI = \frac{c_f \pi}{4} \cdot \frac{D^4 w}{L} \qquad \ldots (153)$$

Shanley [11] noted from his data that the value of c_f for which a panel failure confined between frames was as likely to occur as a more general instability was about 6.25×10^{-5}. Following an analogous argument, Gerard [13] gives $c_f = 6.80 \times 10^{-5}$.

These various possibilities are encompassed, if required transverse frame stiffness is taken to be specified by the equation

$$EI = C.\frac{c^4 w}{L} \qquad \ldots (154)$$

where the chord c should be taken either as the width of a flat panel, or the diameter of a cylindrical shell as required, together with the appropriate value of the coefficient C.

Support weight

Now that the required bending stiffness of the supports has been formulated, this must in turn be related to support weight.

Ideally any analysis should realistically envisage a number of practical possibilities, while admitting of the maximum degree of generalisation. Thus if the family of beams under consideration were all geometrically similar in cross-section, area A would be proportional to the square root of the second moment of area I.

Alternatively, such members are often fabricated as thin walled sections of constant overall size, but with variable wall thickness, which leads to a linear relationship between A and I.

Again, when a structure is lightly loaded, the stiffness criteria discussed above may be comfortably met by members of an irreducibly minimum size, in which case their area will take a constant value, insensitive to span, loading intensity, etc.

All of these concepts can be included if the following relationship is assumed.

$$A = A_o I^m \qquad \ldots (155)$$

where the index m takes the following values

$$\left.\begin{array}{ll} \text{constant frames,} & m = 0 \\ \text{geometrically similar "} & m = 1/2 \\ \text{linear frames,} & m = 1 \end{array}\right\} \qquad \ldots (156)$$

Obviously more complex, perhaps hybrid possibilities may be envisaged. However equation (155) does cover a very wide rage of design policies of practical significance.

Analysis of optimum spacing

The objective of this analysis is to determine the support spacing which minimises the total weight of the structure including surface and supports.

This objective is best expressed as the equivalent surface thickness of the structure, t_e, which is given by

$$t_e = \frac{w}{f} + \frac{A}{L} \qquad \ldots (157)$$

Equation (157) may never be developed as an explicit function of support spacing, if the non-linear effects of plasticity are to be incorporated.

However, it proves possible to express (157) completely in terms of surface stress which provides an entirely acceptable independent variable in the analysis. This is feasible because of the inverse monotonic relationship between support spacing and surface stress which may be noted from equation (120), which gives

$$L = \frac{F^2 W}{E} \cdot \frac{1}{(f/E)^2(1+n\phi)} \qquad \ldots (158)$$

Equations (154), (155) and (157) may now be combined in parametric form to give the following non-dimensional expression for equivalent surface thickness as a function of surface stress

$$\bar{t}_e = \frac{\bar{w}}{f/E} + \frac{(f/E)^{2(1+m)} (1+n\phi)^{(1+m)}}{\bar{w}} \qquad \ldots (159)$$

where

$$\bar{t}_e = \frac{F^{(1+m)} t_e}{A_o^{\frac{1}{2}} C^{m/2} c^{2m}} \qquad \ldots (160)$$

$$\bar{w} = \frac{F^{(1+m)} w}{A_o^{\frac{1}{2}} C^{m/2} c^{2m} E} \qquad \ldots (161)$$

and from (A4)

$$\phi = \alpha\left(\frac{f}{E}\right)^{n-1}$$

For any given value of the load intensity parameter $\bar{w}$, and any particular stress-strain relation (α, n), equation (159) has a single natural minimum value with respect to surface stress which may be determined in a straightforward fashion by applying the condition

$$\frac{\partial \bar{t}_e}{\partial (f/E)} = 0$$

which process leads to the following results for the optimum structure.

$$\bar{t}_{eo} = \left\{\left(\frac{f}{E}\right)^{2m+1} \frac{(1+n\phi)^m [(1+m)[(1+n)n\phi+2]+1+n\phi]^2}{(1+m)[(1+n)n\phi+2]}\right\}^{\frac{1}{2}} \qquad \ldots (162)$$

$$\bar{w} = \left\{\left(\frac{f}{E}\right)^{2m+3} (1+m)(1+n\phi)^m [(1+n)n\phi+2]\right\}^{\frac{1}{2}} \qquad \ldots (163)$$

The associated optimum dimensions are found by substitution into (120), (121) and (122) which lead to

$$\bar{L} = \left\{\left(\frac{f}{E}\right)^{2m-1} (1+m) \frac{[(1+n)n\phi+2]}{(1+n\phi)^{2-m}}\right\}^{\frac{1}{2}} \qquad \ldots (164)$$

$$\bar{t} = \left\{\left(\frac{f}{E}\right)^{2m+1}(1+m)(1+n\phi)^{m}\left[(1+n)n\phi+2\right]\right\}^{\frac{1}{2}} \quad \ldots (165)$$

$$\bar{b} = \left\{\left(\frac{f}{E}\right)^{2m}(1+m)\frac{\left[(1+n)n\phi+2\right]}{(1+n\phi)^{1-m}}\right\}^{\frac{1}{2}} \quad \ldots (166)$$

where $$\bar{L} = \frac{F^{m-1}L}{A_o^{\frac{1}{2}}\, C^{m/2} c^{2m}} \quad \ldots (167)$$

$$\bar{t} = \frac{F^{m}t}{A_o^{\frac{1}{2}}\, C^{m/2} c^{2m} T} \quad \ldots (168)$$

$$\bar{b} = \frac{F^{m-\frac{1}{2}}b}{A_o^{\frac{1}{2}}\, C^{m/2} c^{2m} B} \quad \ldots (169)$$

The analysis also makes possible the separate identification of support weight as a proportion of total weight in the following form

$$\frac{t_r}{t_e} = \frac{1+n\phi}{(1+m)\left[(1+n)n\phi+2\right]+1+n\phi} \quad \ldots (170)$$

It may be noted that the above quantities are functions of surface stress alone together with material stress strain parameters.

They may therefore be used to prepare design data sheets for any given material, thus allowing ideal optimum dimensions to be read off directly for the appropriate form of construction.

The programme ZEDS, described in Appendix E performs the necessary calculations, and has been used to produce figures (57) to (61) which illustrate the character of the results for a range of materials.

Before discussing these,the special case of ideal elastic design will be considered.

Elastic analysis

The results for a perfectly elastic structure may be rapidly obtained from equations (162) to (170) by noting that in the absence of plasticity effects, $\phi = 0$. The application of this condition allows relationships to be developed explicitly, giving the following results.

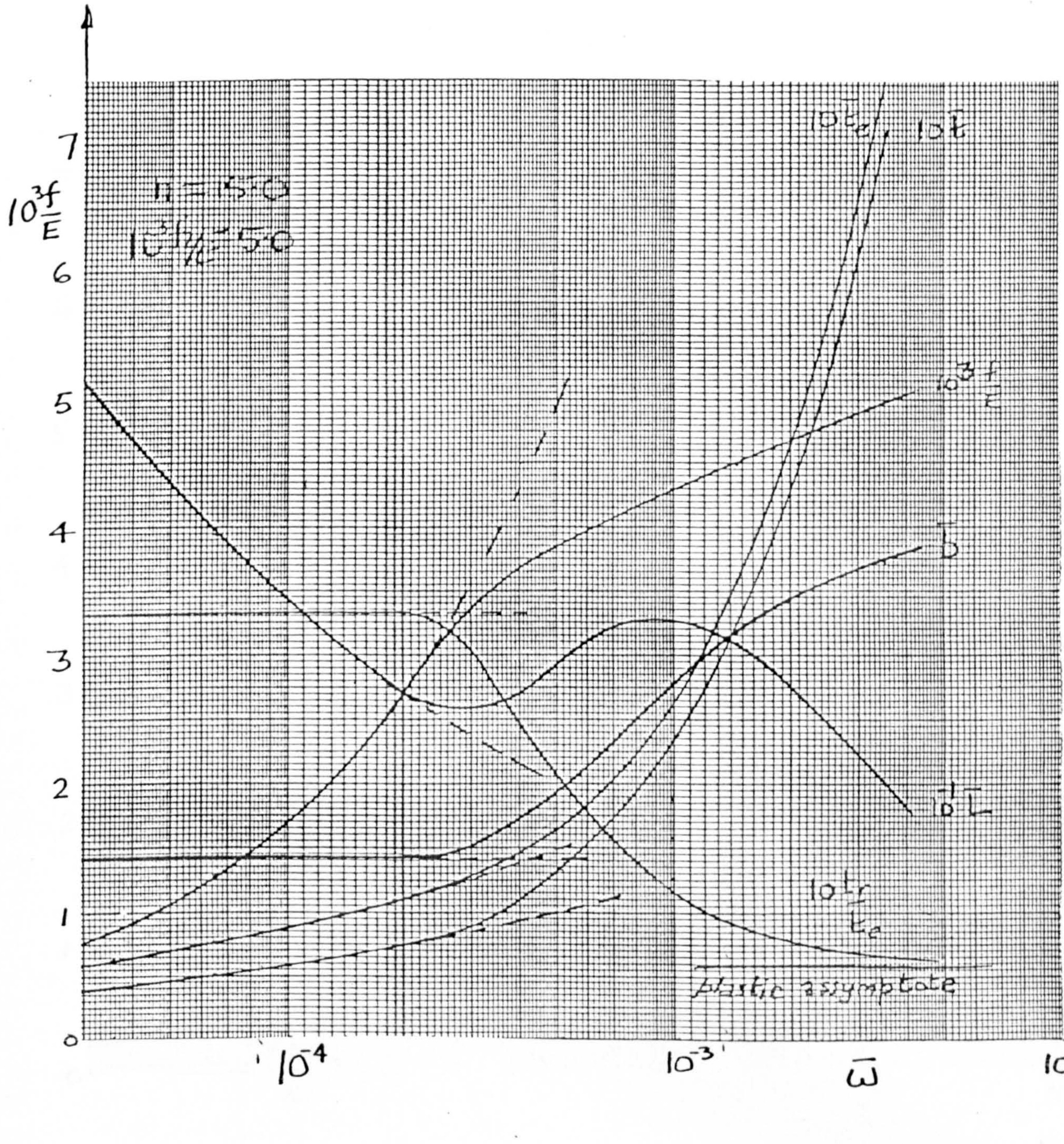

Figure 57. DESIGN DATA FOR WIDE COLUMN SURFACES WITH OPTIMUM SUPPORT LOCATIONS (CONSTANT SUPPORTS, m = 0)

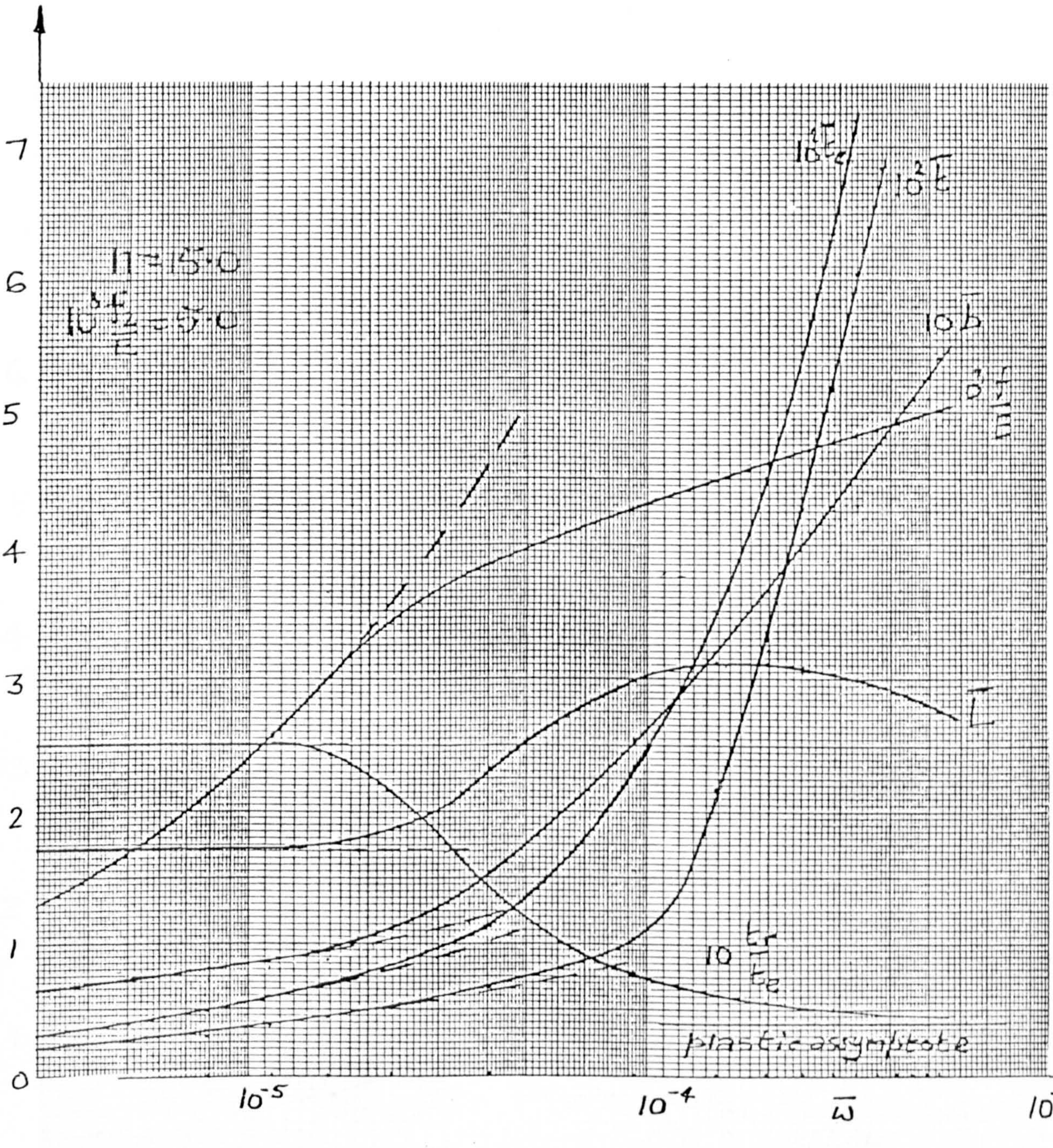

Figure 58. DESIGN DATA FOR WIDE COLUMN SURFACES WITH OPTIMUM SUPPORT LOCATIONS (GEOMETRIC SUPPORTS, $m = \frac{1}{2}$)

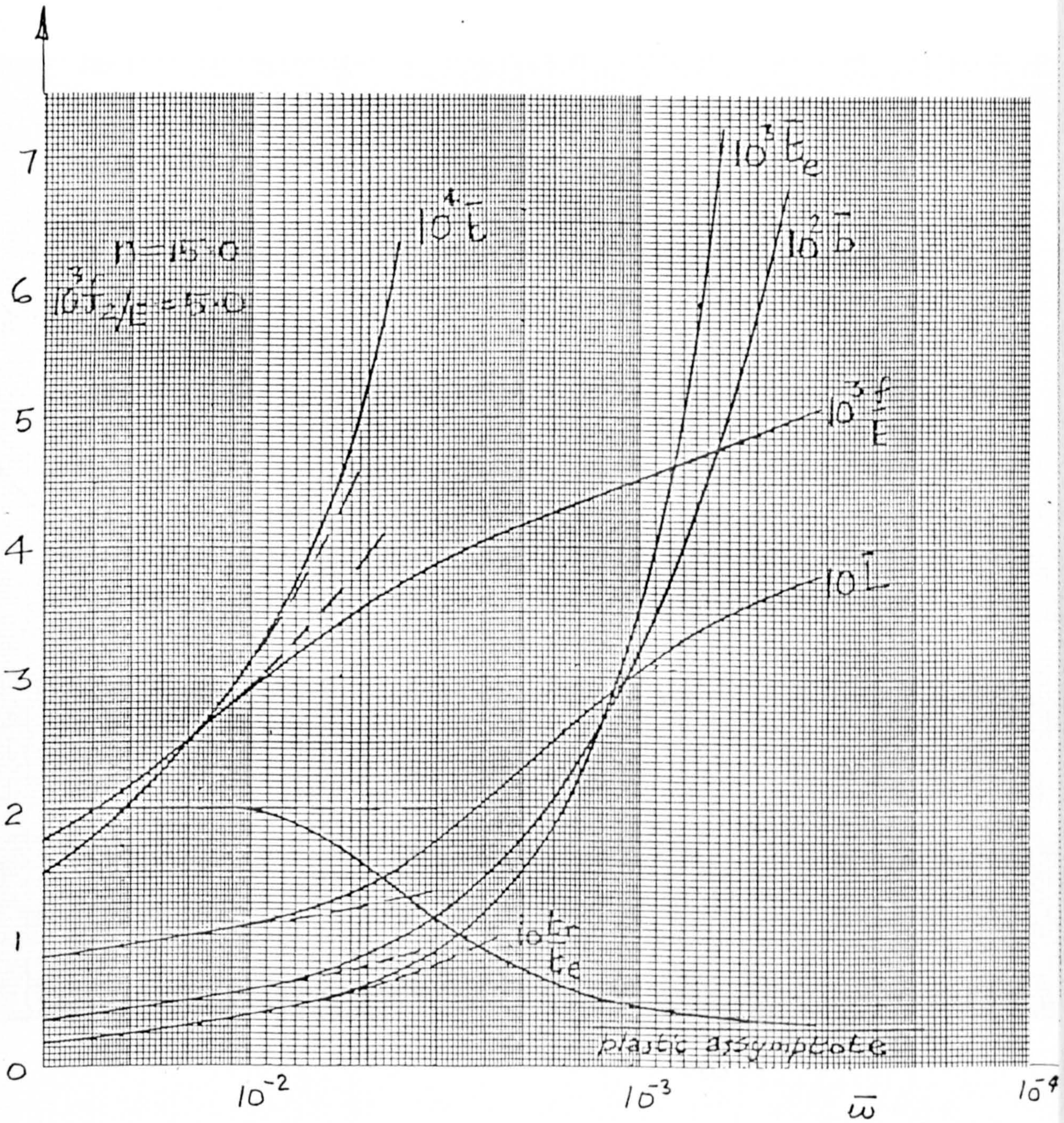

Figure 59. DESIGN DATA FOR WIDE COLUMN SURFACES WITH OPTIMUM SUPPORT LOCATIONS (LINEAR RIBS, m = 1).

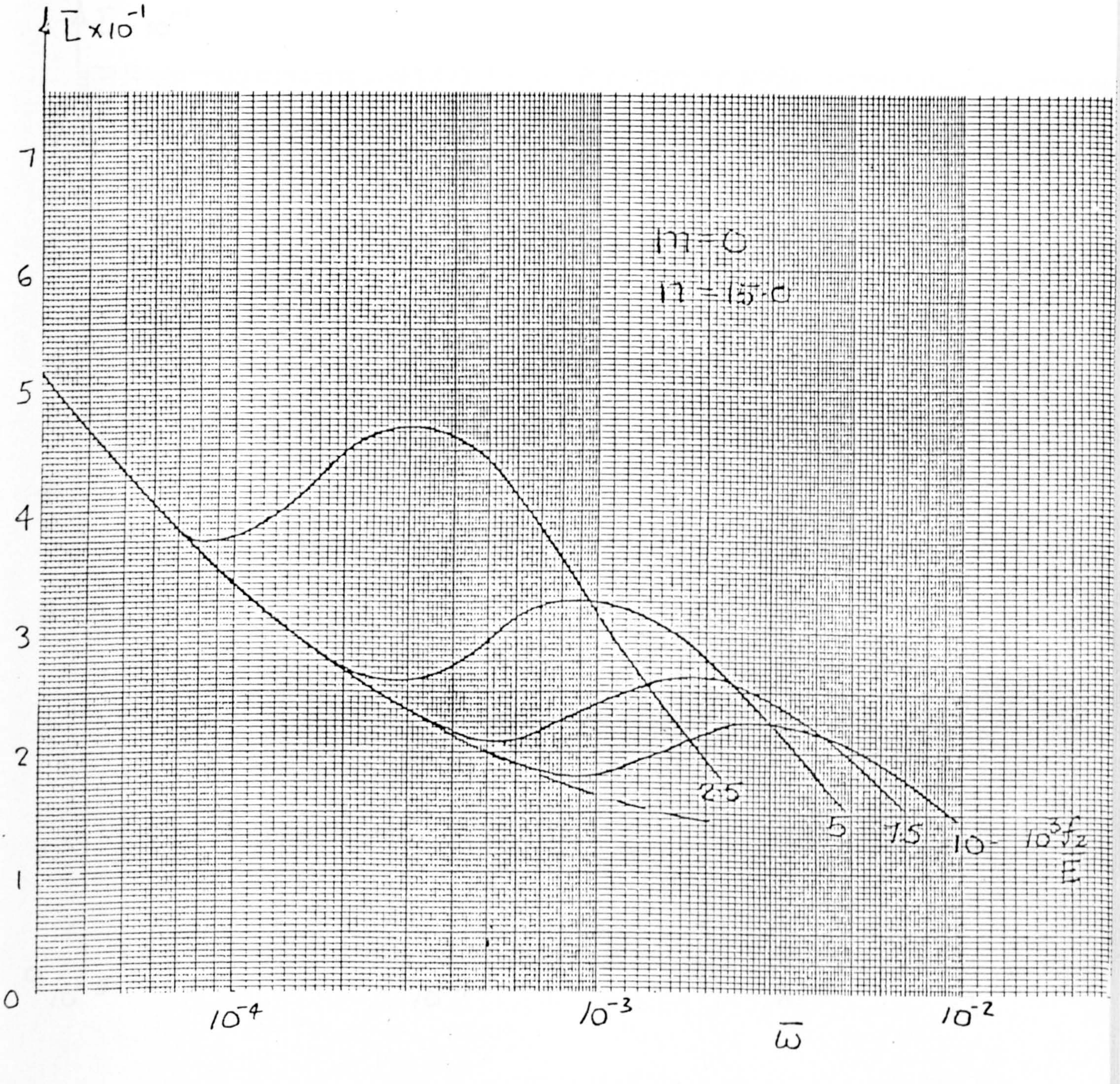

Figure 60. OPTIMUM SUPPORT SPACING FOR WIDE COLUMN SURFACES RELATED TO SURFACE MATERIAL PROOF STRESS

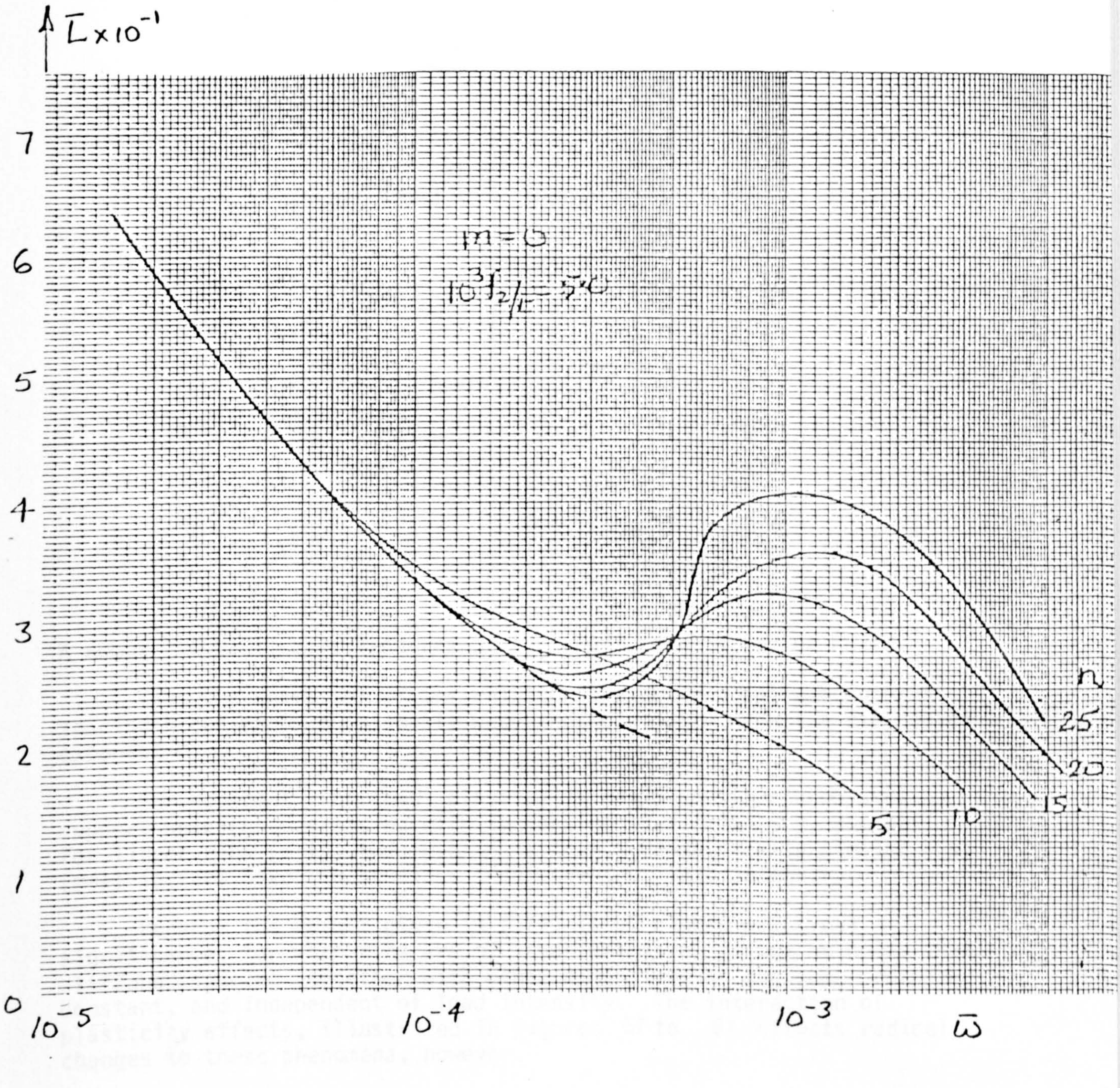

Figure 61. OPTIMUM SUPPORT SPACING FOR WIDE COLUMN SURFACES RELATED TO SURFACE MATERIAL PLASTIC STRAIN EXPONENT

$$\frac{f}{E} = \left[\frac{\bar{w}^2}{2(1+m)}\right]^{\frac{1}{2m+3}} \qquad \ldots (171)$$

$$\bar{L} = \left[4(1+m)^2 \bar{w}^{2m-1}\right]^{\frac{1}{2m+3}} \qquad \ldots (172)$$

$$\bar{t} = \left[2(1+m)\bar{w}^{2m+1}\right]^{\frac{1}{2m+3}} \qquad \ldots (173)$$

$$\bar{b} = \left\{\left[2(1+m)\right]^{3/2} \cdot \bar{w}^{2m}\right\}^{\frac{1}{2m+3}} \qquad \ldots (174)$$

$$\bar{t}_{eo} = (3+2m)\left\{\frac{\bar{w}^{2m+1}}{\left[2(1+m)\right]^{2(1+m)}}\right\}^{\frac{1}{2m+3}} \qquad \ldots (175)$$

$$\frac{t_r}{t_e} = \frac{1}{3+2m} \qquad \ldots (176)$$

A number of particular features of the above results may be noted.

Thus the character of the relationship between optimum support spacing L and endload intensity w depends crucially upon the rib design exponent m.

For constant ribs (m=0) elastically designed structures show support spacings decreasing with increasing load intensity, whereas for linear ribs (m=1), the reverse is true. Geometrically similar ribs ($m=\frac{1}{2}$) in fact have rib spacings independent of load intensity.

Perhaps the result given in (174) is of a more practical significance, for when ribs are of invariant size, it may be noted that stiffener spacing (together with other dimensions of the same order) is constant, and independent of load intensity. The interaction of plasticity effects, illustrated in figures 57 to 61 effects radical changes to these phenomena, however.

The optimum proportion of support material given by equation (176) is a generalisation of a result due to Farrar[10] who considered the case of constant ribs only.

The effect of increasing plasticity as load intensity rises is to progressively reduce the proportion of support material. A limit to this process may be distinguished by noting, from equation (170),

as $\phi \to \infty$

$$\frac{t_r}{t_e} \to \frac{1}{1+(1+m)(1+n)} \qquad \ldots (177)$$

Values for the three rib design cases are tabulated below, utilising a typical aluminium alloy value of 15 for the plasticity exponent n.

Rib material proportion ranges (n = 15)

m	0	1/2	1	
$\lim_{\phi \to 0} t\left(\frac{t_r}{t_e}\right)$	$\frac{1}{3}$	$\frac{1}{4}$	$\frac{1}{5}$	perfect elasticity
$\lim_{\phi \to \infty} t\left(\frac{t_r}{t_e}\right)$	$\frac{1}{17}$	$\frac{1}{25}$	$\frac{1}{33}$	extreme plasticity

Maximum stress limitation

At some point, as load intensity increases the design stress given implicitly by equation (163) will exceed a maximum allowable value which may be specified.

In chapter 5 for individual panels this restriction was met by the introduction of a reserve factor which gave a margin of safety in each instability mode. This had the effect of reducing the efficiency of the panel to a level corresponding to the maximum stress.

Such a strategy could be employed when the panels are of variable length, but it will be shown to lead to unnecessarily large weight penalties at low load intensities. A preferable approach over a wide load range is found to be the method explored here, which involves the expansion of support spacing from its ideal optimum value until surface stress drops to an acceptable level. Not only is this often found to give a lighter structure, but a number of significant benefits might be expected to follow.

Thus a smaller number of supports will be required for the structure as a whole, which should be cheaper. Also, individual structural dimensions (e.g. stiffener spacing) will become larger and their realisation may therefore be more practical.

Suppose the limited maximum stress is f*. Then an adjusted support spacing will lead to an equivalent surface thickness given by (159) to be

$$\bar{t}_{ec} = \frac{\bar{w}}{f^*/E} + \frac{\left[(f^*/E)^2(1+n\phi^*)\right]^{(1+m)}}{\bar{w}} \qquad \ldots (178)$$

and the adjusted panel span will be, from (158)

$$\bar{L}_c = \frac{\bar{w}}{(f^*/E)^2(1+n\phi^*)} \qquad \ldots (179)$$

The net effect of this process may be explored in the following way

(i) Choose a range of stresses $f \geq f^*$.

(ii) Use (162), (163) to find corresponding endload intensity $\bar{w}$ and ideal equivalent thickness $\bar{t}_e$.

(iii) Use (178) to find constrained equivalent thickness $\bar{t}_{ec}$.

(iv) Individual stiffener dimensions may be found from equations (121), (122).

This process has been carried out for the case $f^* = f_2 = 0.005E$, $n = 15.0$, $m = 0$ and the results are shown plotted in figure (62) which shows quite small weight increases compared with the optimum over wide range endload intensities.

For a direct comparison with the policy of reducing surface efficiency, the case of ideal elastic behaviour will be considered.

For elastic designs ($\phi^* = 0$) equations (171), (175) and (178) may be combined to give

$$\frac{t_{ec}}{t_e} = \frac{1}{(3+2m)}\left\{2(1+m)\left(\frac{w}{w^*}\right)^{\frac{2}{2m+3}} + \left(\frac{w}{w^*}\right)^{\frac{4(1+m)}{2m+3}}\right\} \qquad \ldots (180)$$

where $\bar{w}^* = [2(1+m)]^{\frac{1}{2}}(f^*/E)^{(m+3/2)}$

is the load intensity at which the maximum stress limitation begins to operate.

The policy of deliberately reducing surface efficiency may be characterised by noting from (161) and (171) that the surface stress is related to endload intensity and surface efficiency by

$$f \propto w^{\frac{2}{2m+3}} F^{\frac{2(1+m)}{2m+3}}$$

Thus the constrained (reduced) value of efficiency factor, F_c compared with the best obtainable value F is given by

$$\frac{F_c}{F} = \left(\frac{w^*}{w}\right)^{\frac{1}{1+m}} \left(\frac{f}{f^*}\right)^{\frac{2m+3}{2(1+m)}}$$

but from (171) $f \propto w^{\frac{2}{2m+3}}$

$$\therefore \frac{F_c}{F} = \left(\frac{w^*}{w}\right)^{\frac{1}{(1+m)(2m+3)}} \quad \ldots (181)$$

The ratio between surface and support weight remains invariant, and surface weight is inversely proportional to efficiency factor. Thus from (181)

$$\frac{t_{ec}}{t_e} = \frac{F}{F_c} = \left(\frac{w}{w^*}\right)^{\frac{1}{(1+m)(2m+3)}} \quad \ldots (182)$$

The results, which are compared with those from equation (180) in figure 63 show that for each value of the rib design parameter m, a significant range of load intensities above the transition value w* exists for which the support spacing expansion policy is superior.

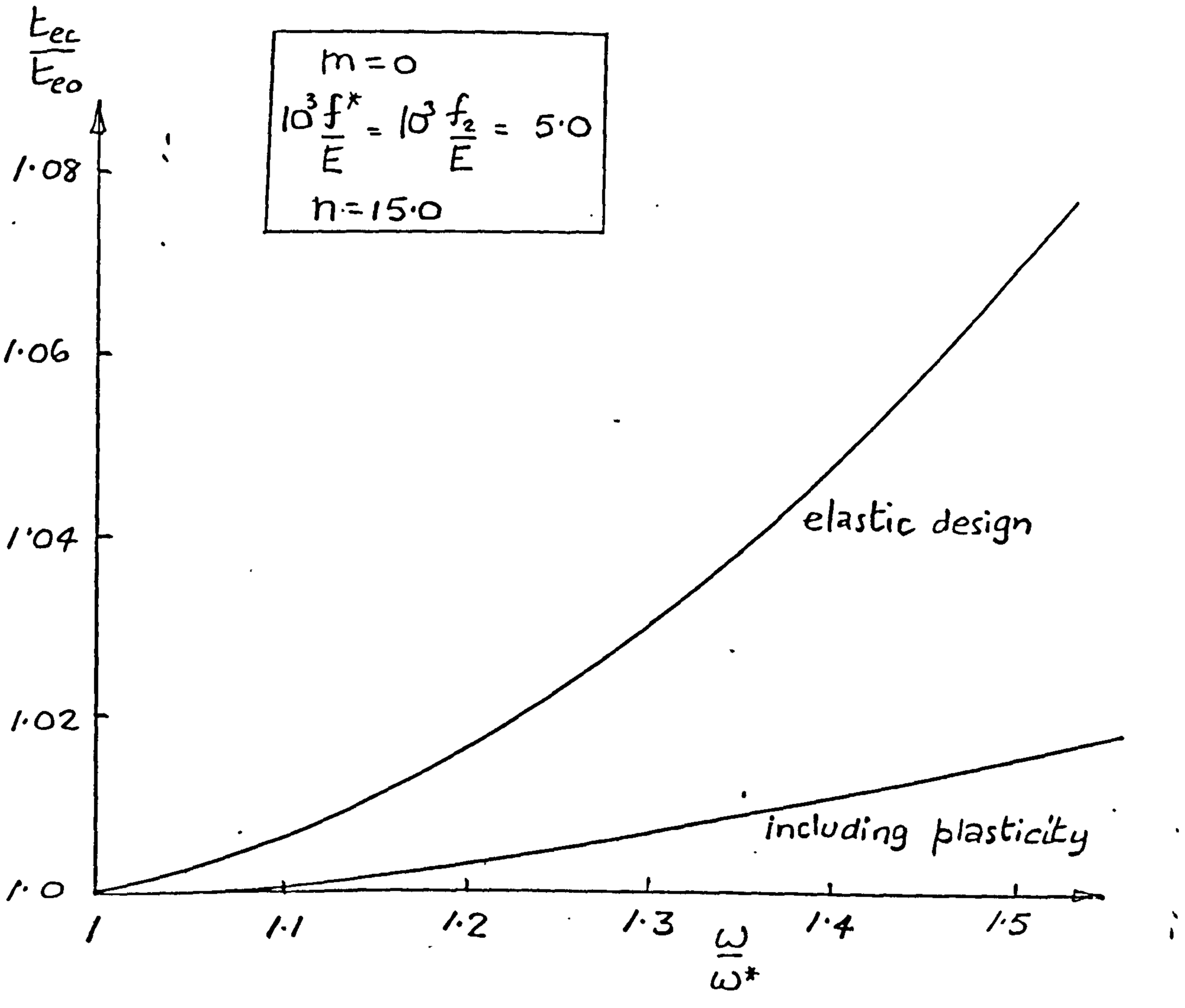

Figure 62. WEIGHT PENALTY FOR SURFACE STRESS CONSTRAINT RELATED TO DESIGN ENDLOAD INTENSITY

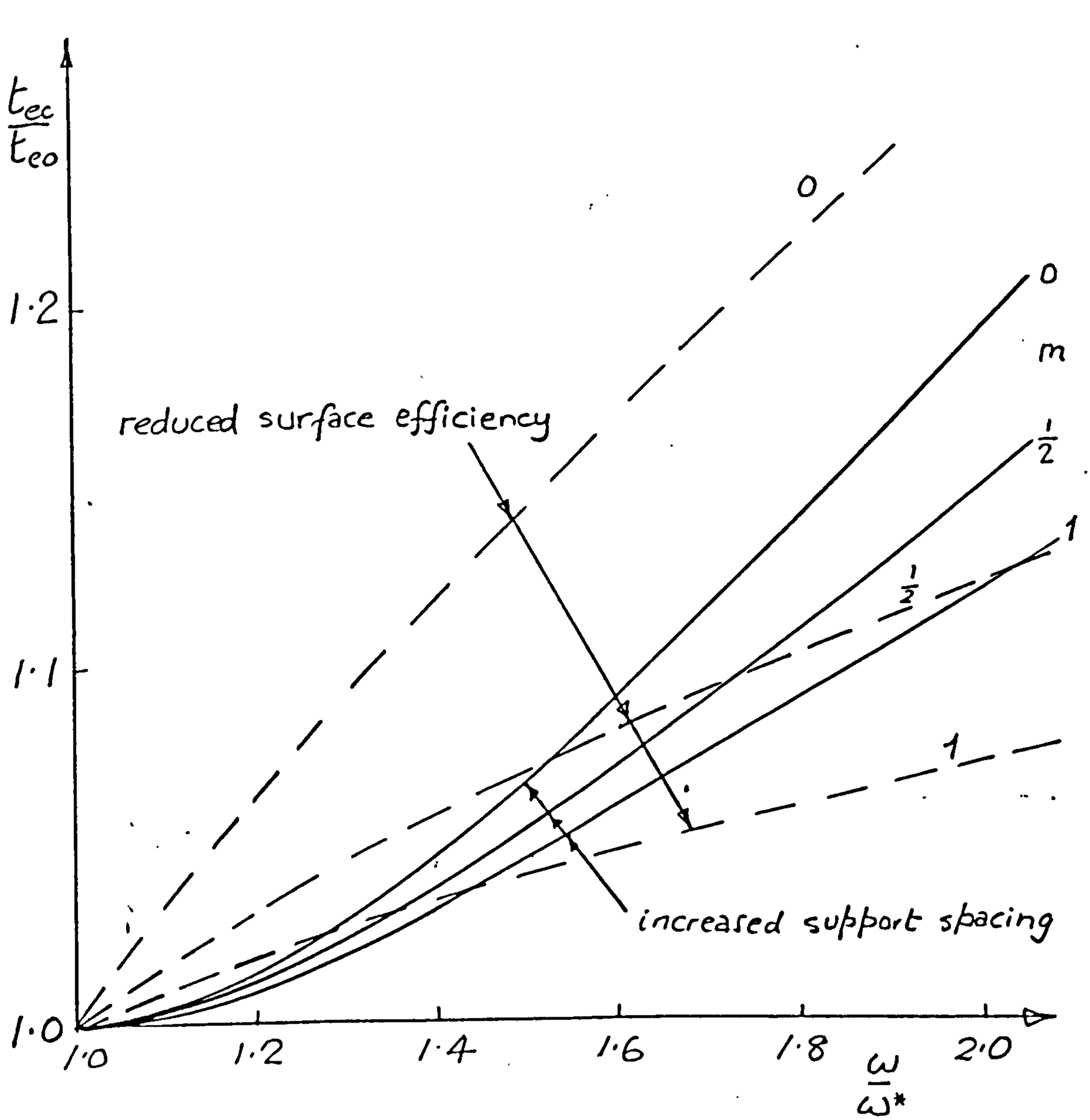

Figure 63. COMPARATIVE WEIGHT PENALTIES ASSOCIATED WITH STRESS CONSTRAINT DESIGN POLICIES.

Chapter 7

THE REINFORCED CIRCULAR CYLINDRICAL SHELL

General

The design of stiffened cylindrical shells has been extensively studied by a number of authors. The principal motivation for this effort has arisen from the requirement for very light structures of this kind for aerospace applications, e.g. aeroplane fuselages, and spacecraft booster rocket shells, although additional demand has occurred for submarine and offshore oil structures.

The most recent papers which have been published, such as the work of Simitses and Ungbhakorn[57], Bronowicki, Nelson, Felton and Schmit[58] and Pappas and Allentuch[59] [60] have been concerned with the application of non-linear mathematical programming optimisation procedures incorporating sophisticated shell buckling analysis schemes demanding large dedicated computer systems for their solution. The analysis described here has more in common perhaps with a more analytic approach often identified with the era immediately before the general application of powerful high speed computing facilities directly to optimisation problems. This approach is typified by the work of Peterson[61], Singer and Baruch[62] and Block[63]. Indeed some comparisons have been made with the results obtained by Peterson and Block towards the end of this chapter.

The results obtained in the previous two chapters have been built upon to produce solutions appropriate to the reinforced cylindrical shell. This has been possible because with primarily axial reinforcement, the transverse curvature of the shell wall has negligible effect on behaviour in the modes of buckling considered. Shell buckling per se, which has been the subject of an enormous expenditure of research resources in the last thirty years has very little influence in this context, especially if frame stiffness criteria are used which ensure the imposition of nodes and effectively simple support at each location as described in chapter 6.

Some of the work described here was published earlier (Richards[56]) in an abbreviated form which was somewhat less general than the present analysis.

Analysis with plasticity

The design of a circular cylindrical shell of diameter D will be considered.

The shell is required to carry a given bending moment M which induces a maximum compressive loading w in the shell surface given by

$$w = \frac{4M}{\pi D^2} \qquad \ldots (183)$$

The shell surface is fabricated from wide column stiffened panels of the sort already described in chapter 5, supported at regular intervals L by ring frame stiffeners, which provide simple support in the Euler mode of buckling.

The frames will be designed according to the criteria discussed in chapter 6, which includes the possibility that their size may be constant i.e. independent of pitch, diameter, loading, etc. ($m = 0$). The shell diameter will be regarded as a design variable, and its optimum value sought.

The support span dimension c as defined in equation (154) is precisely equivalent to shell diameter D, and the corresponding support stiffness coefficient is therefore given by (153) to be

$$C = \frac{\pi}{4} C_f = 6.25 \times 10^{-5} \times \frac{\pi}{4} = \underline{49.09 \times 10^{-6}}$$

(using Gerards'[13] figure with $c = D$).

The shell diameter may then be related to the endload intensity parameter $\bar{w}$ by using (161) and (183) to give

$$\bar{D} = \left[\frac{1}{\bar{w}}\right]^{\frac{1}{2(1+m)}} \qquad \ldots (184)$$

where

$$\bar{D} = \left[\frac{\pi A_o^{\frac{1}{2}} C^{m/2} E}{4MF^{(1+m)}}\right]^{\frac{1}{2(1+m)}} . \; D \qquad \ldots (185)$$

The total equivalent cross section area of the shell is given by

$$A_e = \pi D t_e \qquad \ldots (186)$$

Thus from (184), (163), (162) etc.

$$\bar{A}_e = \left[\frac{(1+n\phi)^m [(1+m)[(1+n)n\phi+2] + 1+n\phi]^{4(1+m)}}{(\frac{f}{E})^{(2m+1)} [(1+m)[(1+n)n\phi+2]]^{(3+4m)}}\right]^{\frac{1}{4(1+m)}} \qquad \ldots (187)$$

which is a function of surface stress alone.

Corresponding expressions for diameter and frame pitch also in terms of surface stress may be derived as follows

$$\bar{D} = \frac{1}{\left\{\left(\frac{f}{E}\right)^{(2m+3)}(1+m)(1+n\phi)^{m}\left[(1+n)n\phi+2\right]\right\}^{\frac{1}{4(1+m)}}} \quad \ldots (188)$$

$$\bar{L} = \left\{\frac{(1+m)[(1+n)n\phi+2]}{\left(\frac{f}{E}\right)^{(2m+1)}(1+n\phi)^{(2+m)}}\right\}^{\frac{1}{2(1+m)}} \quad \ldots (189)$$

where

$$\bar{A}_e = \left\{\frac{F^{(1+m)}}{\pi A_o^{\frac{1}{2}} C^{m/2}}\left[\frac{E}{4M}\right]^{(2m+1)}\right\}^{\frac{1}{2(1+m)}} \cdot A_e \quad \ldots (190)$$

$$\bar{L} = \left\{\left[\frac{\pi E}{4M}\right]^{m}\frac{1}{(A_o C^m)^{\frac{1}{2}}}\right\}^{\frac{1}{1+m}} \cdot \frac{L}{F} \quad \ldots (191)$$

Equation (188) indicates that the surface stress increases monotonically as shell diameter is reduced.

For elastic designs ($\phi=0$), equation (187) gives

$$\bar{A}_c = \frac{3+2m}{\left[\left(\frac{f}{e}\right)^{(1+2m)}[2(1+m)]^{(3+4m)}\right]^{\frac{1}{4(1+m)}}} \quad \ldots (192)$$

Thus without plasticity effects, a continuously lighter design is indicated as shell diameter is reduced.

However a numerical investigation of equation (187) (for for example, figure (64)), indicates that the intervention of plasticity eventually reverses this trend, and shell weight then increases with decreasing diameter. This tendency will be confirmed by noting from (187) that as $\phi \to \infty$.

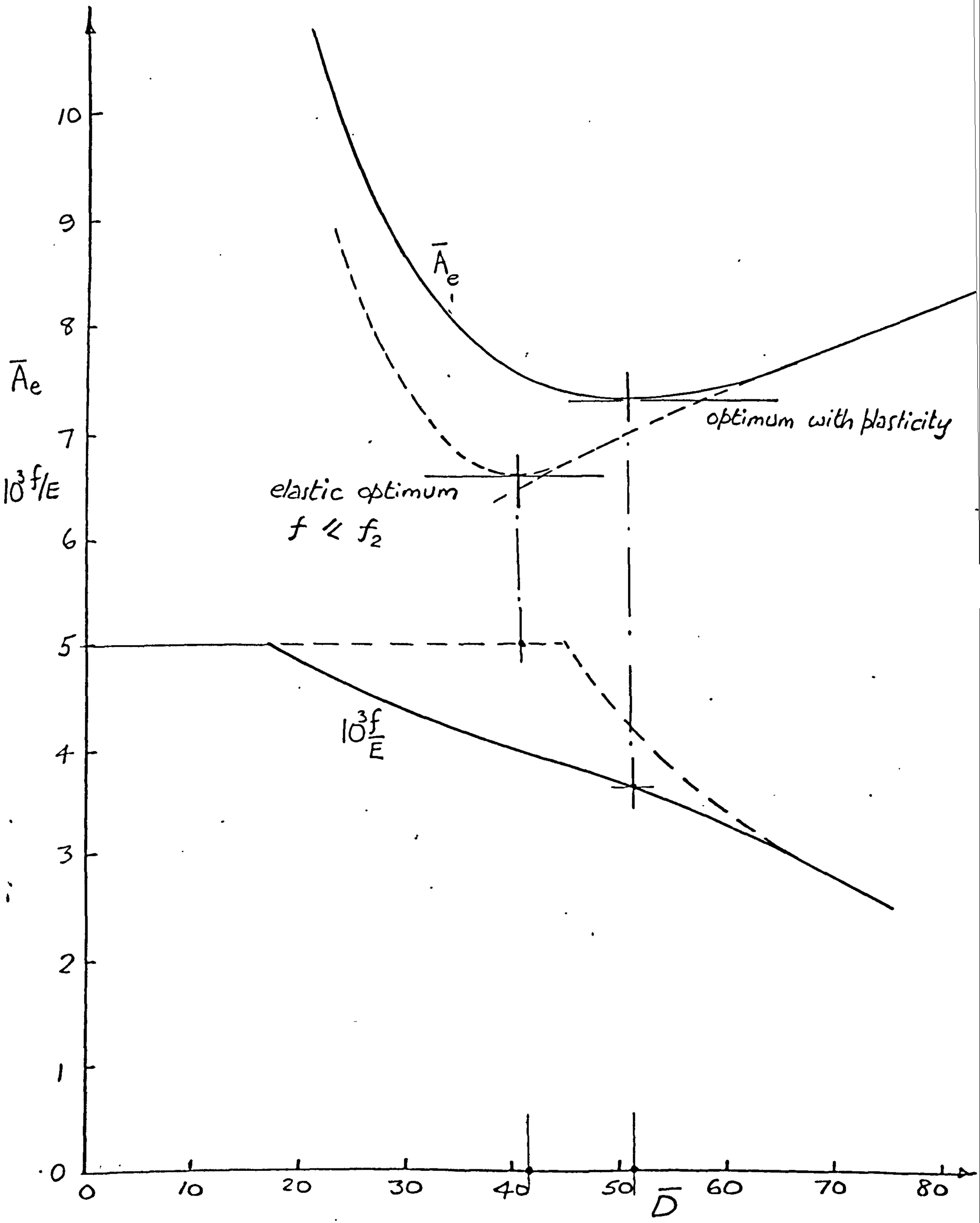

Figure 64. DESIGN OF REINFORCED CYLINDRICAL SHELLS WITH AND WITHOUT PLASTICITY

$$\bar{A}_e \rightarrow \left\{ \frac{\alpha^{(1+m)}[1+(1+m)(1+n)]^{4(1+m)}}{[(1+m)(1+n)]^{(3+4m)}} \cdot \left(\frac{f}{E}\right)^{[n(1+m)-(3m+2)]} \right\}^{\frac{1}{4(1+m)}}$$

$\rightarrow \infty$, provided that $n > \frac{3m+2}{m+1}$.

Relevant values for this criterion are

$$\left\{ \begin{matrix} m = 0 , & 1/2 , & 1 \\ n \geq 2 , & 7/3 , & 5/2 \end{matrix} \right\} \qquad \ldots (193)$$

There are no important structural materials with values of n much less than 10, so that it may be assumed that (193) will be comfortably met.

Thus the existence of an optimum value of surface stress giving minimum shell weight is indicated. Moreover, this value will be specific to all shells designed with a particular given material defined by the parameters f_2/E and n, and will thus be a fundamental property of that material.

Equation (187) is rather too complex to allow the minimum to be found analytically by differentiation. However, a numerical search is straightforward, and the programme ORCS described in Appendix E has been devised for that purpose.

ORCS gives optimum values of equivalent shell area, surface stress, shell diameter and frame spacing for any given material. Off optimum values for the complete range of surface stresses are given by ZEDS.

Results obtained using ORCS for a representative range of materials are shown plotted in figures 65 to 72.

Elastic design

The question of the design of reinforced shells when the material is elastic remains open.

It has already been noted that theoretically structure weight will decrease without limit as shell diameter is decreased.

However this process involves a monotonic increase in surface stress, and at some point a maximum allowable stress limit will be imposed.

With surface stress now constrained, any further reduction in shell diameter will lead to higher endload intensities for a given design bending moment which will activate the procedure discussed in chapter 6 for the design of surfaces with a maximum stress limitation operative.

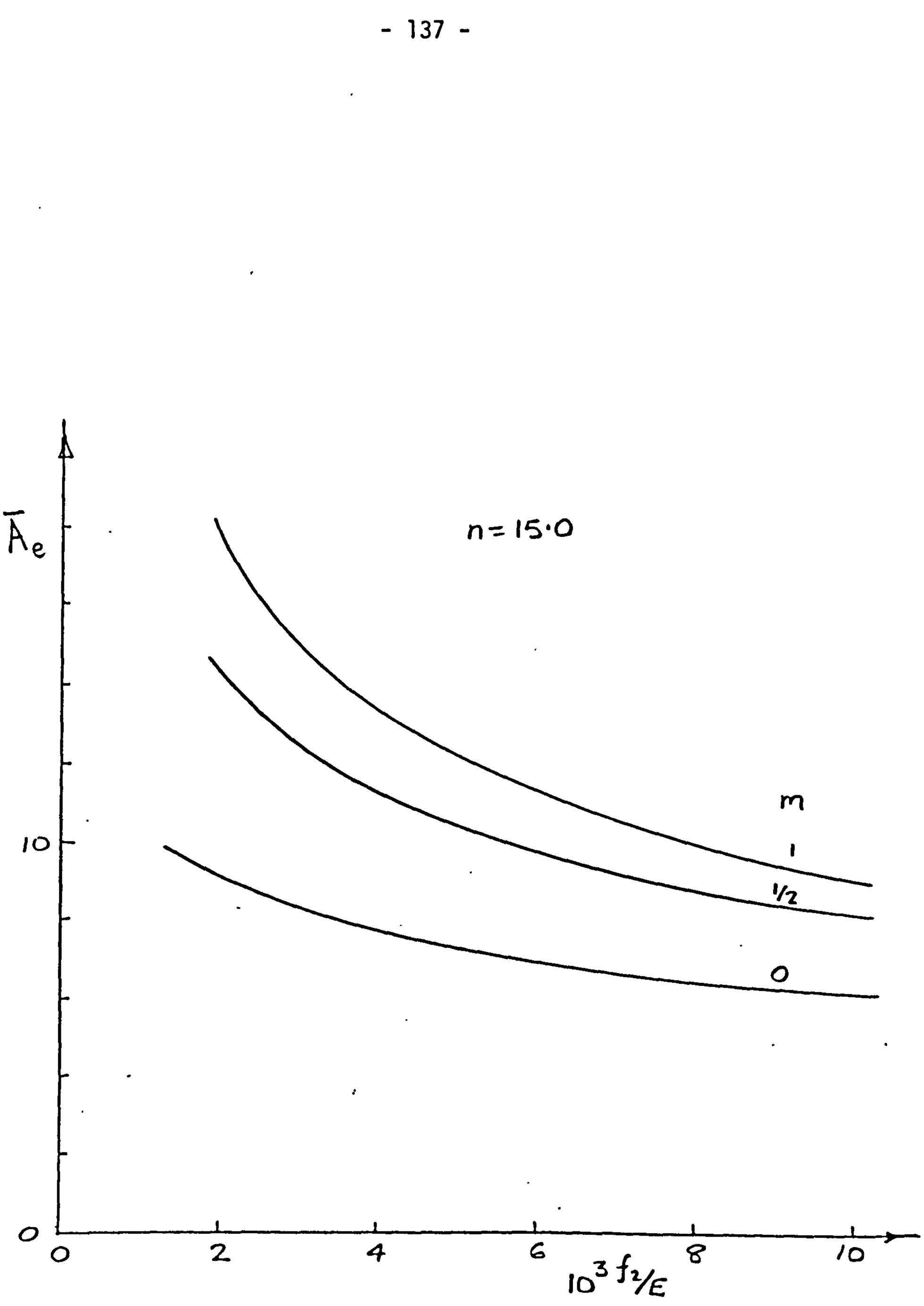

Figure 65. SHELL EQUIVALENT CROSS SECTION AREA RELATED TO PROOF STRESS

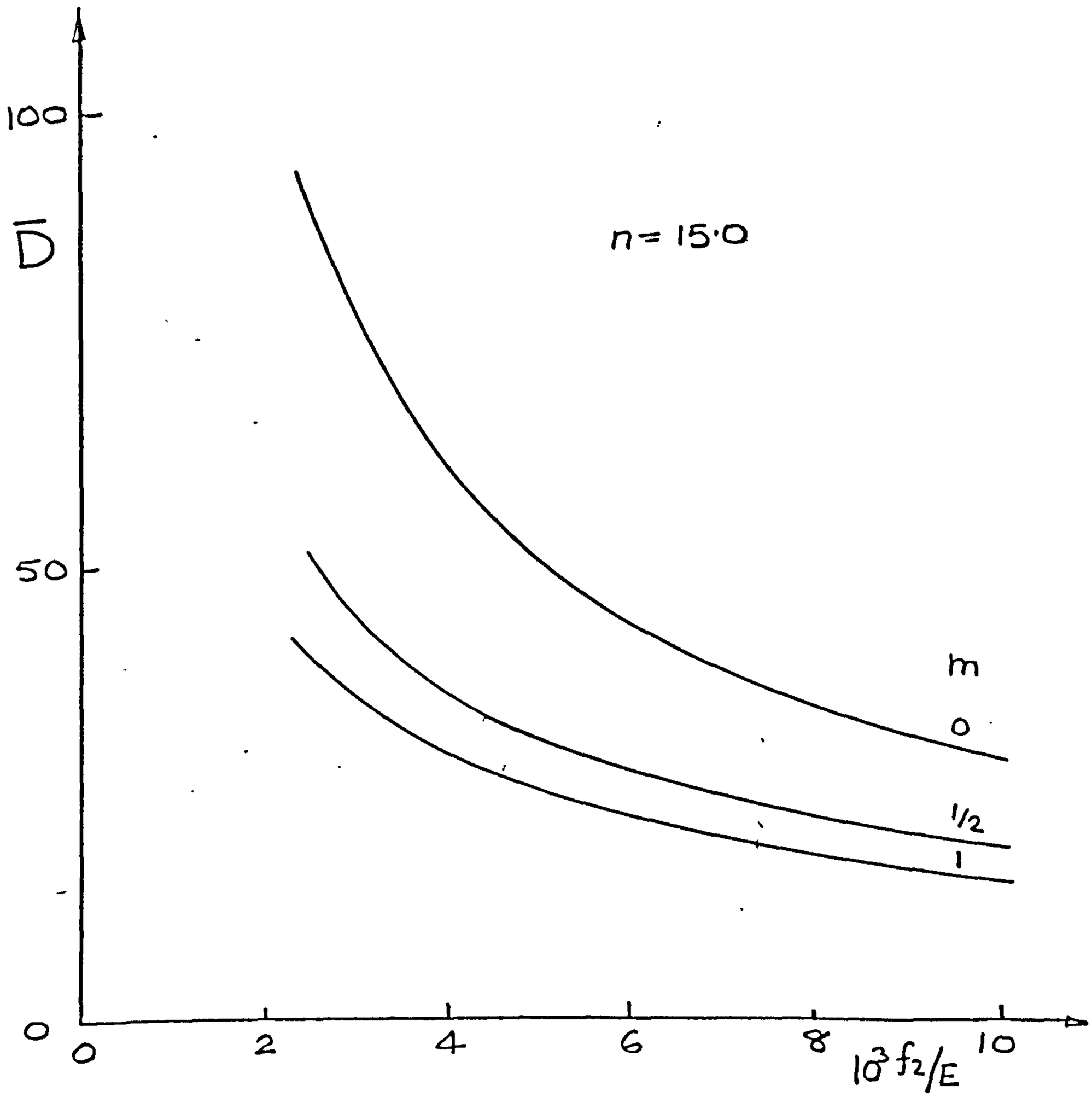

Figure 66. OPTIMUM SHELL DIAMETER RELATED TO MATERIAL PROOF STRESS

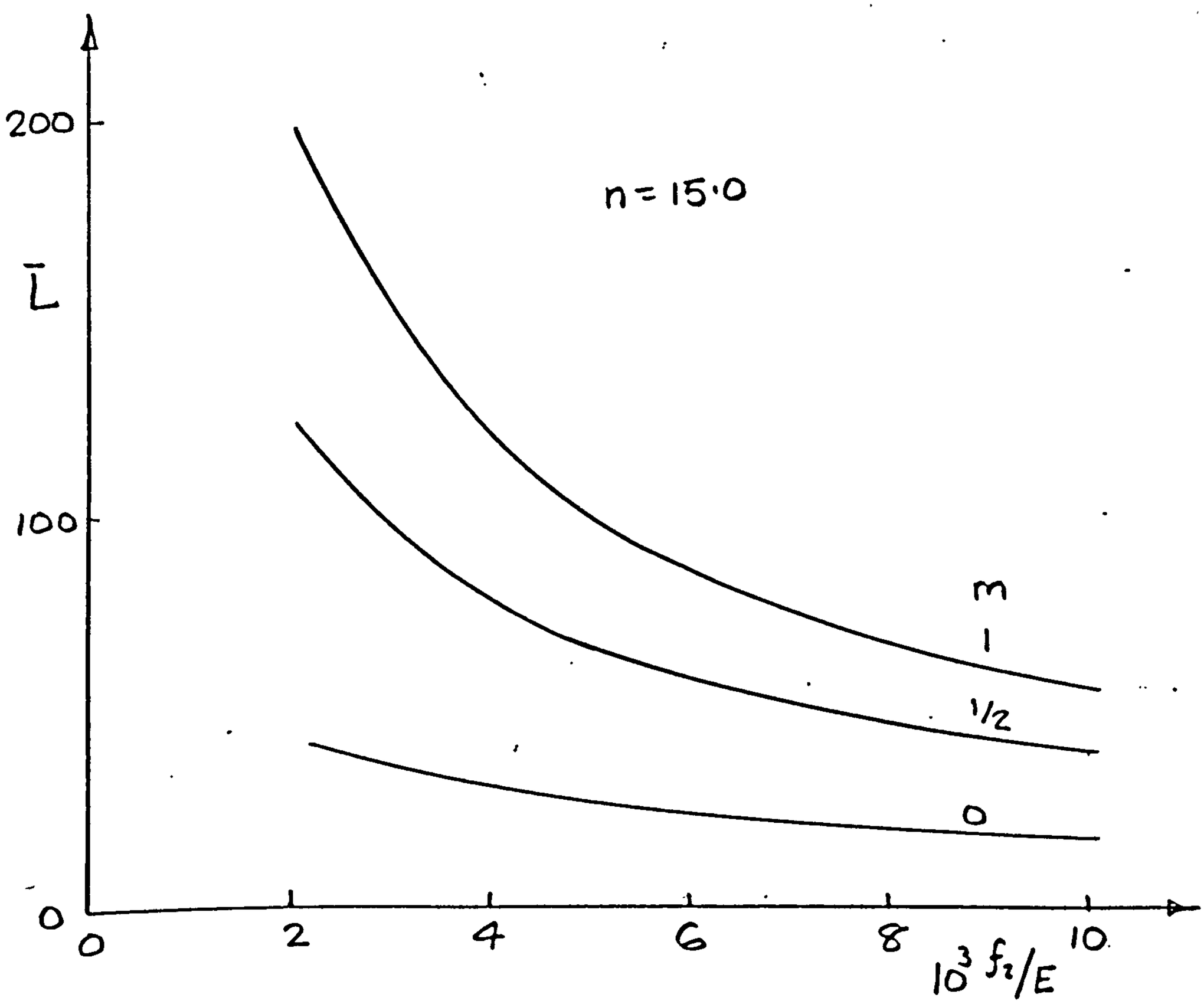

Figure 67. SHELL FRAME PITCH RELATED TO MATERIAL PROOF STRESS

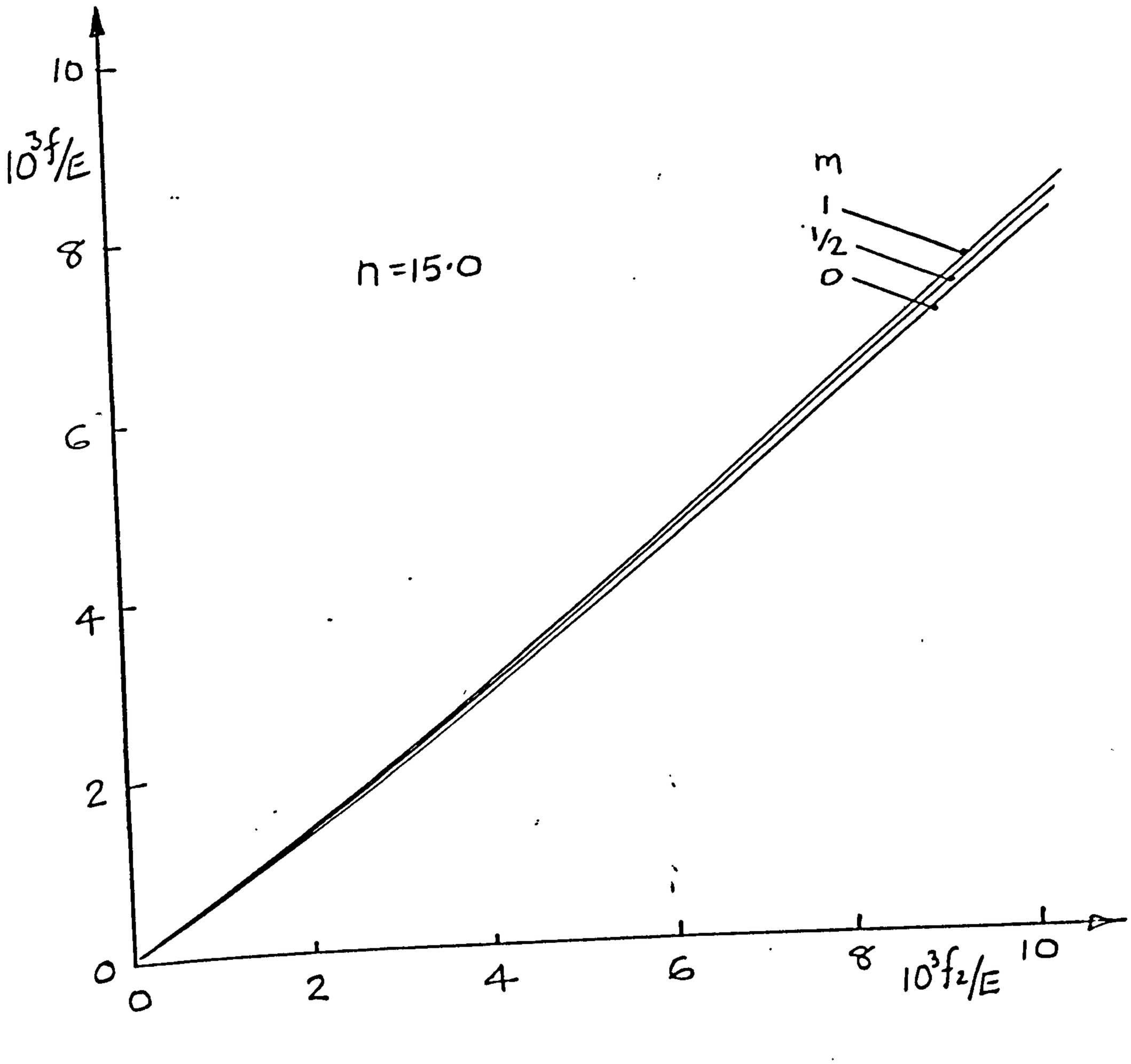

Figure 68. SHELL SURFACE STRESS RELATED TO MATERIAL PROOF STRESS

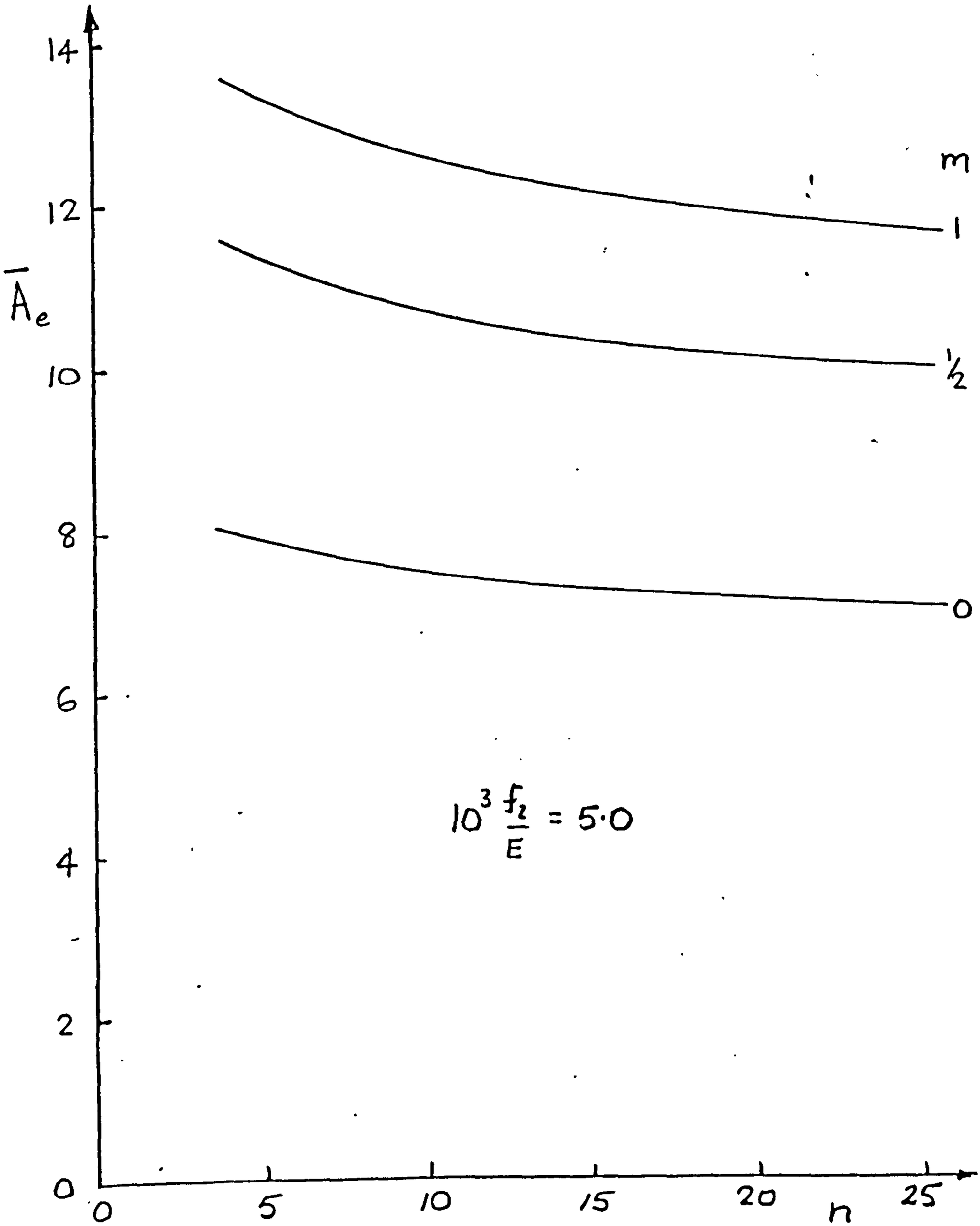

Figure 69. SHELL EQUIVALENT CROSS SECTION AREA RELATED TO PLASTIC STRAIN EXPONENT

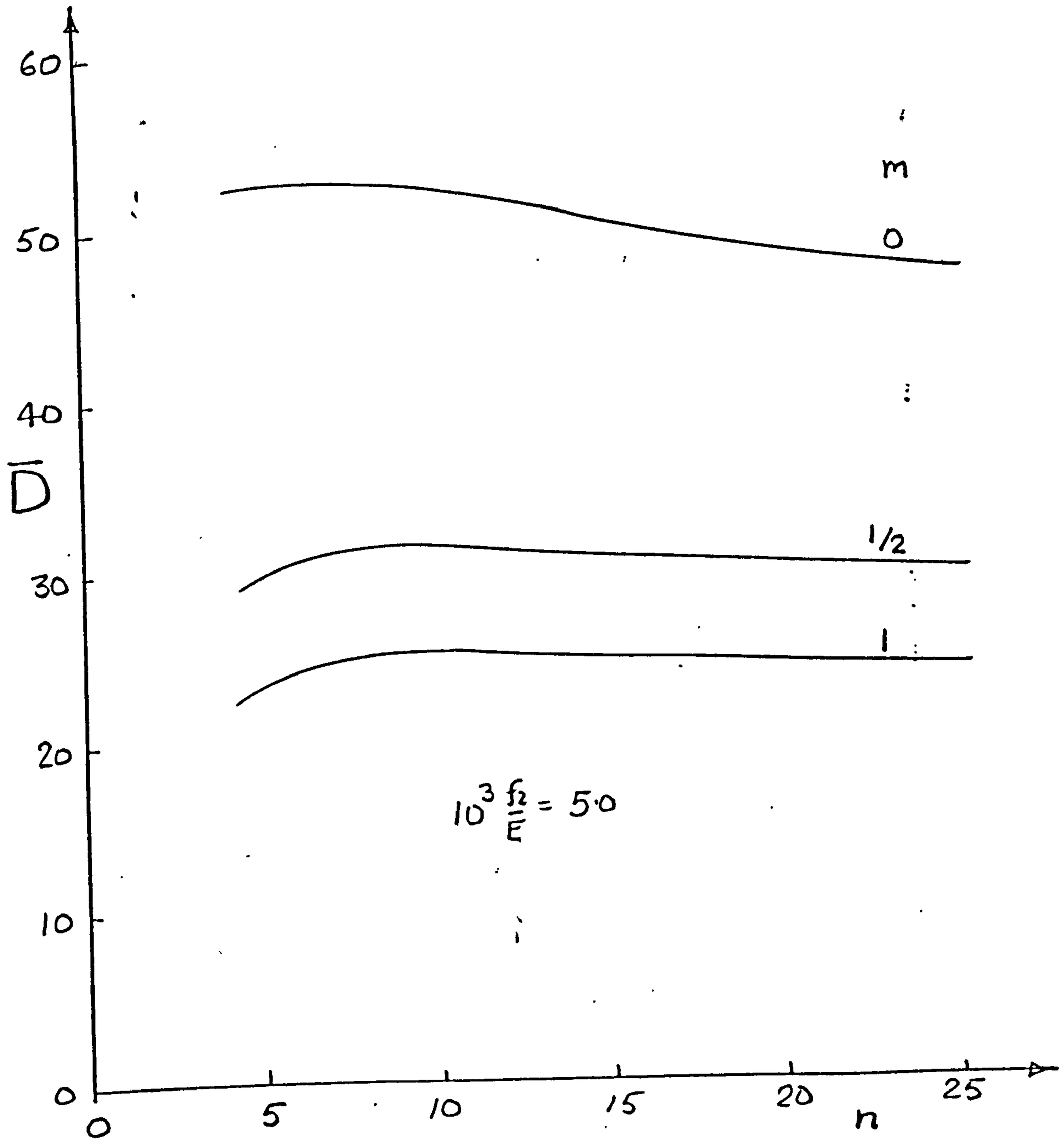

Figure 70. OPTIMUM SHELL DIAMETER RELATED TO PLASTIC STRAIN EXPONENT.

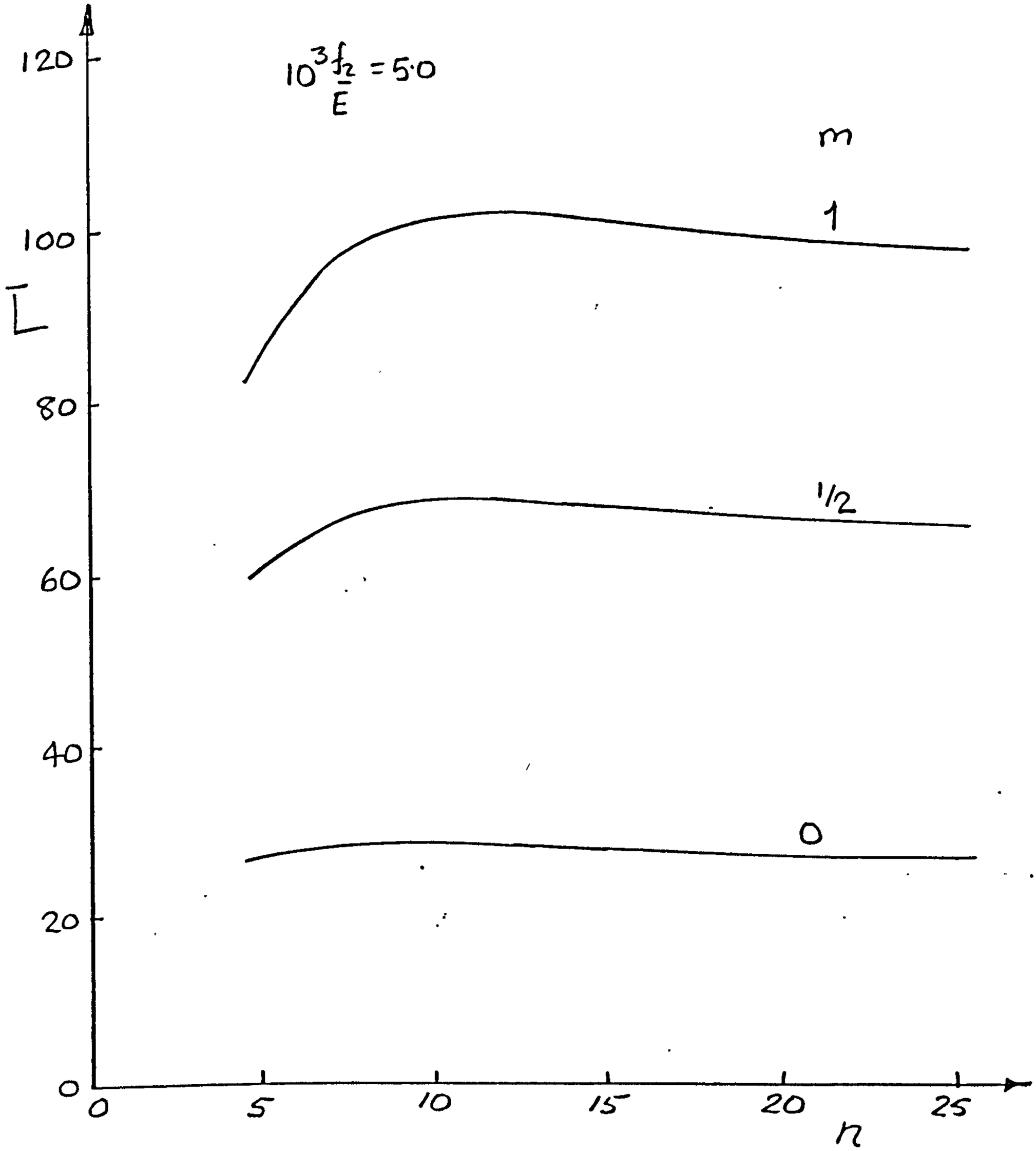

Figure 71. OPTIMUM FRAME PITCH FOR STIFFENED SHELLS RELATED TO PLASTIC STRAIN EXPONENT.

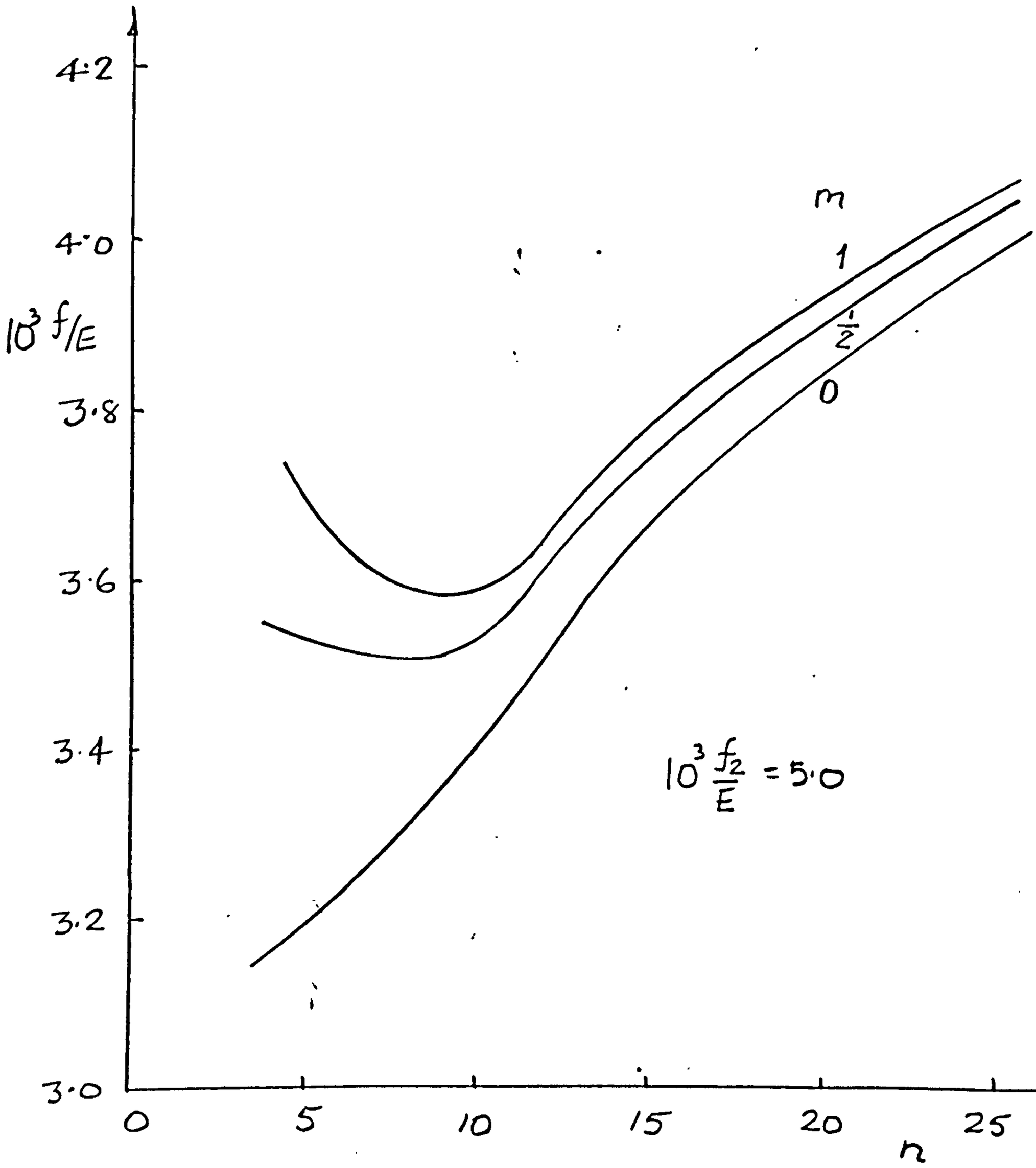

Figure 72. SHELL SURFACE STRESS RELATED TO PLASTIC STRAIN EXPONENT

This process will now be considered in detail as it applies to cylindrical shell design.

For elastic designs, from (188) and (189)

$$\bar{D} = \frac{1}{\left[2\left(\frac{f}{E}\right)^{(2m+3)}_{(1+m)}\right]^{\frac{1}{4(1+m)}}} \qquad \ldots (194)$$

$$\bar{L} = \left\{\frac{2(1+m)}{(f/E)^{(2m+1)}}\right\}^{\frac{1}{2(1+m)}} \qquad \ldots (195)$$

(194) may be used to express the relevant quantities in terms of shell diameter.

Thus

$$\bar{A}_e = (3+2m)\left\{\frac{D^{(2m+1)}}{[2(1+m)]^{2(m+1)}}\right\}^{\frac{1}{2m+3}} \qquad \ldots (196)$$

$$\bar{L} = \left[2(1+m)\right]^2 \bar{D}^{\frac{2(2m+1)}{2m+3}} \qquad \ldots (197)$$

From (183), (192)

$$\bar{w}^* = \frac{1}{\bar{D}^{*2}} \qquad \ldots (198)$$

$$\left(\frac{f}{E}\right)^* = \left[\frac{1}{2(1+m)D^{*4(1+m)}}\right]^{\frac{1}{(2m+3)}} \qquad \ldots (199)$$

where D^*, w^* are the diameter and corresponding load intensity at which the maximum stress limitation begins to apply.

From (178), if surface stress is constrained to be f^*, equivalent surface thickness will be

$$\bar{t}_{ec} = \frac{\bar{w}}{f^*/E} + \frac{(f^*/E)^{(1+m)}}{\bar{w}} \qquad \ldots (200)$$

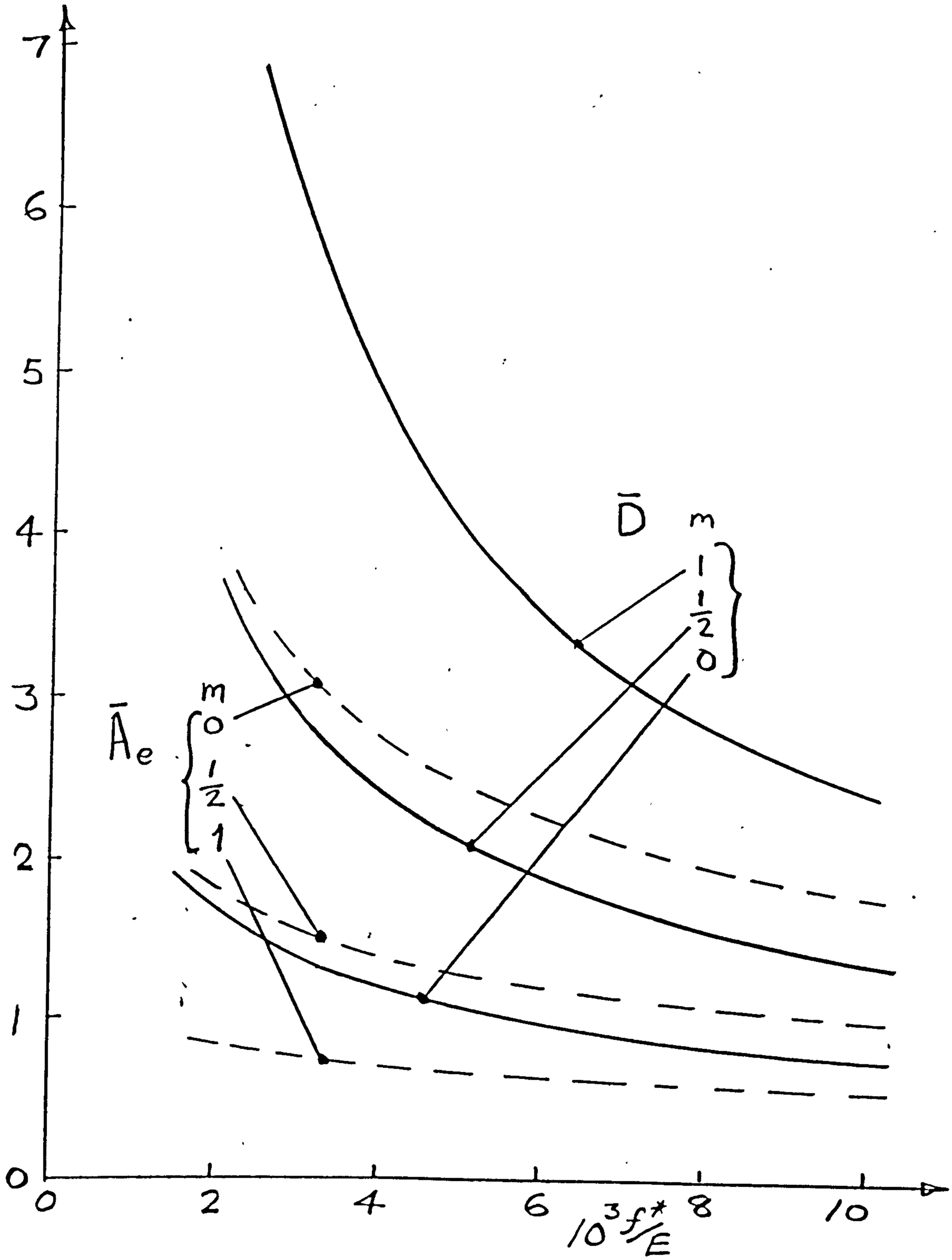

Figure 73. OPTIMUM ELASTIC DESIGNS FOR REINFORCED SHELLS

Shell equivalent cross-section area is

$$\bar{A}_{ec} = \bar{D}\,\bar{t}_{ec}$$

so that, from (198), (199), (200)

$$\bar{A}_{ec} = \frac{1}{\bar{D}f^*/E} + \bar{D}^3(f^*/E)^{(1+m)} \qquad \ldots (201)$$

Equation (201) may be differentiated to determine the optimum diameter at which constrained shell weight takes its minimum value.

$$\therefore \frac{\partial \bar{A}_{ec}}{\partial \bar{D}} = -\frac{1}{\bar{D}^2(f^*/E)} + 3\bar{D}^2(f^*/E)^{(1+m)} = 0$$

so that

$$\bar{D}_o = \left\{\frac{1}{3(f^*/E)^{2+m}}\right\}^{\frac{1}{4}} \qquad \ldots (202)$$

$$\bar{A}_{eco} = \frac{4}{3}\left\{\frac{3}{(f^*/E)^{2-m}}\right\}^{\frac{1}{4}} \qquad \ldots (203)$$

$$\bar{L}_o = 4(1+m)^2\left\{\frac{1}{3(f^*/E)^{2+m}}\right\}^{\frac{2m+1}{2(2m+3)}} \qquad \ldots (204)$$

It may be noted that the optimum design invariably is composed of 25% frames, 75% shell surface. These results are illustrated in figure 64 which reveals the relationship between elastic designs and those affected by plasticity, and figure 73, where the interdependence of maximum allowable stress and optimum dimensions is shown.

Comparisons

It may be of interest to compare the results obtained above with those due to two earlier authors, who employed rather different approaches to the reinforced shell design problem. Both have relied on an analysis by Block, Card and Mikulas[64] for the characteristics of orthotropic buckling behaviour, together with standard local and Euler analysis.

Peterson[61] considered a cylinder with trapezoidally corrugated walls reinforced by ring stiffeners of various cross-sections fitted both inside and outside the shell. The cylinders with external rings proved to be lighter, as indicated in Figure 75 which has been adapted from reference 61

In terms of the present notation, the scales of Petersons figure require interpretation.

The load intensity parameter is $2w/D$, while the structure weight quantity is $2\rho t_e/D$, where ρ is material density.

Equations (183), (185) and (190) may be used (together with m = 0) to transform these quantities, giving

$$\frac{2w}{D} = \frac{\Psi}{\bar{D}^3} \qquad \ldots (205)$$

$$\frac{2\rho t_e}{D} \doteq \frac{\rho}{EF^{\frac{3}{2}}} \cdot \psi \cdot \frac{\bar{A}_e}{\bar{D}^2} \qquad \ldots (206)$$

where

$$\psi = \left[\frac{\pi E^3 A_o^{\frac{3}{2}}}{M}\right]^{\frac{1}{2}} \qquad \ldots (207)$$

For a typical aluminium alloy (n = 15.0, $f_2/E = 0.005$) ORCS gives the optimum equivalent area and diameter parameters

$$\bar{A}_c = 7.266$$

$$\bar{D} = 50.097$$

For aluminium alloys, $\rho = 0.1$ lb/in^3, $E = 10^7$ lbf/in^2 and for the optimum trapezoidal corrugation, F = 1.26.

Thus to plot the results from the present work, appropriate values of $\frac{2w}{D^2}$ are chosen from which (205) is used to calculate the corresponding values of ψ, then (206) gives the corresponding value of $\frac{2\rho t_e}{D}$

The results are shown in Figure 75, indicating a substantial weight saving compared with Petersons solution.

Details of a design by Block[63] are shown in figure 74. T section frames and stiffeners were utilised to produce a number of designs for differing diameters and load intensities.

For Blocks example

$A_o = 0.117$ in^2

L = 20 in

EI = 5.51×10^6 lbf/in^2

F = 0.906

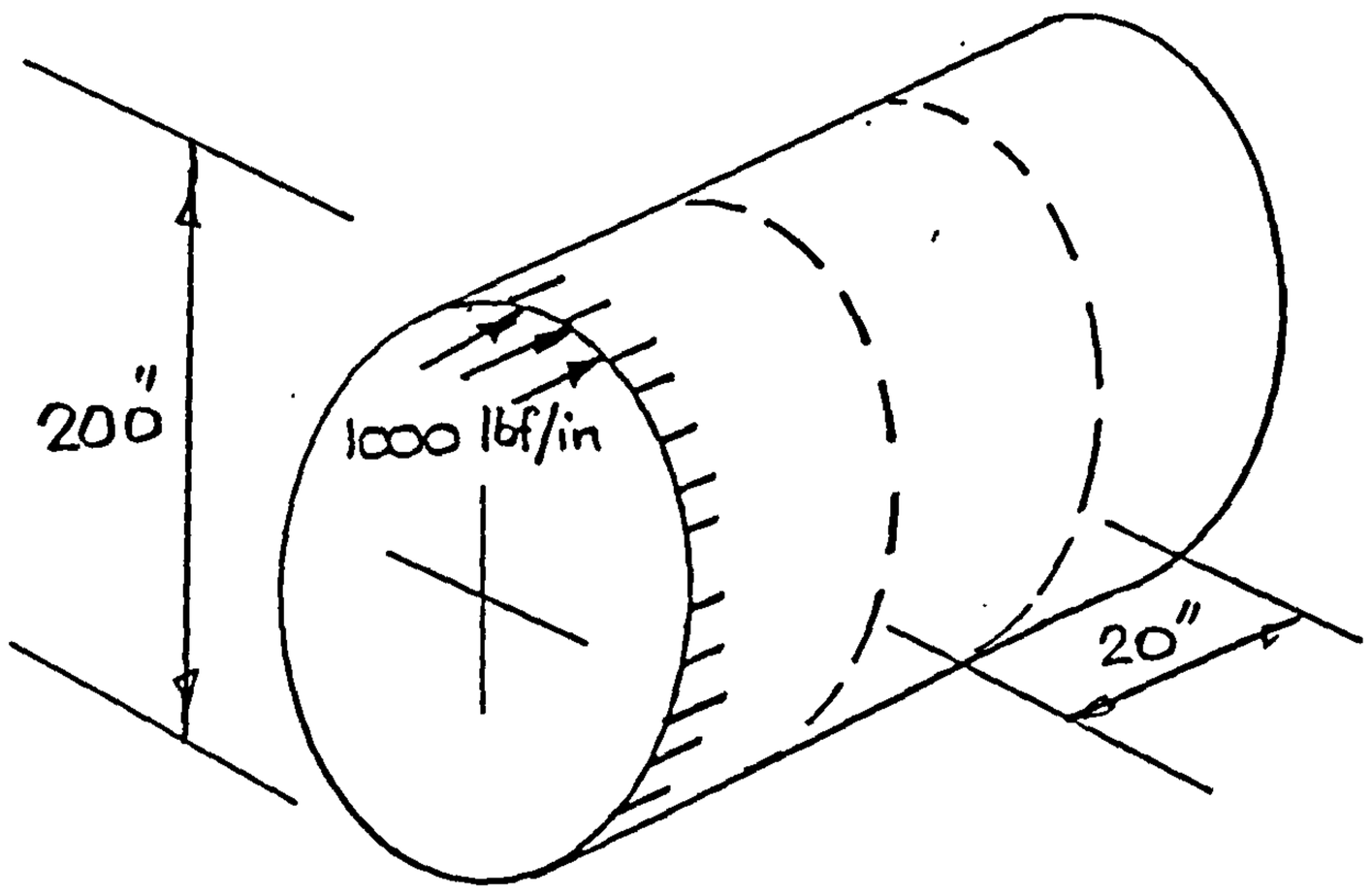

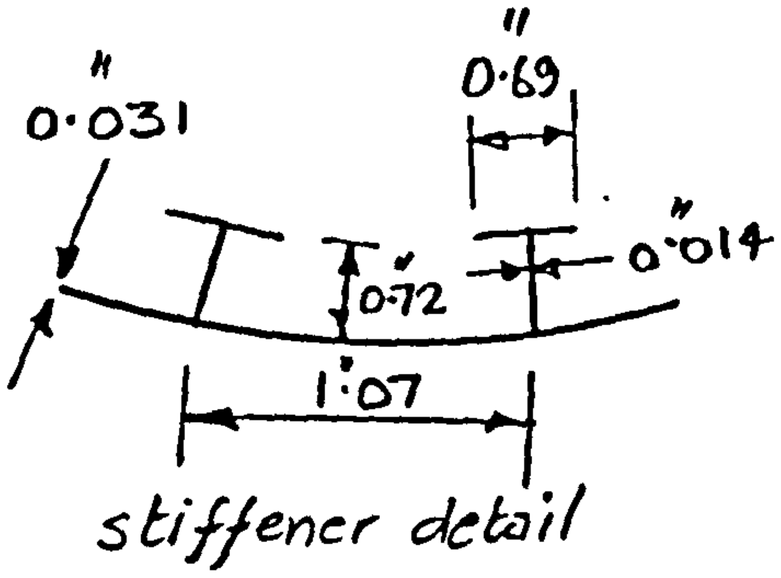

stiffener detail

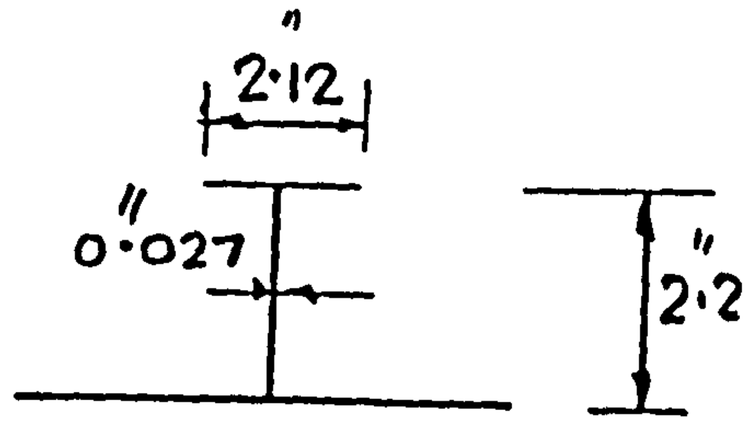

frame detail

Figure 74. SHELL DESIGN DUE TO BLOCK (REF. 63).

$f = 20{,}250\ \text{lbf/in}^2$

$M = 1.257 \times 10^8\ \text{lbf/in}$

$D = 400\ \text{in}$

$A_e = 69.45\ \text{in}^2$

Translated into the parametric form of the present work, this data gives

$$\bar{A}_e = 8.96\ ;\quad \bar{L} = 64.96\ ;\quad \bar{D} = 61.64\ ;\quad \frac{f}{E} = 0.00203$$

The optimum design generated by ORCS has the following properties

$$\bar{A}_e = 7.27\ ;\quad \bar{L} = 27.58\ ;\quad \bar{D} = 50.10\ ;\quad \frac{f}{E} = 0.00366$$

This design is radically different to Blocks, exhibiting a smaller diameter and frame pitch, but much large surface stress. It is some 19% lighter.

If Blocks diameter is preserved, output from ZEDS gives

$$\bar{A}_e = 7.48\ ;\quad \bar{L} = 26.16\ ;\quad \bar{D} = 61.64\ ;\quad \frac{f}{E} = 0.0032$$

On the other hand, if the suggested surface stress is maintained,

$$\bar{A}_e = 8.29\ ;\quad \bar{L} = 30.55\ ;\quad \bar{D} = 84.38\ ;\quad \frac{f}{E} = 0.00203$$

both of which designs are significantly lighter than the original solution.

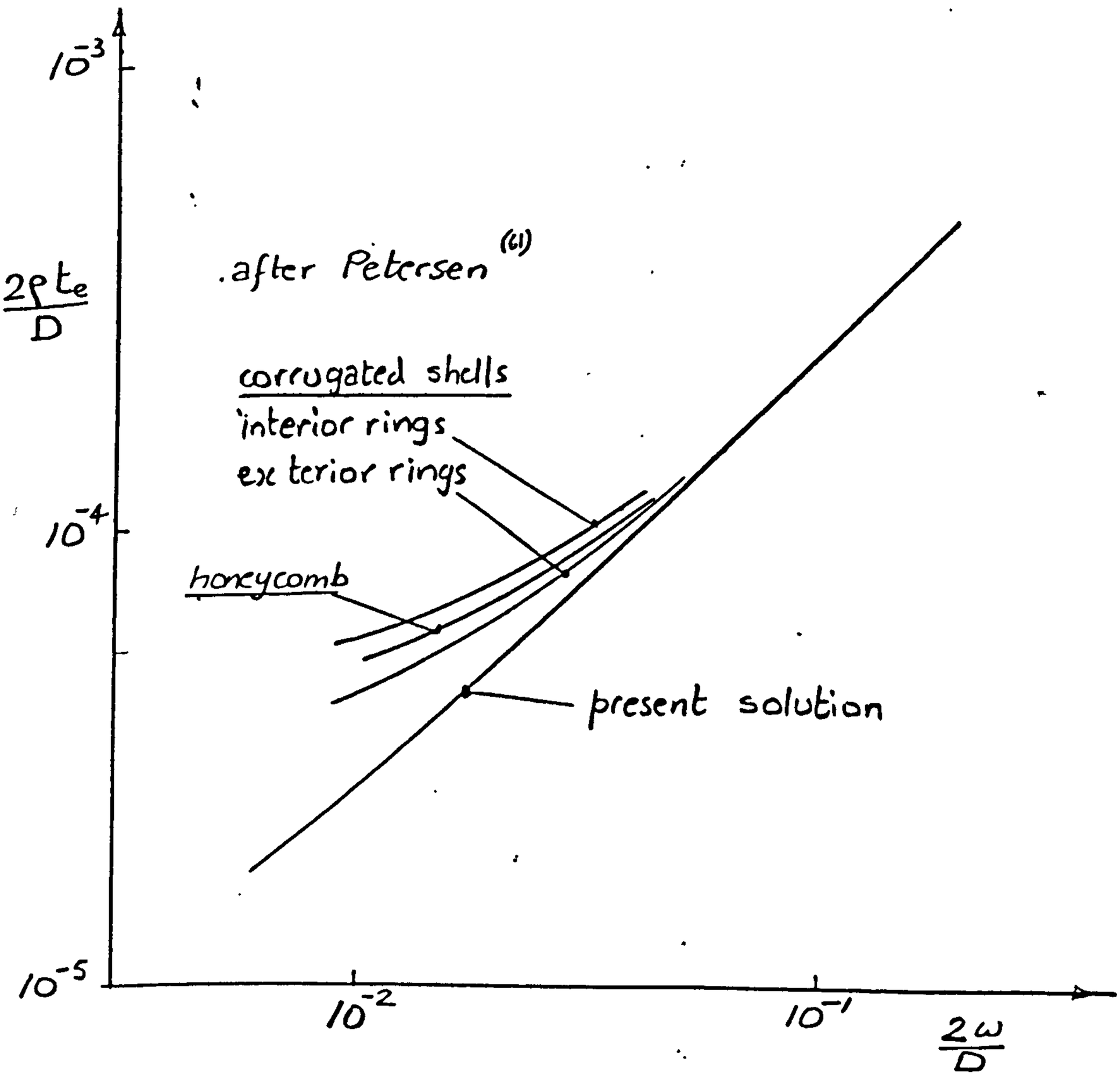

Figure 75. SHELL DESIGNS COMPARED

Chapter 8

CORRUGATED TOWER WITH IMPERFECTIONS

General

The effects of small imperfections on structures which are vulnerable to various forms of instability have been studied extensively recently.[27, 28, 29, 50] Most authors have been concerned to illustrate the way in which the nominal strength of a given structure may be eroded by imperfections. The rate at which strength is reduced as imperfection magnitude increases is characterised by the often ill-defined term 'imperfection sensitivity'.

From the point of view of design, for which the loads are given and the structural dimensions are to be found, a number of authors have discussed these phemomena by illustrating how the strength of structures which are designed without regard for imperfections, may be found to be seriously weakened.

This paper utilises a comparatively simple example to show how, by acknowledging a priori the existence of imperfections in the final structure, optimum designs may be derived to achieve a given strength so that that factor which is most important from the design point of view, i.e. the sensitivity of structure weight to imperfection magnitude, may be quantified.

Design Example

The example chosen is a square tower of width B and total height L, which is required to support a uniform axial compressive force P applied evenly over the tower cross section (see Figure 76).

The tower walls are made from trapezoidally corrugated panels, which are stabilised at regular intervals ℓ by transversely rigid diaphragms of given equivalent thickness t_0, which provide simple support at their intersections with the wall panels.

The structure is everywhere perfectly manufactured except in one respect; the panels each have an imperfection of sinusoidal form, of wavelength equal to the diaphragm spacing ℓ. The imperfection magnitude is characterised by the quantity $\frac{\delta_o}{k}$, where δ_o is the initial imperfection amplitude midway between diaphragms, and k is the corrugation local radius of gyration.

The purpose of the analysis is to establish optimum values for corrugation dimensions, tower width and diaphragm spacing, so that total tower weight is minimised.

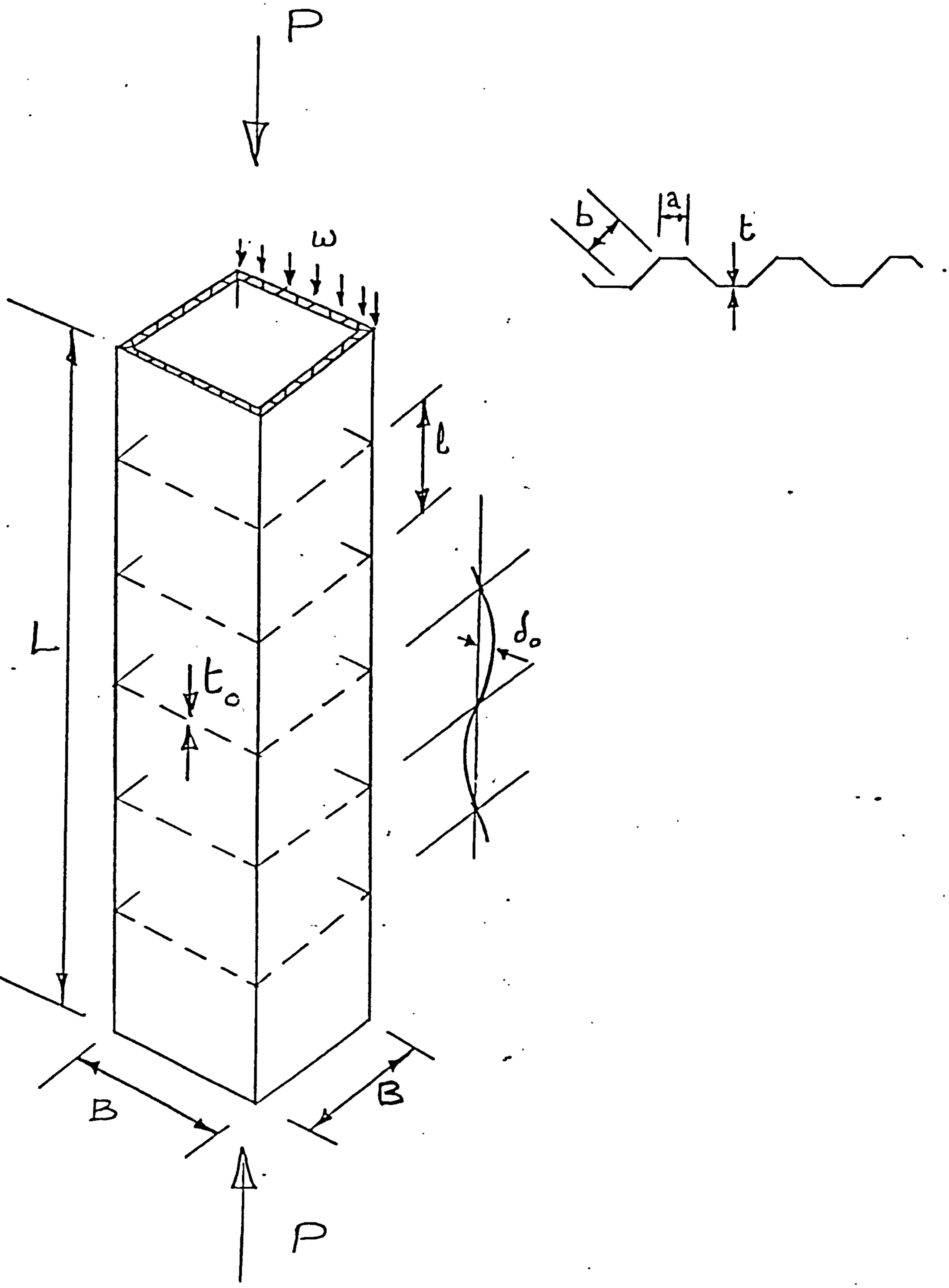

Figure 76. IMPERFECT CORRUGATED TOWER

Analysis

The principal effect of the specified imperfection will be to reduce the axial stiffness of the panels and consequently the overall Euler buckling strength of the tower.

Thus the panels must be designed to work at a load somewhat lower than their own buckling load.

Ideal optimum dimensions for perfectly manufactured trapezoidally corrugated panels[49] are given below (refer to figure 76 for key to dimensions).

$$t = 0.5881 \left[\frac{w\ell}{E}\right]^{\frac{1}{2}}$$

$$b = 1.0477 \left[\frac{w\ell^3}{E}\right]^{\frac{1}{4}}$$

$$a = 0.87\ b \qquad \ldots (208)$$

$$t_e = 1.3423t$$

$$\theta = 59^{o}$$

where w is design end load per unit width when local buckling coincides with flexural buckling, and t_e is panel equivalent thickness.

Let the nominal strength of the panels be a factor r greater than the given design load, so that

$$w = \frac{rP}{4B}$$

which gives

$$t = 0.2941 \left[\frac{rP\ell}{EB}\right]^{\frac{1}{2}}$$

$$t_e = 0.3947 \left[\frac{rP\ell}{EB}\right]^{\frac{1}{2}}$$

$$b = 0.7408 \left[\frac{rP\ell^3}{EB}\right]^{\frac{1}{4}} \qquad \ldots (209)$$

$$f = 0.6334 \left[\frac{PE}{r\ell B}\right]^{\frac{1}{2}}$$

where f = surface working stress.

The total equivalent cross-section area, to which the weight of the tower is proportional, may now be written down

$$A = 4Bt_e + \frac{t_o B^2}{\ell}$$

$$= 1.5788 \left[\frac{rP\ell B}{E}\right]^{\frac{1}{2}} + \frac{t_o B^2}{\ell}$$

which is minimised when

$$\ell = 1.1708 \left[\frac{t_o^2 EB^3}{rP}\right]^{\frac{1}{3}} \qquad \ldots (210)$$

so that structural material is divided between panels and diaphragms in the ratio 2:1.

The list of design variables may now be reformed to give

$$t = 0.3182 \left[\frac{rPt_o}{E}\right]^{\frac{1}{3}}$$

$$b = 0.8338 \left[t_o B\right]^{\frac{1}{2}}$$

$$t_e = 0.4271 \left[\frac{rPt_o}{E}\right]^{\frac{1}{3}} \qquad \ldots (211)$$

$$f = 0.5854 \left[\frac{P^2 E}{t_o rB}\right]^{\frac{1}{3}}$$

$$A = 2.5626 \left[\frac{rPt_o}{E}\right]^{\frac{1}{3}} . B$$

Note that corrugation dimension b is independent of load intensity and Youngs modulus.

The overall stability of the tower must now be considered.

If the top of the tower is free and the base fixed, provided loading is conservative the buckling load is given by

$$P = \frac{\pi^2 E^* I}{4L^2} \qquad \ldots (212)$$

where I = second moment of area = $\frac{2}{3} t_e B^3$

and E^* = effective axial modulus of imperfect panels given by[29]

$$\frac{E^*}{E} = \frac{\left[1 - \frac{p}{p_E}\right]^3}{\frac{1}{2}\left(\frac{\delta_o}{k}\right)^2 + \left[1 - \frac{p}{p_E}\right]^3}$$

p_E = panel Euler buckling load

p = panel applied load, so that $\frac{p_E}{p} = r$.

($\frac{\delta_o}{k}$ is defined above)

Equation (212) may now be solved for B, the tower width which ensures that the tower has adequate overall buckling strength, giving

$$B = 1.1248\left[\frac{\frac{1}{2}\left(\frac{\delta_o}{k}\right)^2 + \left(1 - \frac{1}{r}\right)^3}{r^{1/3}\left(1 - \frac{1}{r}\right)^3}\right]^{\frac{1}{3}}\left[\frac{L^6 p^2}{E^2 t_o}\right]^{\frac{1}{9}} \quad \ldots (213)$$

It may be noted from (211) that equivalent cross section area is proportional to B, so that from (213), tower weight will be minimised with respect to panel reserve factor r when the quantity

$$R = \frac{\frac{1}{2}\left(\frac{\delta_o}{k}\right)^2 + \left(1 - \frac{1}{r}\right)^3}{r^{1/3}\left(1 - \frac{1}{r}\right)^3}$$

is a minimum.

In order to proceed further, it is convenient to write

$$z = 1 - \frac{1}{r} \quad \ldots (214)$$

so that

$$\frac{\frac{1}{2}\left(\frac{\delta_o}{k}\right)^2 \frac{1}{z^3} + 1}{(1 - z)^{\frac{1}{3}}}$$

which is minimised when

$$\left(\frac{\delta_o}{k}\right)^2 = \frac{4z^4}{9 - 11z} \quad \ldots (215)$$

Note that for

$$0 < \frac{\delta_o}{k} < \infty$$

$$0 < z < 9/11$$

and

$$1 < r < 11/2$$

The complete design may now be specified as follows

$$A = 2.8824\Phi_A \left[\frac{L^6 t_o^2 p^5}{E^5}\right]^{\frac{1}{9}}$$

$$B = 1.1248\Phi_B \left[\frac{L^6 p^2}{E^2 t_o}\right]^{\frac{1}{9}}$$

$$f = 0.5204\Phi_f \left[\frac{E^5 p^4}{L^6 t_o^2}\right]^{\frac{1}{9}}$$

$$\ell = 1.3169\Phi_\ell \left[\frac{L^6 t_o^5 E}{p}\right]^{\frac{1}{9}} \quad \ldots (216)$$

$$b = 0.8843\Phi_b \left[\frac{L^3 t_o^4 p}{E}\right]^{\frac{1}{9}}$$

$$t = 0.3182\Phi_t \left[\frac{p t_o}{E}\right]^{\frac{1}{3}}$$

$$t^* = 0.4271\Phi_t \left[\frac{p t_o}{E}\right]^{\frac{1}{3}}$$

The Φ functions contain completely the effects of imperfections and are given below.

$$\Phi_A = \left[\frac{9(1-z)^{\frac{1}{3}}}{9-11z}\right]^{\frac{1}{3}}$$

$$\Phi_B = \left[\frac{9(1-z)^{\frac{4}{3}}}{9-11z}\right]^{\frac{1}{3}}$$

$$\Phi_f = \left[\frac{9-11z}{9(1-z)^{\frac{1}{3}}}\right]^{\frac{1}{3}}$$

$$\Phi_\ell = \left[\frac{9(1-z)^{\frac{7}{3}}}{9-11z}\right]^{\frac{1}{3}}$$

$$\Phi_t = \left[\frac{1}{1-z}\right]^{\frac{1}{3}}$$

$$\Phi_b = \left[\frac{3(1-z)^{\frac{2}{3}}}{(9-11z)^{\frac{1}{2}}}\right]^{\frac{1}{3}}$$

Note that when $\frac{\delta_o}{k} = 0$, $r = 1$, $z = 0$ and all $\Phi = 1$.

Three of the factors are shown plotted in figure 77 as functions of imperfection magnitude.

The effect of imperfections on the strength of the tower for given tower weight may be deduced from the first of equations (216), which gives

$$\frac{P}{P_o} = \left[\frac{1}{\Phi_A}\right]^{\frac{9}{3}} = \left[\frac{(9-11z)}{3(1-z)^{\frac{1}{3}}}\right]^{\frac{3}{5}} \quad \ldots (218)$$

where P_o = strength of perfect structure

P = strength of imperfect structure of same weight.

This is plotted in figure 78, which shows how strength for given structure weight appears to be more 'sensitive' to imperfection magnitude.

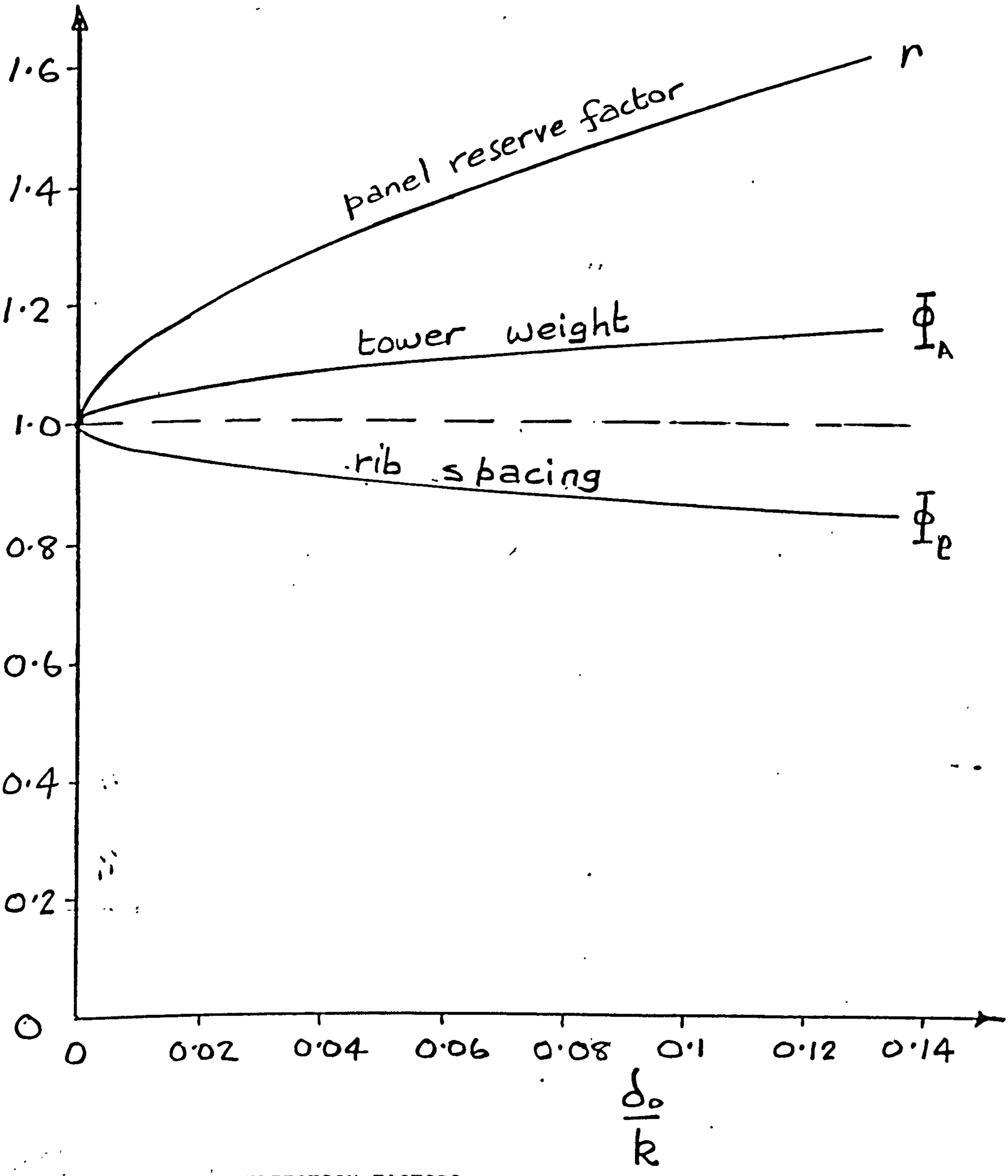

Figure 77. IMPERFECTION FACTORS

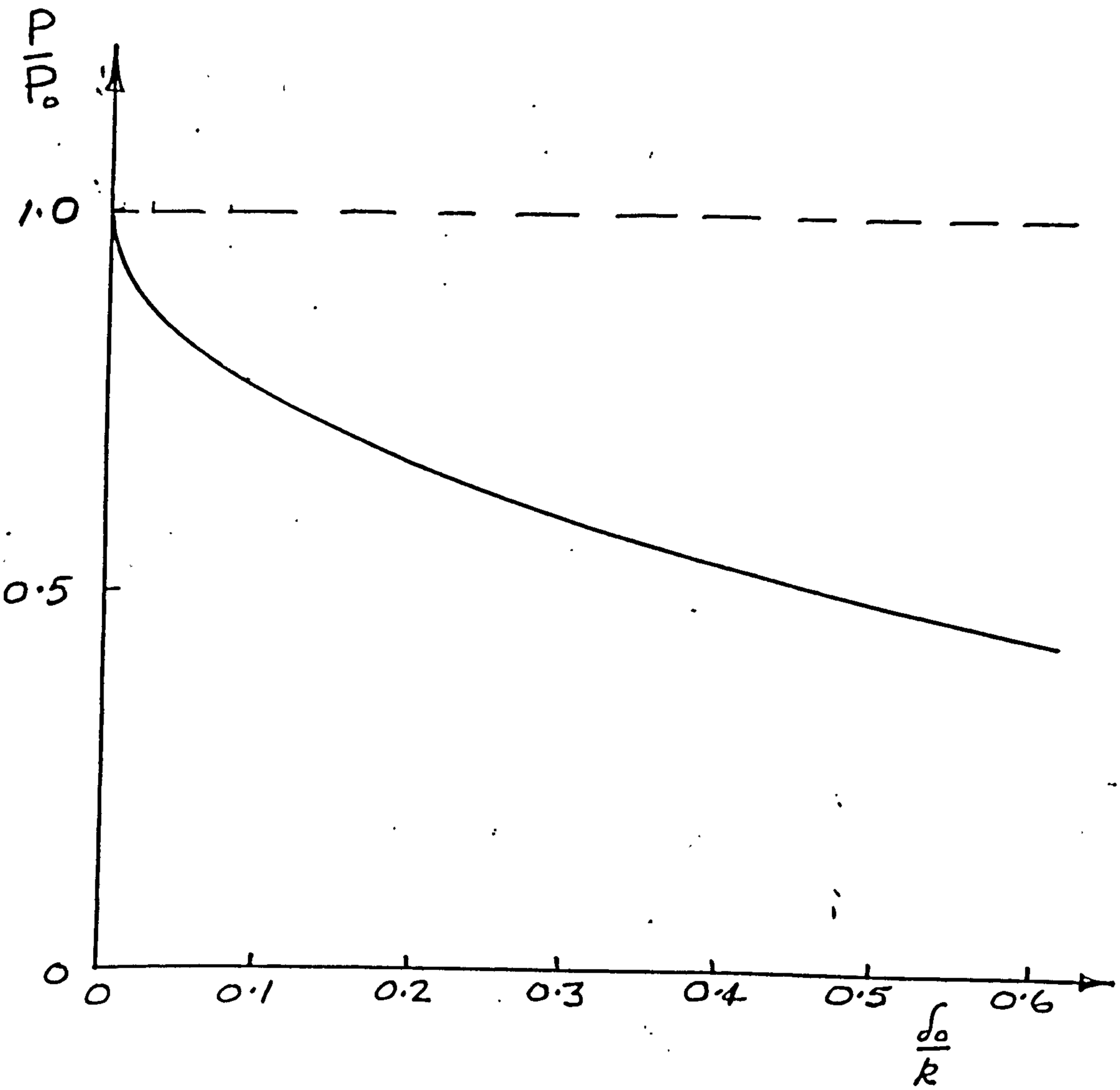

Figure 78. TOWER STRENGTH EROSION DUE TO IMPERFECTIONS

Chapter 9

CONCLUSIONS

The effects of plasticity on the design of a number of structural elements has been considered for which compression is the principal loading. In particular methods have been developed for the minimum weight design of a wide range of columns, the thin rectangular plate, honeycomb sandwich panels, and wide column stiffened panels.

Further consideration has been given to the design of supports for stiffened panels and the results thus obtained have to be utilised to determine minimum weight designs for circular cylindrical shells loaded by bending moment.

It has generally proved possible to derive explicit expressions relating design loading to compressive stress, and also the dimensions required to specify the structure in complete detail. In each case these have been used to develop computer programmes capable of generating the necessary data for design given the loading and material.

It has frequently been possible to directly incorporate the effects of dimensional constraints which may be imposed by considerations of engineering practicality and also restriction on maximum design stress.

The materials which can be contemplated are restricted to those which exhibit smooth and continuous yielding behaviour, and are isotropic in character. However this admits of a very wide class of materials currently utilised in practical structures.

Methods of analysis used to characterise buckling behaviour are precisely those which are standard procedures in engineering organisations. No attempt has been made to introduce elaborations in this respect.

The treatment of manufacturing imperfections has been confined to noting their influence on the above mentioned methods of analysis, together with a study of a corrugated tower which has a very restricted type of imperfection inherent in its construction. Perhaps the most useful feature of the results is in the way in which they may be directly used to systematically quantify the effects of material properties upon weight in the design of structures. This should prove to be a valuable guide to material development.

REFERENCES

1. CILLY, F.K. (1900) The Exact Design of Statically Indeterminate Frameworks. Trans. ASCE V.42, pp.353-407.

2. RICHARDS, D.M. (1968) The Sequential Design of Redundant Elastic Structures. JBCSA Conf. London 1968.

3. RICHARDS, D.M. (1973) The Design of Compatible Structures. 2nd AGARD Symp. Struct. Optimisation, Milan, 1973.

4. POPE, G.G., and SCHMIT, L.A. (1971) Structural Design Application of Mathematical Programming Techniques. AGARDograph No.149.

5. SCHMIT, L.A., and FOX, R.L. (1965) An Integrated Approach to Structural Synthesis and Analysis. AIAA Journal V.3, No.6, p.1104.

6. GELLATLEY, R.A. and BERKE, L. (1972) Structural Design with Optimally Based Algorithms. Conf. Opt. in Struct.Design. Swansea 1972.

7. KHOT, N.S., VENKAYYA, B.B., JOHNSON, C.D., and TISCHLER, V.A. (1973) Application of Optimality Criterion to Fiber-Reinforced Composites. AFFDL-TR-73-6.

8. BUTTERWORTH, D.L. (1969) Correlation of Empirical Stress Strain Properties. College of Aeronautics CIT MSc Thesis.

9. LAGRANGE, A. (1970) Sur la Figure des Colonnes. Mi sc Taurinensia, V.5.

10. FARRAR, D.J. (1949) The Design of Compression Structures for Minimum Weight. J.R.Ae.S., V.53, No.467, p.1041.

11. SHANLEY, F.R. (1952) Weight Strength Analysis of Aircraft Structures. McGraw Hill, New York 1952.

12. HOFF, N.J. (1953) Buckling and Stability J.R.Ae.S. V.58, No.517, p.3.

13. GERARD, G. (1956) Minimum Weight Analysis of Compression Structures. N.Y. University Press 1956.

14. KELLER, J.B. (1960) The Shape of the Strongest Column. Arch.Rat.Mech.Anal. V.5, p.275.

15. COX, H.L. (1943) Structures of Minimum Weight.
ARC, R and M No. 1923.

16. COX, H.L. (1958) The Application of the Theory of Stability in Structural Design.
J.R.AeS. V.162, No.571, p.497.

17. COX, H.L. (1965) The Design of Structures of Least Weight.
Pergamon, Oxford, 1965.

18. NADAI, A. (1950) Theory of Flow and Fracture of Solids
MacGraw Hil, New York.

19. YLINEN, A. (1948) Teknillinen Aikakauslehti, V.38, p.9.

20. HSU, T.R., and BERTELS, A.W.M. (1974) Improved Approximation of Constitutive Relationship for Finite Element Analysis.
AIAA Journal, V.12, No.10, p.1450.

21. RAMBERG, W., and OSGOOD, W.R. (1943) Description of Stress-Strain Curves by Three Parameters.
NACA TN902.

22. NEUT, A van der (1968) The Interaction of Local Buckling and Column Failure of Thin Walled Compression Members.
Univ. Delft. Rept. VTH149.

23. THOMPSON, J.M.T., and SUPPLE, W.J. (1973) Erosion of Optimum Designs by Compound Branching Phenomena.
J.Mechs.Phys.Sols. Vol.12, p.135.

24. ILYUSHIN, A.A. (1947) The Elasto-Plastic Stability of Plates.
NACA TN No.1188.

25. STOWELL, E.Z. (1947) A Unified Theory of Plastic Buckling of Columns and Plates.
NACA TN 1556.

26. BUDIANSKY, B., and HUTCHINSON, J.W. (1964) Dynamic Buckling of Imperfection Sensitive Structures.
Proc. Int. Cong. Appl.Mech. 12th Munich.

27. THOMPSON, J.M.T., and LEWIS, G.M. (1972) On the Optimum Design of Thin-Walled Compression Members.
J.Mechs.Phys.Sols. vol.20,p.101.

28. COX, H.L. and GRAYLEY, M.E. (1972) The Influence of Production Imperfections on the Design of Optimum Structures.
Contrib.Thi.Airc.Structs.Delft Univ.Press 1972.

29. CRAWFORD, R.F. and HEDGEPETH, J.M. (1975) Effects of Initial Waviness of the Strength and Design of Built-Up Structures.
AIAA Journal V.13, No.5, p.672.

30. PRAGER, W., and TAYLOR, J.E. (1968) Problems of Optimal Structural Design.
J.Appl.Mechs. Vo.35, p.102.

31. VENKAYYA, V.B., KHOT, N.S. and BERKE, L. (1973) Application of Optimality Criteria Approaches to Automated Design of Large Practical Structures.
2nd AGARD Symp. Strut. Optimisation, Milan.

32. Structures Data Sheets Engineering Sciences Data Unit.
Royal Aeronautical Society, London.

33. GERARD, G, and BECKER, H. (1957) Handbook of Structural Stability.
NACA TN 3781/3786 and NASA TN D-162.

34. BULSON, P.S. (1970) The Stability of Flat Plates.
Chatto and Windus, London.

35. TIMOSHENKO, S.P., and GERE, J.M. (1961) Theory of Elastic Stability
McGraw Hill, New York.

36. WITTRICK, W.H. (1945) A Theoretical Analysis of the Efficiency of Sandwich Construction under Compressive End Load.
ARC R and M 2016.

37. PLANTEMA, F.J. (1966) Sandwich Construction
Wiley, New York.

38. DUBERG, J.E., and WILDER, T.W. (1951) Inelastic Column Behaviour
NACA TN 2267.

39. HANDELMAN, F.A., and PRAGER, W. (1948) Plastic Buckling of a Rectangular Plate under Edge Thrusts.
NACA TN 1530

40. HUTCHINSON, J.W. (1975) Plastic Buckling
Ch.2, Advances in Appl. Mechs. V.14.

41. GOUGH, G.S., ELAM, C.F., and de BRAYNE, N.A. (1940) The Stabilisation of a Thin Sheet by a Continuous Supporting Medium.
J.R.Ae.S. V.44, p.12.

42. HOFF, N.J. and MAUTNER, S.E. (1960) J.Ae.Sci. V.12, No.3, p.285.

43. YUSUFF, S. (1960) Face Wrinkling and Core Strength in Sandwich Construction.
J.R.Ae.S. V.64, p.164.

44. WILLIAMS, D. (1951) Sandwich Construction - a Practical Approach for the Use of Designers.
ARC R and M 2466.

45. BIJLAARD, P.P. (1950) Optimum Distribution of Material in Sandwich Plates Loaded in their Plane. Rep. SA-247-S-8 Cornell Aero Lab.

46. KAECHELE, L.E. (1957) Minimum Weight Design of Sandwich Panels Rand Rep. RM-1895.

47. ALLEN, H.G. (1969) Analysis and Design of Sandwich Panels Pergamon, Oxford.

48. CATCHPOLE, E.J. (1954) The Optimum Design of Compression Surfaces having Unflanged Integral Stiffeners J.R.Ae.S. V.58, No.527, p.765.

49. RICHARDS, D.M. (1971) Optimum Design of Fibre Reinforced Corrugated Panels. CofA Report Aero No.209.

50. TVERGAARD, V. (1973) Imperfection Sensitivity of a Wide Integrally Stiffened Panel under Compression. Int.J.Sols.Structs. V.9, p.177.

51. EMERO, D.H., and SPUNT, L. (1966) Wing Box Optimisation under Combined Stresses and Bending. J. Aircraft, V.3, No.2, p.130.

52. COX, H.L. (1954) Computation of Initial Buckling Stress for Sheet Stiffener Combinations. J.R.Ae.S. V.58, p.634.

53. YUSUFF, S. (1976) Buckling and Failure of Flat Stiffened Panels. J. Aircraft. V.13, No.3, p.198.

54. FEWS, R. (1972) Fuselage Design. CIT College of Aeronautics MSc Thesis.

55. WILLIAMS, J.G., and MIKULAS, M.M. (1975) Analytical and Experimental Study of Efficient Compression Panels. 16th ASME/AIAA/SAE Conf. paper 75-754.

56. RICHARDS, D.M. (1977) Minimum Weight Design of Compression Surfaces Including Plasticity Effects. RAE Tech. Memo Structures 901.

57. SIMITSES, G.J. and UNGBHAKORN, V. (1975) Weight Optimisation of Stiffened Cylinders under Axial Compression Comps. and Structs. V.5, p.305.

58. BRONOWICKI, A.J., et al (1975) Optimisation of Ring Stiffened Cylindrical Shells. AIAA Journal V.13, No.10, p.1319.

59. PAPPAS, M, and ALLENTUCH, A. (1972) Optimal Design of Submersible Frame Stiffened Circular Cylindrical Shells.
NCE Report NV6.

60. PAPPAS, M, and ALLENTUCH, A. (1973) Mathematical Programming Procedures for Mixed Discrete-Continuous Design Problems.
NCE Report NV7.

61. PETERSON, J.P. (1967) Structural Efficiency of Ring Stiffened Corrugated Cylinders in Axial Compression
NASA TN D-4073

62. SINGER, J, and BARUCH, M. (1966) Recent Studies on Optimisation for Elastic Stability of Cylindrical and Conical Shells.
ICAS 5th Cong. London

63. BLOCK, D.L. (1971) Minimum Weight Design of Axially Compressed Ring and Stringer Stiffened Cylindrical Shells.
NASA CR-1766

64. BLOCK, D.L. Card, M.F., and MIKULAS, M.M. (1965) Buckling of Eccentrically Stiffened Orthotropic Cylinders.
NASA TN D-2960.

Appendix A

RAMBERG OSGOOD STRESS STRAIN FUNCTIONS

The Ramberg Osgood [21] equation for uniaxial strain ε in terms of uniaxial stress f is

$$\varepsilon = \frac{f}{E} + \alpha\left(\frac{f}{E}\right)^n \qquad \ldots (A1)$$

where E = Youngs modulus.

The individual terms may be indentified as elastic and plastic (or irrecoverable) strain, so that

$$\varepsilon = \varepsilon_e + \varepsilon_p$$

where

$$\varepsilon_e = f/E \quad \text{and} \quad \varepsilon_p = \alpha(f/E)^n$$

The plastic strain coefficient has no immediately obvious physical significance, and is usually a very large number which can prove an embarrassment during computation.

Proof stress is defined as the stress at which a given degree of plastic strain is developed, so that at f_2 the 0.2% proof stress,

$$\varepsilon_p = 0.002 = \alpha\left(\frac{f_2}{E}\right)^n$$

$$\therefore \quad \alpha = \frac{0.002}{(f_2/E)^n} \qquad \ldots (A2)$$

Equation (A1) may therefore be written

$$\varepsilon = f/E(1 + \phi) \qquad \ldots (A3)$$

where

$$\phi = \alpha(f/E)^{n-1} \qquad \ldots (A4)$$

which is the ratio between plastic and elastic strain at the stress f. This quantity occurs repeatedly throughout this work. The following form which is particularly convenient for compution, is obtained by substituting (A2) into (A4), giving

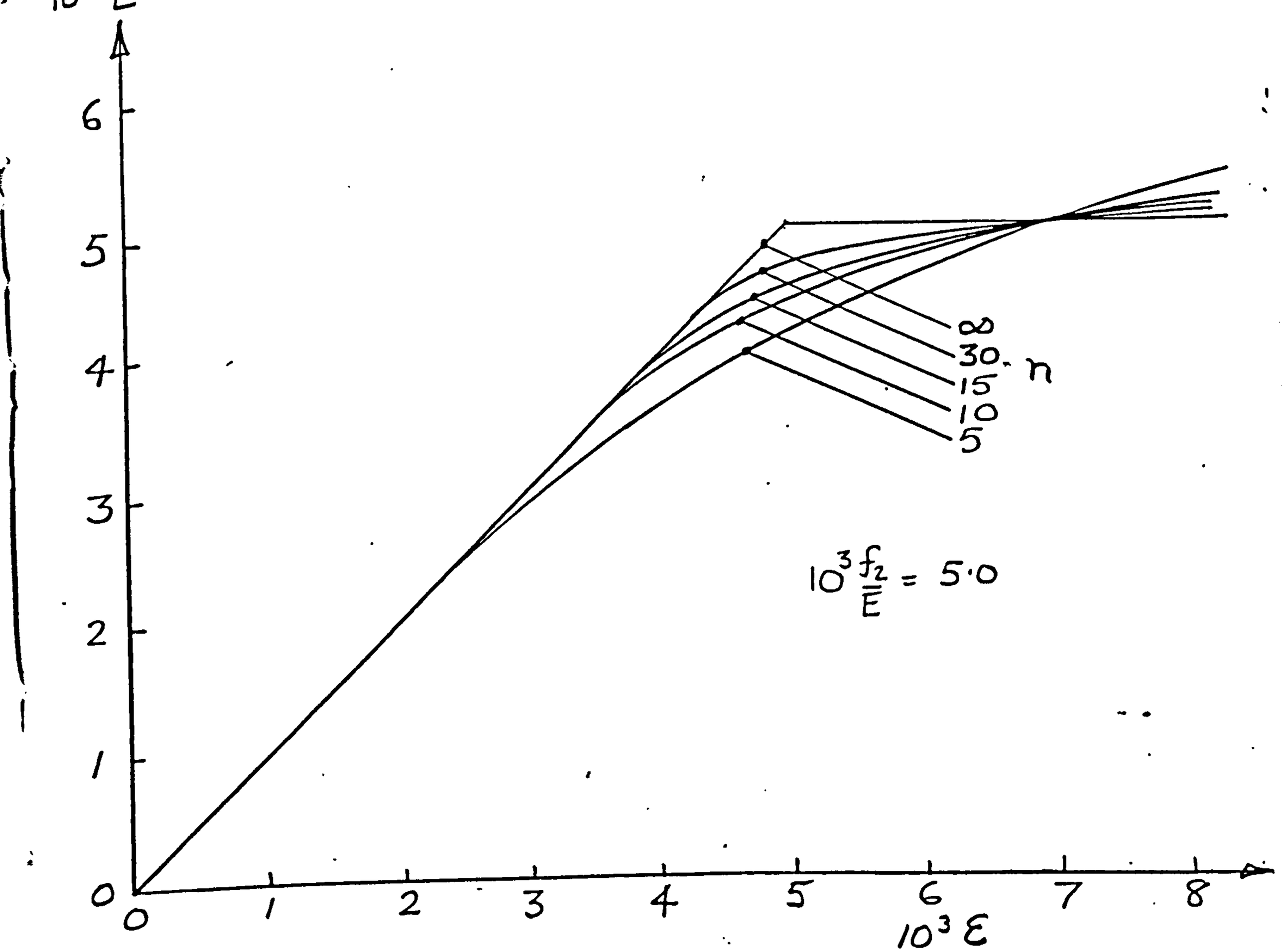

Figure A1. RAMBERG-OSGOOD STRESS STRAIN CURVES.

$$\phi = \frac{0.002}{f_2/E}\left(\frac{f/E}{f_2/E}\right)^{n-1} \qquad \ldots (A5)$$

A range of stress-strain curves based on equation (A3) is shown in Figure A1.

The two fundamental moduli required in buckling analysis are the secant and tangent moduli E_s and E_t. They may now be found directly from (A1), (A3) and (A5) with the following results

$$\frac{E_s}{E} = \frac{f}{\varepsilon E} = \frac{1}{1+\phi} \qquad \ldots (A6)$$

$$\frac{E_t}{E} = \frac{1}{E}\cdot\frac{\partial f}{\partial \varepsilon} = \frac{1}{1+n\phi} \qquad \ldots (A7)$$

Two important derived quantities are the reduced and geometric moduli E_r and E_g, given by

$$\frac{E_r}{E} = \frac{2E_t}{E+E_t} = \frac{2}{2+n\phi} \qquad \ldots (A8)$$

$$\frac{E_g}{E} = \frac{4E_t}{(E^{\frac{1}{2}}+E_t^{\frac{1}{2}})^2} = \frac{4}{\left[(1+n\phi)^{\frac{1}{2}}+1\right]^2} \qquad \ldots (A9)$$

These quantities are illustrated for a typical material in Figure A2.

The plastic strain exponent n which for engineering metals is a number in the range 10-30 may sometimes be quoted in a specification. However, more often a second proof stress f_1 will be given in which case n may be obtained in the following way.

If f_1 is the 0.1% proof stress

$$0.001 = \alpha(f_1/E)^n$$

and $$0.002 = \alpha(f_2/E)^n$$

so that by division, and taking logs to some base,

$$n = \frac{\log 2}{\log(f_2/f_1)} \qquad \ldots A10)$$

Typical values are shown in Figure A3.

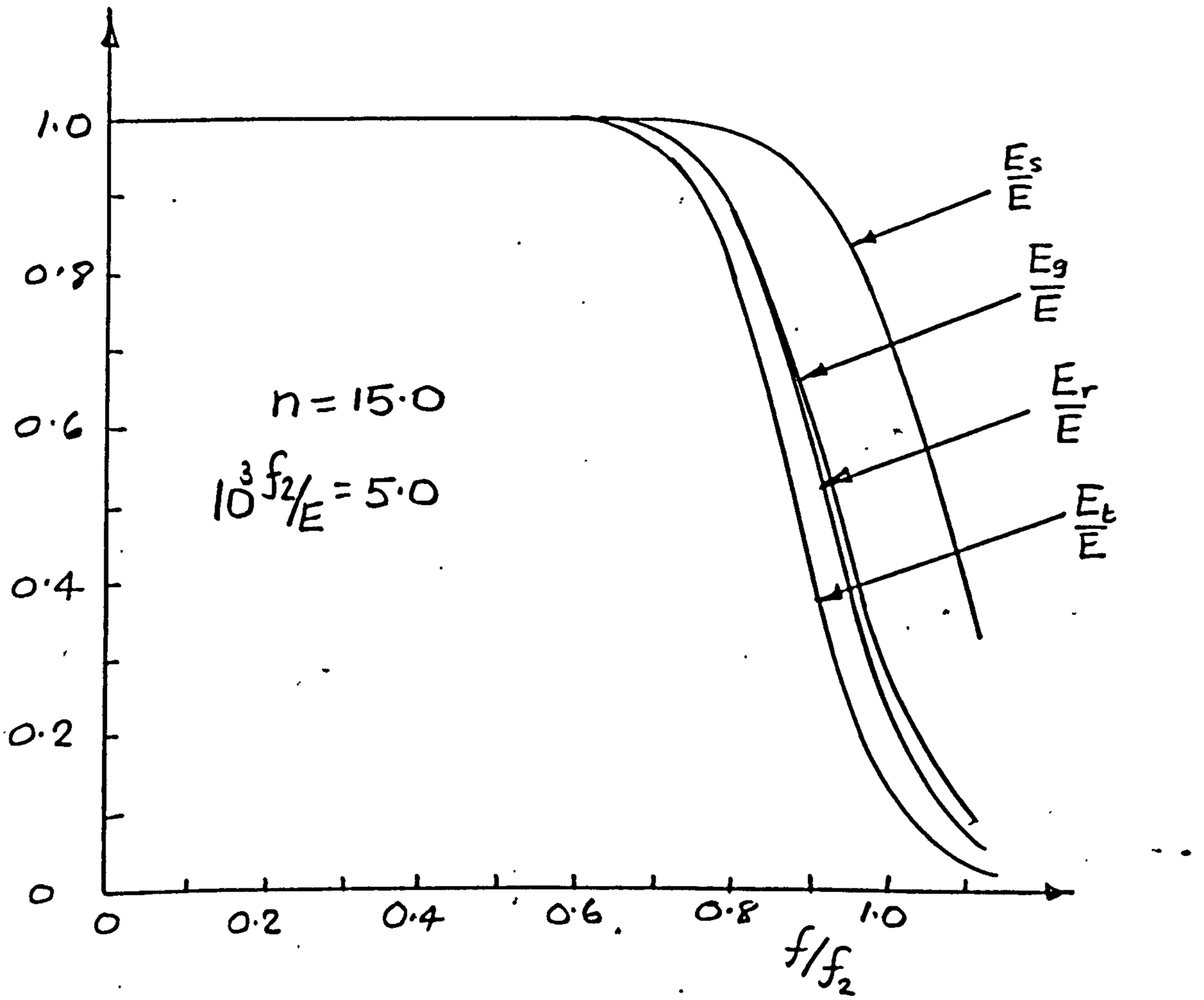

Figure A2. PLASTIC MODULI FOR TYPICAL RAMBERG-OSGOOD MATERIAL

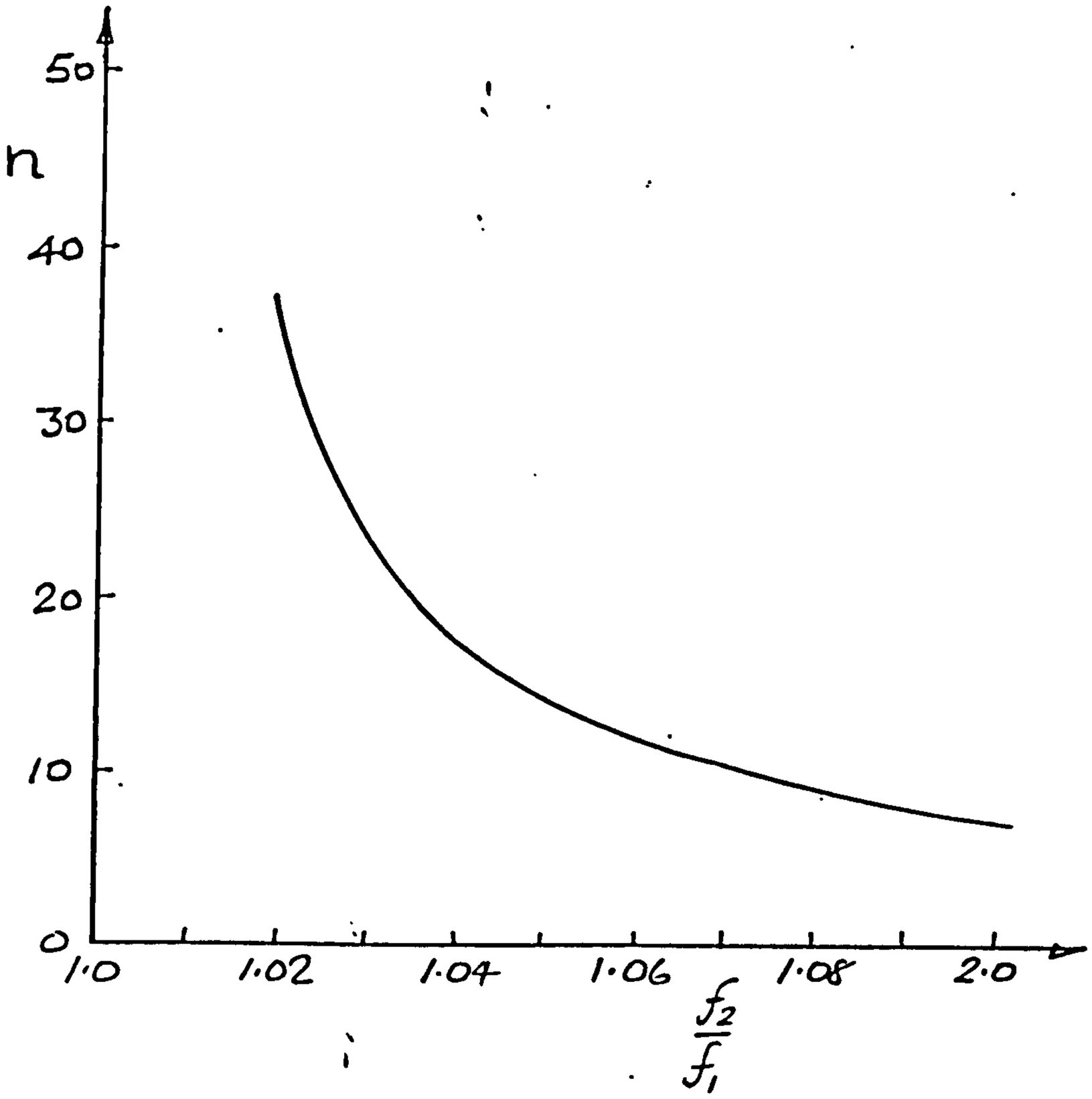

Figure A3. PLASTIC STRAIN EXPONENT RELATED TO PROOF STRESS RATIO

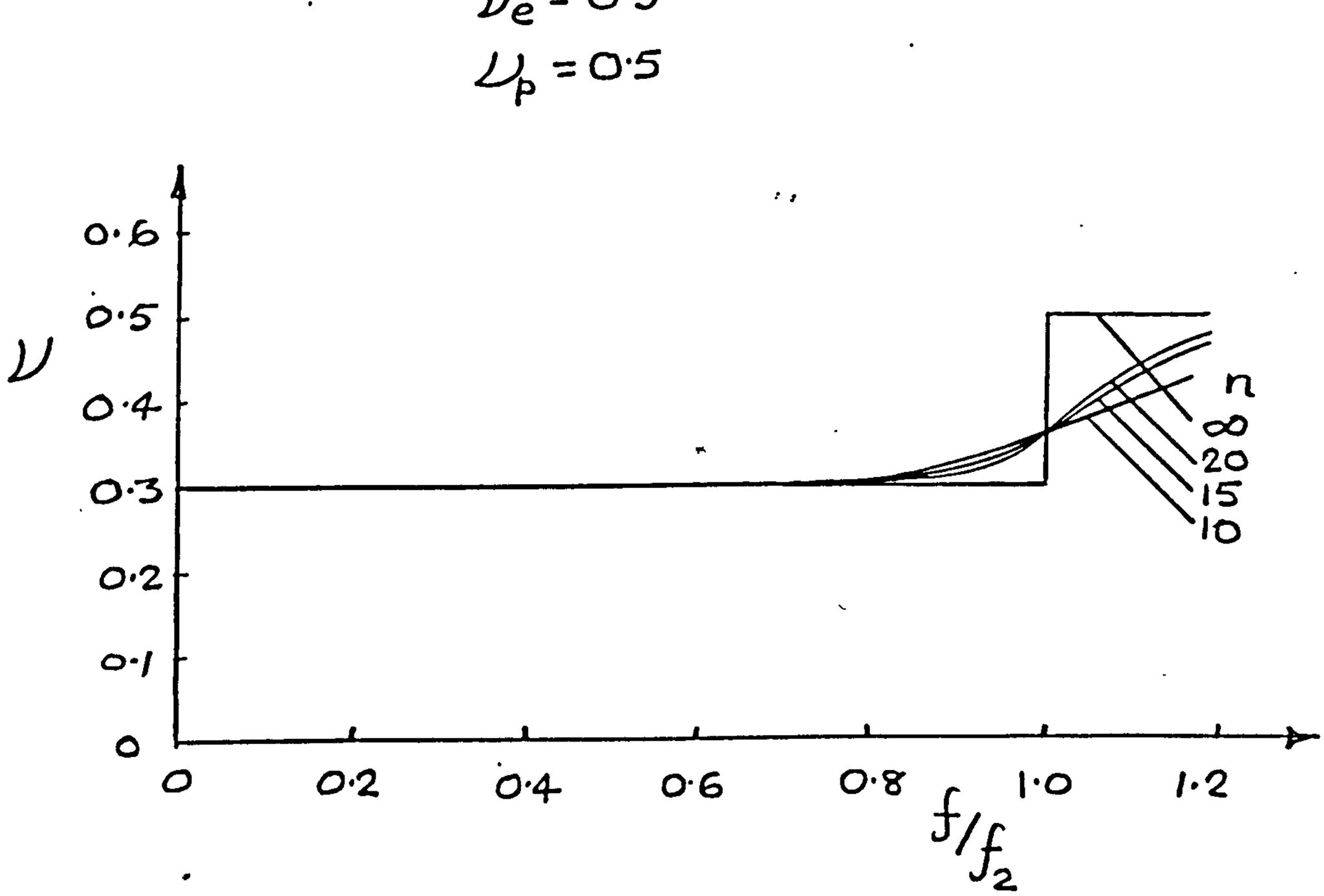

Figure A4 PLASTICITY EFFECTS ON POISSONS RATIO

The segregation into separate terms of elastic and plastic strains in equation (A1) suggests a method for dealing with the transition of Poisson's ratio between the elastic value which is usually about 0.3, and the fully plastic value of 0.5 which corresponds to strain at constant volume.

If it is assumed that each type of strain occurs independently, the rule of mixtures leads to the following expression for Poisson's ratio, or more correctly transverse strain ratio.

$$\nu = \frac{\nu_e(f/E) + \nu_p\alpha(f/E)^n}{(f/E) + \alpha(f/E)^n}$$

where ν_e = ideal elastic value

ν_p = fully plastic value

If this expression is divided throughout by f/E, equation (A4) may be used to give

$$\nu = \frac{\nu_e + \nu_p\phi}{1 + \phi} \qquad \ldots (A11)$$

This idea was originally suggested in principle by Shanley[11] as a graphical construction. Values of ν based on equation (A11) are shown plotted in Figure A4.

Appendix B

STRUT PROGRAMMES : SCOM and SAST

SCOM

The programme SCOM is designed to solve the equation

$$W = C\left(\frac{f}{E}\right)^{R}(1+n\phi)^{S} \qquad \ldots (B1)$$

where ϕ is defined in Appendix A.

Equations of this form occur frequently in Chapter 2 which is concerned with the design of struts of a variety of cross-section configurations.

The given quantity W corresponds to applied compressive load intensity and f/E is the required optimum design stress for the given parameters C, R and S.

Various values of C, R and S are given in Chapter 2. Input is in three stages

(i) Material properties $10^3 f_2/E$
(ii) Configuration parameters R, S, C.
(iii) Load intensity data W, XW and M.

W = initial value of load intensity
XW = number of values of W per decade
M = total number of W values to be computed.

XW is a round (but real) number which ensures regular spacing of W values on a logarithmic scale.

This is important because of the typically large range of W extending over a number of decades.

Output includes W and design stress f/E for each case.

Finally after each case is dealt with various options are exercised including

(i) New material (enter 1)
(ii) New configuration parameters (enter 2)
(iii) New load range (enter 3)
(iv) Exit (enter 4)

A listing for SCOM follows.

```
      LIST SCOM
     MASTER SCOM
200  FORMAT(2F0.0)
201  FORMAT (14H  10*3F2/E    N)
202  FORMAT(2F0.0,I0)
203  FORMAT( 19H   W/EL      10*3F/E)
204  FORMAT(3F0.0)
205  FORMAT( 7H R,S,C=,F10.4,F10.4,F10.4)
206  FORMAT(E12.4,F10.4)
207  FORMAT(I0)
208  FORMAT(F10.4,F8.2)
   1 READ (1,200)F2,XN
     WRITE(2,201)
     WRITE(2,208)F2,XN
     A=2.0*XN/F2
   2 READ(1,204)R,S,C
     WRITE(2,205)R,S,C
   3 READ(1,202)W,XW,M
     WRITE(2,203)
     RW=10.0**(1.0/XW)
     DO 12,J=1,M
     WX=W*(10.0**(3.0*R))/(C*(F2**R))
     S1=WX**(1.0/R)
     CONTINUE
  11 XP=1.0+A*S1**(XN-1.0)
     X=R+S*A*(XN-1.0)*(S1**(XN-1.0))/XP
     S2=1.0-(1.0-WX/((XP**S)*(S1**R)))/X
     DS2=ABS(S2-1.0)
     IF(DS2.LE.0.0001)GO TO 10
     S1=S2*S1
     GO TO 11
  10 S1=S2*S1*F2
     WRITE(2,206)W,S1
  12 W=W*RW
     READ(1,207)L
     GO TO(1,2,3,4),L
   4 CONTINUE
     STOP OK
     END
     FINISH
```

SAST

The programme SAST has been written to produce data for the optimum design of sandwich struts, utilising the method developed in Chapter 2, equations (46)-(52).

Euler buckling (including transverse shear flexibility) and face wrinkling modes of failure are considered.

Input includes

(i) Material properties $10^3 f_2/E$, n
(ii) Load intensity data W, XW, M

where W = initial load intensity parameter value
XW = number of load values per decade
M = total number of loads to be computed.

Output is tabulated for each load, giving

(i) load intensity $10^6 w/EL$
(ii) faceplate stress $10^3 f/E$
(iii) faceplate thickness $10^6 t/L$
(iv) sandwich depth $10^3 h/L$
(v) honeycomb core modulus $10^6 G_c/E$
(vi) face material proportion $2t/t_e$
(vii) total equivalent thickness $10^6 t_e/L$
(viii) equivalent endload stress $10^3 f_e/E$

Rerun options are

(i) New material (enter 1)
(ii) New load data (enter 2)
(iii) Exit (enter 3)

A listing of SAST follows.

```
      LIST SAST
     MASTER SAST
200  FORMAT(2F0.0)
201  FORMAT(2F0.0,I0)
202  FORMAT(34H 10*6W/EL,10*3F/E,10*6T/L,10*3H/L,)
209  FORMAT(33H 10*6GC/E,2T/TE,10*6TE/L,10*3FE/E)
203  FORMAT(E10.3,F7.4,E10.3,E10.3,E10.3,F6.3,E10.3,F7.4)
204  FORMAT(I0)
205  FORMAT(17H    N      10*3F2/E)
206  FORMAT(F4.2,F10.4)
207  FORMAT(10H 10*6W/EL=,E10.4)
208  FORMAT(F10.4)
   1 READ(1,200)XN,F2
     WRITE(2,205)
     WRITE(2,206)XN,F2
   2 READ(1,201)W,XW,M
     WRITE(2,202)
     WRITE(2,209)
     RW=10.0**(1.0/XW)
     DO 11,J=1,M
     DDF=0.00011*F2
     F=F2
     DF=-0.099*F2
     NR=1
     GO TO 100
   3 GZ=G
     TEZ=TE
     FZ=F
     F=0.9*F2
     NR=2
     GO TO 100
   4 IF(TE.LE.TEZ)GO TO 5
     F=1.1*F2
     NR=3
     DF=-DF
     GO TO 100
   5 GZ=G
     TEZ=TE
     F=F+DF
     NR=3
     GO TO 100
   6 GZ=G
     IF(TE.GE.TEZ)GO TO 7
     TEZ=TE
     F=F+DF
     GO TO 100
```

```
      7 DFP=ABS(DF)
        IF(DFP.LE.DDF)GO TO 8
        DF=-0.1*DF
        TEZ=TE
        F=F+DF
        GO TO 100
      8 CONTINUE
        TX=2.0*T/TE
        FE=1000.0*W/TE
        GO TO 10
    100 IF(F.GE.DDF)GO TO 101
        F=DDF
    101 CONTINUE
        S=(2.0/F2)*((F/F2)**(XN-1.0))
        S=1.0+XN*S
        G=18.99*(F**1.5)*((S**0.5)+1.0)
        H=500.0*W/G+10.0*((2500.0*((W/G)**2.0)
       1+4.053*S*F)**0.5)
        T=500.0*W/F
        TE=2.0*T+0.005547*H*G
        GO TO (3,4,6),NR
     10 WRITE(2,203)W,F,T,H,G,TX,TE,FE
     11 W=W*RW
        READ(1,204)L
        GO TO (1,2,9),L
      9 CONTINUE
        STOP OK
        END
        FINISH
```

Appendix C

THIN PLATE PROGRAMMES: PDES and PDEP

The programmes PDES and PDEP are devised to produce designs for simply supported thin rectangular plates loaded in compression, including plasticity effects.

The two programmes operate in a completely parallel way, but differ in that they are based on different plate buckling analyses.

PDES utlises the Stowell-Ilyushin[25] analysis, while PDEP is based on that due to Prager and Handelman.[39]

Both methods are described in detail in Chapter 3, where they are adapted for design purposes.

Realistic account is taken of plasticity effects on buckling behaviour, including the wavelengths involved for plates of finite aspect ratio.

Input includes

(i) Material property data $10^3 f_2/E$, n, ν_e, ν_p

(ii) Endload intensity parameter w/Eb

(iii) Aspect ratio data A, dA, J.

where A = initial value of aspect ratio a/b
dA = increment of A
J = number of values of A to be computed.

Output comprises in tabular form

(i) Aspect ratio a/b

(ii) Plate design stress $10^3 f/E$

(iii) Number of half-waves in buckling mode m

(iv) Plate thickness t/b

(v) Normalised plate thickness.

A listing of each programme is given below.

```
      LIST PDES
     MASTER PDES
300  FORMAT(4F0.0)
301  FORMAT(F0.0)
302  FORMAT(2F0.0,I0)
303  FORMAT(I0)
200  FORMAT(39H  N,S2P/E(E3),A(E-30),PRE,PRP,S01P/E(E3))
201  FORMAT(F7.3,F10.4,E12.4,F7.4,F7.4,F10.4)
202  FORMAT(6H W/EB=,E12.4)
203  FORMAT(44H     AR     S/E(E3)     M    T/B              (T/B)N)
204  FORMAT(F8.4,F8.4,I5,3X,E13.6,F8.4)
   1 READ(1,300)XN,S2P,RE,RP
     PI=3.141593
     A=2.0*(10.0**(3.0*XN-33.0))/(S2P**XN)
     F2=2.0/S2P
     S01P=(0.05**(1.0/XN))*S2P
     F01=(0.05**((XN-1.0)/XN))*F2
     WRITE(2,200)
     WRITE(2,201)XN,S2P,A,RE,RP,S01P
205  FORMAT(18H   ILYUSHIN-STOWELL)
     WRITE(2,205)
   2 READ(1,301)W
     WRITE(2,202)W
     DW=0.0001*W
   3 READ(1,302)AR,DAR,JM
     WRITE(2,203)
     DO 500 JAR=1,JM
     M1=INT(AR)
     MT=M1*(M1+1)
     AM=1.0*MT
     ART=SQRT(AM)
     IF(AR.LE.ART)GO TO 10
     M1=M1+1
  10 R=(PI*(M1+(AR*AR/M1)))**2.0
     R=R/(12.0*(1.0-(RE*RE)))
     R=R/(AR*AR)
     ML=5*M1
     FW=F01
     SW=S01P
     IR=1
     GO TO 100
  11 IF(WS.GE.W)GO TO 12
     W1=WS
     E1=1.0
     S1=S01P
     FW=F2
     SW=S2P
     IR=2
     GO TO 100
  13 W2=WS
     S2=SW
     E2=20.0*(SW/S2P)**XN
     E=(W-W1)*(E2-E1)/(W2-W1)+E1
     E=ABS(E)
```

```
      SW=S2P*((E/20.0)**(1.0/XN))
      FW=F2*((E/20.0)**((XN-1.0)/XN))
      IF(ABS(W-W2).LE.DW)GO TO 20
      S=S2
      E1=E2
      W1=W2
      GO TO 100
   12 SW=1000.0*((R*W)**(1.0/3.0))*(W**(1.0/3.0))
      FW=(SW/S2P)**(XN-1.0)
      IR=3
      GO TO 100
   14 W2=WS
      FS2=SW**1.5
      S2=SW
      IF(ABS(W-W2).LE.DW)GO TO 20
      FS1=FS2
      W1=W2
      S1=S2
      SW=0.95*SW
      FW=(SW/S2P)**(XN-1.0)
      IR=4
      GO TO 100
   15 S2=SW
      FS2=SW**1.5
      W2=WS
      FS=(W-W1)*(FS2-FS1)/(W2-W1)+FS1
      SW=FS**(2.0/3.0)
      FW=(SW/S2P)**(XN-1.0)
      IF(ABS(W-W2).LE.DW)GO TO 20
      S1=S2
      FS1=FS2
      W1=W2
  100 WX=((RE+(FW*RP))/(1.0+FW))**2.0
      WX=(SW**3.0)*12.0*(1.0+FW)*(1.0-WX)
      WY=0.25*(1.0+3.0*(1.0+FW)/(1.0+XN*FW))
      WZ=WY*((M1/AR)**2.0)+(AR/M1)**2.0+2.0
      M=M1
      DO 101 MZ=(M1+1),ML
      WZZ=WY*((MZ/AR)**2.0)+((AR/MZ)**2.0) +2.0
      IF(WZZ.GE.WZ)GO TO 102
      M=MZ
  101 WZ=WZZ
  102 WS=SQRT(WX/WZ)/(PI*(10.0**4.5))
      GO TO (11,13,14,15),IR
   20 T=W*1000.0/S2
  207 FORMAT(E8.4)
      TN=T/(W**(1.0/3.0))
      WRITE(2,204)AR,S2,M,T,TN
  500 AR=AR+DAR
      READ(1,303)K
      GO TO (1,2,3,4),K
    4 CONTINUE
      STOP OK
      END
      FINISH
```

```
      LIST PDEP
     MASTER PDEP
300  FORMAT(4F0.0)
301  FORMAT(F0.0)
302  FORMAT(2F0.0,I0)
303  FORMAT(I0)
200  FORMAT(39H  N,S2P/E(E3),A(E-30),PRE,PRP,S01P/E(E3))
201  FORMAT(F7.3,F10.4,E12.4,F7.4,F7.4,F10.4)
202  FORMAT(6H W/EB=,E12.4)
203  FORMAT(44H     AR     S/E(E3)     M    T/B                (T/B)N)
204  FORMAT(F8.4,F8.4,I5,3X,E13.6,F8.4)
   1 READ(1,300)XN,S2P,RE,RP
     PI=3.141593
     A=2.0*(10.0**(3.0*XN-33.0))/(S2P**XN)
     F2=2.0/S2P
     S01P=(0.05**(1.0/XN))*S2P
     F01=(0.05**((XN-1.0)/XN))*F2
     WRITE(2,200)
     WRITE(2,201)XN,S2P,A,RE,RP,S01P
205  FORMAT(18H   HANDELMAN-PRAGER)
     WRITE(2,205)
   2 READ(1,301)W
     WRITE(2,202)W
     DW=0.0001*W
   3 READ(1,302)AR,DAR,JM
     WRITE(2,203)
     DO 500 JAR=1,JM
     M1=INT(AR)
     MT=M1*(M1+1)
     AM=1.0*MT
     ART=SQRT(AM)
     IF(AR.LE.ART)GO TO 10
     M1=M1+1
  10 R=(PI*(M1+(AR*AR/M1)))**2.0
     R=R/(12.0*(1.0-(RE*RE)))
     R=R/(AR*AR)
     ML=5*M1
     FW=F01
     SW=S01P
     IR=1
     GO TO 100
  11 IF(WS.GE.W)GO TO 12
     W1=WS
     E1=1.0
     S1=S01P
     FW=F2
     SW=S2P
     IR=2
     GO TO 100
```

```
   13 W2=WS
      S2=SW
      E2=20.0*(SW/S2P)**XN
      E=(W-W1)*(E2-E1)/(W2-W1)+E1
      IF(E.GT.0.0)GO TO 16
      E=0.05
   16 CONTINUE
      SW=S2P*((E/20.0)**(1.0/XN))
      FW=F2*((E/20.0)**((XN-1.0)/XN))
      IF(ABS(W-W2).LE.DW)GO TO 20
      S=S2
      E1=E2
      W1=W2
      GO TO 100
   12 SW=1000.0*((R*W)**(1.0/3.0))*(W**(1.0/3.0))
      FW=(SW/S2P)**(XN-1.0)
      IR=3
      GO TO 100
   14 W2=WS
      FS2=SW**1.5
      S2=SW
      IF(ABS(W-W2).LE.DW)GO TO 20
      FS1=FS2
      W1=W2
      S1=S2
      SW=0.95*SW
      FW=(SW/S2P)**(XN-1.0)
      IR=4
      GO TO 100
   15 S2=SW
      FS2=SW**1.5
      W2=WS
      FS=(W-W1)*(FS2-FS1)/(W2-W1)+FS1
      SW=FS**(2.0/3.0)
      FW=(SW/S2P)**(XN-1.0)
      IF(ABS(W-W2).LE.DW)GO TO 20
      S1=S2
      FS1=FS2
      W1=W2
  100 PR=(RE+(FW*RP))/(1.0+FW)

      ET=1.0+XN*FW

      C=(ET-1.0)/((5.0-4.0*PR)*ET-((1.0-2.0*PR)*(1.0-2.0*PR)))

      CC=0.002/(5.0-4.0*PR)

      IF(C.GE.CC) GO TO 103
      C=0
      ES=0
      GO TO 104
```

```
103 AL=1.0-2.0/(C*(5.0-4.0*PR))
    IF(AL.LT.-1.0)GO TO 106
    ES=AL
    GO TO 104
106 ES=AL+SQRT(AL*AL-1.0)
104 DE=0.25*(2.0-(3.0*ES)+ES*ES*ES)
    D11=1.0-C*DE*((2.0-PR)**2.0)
    D12=(1.0-C*DE*(2.0-PR)*((2.0*PR)-1.0))*2.0
    D22=(1.0-C*DE*(2.0*PR-1.0)*(2.0*PR-1.0))
    WZ=D11*((M1/AR)**2.0)+D22*((AR/M1)**2.0)+D12
    M=M1
    DO 101 MZ=(M1+1),ML
    WZZ=D11*((MZ/AR)**2.0)+D22*((AR/MZ)**2.0)+D12
    IF(WZZ.GE.WZ)GO TO 102
    M=MZ
101 WZ=WZZ
102 WS=((SW**3.0)*(12.0*(1.0-PR*PR)))/WZ
    WS=SQRT(WS)/(PI*(10.0**4.5))
    GO TO (11,13,14,15),IR
 20 T=W*1000.0/S2
207 FORMAT(E12.4,E12.4,E12.4)
    TN=T/(W**(1.0/3.0))
    WRITE(2,204)AR,S2,M,T,TN
500 AR=AR+DAR
    READ(1,303)K
    GO TO (1,2,3,4),K
  4 CONTINUE
    STOP OK
    END
    FINISH
```

Appendix D

HONEYCOMB SANDWICH PLATE PROGRAMME: COSA

The programme COSA determines optimum designs for rectangular honeycomb core sandwich panels loaded in uniaxial compression. The panels are simply supported at all edges, and are of finite aspect ratio.

Proper account is taken of plasticity and transverse shear flexibility effects in evaluating panel buckling and wrinkling instabilities.

The programme also takes direct account of the following constraining factors.

(i) Maximum faceplate stress.
(ii) Minimum faceplate thickness
(iii) Maximum sandwich depth
(iv) Minimum core stiffness.

Input comprises

(i) Material property data $10^3 f_2/E$, n
(ii) Constraint data $10^3 f_{max}/E$, t_{min}/C, h_{max}/C, G_{min}/E.
(iii) Load intensity data W, XW, J
where W = initial value of loading w/E_c
XW = number of W values per decade
J = total number of W values to be computed
(iv) Aspect ratio A, dA, K.
where A = initial value of aspect ratio
dA = increment of aspect ratio.
K = total number of A values to be computed

For each case, output includes

(a) For the ideal optimum design
(i) Faceplate stress $10^3 f/E$
(ii) Number of half waves in panel buckling mode m
(iii) Face thickness t/c
(iv) Sandwich thickness h/c
(v) Core modulus G_c/E
(vi) Equivalent panel thickness t_e/c
(vii) Core proportion of total weight t_{ec}/t_e
(viii) Equivalent panel stress $10^3 f_e/E$

(b) For the constrained design, all data as given under (a) above.

A listing of COSA is given below.

```
      MASTER COSA
  200 FORMAT(2F0.0)
  201 FORMAT(F0.0)
  204 FORMAT(4F0.0)
  205 FORMAT(I0)
  250 FORMAT(18H  N,S2(E3),A(E-30))
  251 FORMAT(F8.3,F10.4,E12.4)
  252 FORMAT(3H W=,E12.4)
  253 FORMAT(4H AR=,F8.3)
  254 FORMAT(21H SMAX,TMIN,HMAX,GCMIN)
  255 FORMAT(F8.3,E12.4,E12.4,E12.4)
  256 FORMAT(22H UNCONSTRAINED OPTIMUM)
  257 FORMAT(37H    SO,M,T/C,H/C,GC/E,T*/C,TEC/T*,F*/E)
  258 FORMAT(F8.4,I3,E10.3,E10.3,E10.3,E13.6,F7.3,F7.3)
  259 FORMAT(31H MAX STRESS CONSTRAINT VIOLATED)
  260 FORMAT(39H MIN FACE THICKNESS CONSTRAINT VIOLATED)
  261 FORMAT(39H MIN CORE STIFFNESS CONSTRAINT VIOLATED)
  262 FORMAT(36H MAX PANEL DEPTH CONSTRAINT VIOLATED)
  263 FORMAT(27H CONSTRAINED OPTIMUM DESIGN)
  264 FORMAT(2F0.0,I0)
    1 READ(1,200)XN,S2P
      A=(0.002*(10.0**(3.0*(XN-10.0))))/(S2P**XN)
      WRITE(2,250)
      WRITE(2,251)XN,S2P,A
    2 READ(1,204)SMAX,TMIN,HMAX,GCMIN
      WRITE(2,254)
      WRITE(2,255)SMAX,TMIN,HMAX,GCMIN
    3 READ(1,264)W,DW,NW
    4 READ(1,264)AR1,DAR,JM
      DO 300 JW=1,NW
      AR=AR1
      WRITE(2,252)W
      DO 34 JAR=1,JM
      WRITE(2,253)AR
      M1=INT(AR)
      MT=M1*(M1+1)
      AM=1.0*MT
      ART=SQRT(AM)
      IF(AR.LE.ART)GO TO 502
      M1=M1+1
  502 MM=10*M1
      SM=2.0*S2P
      KC=0
      KG=0
  802 TE1=10000.0
      NN=11
      S=SM
      DS=-SM/10.000
```

```
      DO 800 ND=1,5
      DO 801 NS=1,NN
      FS=XN*A*(S**(XN-1.0))*(10.0**(3.0*(11.0-XN)))
      F1=1.0+FS/2.0
      GC=(0.25*SQRT((15.0/2.6)*S*S*S))/(10.0**4.5)
      GC=GC*(1.0+SQRT(1.0+FS))
      IF(KG.EQ.0)GO TO 807
      GC=AMAX1(GC,GCMIN)
  807 T=500.0*W/S
      HM=0.0
      DO 150 M=M1,MM
      FL=AR*AR/(M*M)
      H=F1*W*(1.0+SQRT(1.0+0.73762*GC*GC*FL/(F1*W*T)))
      H=H/(2.0*GC*(1.0+FL))
      IF(H.LE.HM)GO TO 149
      HM=H
      MS=M
  150 TE=2.0*T+5.54667*GC*H
  149 IF(TE.GE.TE1)GO TO 148
      TE1=TE
      T1=T
      S1=S
      M11=MS
      H1=HM
      GC1=GC
  270 FORMAT(F8.4,E12.4,E12.4,E12.4,I4)
      WRITE(2,270)S1,H1,GC1,TE1,M11
      CONTINUE
      S=S+DS
      IF(S.LE.0.05)S=0.05
  801 IF(S.GE.SM)S=SM
  148 TE1=TE
      T1=T
      NN=21
      S1=S
      M11=MS
      H1=HM
      GC1=GC
      WRITE(2,270)S1,H1,GC1,TE1,M11
      DS=-DS/10.0
      S=S+DS
      IF(S.LE.0.05)S=0.05
  800 IF(S.GE.SM)S=SM
      IF(KG.EQ.1)GO TO 806
      IF(KC.EQ.1)GO TO 803
      TC=1.0-2.0*T1/TE1
      FE=10.0*10.0*10.0*W/TE1
      WRITE(2,257)
      WRITE(2,258)S1,M11,T1,H1,GC1,TE1,TC,FE
      KC=1
      TSM=500.0*W/SMAX
      SM=SMAX
      IF(TSM.GE.TMIN)GO TO 804
      SM=500.0*W/TMIN
```

```
804 IF(S1.GE.SM)GO TO 802
803 IF(GC1.GE.GCMIN)GO TO 805
    GC=GCMIN
    KG=1
    GO TO 802
806 S=S1
    MS=M11
    T=T1
    HM=H1
    GC=GC1
    TE=TE1
805 IF(H1.LE.HMAX)GO TO 33
    HM=HMAX
    GL=10000.0*W+SMAX
    TE1=2.0*AMAX1(TMIN,TSM) +6.0*GL*HMAX
    NN=11
    DS=-SM/10.000
    S=SM
    DO 500 NH=1,5
    DO  501 NS=1,NN
    FSG=XN*A*(S**(XN-1.0))*(10.0**(3.0*(11.0-XN)))
    GW=(0.25*SQRT((15.0/2.6)*S*S*S))/(10.0**4.5)
    GW=GW*(1.0+SQRT(1.0+FSG))
    ER=2.0/(2.0+FSG)
    G1=0.0
    DO 503 M=M1,MM
    FL=AR*AR/(M*M
    A1=(0.36881E-3)*S*FL/(HM*(1.0+FL))
    A2=HM*ER*(1.0+FL)
    DAA=A2-A1
    IF(DAA.GE.0.0001) GO TO 504
    G=10000.0*W+S
    GO TO 505
504 G=W/(A2-A1)
505 IF(G.LE.G1) GO TO 506
503 G1=G
506 M=M-1
    G=AMAX1(G1,GW,GCMIN)
    T=500.0*W/S
    TE=2.0*T+5.54667*G*HM
    IF(TE.GT.TE1) GO TO 510
    M11=M
    S1=S
    S=S+DS
    G1=G
    T1=T
    IF(S.LE.0.05)S=0.05
    IF(S.GE.SM)S=SM
```

```
501 TE1=TE
510 TE1=TE
    T1=T
    G1=G
    S1=S
    M11=M
    DS=-DS/10.0
    S=S+DS
    IF(S.LE.0.05)S=0.05
    IF(S.GE.SM)S=SM
    NN=21
500 CONTINUE
    H1=HM
    GC1=G1
 33 TC=1.0-2.0*T1/TE1
    FE=10.0*10.0*10.0*W/TE1
    WRITE(2,258)S1,M11,T1,H1,GC1,TE1,TC,FE
 34 AR=AR+DAR
300 W=W*(10.0**(1.0/DW))
    READ(1,205)L
    GO TO(1,2,3,4,5)L
  5 CONTINUE
    STOP OK
    END
    FINISH
```

Appendix E

WIDE COLUMN PROGRAMMES: ZEDS AND ORCS

The programmes ZEDS and ORCS are based on the work described in chapters 6 and 7.

They are designed to allow parametric studies of materials and load intensities for

(i) Wide column plates of given span.

(ii) Wide column surfaces supported at optimum intervals by supports designed according to various policies.

(iii) Circular cylindrical shells fabricated from the surfaces described in (ii), with the shell diameter optimised.

The programme ZEDS is based on a coding by Fews[54] with modifications to account for recent developments in analysis.

ZEDS gives load intensities and dimensions for the complete working range of stresses for any given material for each of the configurations above, together with stress-strain data, tangent and secant moduli, and Poisson's ratios modified to allow for plasticity.

The programme is documented to allow for the exercise of a variety of options for information output.

Three support design policies are considered

(i) Constant size supports (m = 0)

(ii) Linear relation between size and stiffness (m = 1)

(iii) Geometric relation between size and stiffness (m = $\frac{1}{2}$)

A listing of the programme is given below.

```
MASTER SEGMENT

      MASTER COMPSURF
      COMMON/COM1/F1(30),ES(30),ET(30),AMU(30),EPS(30)
      COMMON/COM2/F2(30),W1(30),T11(30),B1(30),TS1(30)
      COMMON/COM3C/F2C(30),W21(30),AL1(30),T21(30),B21(30),
     1TS21(30),RR1(30)
      COMMON/COM3L/F2L(30),W22(30),AL2(30),T22(30),B22(30),
     1TS22(30),RR2(30)
      COMMON/COM3G/F2G(30),W23(30),AL3(30),T23(30),B23(30),
     1TS23(30),RR3(30)
      COMMON/COM4C/F3C(30),A1(30),D1(30),S1(30)
      COMMON/COM4L/F3L(30),A2(30),D2(30),S2(30)
      COMMON/COM4G/F3G(30),A3(30),D3(30),S3(30)
   10 FORMAT (5F0.0)
   20 FORMAT (//2X,18HSTRESS-STRAIN DATA,/,
     12X,18H------------------,//)
   30 FORMAT (6X,3HF/E,9X,4HES/E,9X,4HET/E,
     17X,10HSTR/(F2/E),4X,7HPOS-RAT,/)
   40 FORMAT (1X,5(1X,E12.5))
   50 FORMAT (//2X,31HOPTIMUM PANELS OF FIXED SUPPORT,/,
     12X,31H-------------------------------,//)
   60 FORMAT (6X,3HF/E,6X,12HF**2*W/(E*L),2X,10HF*TS/(T*L)
     1,1X,15HF**0.5*SP/(B*L),1X,10HF**2*TES/L,/)
   70 FORMAT (//2X,41HSURFACES WITH OPTIMISED SUPPORT LOCATIONS,/,
     12X,41H-----------------------------------------,/)
   80 FORMAT (//2X,13HCONSTANT RIBS,/)
   90 FORMAT (1X,5HF    3,/,1X,4H-*10,7X,2HW1,10X,2HL1,10X,2HT1,
     110X,2HB1,9X,3HTE1,6X,2HR1,/,1X,1HE,/)
   97 FORMAT (1X,5HF    3,/,1X,4H-*10,7X,2HW2,10X,2HL2,10X,2HT2,
     110X,2HB2,9X,3HTE2,6X,2HR2,/,1X,1HE,/)
   98 FORMAT (1X,5HF    3,/,1X,4H-*10,7X,2HW3,10X,2HL3,10X,2HT3,
     110X,2HB3,9X,3HTE3,6X,2HR3,/,1X,1HE,/)
  100 FORMAT (1X,F5.3,5(E12.5),1X,F5.3)
  110 FORMAT (//2X,11HLINEAR RIBS,/)
  120 FORMAT (//2X,14HGEOMETRIC RIBS,/)
  130 FORMAT (//2X,48HCIRCULAR SHELLS WITH OPTIMISED SUPPORT LOCATION
     12X,48H------------------------------------------------,/)
  140 FORMAT (7X,3HF/E,10X,3HA11,10X,3HD11,9X,4HLS11,/)
  141 FORMAT (7X,3HF/E,10X,3HA12,10X,3HD12,9X,4HLS12,/)
  142 FORMAT (7X,3HF/E,10X,3HA13,10X,3HD13,9X,4HLS13,/)
  150 FORMAT (1X,4(1X,E12.5))
  160 FORMAT (F0.0)
  170 FORMAT (//,2X,39HTYPE 1 FOR DATA DESCRIPTION OTHERWISE 0)
  180 FORMAT (I0)
  190 FORMAT (//,2X,13HMATERIAL DATA,/,
     12X,13H-------------,/)
```

```
200 FORMAT (/,2X,24HPLASTICITY INDEX          =)
210 FORMAT (2X,24HO.2% PROOF STRESS           =)
220 FORMAT (2X,24HYOUNG'S MODULUS             =)
340 FORMAT (2X,24HELASTIC POISON'S RATIO      =)
350 FORMAT (2X,24HPLASTIC POISON'S RATIO      =)
230 FORMAT (//,2X,26HSELECTIVE OUTPUT PARAMETER,/)
240 FORMAT (2X,26HTYPE 1 FOR CIRCULAR SHELLS,/,
   12X,53HTYPE 10 FOR SURFACES WITH OPTIMISED SUPPORT LOCATIONS,/,
   22X,44HTYPE 100 FOR PANELS OF GIVEN SUPPORT SPACING,/,
   32X,32HTYPE 1000 FOR STRESS STRAIN DATA,/,
   42X,50H1001 WILL GIVE BOTH CIRCULAR SHELL INFORMATION AND,/,
   52X,22HSTRESS STRAIN DATA ETC,/)
250 FORMAT (2X,13HOTHER OPTIONS,/,
   12X,13H-------------,/)
260 FORMAT (2X,26HTYPE 2000 FOR NEW MATERIAL,/,
   12X,31HTYPE 3000 TO TERMINATE PROGRAM,/)
270 FORMAT (/,2X,28HSELECTIVE OUTPUT PARAMETER =)
280 FORMAT (//2X,30HRIB DESIGN PARAMETER (SURFACE),/,
   12X,30H-----------------------------,/)
360 FORMAT (//2X,31HRIB DESIGN PARAMETER (CYLINDER),/,
   12X,31H------------------------------,/)
290 FORMAT (2X,25HTYPE 1 FOR GEOMETRIC RIBS,/,
   12X,23HTYPE 10 FOR LINEAR RIBS,/,
   22X,26HTYPE 100 FOR CONSTANT RIBS,/,
   32X,50H101 WILL GIVE BOTH CONSTANT AND GEOMETRIC DATA ETC,/)
300 FORMAT (/2X,22HRIB DESIGN PARAMETER =)
310 FORMAT (//2X,26HMINIMUM WEIGHT COMPRESSION,1X,
   139HSURFACE DESIGN WITH ISOTROPIC MATERIALS,/,
   22X,30H******************************,
   336H**********************************)
320 FORMAT (//2X,19HMATERIAL PROPERTIES,/,
   12X,19H-------------------)
330 FORMAT (//5X,7HYOUNG'S,5X,10HO.2% PROOF,2X,
   110HPLASTICITY,7X,15HPOISON'S RATIOS,/,5X,7HMODULUS,
   26X,6HSTRESS,7X,5HINDEX,8X,7HELASTIC,6X,7HPLASTIC,/)
    CHK=0.999999
 69 WRITE (2,170
    READ (1,180) NDAT
    IF (NDAT.NE.1) GO TO 81
    WRITE (2,190)
    WRITE (2,200)
    READ (1,160) AN
    WRITE (2,210)
    READ (1,160) F2P
    WRITE (2,220)
    READ (1,160) E
    WRITE (2,340)
    READ (1,160) PE
    WRITE (2,350)
    READ (1,160) PP
 67 IF (NDAT.NE.1) GO TO 82
    WRITE (2,230)
    WRITE (2,240)
    WRITE (2,250)
    WRITE (2,260)
    WRITE (2,270)
```

```
      READ (1,160) SO
      IF (SO.LT.1500.0) GO TO 83
      IF (SO-2100.0) 69,69,26
      GO TO 83
   81 READ (1,10) AN,F2P,E,PE,PP
   82 READ (1,160) SO
      IF (SO.LT.1500.0) GO TO 83
      IF (SO-2100.0) 69,69,26
   83 WRITE (2,310)
      WRITE (2,320)
      WRITE (2,330)
      WRITE (2,40) E,F2P,AN,PE,PP
      PS=0.0002
      SEP=0.1**(1.0/AN)
      BIT=0.0
      ST=SEP/10.0
      N1=0
      N2=0
      N3=0
      N4=0
      NC1=0
      NL1=0
      NG1=0
      NC2=0
      NL2=0
      NG2=0
      N=0
      S=ST
      CON=F2P/E
    1 PHY=0.002/CON*S**(AN-1.0)
      N=N+1
      T1=SO/1000.0
      IF (T1-CHK) 13,3,3
    3 CALL TAB1(N,S,PHY,CON,AN,PE,PP)
      N1=1
      BIT=1.0
   13 T2=(T1-BIT)*10.0
      BIT=0.0
      IF (T2-CHK) 14,4,4
    4 CALL TAB2 (N,S,PHY,CON,AN)
      N2=1
      BIT=1.0
   14 T3=(T2-BIT)*10.0
      BIT=0.0
      IF (T3-CHK) 15,5,5
    5 IF (N3.EQ.1) GO TO 11
      N3=1
      IF (NDAT.NE.1) GO TO 84
      WRITE (2,280)
      WRITE (2,290)
      WRITE (2,300)
      READ (1,160) RIBS
      GO TO 11
   84 READ (1,10) RIBS
   11 NS=1
      CALL TAB3 (N,RIBS,NC1,NL1,NG1,S,PHY,CON,AN,NS)
```

```
      BIT=1.0
   15 T4=(T3-BIT)*10.0
      BIT=0.0
      IF (T4-CHK) 2,6,6
    6 IF (N4.EQ.1) GO TO 12
      N4=1
      IF (NDAT.NE.1) GO TO 85
      WRITE (2,360)
      WRITE (2,290)
      WRITE (2,300)
      READ (1,160) RIBC
      GO TO 12
   85 READ (1,10) RIBC
   12 NS=2
      CALL TAB3 (N,RIBC,NC2,NL2,NG2,S,PHY,CON,AN,NS)
    2 IF (N.GT.9) GO TO 7
      S=S+ST
      GO TO 1
    7 PS=PS+0.0002
      IF (PS.GT.0.0023) GO TO 8
      S=(PS/0.002)**(1.0/AN)
      GO TO 1
    8 IF (N1.NE.1) GO TO 21
      WRITE (2,20)
      WRITE (2,30)
      DO 91 I=1,N
   91 WRITE (2,40) F1(I),ES(I),ET(I),EPS(I),AMU(I)
   21 IF(N2.NE.1) GO TO 22
      WRITE (2,50)
      WRITE (2,60)
      DO 92 I=1,N
   92 WRITE (2,40) F2(I),W1(I),T11(I),B1(I),TS1(I)
   22 IF (N3.NE.1) GO TO 23
      WRITE (2,70)
      IF (NC1.NE.1) GO TO 24
      WRITE (2,80)
      WRITE (2,90)
      DO 41 I=1,N
   41 WRITE (2,100) F2C(I),W21(I),AL1(I),T21(I),B21(I),TS21(I),RR1(I)
   24 IF (NL1.NE.1) GO TO 25
      WRITE (2,110)
      WRITE (2,97)
      DO 42 I=1,N
   42 WRITE (2,100) F2L(I),W22(I),AL2(I),T22(I),B22(I),TS22(I),RR2(I)
   25 IF (NG1.NE.1) GO TO 23
      WRITE (2,120)
      WRITE (2,98)
      DO 43 I=1,N
   43 WRITE (2,100) F2G(I),W23(I),AL3(I),T23(I),B23(I),TS23(I),RR3(I)
   23 IF (N4.NE.1) GO TO 67
      WRITE (2,130)
      IF (NC2.NE.1) GO TO 27
      WRITE (2,80)
      WRITE (2,140)
      DO 93 I=1,N
   93 WRITE (2,150) F3C(I),A1(I),D1(I),S1(I)
```

```
 27 IF (NL2.NE.1) GO TO 28
    WRITE (2,110)
    WRITE (2,141)
    DO 94 I=1,N
 94 WRITE (2,150) F3L(I),A2(I),D2(I),S2(I)
 28 IF (NG2.NE.1) GO TO 67
    WRITE (2,120)
    WRITE (2,142)
    DO 95 I=1,N
 95 WRITE (2,150) F3G(I),A3(I),D3(I),S3(I)
    GO TO 67
 26 STOP OK
    END
```

STRESS STRAIN DATA

```
    SUBROUTINE TAB1 (N,S,PHY,CON,AN,PE,PP)
    COMMON/COM1/F1(30),ES(30),ET(30),AMU(30),EPS(30)
    F1(N)=S*CON
    ES(N)=1.0/(1.0+PHY)
    ET(N)=1.0/(1.0+AN*PHY)
    AMU(N)=(PE+PP*PHY)/(1.0+PHY)
    EPS(N)=S*(1.0+PHY)
    RETURN
    END
```

OPTIMUM PANELS OF FIXED SUPPORT

```
    SUBROUTINE TAB2 (N,S,PHY,CON,AN)
    COMMON/COM2/F2(30),W1(30),T1(30),B1(30),TS1(30)
    F2(N)=S*CON
    W1(N)=F2(N)*F2(N)*(1.0+AN*PHY)
    T1(N)=W1(N)/F2(N)
    B1(N)=SQRT(T1(N))
    TS1(N)=T1(N)
    RETURN
    END
```

SURFACES WITH OPTIMISED SUPPORT LOCATIONS

```
    SUBROUTINE TAB3 (N,RIB,NC1,NL1,NG1,S,PHY,CON,AN,NS)
    COMMON/COM3C/F2C(30),W21(30),AL1(30),T21(30),B21(30),TS21(30)
   1,RR1(30)
    COMMON/COM3L/F2L(30),W22(30),AL2(30),T22(30),B22(30),TS22(30)
   1,RR2(30)
    COMMON/COM3G/F2G(30),W23(30),AL3(30),T23(30),B23(30),TS23(30)
   1,RR3(30)
    COMMON/COM4C/F3C(30),A1(30),D1(30),S1(30)
    COMMON/COM4L/F3L(30),A2(30),D2(30),S2(30)
    COMMON/COM4G/F3G(30),A3(30),D3(30),S3(30)
    BIT=0.0
    T1=RIB/100.0
    IF (T1-1.0) 21,3,3
  3 IF (NS.EQ.2) GO TO 13
    CALL CRIBS (N,S,PHY,CON,AN)
    GO TO 14
```

```
   13 CALL CRIBC (N,S,PHY,CON,AN)
   14 NC1=1
      BIT=1.0
   21 T2=(T1-BIT)*10.0
      BIT=0.0
      IF (T2-1.0) 22,4,4
    4 IF (NS.EQ.2) GO TO 15
      CALL LRIBS (N,S,PHY,CON,AN)
      GO TO 16
   15 CALL LRIBC (N,S,PHY,CON,AN)
   16 NL1=1
      BIT=1.0
   22 T3=(T2-BIT)*10.0
      BIT=0.0
      IF (T3-1.0) 2,5,5
    5 IF (NS.EQ.2) GO TO 17



      CALL GRIBS (N,S,PHY,CON,AN)
      GO TO 18
   17 CALL GRIBC (N,S,PHY,CON,AN)
   18 NG1=1
    2 RETURN
      END
```

SURFACES WITH CONSTANT RIBS

```
      SUBROUTINE CRIBS (N,S,PHY,CON,AN)
      COMMON/COM3C/F2C(30),W21(30),AL1(30),T21(30),B21(30),TS21(30)
     1,RR1(30)
      F2C(N)=S*CON
      D1=AN*PHY+1.0
      D2=(1.0+AN)*AN*PHY+2.0
      W21(N)=(F2C(N)**1.5)*SQRT(D2)
      AL1(N)=SQRT(D2/F2C(N))/D1
      T21(N)=SQRT(F2C(N)*D2)
      B21(N)=SQRT(D2/D1)
      TS21(N)=SQRT(F2C(N)/D2)*(D2+D1)
      RR1(N)=D1/(D1+D2)
       F2C(N)=F2C(N)*10**3.0
      RETURN
      END
```

SURFACES WITH LINEAR RIBS

```
      SUBROUTINE LRIBS (N,S,PHY,CON,AN)
      COMMON/COM3L/F2L(30),W22(30),AL2(30),T22(30),B22(30),TS22(30)
     1,RR2(30)
      F2L(N)=S*CON
      D1=1.0+AN*PHY
      D2=((1.0+AN)*AN*PHY+2.0)*2.0
      W22(N)=(F2L(N)**2.5)*SQRT(D1+D2)
      AL2(N)=SQRT(F2L(N)*D2/D1)
      T22(N)=(F2L(N)**1.5)*SQRT(D1*D2)
      B22(N)=F2L(N)*SQRT(D2)
      TS22(N)=(F2L(N)**1.5)*SQRT(D1/D2)*(D1+D2)
      RR2(N)=D1/(D1+D2)
      F2L(N)=F2L(N)*10**3.0
      RETURN
      END
```

SURFACES WITH LINEAR RIBS

```
      SUBROUTINE GRIBS (N,S,PHY,CON,AN)
      COMMON/COM3G/F2G(30),W23(30),AL3(30),T23(30),B23(30),TS23(30)
     1,RR3(30)
      F2G(N)=S*CON
      D1=1.0+AN*PHY
      D2=((1.0+AN)*AN*PHY+2.0)*1.5
      W23(N)=F2G(N)*F2G(N)*SQRT(SQRT(D1)*D2)
      AL3(N)=SQRT(D2)/(D1**0.75)
      T23(N)=W23(N)/F2G(N)
      B23(N)=SQRT(F2G(N)*D2/SQRT(D1))
      TS23(N)=F2G(N)*(D1+D2)*SQRT(SQRT(D1)/D2)
      RR3(N)=D1/(D2+D1)
      F2G(N)=F2G(N)*10**3.0
      RETURN
      END
```

CYLINDRICAL SHELL WITH CONSTANT RIBS

```
      SUBROUTINE CRIBC (N,S,PHY,CON,AN)
      COMMON/COM4C/F3C(30),A1(30),D1(30),S1(30)
      F3C(N)=S*CON
      D11=1.0+AN*PHY
      D2=2.0+(AN+1.0)
      D2=2.0+(AN+1.0)*AN*PHY
      A1(N)=(((D11+D2)**4.0)/(F3C(N)*D2**3.0))**0.25
      D1(N)=1.0/(((F3C(N)**3.0)*D2)**0.25)
      S1(N)=SQRT(D2/(F3C(N)*D11*D11))
      RETURN
      END
```

CYLINDRICAL SHELL WITH LINEARLY VARYING RIBS

```
      SUBROUTINE LRIBC (N,S,PHY,CON,AN)
      COMMON/COM4L/F3L(30),A2(30),D2(30),S2(30)
      F3L(N)=S*CON
      D1=1.0+AN*PHY
      D22=(2.0+(1.0+AN)*AN*PHY)*2.0
      A2(N)=((D1/((F3L(N)**3.0)*(D22**7.0)))**0.125)*(D1+D22)
      D2(N)=1.0/(((F3L(N)**5.0)*D1*D22)**0.125)
      S2(N)=(D22/((F3L(N)*D1)**3.0))**0.25
      RETURN
      END
```

CYLINDRICAL SHELL WITH GEOMETRIC RIBS

```
      SUBROUTINE GRIBC (N,S,PHY,CON,AN)
      COMMON/COM4G/F3G(30),A3(30),D3(30),S3(30)
      F3G(N)=S*CON
      D1=1.0+AN*PHY
      D2=(2.0+(1.0+AN)*AN*PHY)*1.5
      A3(N)=((SQRT(D1)/(F3G(N)*F3G(N)*(D2**5.0)))**(1.0/6.0))
      A3(N)=A3(N)*(D1+D2)
      D3(N)=(1.0/((F3G(N)**4.0)*SQRT(D1)*D2))**(1.0/6.0)
      S3(N)=(D2/(F3G(N)*F3G(N)*(D1**2.5)))**(1.0/3.0)
      RETURN
      END
      FINISH
```

The programme ORCS extracts the optimum value of surface stress for wide column stiffened shells and outputs this together with parameters corresponding to shell diameter, equivalent cross-section area and ring frame spacing.

Again, the three support design policies described above are implemented.

A listing of ORCS is given below.

```
      MASTER ORCS
   10 FORMAT(1F0.0)
   11 FORMAT(//,34H    S1          S2       A(E-30)          N)
   12 FORMAT(F8.4,F8.4,E11.4,F10.4)
   13 FORMAT(F8.4,F11.3,F11.3,F11.3)
   14 FORMAT(/,39H     SO           XW           XD           XL)
   15 FORMAT(///,30H  OPTIMUM SHELL PARAMETERS FOR)
  111 FORMAT(39H  DESIGNS BASED ON CONSTANT AREA FRAMES)
  112 FORMAT(42H  DESIGNS BASED ON LINEAR STIFFNESS FRAMES)
  113 FORMAT(45H  DESIGNS BASED ON GEOMETRIC STIFFNESS FRAMES)
   16 FORMAT(I0)
   99 READ(1,10)XN
  100 READ(1,10)S2
      A=(0.002*(10.0**(3.0*(XN-10.0))))/(S2**XN)
      S1=((0.001/A)**(1.0/XN))*(10.0**(3.0*(1.0-10.0/XN)))
      WRITE(2,11)
      WRITE(2,12)S1,S2,A,XN
      DO 500 NE=1,3
      I=1
      NR=1
      S=1.0
      DS=1.0
      GO TO (101,102,103),NE
   20 SA=S
      WA=XW
      S=2.0
      NR=2
      GO TO(101,102,103),NE
   21 SB=S
      WB=XW
      S=3.0
      NR=3
      GO TO(101,102,103),NE
   24 IF(XW-WB)25,26,26
   25 SA=SB
      WA=WB
      SB=S
      WB=XW
      S=S+DS
      GO TO(101,102,103),NE
   26 I=I+1
      IF(I-4)27,27,28
   27 DS=-DS/10.0
      SA=SB
      WA=WB
      SB=S
      WB=XW
      S=S+DS
      GO TO(101,102,103),NE
```

```
101 FS=A*(S**(XN-1.0))*(10.0**(3.0*(11.0-XN)))
    F1=1.0+XN*FS
    F2=(1.0+XN)*XN*FS+2.0
    XD=(1000.0**0.75)/((S*S*S*F2)**0.25)
    XW=(F1+F2)*(1000.0/(S*F2*F2*F2))**0.25
    XL=SQRT(1000.0*F2/(S*F1*F1))
    GO TO(20,21,24,30),NR
102 FS=A*(S**(XN-1.0))*(10.0**(3.0*(11.0-XN)))
    F1=1.0+XN*FS
    F2=(2.0+(1.0+XN)*XN*FS)*2.0
    XD=((1000.0**5.0)/(S**5.0*F1*F2))**0.125
    XW=(F1+F2)*((F1/(((0.001*S)**3.0)*(F2**7.0)))**0.125)
    XL=(F2/((0.001*S*F1)**3.0))**0.25
    GO TO(20,21,24,30),NR
103 FS=A*(S**(XN-1.0))*(10.0**(3.0*(11.0-XN)))
    F1=1.0+XN*FS
    F2=(2.0+(1.0+XN)*XN*FS)*1.5
    XD=1.0/(((0.001*S)**4.0*SQRT(F1)*F2)**(1.0/6.0))
    XW=(F1+F2)*(SQRT(F1)/(0.000001*S*S*(F2**5.0)))**(1.0/6.0)
    XL=(F2/((0.001*S)*(0.001*S)*(F1**2.5)))**(1.0/3.0)
    GO TO(20,21,24,30),NR
 28 C=(((WB-WA)/(SB-SA))-((XW-WA)/(S-SA)))/(SB-S)
    B=((WB-WA)/(SB-SA))-C*(SA+SB)
    S=-B/(2.0*C)
    NR=4
    GO TO(101,102,103),NE
 30 WRITE(2,15)
    IF(NE.EQ.1) WRITE(2,111)
    IF(NE.EQ.2) WRITE(2,112)
    IF(NE.EQ.3) WRITE(2,113)
    WRITE(2,14)
    WRITE(2,13)S,XW,XD,XL
500 CONTINUE
    READ(1,16)M
    IF(M)99,100,501
501 CONTINUE
    STOP OK
    END
    FINISH
```

BIBLIOGRAPHY

The bibliography which follows is concerned with the general subject of structural optimisation, of which the studies described in this thesis form but a small part.

It is appended here as a useful item in its own right, but it may also serve to indicate the scope and diversity of research interests in this field.

The method of serialisation chosen is by authors names in alphabetical sequence, while any further subdivision that may be required is chronological.

AGARWAL, B, and DAVIS, R.C. (1974) Minimum Weight Designs for Hat-Stiffened Composite Panels Under Uniaxial Compression. NASA TN D-7779.

ALBLAS, J.B. (1977) Optimal Strength of a Compound Column. Int. J. Sols. Structs. Vol.13, pp.307-320.

ANDERSON, R.A. (1957) Weight Efficiency Analysis of Thin Wing Construction. Trans.ASME v.79, No.5, pp.974-979. July 1957.

ARORA, J.S. (1974) Inverse Problem of Structural Optimisation. J.Struct.Div.ASCE, pp.2355-2361.

ARORA, J.S. and GOVIL, A.K. (1977) An Efficient Method of Optimal Structural Design by Substructuring. Comp.Structs. v7, pp.507-515.

ARMAND, J.L. (1971) Minimum Mass Design of a Plate-Like Structure for Specified Fundamental Frequency. AIAA Jour. Vol.9, No.9, pp.1739-1745.

ASHLEY, H, McINTOSH, S.C. and WEATHERILL, W.H. (1970) Optimisation under Aeroelastic Constraints. AGARD Symp. on Struct. Optmisation, AGARD CP-36-70.

BARTA, J. (1956) On the Minimum Weight of Certain Redundant Structures. Acta Tech.Acad.Sci.Hungary, v.18,pp67-76.

BERKE, L. (1972) Convergence Behaviour of Iterative Resizing Procedure Based on Optimality Criteria. AFFDL-TM-72-1-FBR

BIJLAARD, P.P. (1951) On the Optimum Distribution of Material in Sandwich Plates Loaded in their Plane. Proc. 1st U.S. Nat. Con. Appl. Mech. pp.373-380.

BLOCK, D.L. (1971) Minimum Weight Design of Axially Compressed Ring and Stringer Stiffened Cylindrical Shells.
NASA CR-1766

BROCK, J.E. (1974) Analytic Treatment of Minimum Weight Design of Cantilevers.
J.Appl.Mech. (Trans.ASME) pp.512-515.

BRONOWICKI, A.J. et al. (1975) Optimisation of Ring Stiffened Cylindrical Shells.
AIAA J. Vol.13,No.10. Oct. 1973. pp.1319-1325.

BULSON, P.S. (1970). The Stability of Flat Plates. (Chatto and Windus)

CARDOU, A. (1973) Piecewise Uniform Optimum Design for Axial Vibration Requirement.
AIAA Jour. Vol.11,No.12, Dec. 1973, pp.1760-1761.

CARTER, W.J. and RAGSDELL, K.M. (1974). The Optimal Column.
J.Eng.Mat.Tech. (Trans.ASME) pp.71-76.

CATHCHPOLE, E.J. (1954). The Optimum Design of Compression Surfaces having Unflanged Integral Stiffeners.
JRAeS, Vol.58, No.527, p.765.

CELLA, A. and SOOSAR, K. (1972). A Discrete Variable Approach to Structural Optimisation.
Conf. Optmisation of Structural Design, Swansea 1972.

CHAN, A.S.L. (1960) The Design Of Michell Optimum Structures.
College of Aeronautics Report No.142.

CHAN, H.S.Y. (1963) Optimum Michell Frameworks for Three Parallel Forces.
CoA Report Aero. No.167.

CHAN, H.S.Y.(1964) Optimum Structural Design and Linear Programming.
College of Aeronautics Report No.175.

CHAN, H.S.Y.(1964) Tabulation of Some Layouts and Virtual Displacement Fields in the Theory of Michell Optimum Structures.
College of Aeronautics Note Aero. 161.

CHAN, H.S.Y. (1966) Minimum Weight Cantilever Frames with Specified Reactions.
Oxford University Engineering Science Dept. Rep.1010.66.

CHAN, H.S.Y. (1966) Optimum Design of Shells of Revolution Under Edge Loadings.
Oxford University Dept. of Engineering Science Report 1005.66

CHAN, H.S.Y. (1967) Optimum Design of Structures
(PhD Thesis, Oxford University)

CHAN, H.S.Y. (1967) Half-Plane Slip-Line Fields and Michell Structures
Q.J. Mechs.Appl.Math.VXX Part 4, Nov.1967.

CHAN, H.S.Y. (1968) Minimum Volume Design of Frameworks and Discs
for Alternative Loading Systems.
Quart.Appl.Math.V.XXV, No.4, Jan.1968.

CHAN, H.S.Y. (1968) Mathematical Programming in Optimal Plastic Design.
Int.J.Solids Structs. v.4.pp.885-895

CHERN, J.M. (1971) Optimal Structural Design for given Deflection
in the Presence of Body Forces.
Int.J. Solids Structures v.7, pp.373-382.

CHILVER, A.H. (1976) Design Philosophy in Structural Stability
IUTAM Symp. Buckling of Structures 1974, Springer, Berlin.

CILLY, F.H. (1900) The Exact Design of Statically Indeterminate
Frameworks, an Exposition of its Possibility, but Futility.
Trans. ASCE, v.42 pp.353 - 407.

COHN, M.Z. and PARIMI, S.R. (1973) Optimal Design of Plastic Structures
for Fixed and Shakedown Loadings.
J.Appl.Mechs. June 1973, pp.595-599.

COLLATZ, L, and WETTERLING, W. (1975) Optimisation Problems
Springer Verlag, Berlin 1975.

COOK, R.D. (1977) Application of Optimisation and Finite Element Methods
to a Cracking Problem in Timber.
Int.J.Num.Meth.Eng. Vol.11,pp.756-758.

COX, H.L. (1943) Structures of Minimum Weight.
ARC R and M, No.1923.

COX, H.L. (1954) Computation of Initial Buckling Stress for Sheet-
Stiffener Combinations
JRAeS, Vol.58,Sept. 1954 pp.634-638.

COX, H.L. (1958) The Theory of Design.
ARC Report 19791.

COX, H.L. (1958) The Application of the Theory of Stability in
Structural Design.
JRAeS, Vol.62, No.571, p.497.

COX, H.L. (1958) Structures of Minimum Weight. The Basic Theory of
Design Applied to the Beam Under Pure Bending.
ARC Report Struct. 2036.

COX, H.L. (1965). The Design of Structures of Least Weight. (Pergamon)

COX, H.L. and GRAYLEY, M.E. (1972). The Influence of Production Imperfections on Design of Optimum Structures. Contributions to the Theory of Aircraft Structures. Delft University Press 1972.

COX, H.L. (1973) Comment on 'Optimisation as a Generator of Structural Stability' by J.M.T. Thompson. Int.J.Mech.Sci. Vol.15, pp.855-857.

CRAWFORD, R.F., and HEDGEPETH, J.M. (1975). Effects of Initial Waviness on the Strength and Design of Built-Up Structures. AIAAJ Vol.13, No.5, pp.672-675

DALEY, G.C. (1974) Optimisation of Tension and Stinger Length for Offshore Pipeline Installation J.Eng.End. Nov. 1974 pp.1334-1336.

DANTZIG, G.B. (1963) Linear Progamming and Extensions. Princeton University Press.

DAYARATHNAM, P. and SURYANARAYANA, P. (1969) Feasibility of Full Stress Design AIAA V.7, No.4, pp.773-774.

DORN, W.S., GOMORY, R.E., and GREENBERG, H.J. (1964) Automatic Design of Optimal Structures. J. Mécanique v.3, No.1.

DRUCKER, D.C. and SHIELD, R.T. (1956) Design for Minimum Weight. Proc. 9th Int. Cong. Appl. Mechs. Brussels.

DUBERG, J.E. and WILDER, T.W. (1951) Inelastic Column Behaviour NACA TN 2267.

DUFFIN, R.S., PETERSEN, E.L., and ZENER, C.M. (1967) Geometric Programming (Wiley).

DUPUIS, G. (1971) Optimal Design of Statically Determinate Beams Subject to Displacement and Stress Constraints. AIAAJ Vol.9, No.5, pp.981-984.

DWIGHT, J.B., LITTLE, G.H. and ROGERS, N.A. (1973) An Approach to Stiffened Steel Compression Panels. Cambridge University Engineering Department CUED/C-Struct/ TR 32 (1973)

DWYER, W.J, EMERTON, R and OJALVO, I.U. (1971) An Automated Procedure for the Optimisation of Practical Aerospace Structures, Vols. I and II. AFFDL TR-70-118.

DWYER, W.J. (1972) Finite Element Modelling and Optimisation of Aerospace Structures. AFFDL-TR-72-59.

DYM, C.L. (1974) On Some Recent Approaches to Structural Optimisation. J. Sound and Vib. Vol.32, No.1, pp 49-70.

EASON, G. (1960) The Minimum Weight Design of Circular Sandwich Plates, ZAMP Vol.XI, pp.368-375.

EMERO, D.H. and SPUNT, L. (1966) Wing Box Optimisation under Combined Stress and Bending. Journal of Aircraft, Vol.3, No.2, p.130.

ENGINEERING SCIENCES DATA. Aeronautical (Structures) Series.

FARRAR, D.J. (1949) The Design of Compression Structures for Minimum Weight. JRAeS, Vol.53, No.467, p.1041.

FELTON, L.P. and NELSON, R.B. (1971) Optimised Components in Frame Synthesis.
AIAAJ Vol.9, No.6,pp.1027-1031.

FELTON, L.P., NELSON, R.B. and BRONOWICKI, A.J. (1973). Thin-Walled Elements in Truss Synthesis.
AIAA Journal, Vol.11, No.12, Dec. 1973, pp.1780-1782.

FLERON, P. (1964) The Minimum Weight of Trusses.
Bygningsstatiske Meddelelser v.35,No.3,pp.81-96.

FLETCHER, R. (1972) Methods of Solving Optimisation Problems.
Conf. Optimisation of Struct. Design, Swansea 1972.

FOULKES, J. (1954) Minimum Weight Design of Structural Frames.
Proc. Royal Society of London, Series A. Vol.223, p.482.

FRANCIS, A.J. (1953) Direct Design of Elastic Statically Indeterminate Triangulated Frameworks for Single Systems of Loads.
Australian J. of Appli.Sci. v4, pp.175-185.

FRAUENTHAL, J.C. (1973) Initial Postbuckling Behaviour of Optimally Designed Columns and Plates.
Int.J.Solids Structures, 1973, v.9, pp.115-127.

FRENCH, M.J. (1964) The Design of Rotors to have Minimum Weight Consistent with Required First Critical Speed.
J.Mech.Eng.Sci. v.6, No.1.

FREUDENTHAL, A.M. (1956) Safety and the Probability of Structural Failure.
Trans.ASCE, Vol.121 (also AGARD Symposium on Structural Optimisation, AGARD CP-36-70)

FREUDENTHAL, A.M. and others (1966) The Analysis of Structural Safety.
Journal ASCE, V.92.

FULLER, B. (1968) Design Science Initiative Q.M.C. Course notes.
April 1968.

FULTON, R.E. and McCOMB, H.G. (1974) Automated Design of Aerospace
Trans.ASME J.Eng.Ind. pp.217-225.

GALLAGHER, R.H. (1977) Computerised Structural Analysis and Design -
the Next Twenty Years.
Comp. Structs. v.7, pp.495-501.

GELLATLEY, R. (1966) Development of Procedures for Large Scale
Automated Minimum Weight Structural Design.
AFFDL-TR-66-180.

GELLATLEY,R.A. and GALLAGHER, R.H. (1967) Instability Effects in
Automated Minimum Weight Design.
Conf. Struct. Stability and Optimisation, Loughborough,
March 1967.

GELLATLEY, R.L. and BERKE, L. (1971) Optimal Structural Design.
AFFDL-TR-70-165.

GELLATLEY, R.A. and BERKE, L. (1972) Structural Design with
Optimally-Based Algorithms.
Conf. Optimisation of Structural Design, Swansea 1972.

GERARD, G. (1956) Minimum Weight Analysis of Compression Structures.
(New York University Press)

GERARD, G. (1957) Thermostructural Efficiencies of Compression Elements
and Materials.
Trans.ASME v.79, No.5, July 1957

GERARD, G. and BECKER, H. (1957) Handbook of Structural Stability.
NACA TN 3781 to 3786 and NASA TN D-162.

GERARD, G. (1965) Optimum Structural Design Concepts for Aerospace
Vehicles: Bibliography and Assessment.
AFFDL-TR-65-9.

GHISTA, D.N. (1966) Structural Optimisation with Probability of
Failure Constraint
NASA TN D-3777.

GILES, G.L. (1971) Structural Efficiencies of Five Compression
Panels with Curved Elements.
NASA TN D-6474.

GJELSVIK, A. (1971) Minimum Weight Design of Continuous Beams.
Int.J. Solids Structures, Vol.7, pp.1411 to 1425

GUNNLAUGSSON, G.A. and MARTIN, J.B. (1972) A Note of Optimality
Conditions for Trusses with Zero Minimum Cross-Section.
Int.J. Mech. Sc. V.14, pp.643-650.

HACKMAN, L.E. and RICHARDSON, J.E. Design Optimisation of Aircraft Structures with Thermal Gradients
J. Aircraft Vol.1, No.1.

HADLEY, G. (1962) Linear Programming (Addison-Wesley)

HAFTKA, R.T. (1973) Automated Procedure for Design of Wing Structures to Satisfy Strength and Flutter Requirements.
NASA TN-D-7264 July 1973

HARRIS, G.Z. (1968) Optimum Fibre Arrangements for Reinforced Sheets Under Combined Loading.
ARC.CP. No. 975.

HARRIS, G.Z. (1972) Instability of Laminated Composite Plates.
AGARD-CP1112, pp.14-1 to 14-19.

HARRIS, G.Z. (1975) The Buckling of Orthotropic Rectangular Plates, Including the Effect of Lateral Edge Restraint.
Int.J. Sols.Structs (11) pp.887-88

HARRIS, G.Z. (1975) Buckling and Post-Buckling of Orthotropic Laminated Plates.
ASME/AIAA/SAE Conf. AIAA paper 75-813.

HARRIS, G.Z. (1975) The Buckling and Post-Buckling Behaviour of Composite Plates under Biaxial Loading.
Int.T.Mech.Sci. (17) pp.187-202.

HAUG, E.J. (1969) Optimal Design of Elastic Structural Elements.
U.S.A. Weapon Command. SY1R1-69.

HAUG, E.J., PAN, K.C. and STREETER, T.D. (1972) A Computational Method for Optimal Structural Design (1) Piecewise Uniform Structures. Int. J. Num. Meths in Eng. V.5, pp.171-184.

HEMP, W.S. (1958) Notes on the Problem of the Optimum Design of Structures. C.o.A. Note No.73.

HEMP, W.S. (1958) Theory of Structural Design.
AGARD Report 214.

HEMP, W.S. and CHAN, H.S.Y. (1965) Optimum Structures.
College of Aeronautics Memo No.70.

HEMP, W.S. (1966) Michell Frameworks for Alternative Loading Systems.
Unpublished Note.

HEMP, W.S. (1968) Optimum Structures.
Lecture course abstract, Oxford.

HEMP, W.S. (1970) Optimum Design of Circular Sandwich Plates.
Oxford Dept. Eng.Sci. Rep. 1120/70.

HEMP, W.S. (1970) Optimum Design of Girder of Uniform Depth.
Oxford Dept. Eng. Sci. Rep. 1124/70.

HEMP, W.S. and SUPPLE, W.J. (1970) Optimum Half-Plane Structures for Simply Supported Uniform Loading.
Oxford University Note.

HEMP, W.S. (1971) Upper Bounds for Optimum Half-Plane Structures for Simply Supported Uniform Loading.
Oxford Dept. Eng. Sci. Report 1010/71.

HEMP, W.S. (1973) Optimum Structures (Oxford)

HESS, T.E. et al. (1963) Re-entry Optimisation and Synthesis Program.
Proc. ASCE Struct. Div. Aug. 1963 pp.249-267.

HEYMAN, J. (1951) Plastic Design of Beams and Frames for Minimum Material Consumption.
Quarterly of Applied Mathematics, Vol.8, p.373.

HODGE, P.G. (1959) Plastic Analysis of Structures (McGraw-Hill)

HOFF, N.J. (1941) The Proportioning of Aircraft Frameworks.
J.Ae.Sci. Vol.8, No.8.

HOFF, N.J. (1953) Buckling and Stability.
J.R.Ae.S. (58); 517 pp.3-52.

HOFF, N.J. (1967) Inelastic Buckling of Columns in the Conventional Testing Machine.
Proc.Symp. Theory of Shells.
L.H. Donnell 70th Anniv. Vol, U. Houston.

HOFF, N.J. (1969) Some Recent Studies of the Buckling of Thin Shells.
The Aeronautical Journal, Vol.73, Dec. 1969.

HOFF, N.J. (1972) Creep Buckling of Plates and Shells.
Proc. 13th Int. Cong. Th. Applied Mechs. Moscow 1972.

HOFLER, A, LEYSSNER, U and WIEDEMANN, J. (1973) Optimisation of the Layout of Trusses Combining Strategies Based on Michell's Theorem and the Biological Principles of Evolution.
AGARD C-P123, pp.A1 to A8.

HOFMEISTER, L.D. and FELTON, L.P. (1969) Synthesis of Waffle Plates and Multiple Rib Sizes
AIAA Journal V.7, No.12 pp.2193-2199.

HOFMEISTER, L.D. and FELTON, L.P. (1970) Prestressing in Structural Synthesis.
AIAA J. Vol.8, No.2, pp.363-364.

HORNE, M.R. and MORRIS, L.J. (1972) Optimum Design of Multi-Storey Rigid Frames.
Cont. Optimisation of Structural Design, Swansea 1972.

HOUGHTON, D.S. (1961) Optimum Design of a Band Reinforced Pressurised Cylinder.
College of Aeronautics Note 116, April 1961.

HOWARD, H.B. (1953) Tube of Least Weight for Given Torsional Stiffness.
JRAeS, V.57, Jan.1953.

HSU, T.R. and BERTELS, A.W.M. (1974) Improved Approximation of Constitutive Elasto-Plastic Stress-Strain Relationship for Finite Element Analysis.
AIAA Jour. (12) 10, pp.1450-1452.

HU, T.C, and SHIELD, R.T. (1961) Minimum Volume Design of Discs.
ZAMP Vol.XII, pp.414-433.

HU, T.C. and SHIELD, R.T. (1961) Uniqueness in the Optimum Design of Structures.
J.Appl.Mech. June 1961 pp.284-287.

HUANG, N.C. (1971) The Effect of Shear Deformation on Optimal Design of Elastic Beams.
Int.J.Solids Structures, Vol.7, pp.321 to 326.

HUANG, N.C. (1973) Inelastic Buckling of Eccentrically Loaded Columns.
AIAA J (11) 7 pp.974-979.

HUANG, N.C. (1975) Minimum Weight Design of Vibrating Elastic Structures with Dynamic Deflection Constraint.
Univ. Wisconsin MRC Tech.Summ.Rep.1579.

HUANG, N.C. (1975) Minimum Volume Design of Elastic Trusses with Deflection Constraints.
J.Appl.Maths.Phys. (ZAMP) V.26, pp.437-452.

JAEGER, L.G. and CHILVER, A.H. (1959) The Design of Frameworks to Give Specific Deflections.
Mem.Int.Ass.Bridge Struct.Eng. No.19,pp.81-110.

JOHNS, K.C. (1976) Some Statistical Aspects of Coupled Buckling Structures.
IUTAM Symp. Buckling of structures 1974 Springer Berlin.

JOHNSON, J.R. MELOSH, R.J. and LUIK, R. (1967) Optimum Structural Design.
AFFDL TM-67-1-FDTR.

JOHNSTON, B.G. (1960) Design Criteria for Metal Compression Members (2nd Edition 1966). Column Research Council. Wiley. New York.

KAECHELE, L.E. (1957) Minimum Weight Design of Sandwich Panels.
Project Rand RM-1895.

KATO, B and AKIYAMA, H. (1975) The Equilibrium of Strain-Hardening Steel Columns.
Int. J. Sols. Struct. (11) pp.305-320.

KELLER, J.B. (1960) The Shape of the Strongest Column.
Arch.Rat. Mech.Anal. Vo.5, pp.275-285.

KHOT, N.S. VENKAYYA, V.B, JOHNSON, C.D. and TISCHLER, V.A. (1972) Optimisation of Fiber Reinforced Composite Structures.

KHOT, N.S., VENKAYYA, V.B. and BERKE, L. (1976) Optimum Design of Composite Structures with Stress and Displacement Constraints AIAA J. Bol.14,No.2, Feb.1976.

KIUSALAAS, J. (1972) Minimum Weight Design of Structures via Optimality Criteria. NASA TN D-7115.

KUHN, P. (1956) Stresses in Aircraft and Shell Structures (McGraw-Hill)

KYSER, A.C. (1965) Uniform Stress Spinning Filamentary Disc. AIAA J V.3, No.7, pp.1313-1316.

LAAKSO, J.H. and STRAAYER, J.W. (1974) Evaluation of Metal Shear Web Selectively Reinforced with Filamentary Composites for Space Shuttle Application. NASA CR-2409 August 1974.

LAMBLIN, D. (1972) Minimum-Weight Plastic Design of Continuous Beams Subjected to One Single Moveable Load J.Struct.Mech, Vol,1, No.1, pp.133-157.

LITTLE, G.H. (1973) Plate Failure in Stiffened Steel Compression Panels. Cambridge University Engineering Department. Technical Report CUED/C-Struct/TR.33(1973)

LIVESLEY, R.K. (1972) Linear Programming in Structural Analysis and Design. Conf. Optimisation of Structural Design, Swansea.

LUSSER, R. (1958) Reliability through Safety Margins. United States Army Ordnance Missile Command ASTIA, AD-212-476.

MAIER, G. (1972) Constrained Optimisation in Elasto Plastic Analysis. Conf. Optimisation of Structural Design Swansea.

MANSFIELD, E.H. (1963) Loading and Heating of a Simple Structure with Linear Work Hardening. J.R.Ae.S (67) 626 pp.92-102.

MANSFIELD, E.H. (1970) Analysis of a Class of Variable Thickness Reinforcement Around a Circular Hole in a Flat Sheet Aero. Quart, (21) pp.303-312.

MANSFIELD, E.H. (1970) Optimum Variable Thickness Reinforcement Around a Circular Hole in a Flat Sheet under Radial Tension. Q.J.Mech.Appl.Math. (26)4.

MANSFIELD, E.H. (1972) Inverse Methods in Two-Dimensional Elasticity. RAE Tech.Memo Structures 820, March 1972.

MASUR, E.F. (1970) Optimum Stiffness and Strength of Elastic Structures. J.Eng.Mech.Div., Proc. ASCE 96, EM5, pp.621-640.

MAXWELL, C. (1890) Scientific Papers II, P.175 (Cambridge University Press)

MICHAEL, M.E. (1960) Buckling of Unstiffened Shear Webs with Flanged Lightening Holes.
Aero.J. of the RAeS, Vol.64, p.298.

MICHELL, A.G.M. (1904) The Limit of Economy of Material in Frame Structures.
Philosophical Magazine, S.6,Vol.8, No.47.

MICKS, W.R. (1954) A Method for Determining the Effects of Elevated Temperature on Structural Design and Weight.
RAND Corp. Rep.P-488. March 1954.

MOE, J. (1972) Ship Structures Optimisation.
Conf. Optimisation of Structural Design, Swansea.

MORLEY, C.T. (1970) Optimum Reinforcement of Concrete Slab Elements Against Combination Moments and Membrane Forces.
Mag.Concrete Research, Vol.22, No.72, Sept. 1970.

MORRIS, A.J. (1972) Structural Optimisation by Geometric Programming.
Int.J. Solids Structures, Vol.8, pp.847-864.

MORRIS, A.J. (1974) A Primal-Dual Method for Minimum Weight Design of Statically Determinate Structures with Several Systems of Load.
Int.J.Mech.Sci. (16) pp.801-807.

MOSES, F. (1971) Optimisation of Structures with Reliability Constraints.
Structural Design Applications of Mathematical Programming Techniques, AGARD-A6-149-71.

MOSES, F. (1972) Design for Reliability; Concepts and Application.
Conf. Optimisation of Structural Design. Swansea.

MOSS, W.L. and BODDY, J.A. (1970) Weight Optimisation using Geometric Programming.
Soc. Aero. Wt. Engrs, Annual Conference.

MURTHY, K.N. and CHRISTIANO, P. (1973) Design of Least Weight Structures for Prescribed Buckling Load.
AIAA Journal Vol.11, No.12, Dec. 1973 pp.1773-1775.

NEUT, A. Van der (1949) Design of Structures on the Basis of Assumed Deformations.
Engineering Structures, Butterworth, London.

NEUT, A. Van der (1962) The Post Buckling Stiffness of Rectangular Simply Supported Plates.
Delft Technical University Report VTH-113.

NEUT, A. Van der (1968) The Interaction of Local Buckling and Column Failure of Thin-Walled Compression Members
University of Delft Report VTH-149.

NEUT, A. Van der (1972) The Sensitivity of Thin-Walled Compression Members to Column Axis Imperfection.
Delft University Report VTH-172.

NIORDSON, F.I. (1965) On the Optimal Design of a Vibrating Beam.
Quarterly of Applied Mechanics, Vol.23, No.1, p.47.

NIORDSON, F.I. and PEDERSEN, P. (1972) A Review of Optimal Structural Design. Tech. Univ. Denmark. DCAMM Rep. 31.

NOOR, A.K. and LOWDER, H.E. (1974) Approximate Techniques of Structural Re-Analysis.
Comp. and Structs. (4) pp.801-812.

NOOR, A.K. and LOWDER, H.E. (1975) Approximate Re-Analysis Techniques with Substructuring.
J.Struct.Div.ASCE PP.1687-1698.

PALMER, A.C. (1972) Dynamic Programming and Structural Optimisation.
Conf. Optimisation of Structural Design, Swansea.

PAPPAS, M, and AMBA-RAO, C.L. (1971) A Direct Search Algorithm for Automated Optimum Structural Design.
AIAA J V.9, No.3, March 1971, pp.387-393.

PAPPAS, M and ALLENTUCH, A. (1972) Optimal Design of Submersible Frame Stiffened Circular Cylindrical Hulls.
NCE Report No.NV6, July 1972.

PAPPAS, M. (1972) Use of Direct Search in Automated Optimal Design.
J.Eng.for.Ind. May 1972, pp.395-401.

PAPPAS, M, and ALLENTUCH, A. (1973) Mathematical Programming Procedures for Mixed Discrete-Continuous Design Problems.
Newark C.E. Report No.NV7, April 1973.

PAPPAS, M and ALLENTUCH, A. (1973) Pressure Hull Optimisation using General Instability Equations Admitting More Than One Longitudinal Buckling Half Wave.
Newark C.E. Report No.NV9, June 1973.

PAPPAS, M and ALLENTUCH, A. (1974) Structural Synthesis of Frame Reinforced Submersible Circular Cylindrical Shells.
Comps. and Structs. V.4, pp.253-280.

PAPPAS, M, and ALLENTUCH, A. (1974) Extended Capability for Automated Design of Frame Stiffened Submersible Cylindrical Shells.
Comps. and Structs. V.4, pp.1025-1059.

PAPPAS, M and MORADI, J.Y. (1975) An Improved Direct Search Mathematical Programming Algorithm.
ASME paper 75-DET-90.

PARSONS, H.W. and BEARD, D.W. (1973) The Optimum Distribution of Diagonal Stiffeners Reinforcing a Clamped Infinitely Long Plate Buckling under Stress.
The Aeronautical Journal, V.77, No.747, pp.148-150, March 1973.

PATNAIK, S.N. and SANKARAN, G.V. (1976) Optimum Design of Stiffened Cylindrical Panels with Constraint on Frequency in the Presence of Initial Stresses.
Int. J. Num. Meth. Eng. V.10, pp.283-299.

PEDERSEN, P. (1971) On the Optimal Layout of Multi Purpose Trusses.
Tech. Univ. Denmark DCAMM Rep. 18.

PEDERSEN, P. (1973) Optimal Joint Positions for Space Trusses.
2nd AGARD Conf. Struct. Optimisation, Milan.

PERRY, S.H. and CHILVER, A.H. (1976) The Statistical Variation of Buckling Strengths of Columns.
Proc. Inst. Civ. Eng. Pt.2, Mar. 1976, pp.109-125.

PETERSON, J.P. (1967) Structural Efficiency of Ring Stiffened Corrugated Cylinders in Axial Compression.
NASA TN D-4073.

PICKETT, R.M., RUBINSTEIN, M.F, and NELSON, R.B. (1973) Automated Structural Synethesis Using a Reduced Number of Design Coordinates.
AIAAJ, V.11, No.4, pp.489-494.

PIERRE, D.A. (1977) Robust Code for Optimisation.
AIAA J. Vol.15, No.6, pp.877-878.

PILKEY, W.D., WANG, B.P., YOO, Y, and CLARK, B. (1973) Perform - a Performance Optimising Computer Program for Dynamic Systems Subject to Transient Loadings.
NASA CR-2268, June 1973.

PIPPARD, A.J.S. (1922) On a Method for the Direct Design of Framed Structures having Redundant Bracing.
R and M No.793 (Ae50).

PLANTEMA, F.J. (1966) Sandwich Construction (Wiley)

POPE, G.C. (1966) On the Closer Integration of the Digital Computer with Design Procedures.
RAE Tech. Memo. Structures 666.

POPE, G.G. (1967) The Design of Optimum Structures of Specified Basic Configuration.
RAE TR 67284.

POPE, G.G. (1970) The Application of Linear Programming Techniques in the Design of Optimum Structures.
AGARD Symposium on Structural Optimisation, AGARD CP-36-70.

POPE, G.G. and SCHMIT, L.A. (1971) Structural Design Applications of Mathematical Programming Techniques.
AGARDograph No.149.

POPE, G.G. (1973) Optimum Design of Stressed Skin Structures.
AIAA Journal Vol.11, No.11, Nov. 1973, pp.1545-1552.

PORTER, B. (1969) Synthesis of Dynamical Systems
Nelson, London 1969.

PRAGER, W. and TAYLOR, J.E. (1968) Problems of Optimal Structural Design.
Trans. ASME, Journal of Applied Mechanics, Vol.35, p.102.

PRAGER, W. and SHIELD, R.T. (1968) Optimal Design of Multi-Purpose Structures.
Int.J.Sols.Structs. Vol.4, pp.469-475.

PRAGER, W, and MARCAL, P.V. (1971) Optimality Criteria in Structural Design.
AFFDL TR-70-166

PRAGER, W. (1973) Minimum Weight Design of a Statically Determinate Truss Subject to Constraints on Compliance, Stress and Cross-Sectional Area.
J. Appl. Mech. March 1973, pp.313-314.

PRAGER, W. (1973) Necessary and Sufficient Conditions for Global Structural Optimality.
AGARD C-P123, pp.1-1 to 1-12.

PRAGER, W. and ROZVANY, G.I.N. (1975) Plastic Design of Beams: Optimal Locations of Supports and Steps in Yield Moment.
Int.J.Mech.Sci. 17, pp.627-631.

RAMBERG, W. and OSGOOD, W.R. (1943) Description of Stress-Strain Curves by Three Parameters. NACA TN 902.

RAZANI, R. (1965) Behaviour of Fully Stressed Design of Structures and its Relationship to Minimum Weight Design.
AIAA J. Vol.3, No.12, pp.2262-2268.

RICHARDS, D.M. (1965) Michell Optimum Structures.
Eng. Mats. and Des. Dec. 1965.

RICHARDS, D.M. and CHAN, H.S.Y. (1966) Developments in the Theory of Michell Optimum Structures.
AGARD Report 543.

RICHARDS, D.M. (1968) The Sequential Design of Redundant Elastic Structures.
JBCSA Conf. on Recent Advances in Stress Analysis.

RICHARDS, D.M. (1969) Optimum Design of Fibre Reinforced Corrugated Compression Panels.
College of Aeronautics Report Aero. No.209.

RICHARDS, D.M. (1971) Material Property Effects in the Design of Inflated Structures.
Cranfield Memo No.56.

RICHARDS, D.M. (1973) The Design of Compatible Structures.
AGARD C-P123, pp.10-1 to 10-13.

RICHARDS, D.M. and WEBB, J.H. (1974) The Analysis and Design of Isovoid Plates (1) Analysis and Preliminary Optimisation.
MOD Contract Report.

RICHARDS, D.M. and WEBB, J.H. (1975) The Analysis and Design Of Isovoid Plates (2) Transverse Shear Flexibility Effects.
MOD Contract Report.

RICHARDS, D.M. (1975) Optimisation of Airship Structures.
RAeS Symp. "Future of the Airship", London Nov. 1975.

RICHARDS, D.M. and WEBB, J.H. (1976) The Analysis and Design of Isovoid Plates (3) Comparison and Conclusions.
MOD Contract Report.

RICHARDS, D.M. (1976) The Application of Empirical Stress-Strain Functions to Structural Optimisation Problems.
Xth Congress ICAS Ottawa, Oct. 1976.

RICHARDS, D.M. (1976) The Optimum Design of Stiffened Shear Webs with Supplementary Skin Stabilisation.
Int.J.Sols.Structs. V.12, pp.791-802.

RICHARDS, D.M. (1977) Minimum Weight Design of Compression Surfaces.
RAE Tech. Memo. Structures 901, Jan. 1977.

RIFE, C.D. (1964) Bibliography of Aeronautical Weight Estimation and Control. Lockheed-Georgia Int.Rep. Aug. 1st 1964.

RIKARDS, R.B. et al (1972) Synthesis of Optimum Cylindrical Shells of Reinforced Plastics for an External Pressure and Axial Compression.
Mekhanika Polmerov, No.2, pp.301-309, Mar. 1972.

ROSSOW, M.P. and TAYLOR, J.E. (1973) A Finite Element Method for the Optimal Design of Variable Thickness Sheets.
AIAA Journal Vol.11, No.11, November 1973, pp.1566-1569.

ROTHWELL, A. (1969) Optimum Fibre Orientations for the Buckling of Thin Plates of Composite Material.
Fibre Science and Technology, Vol.2, p.111.

ROZVANY, G.I.N, and HAMPSON, A.J.K. (1963) Optimum Design of Prestressed Plates.
J.Amer.Concrete Inst. No.60-53, pp.1065-1083.

ROZVANY, G.I.N. (1972) Grillages of Maximum Strength and Maximum Stiffness. Int.J.Mech.Sci., V.14, pp.651-666.

ROZVANY, G.I.N. (1976) Optimal Design of Flexural Systems. Pergamon, Oxford, 1976.

RUBIN, C. (1975) Optimum Design for a Corrugated Diaphragm Clamped to a Shaft Undergoing Axial or Angular Displacement. J.Eng.Mat.Tech. Oct. 1975, pp.363-366.

SAVE, M.A. (1972) A Unified Formulation of the Theory of Optimal Plastic Design with Convex Cost Function. J.Struct.Mech.,1 (2) pp.247-276.

SCHMIT, L.A., KICHER, T.P. and MORROW, W.M. (1963) Structural Synthesis Capability of Integrally Stiffened Waffle Plates. AIAA J. Vol.1, No.12, pp.2820 to 2836.

SCHMIT, L.A. and MALLETT, A.M. (1963) Structural Synthesis and Design Parameter Hierarchy. Proc. ASCE.Struct.Div. Aug. 1963, pp.269-299.

SCHMIT, L.A. and FOX, R.L. (1965) An Integrated Approach to Structural Synthesis and Analysis. AIAA Journal, Vol.3, No.6, p.1104.

SCHMIT, L.A. and FARSHI, B. (1977) Optimum Design of Laminated Fibre Composite Plates. Int.J. Num. Meth. Eng. Vol.11, pp.623-640.

SCHUERCH, H.U. and BURGGRAF, O.R. (1964) Analytical Design for Optimum Filamentary Pressure Vessels. AIAA Journal, Vol.2, No.5, p.809.

SCHUERCH, H. (1966) Large-Sized Orbiting Radio Telescopes. Astro Res.Corp. ARC-R-224.

SCHUERCH, H. (1966) Performance-Weight Relations and Shape Parameters for Maxwell Structures. Astro Research Corp. (unpublished)

SHANLEY, F.R. (1960) Weight Strength Analysis of Aircraft Structures. (Dover: also McGraw-Hill, 1952)

SHEU, C.Y. and PRAGER, W. (1968) Recent Developments in Optimal Structural Design. Applied Mechanics Reviews, Vol.21, No.10, p.98b.

da SILVA, B.M.A. (1972) Application of Feasible Direction Methods to Structural Optimisation Problems. Conf. Optimisation of Structural Design, Swansea.

SIMITSES, G.J. (1973) Optimal vs. Stiffened Circular Plate. AIAA Journal Vol.11, No.10, Oct. 1973, pp.1409-1412.

SIMITSES, G.J. and UNGBHAKORN, V. (1975) Weight Optimisation of Stiffened Cylinders under Axial Compression. Comps. and Structs. V.5, pp.305-314.

SINGER, J. and BARUCH, M. (1966) Recent Studies on Optmisation for Elastic Stability of Cylindrical and Conical Shells. ICAS paper 66-13.

SLYSH, P. et al. (1975) Isogrid Weight Optimum Structures. 34th SAWE Conference.

SPUNT, L. (1970) Weight Optimisation of the Post Buckling Integrally Stiffened Wide Column. J.Aircraft, V.7, No.4, pp.331-333.

SOBIESZCZANSKI, J. and LOENDORF, D. (1973) Automated Sizing of Large Structures by Mixed Optimisation Methods. AGARD CP-123, pp.15-1 to 15-12.

SOBIESZCZANSKI, J. (1975) Building A Computer-Aided Design Capability Using a Standard Time Share Operating System. ASME Winter Annual Meeting, Houston Dec. 5.

STEPHENSON, G. (1971) Inequalities and Optimal Problems in Mathematics and the Sciences. Longman, London 1971

STEPNIEWSKI, W.Z. and KALMBACH, C.F. (1969) Multivariable Search and its Application to Aircraft Design Optimisation Boeing Vertol. Sept. 1969.

STOKER, J.J. (1949) Prestressing a Plane Circular Plate to Stiffen it against Buckling. Reissner Aniv. Vol. : Contrib. to Appl. Mechs. pp.268-278 Edwards,(Michigan)

STOWELL, E.Z. (1947) A Unified Theory of Plastic Buckling of Columns and Plates. NACA TN 1556.

STRAUB, W.L. (1974) Managerial Implications of Computerised Aircraft Design Synthesis. J. Aircraft (11), 3, pp.129-135.

SVED, G. (1954) The Minimum Weight of Certain Redundant Structures. Australian J. of Appl. Sci. V.5, No.1, pp.1-9.

SVED, G. and GINOS, Z. (1968) Structural Optimisation under Multiple Loading. Int.J.Mech.Sci. Vol.10, pp.803-805.

SYMONDS, M.F. (1956) Minimum Weight Design of a Simply Supported Transversely Stiffened Plate in Shear. Journal of the Aeronautical Sciences, Vol.23, No.7, p.685

SZCZEPINSKI, W. (1972) Limit Analysis and Plastic Design of Structural Elements of Complex Shape.
Progress in Aerospace Sciences, Pergamon, 1972.

TAIG, I.C. and KERR, R.I. (1973) Optimisation of Aircraft Structures with Multiple Stiffness Requirements.
AGARD C-P 123, pp.16-1 to 16-14.

TALEB-AGHA, G and NELSON, R.B. (1976) Method for the Optimum Design of Truss-Type Structures.
AIAA J. V.14, Bo.4, pp.436-445.

TAYLOR, J.E. (1967) The Strongest Column: An Energy Approach.
J.Appl.Mech. June 1967, pp.486-487.

TAYLOR, J.E. (1969) Maximum Strength Elastic Structural Design.
J.Eng.Mech.Div. ASCE, June, p.653.

TAYLOR, J.E. (1971) Optimal Prestress Against Buckling: An Energy Approach.
Int.J.Sols.Structs. V.7, pp.213-223.

TAYLOR, R.F. and GWIN, L.B. (1973) Application of a General Method for Flutter Optmisation.
AGARD C-P123, pp.13-1 to 13-14.

THOMAS, J.M. and HANAGUD, S. (1974) Reliability Based Econometrics of Aerospace Structural Systems: Design Criteria and Test Options.
NASA TN D-7646.

THOMPSON, J.M.T. and LEWIS, G.M. (1972) On the Optimum Design of Thin-Walled Compression Members.
J.Mech.Phys.Solids, Vol.20, pp.101 to 109.

THOMPSON, J.M.T. (1972) Optimisation as a Generator of Structural Instability.
Int.J.Mech.Sci. V.14, pp.627-629.

THOMPSON, J.M.T. and SUPPLE, W.J. (1973) Erosion of Optimum Designs by Compound and Branching Phenomenona.
J.Mech.Phys.Sols.Vol.21, pp.135-144.

TVERGAARD, V. (1973) Imperfection-Sensitivity of a Wide Integrally Stiffened Panel under Compression.
Int.J.Solds Structures 1973, V.9, pp.177-192.

TVERGAARD, V. and NEEDLEMAN, A. (1975) Buckling of Eccentrically Stiffened Elasti-Plastic Panels on Two Simple Supports or Multiply Supported.
Int.J.Sols.Structs. (11) pp.647-663.

VAJDA, S. (1961) Mathematical Programming.
Addison-Wesley.

VENKAYYA, V.B, KHOT, N.A, and REDDY, V.S. (1969) Energy Distribution in an Optimum Structural Design.
AFFDL-TR-68-156.

VENKAYYA, V.B. (1971) Design of Optimum Structures.
Computers and Structures, Vol.1, pp.365-309.

VENKAYYA, V.B, KHOT, N.S, TISCHLER,V.A, and TAYLOR, R.F. (1971)
Design of Optimum Structures for Dynamic Loads.
3rd AF Conf. on Matrix Methods in Struct. Mechs.

VENKAYYA, V.B, KHOT, N.S, and BERKE, L. L973) Application of Optimality Criteria Approaches to Automated Design of Large Practical Structures.
AGARD C-P123, pp.3-1 to 3-19.

VISWANATHAN, A.V, SOONG, TSAI-CHEN, and MILLIER, R.E. (1971) Buckling Analysis for Axially Compressed Flat Plates, Structural Sections, and Stiffened Plates Reinforced with Laminated Composites.
NASA CR-1887.

VISWANATHAN, A.V, and TAMEKINI, M. (1973) Elastic Buckling Analysis for Composite Stiffened Panels and Other Structures Subjected to Biaxial Inplane Loads.
NASA CR-2216.

WHITTLE, P. (1971) Optimisation under Constraints.
(Wiley).

WILDER, T.W, BROOKS, A.B, and MATHAUSER, E.E. (1953) The Effect of Initial Curvature on the Strength of an Inelastic Column
NACA TN 2872.

WILLIAMS, D. (1951) Sandwich Construction - a Practical Approach for the Use of Designers.
R & M No.2466.

WILLIAMS, F.W. (1973) Stiffened Panels with Varying Stiffener Sizes.
The Aeronautical Journal, V.77, pp.350-354. July 1973.

WILLIAMS, J.G. and MIKULAS, M.M. (1975) Analytical and Experimental Study of Structurally Efficient Composite Hat-Stiffened Panels Loaded in Axial Compression.
16th ASME/AIAA/SAE Conf. AIAA paper 75-754.

WILSON, J.F. HOLLOWAY, D.M, and BIGGERS, S.B. (1971) Stability Experiments on the Strongest Columns and Arches.
Experimental Mechanics July 1971, pp.303-308.

WITTRICK, W.H. (1945) A Theoretical Analysis of the Efficiency of Sandwich Construction under Compressive Endload.
R & M 2016.

YASAKA, T. (1970) A Method of Minimum Weight Design with Requirements Imposed on Stresses and Natural Frequencies. Institute of Space and Aero. Science, University of Tokyo Rep.No. 452.

YUSUFF, S. (1975) Buckling Failure of Flat Stiffened Panels. J. Aircraft. Vol.13, No.3, pp.198-204.

ZIEGLER, H. (1958) Kuppeln Gleicher Festigkeit. Ingenieur-Archiv XXVI Band 1958, pp.378-382.